THE CHEMICAL AND MECHANICAL PROPERTIES

OF THIOL MODIFIED ABS

by

MOSA GHAEMY

A Thesis Submitted for the Degree of

DOCTOR OF PHILOSOPHY

of The University of Aston in Birmingham

June 1980

SUMMARY

CHEMICAL AND MECHANICAL PROPERTIES OF THIOL MODIFIED ABS

MOSA GHAEMY

Submitted for the Degree of PhD   June 1980

The oxidative degradation (photo and thermal) of unstabilised and
stabilised acrynonitrile-butadiene-styrene graft copolymer (ABS)
has been studied using a viscoelastomeric technique (Rheovibron),
falling weight impact tester and infra-red spectrometry to measure
mechanical and chemical changes occurring in the polymer. Linear
correlations were obtained between the loss of unsaturation in
the polybutadiene segment of the polymer and loss of impact
resistance. The parameters were also correlated with decrease in
tan δ at -80°C.

Stabilisers containing the thiol group, notably 3,5-di-tert-butyl-
4-hydroxybenzyl mercaptan (BHBM), an antioxidant, and 4-benzoyl-3-
hydroxyphenyl-O-ethyl thioglycollate (EBHPT), a uv stabiliser, have
been bound to ABS in latex and during processing in a high
temperature mixing operation through the thiol group by free radical
addition to the double bond. The bound stabilisers produced in
concentrated form (masterbatches) have been diluted to normal
concentration (1%) with unstabilised ABS and their stabilising
properties followed by the above techniques. The adducts were
effective thermal and photo-oxidative stabilisers and their
effectiveness was not substantially reduced by solvent extraction
of the polymer. The presence of bound stabilisers in normal
concentration did not effect the initial mechanical properties
of ABS compared with unstabilised ABS. Furthermore, ABS
containing synergistic combinations of the two stabilisers showed
remarkable synergism in stabilising the mechanical properties of
ABS towards photodegradation.

Keywords

ABS
Photo and Thermal Degradation
Bound Antioxidants
Bound uv Stabilisers

ACKNOWLEDGMENTS

The work described herein was carried out at the University of

Aston in Birmingham between October 1977 and March 1980.

It has been done independently and submitted for no other degree.

M. GHAEMY

June 1980

CONTENTS

(vi)

LIST OF FIGURES

LIST OF TABLES

CHAPTER ONE

INTRODUCTION

1.1 Chemistry and Structure of ABS Polymer

Commercial acrylonitrile-butadiene-styrene (ABS) resins have been
characterised as two phase systems. The polybutadiene (PB)
constitutes a rubber phase and exists as particles in a glassy
matrix of ~ poly(styrene-co-acrylonitrile), ie SAN[1,2].

The development of this styrene based polymer dates back almost
one hundred years, to the discovery of polystyrene (PS). The
increase in production and use of PS has been due to its low cost,
ease of processing and useful physical properties, such as
hardness, rigidity, high refractive index, good electrical
properties and good resistance to water. The chief defect of PS
is brittleness, manifested as low resistance to impact[3].

Attempts to overcome this deficiency have culminated in the
development of the so-called 'impact-resistant polystyrene',
wherein an elastomer is incorporated in the polymerised styrene
to improve greatly the impact resistance of the plastic[4].

Polybutadiene (PB) can be blended with PS to give only a
marginal improvement in impact strength[5]. However, if the
rubber is first dissolved in styrene monomer and then polymerised

1

a graft copolymer of short PS side chains attached to SBR is obtained which gives a great improvement in the reistance to impact of the plastic[6].

One of the methods used to make ABS polymer is copolymerisation of styrene and acrylonitrile to give a resinous copolymer and then mixing this copolymer with a minor proportion of a rubbery copolymer of butadiene and acrylonitrile. It was considered necessary in producing this type of product that the resinous copolymer be mixed with a butadiene-acrylonitrile rubber in order to obtain satisfactory compatibility of the ingredients. The resinous copolymer and the rubbery copolymer must be mixed at high temperatures and then worked on a cold mill. The resulting blend is always a mixture capable of mechanical separation[7].

Another method used commercially to make ABS polymers is 'graft copolymerisation'[8]. A mixture of styrene-acrylonitrile monomers are polymerised in the presence of polybutadiene latex to form a grafted polymer[9]. A water soluble initiator such as potassium persulphate is added to polymerise styrene and acrylonitrile. The resultant material will be a mixture of PBD, PBD-grafted with acrylonitrile and styrene and styrene-acrylonitrile copolymer[10].

Therefore ABS plastics are classified into two different types. Type A is a nitrile rubber modified styrene-acrylonitrile resin

2

made by blending the two copolymers. Type B is a graft-modified
styrene-acrylonitrile resin, produced by copolymerising styrene
and acrylonitrile in the presence of PBD. The following
information regarding the structure of graft copolymerised ABS
is now available:

(1)   It has a two-phase structure.

(2)   Of the two phases, the matrix (SAN) is soluble in most
       solvents and can be separated from the insoluble graft
       polymer by centrifugation.

(3)   The addition sequence of the substrate polymer, PBD is
       exclusively 1,4 and 1,2 and not 1,2, 1,2.

(4)   Tertiary allylic hydrogen and vinylic double bonds are
       common in the graft copolymer.

(5)   There is an appreciable number of cross-links in the
       graft copolymer which are randomly distributed.

1.2   Mechanism Responsible for Toughness in Rubber Toughened Plastics

In general the toughness of a polymer can be explained in terms
of the fracture growth process which occurs by the initiation
of a crack in some microscopic region of the surface. Crack
initiation is followed by a very rapid propagation in a point
perpendicular to the maximum tensile stress. This crack may
fork into a number of directions, thus shattering the material
into several pieces.

In toughened thermoplastics such as ABS which contains a rubbery component, when the propagating crack meets a rubber particle an increase in energy is required to keep the crack moving.

One of the first hypotheses advanced to explain rubber toughening was that the rubber absorbs impact energy by mechanical damping. Buchdahl and Nielsen had observed the secondary loss peak due to the rubber[11]. However, whilst damping might explain some of the energy absorption in impact, it did not account for stress-whitening. The first theory of toughening was published in 1956 by Merz et al[12]. The basic idea was that the rubber particles held together the opposite faces of a propagating crack, so that the energy absorbed on impact was the sum of the energy to fracture the glassy matrix and the work required to break the rubber particles. The multiple crazing theory, advanced by Bucknall and Smith[13] in 1965 was a development of the microcrack theory of Merz et al. The important new feature was that stress-whitening was attributed not to cracks but to crazes. Electron microscope studies on crazing in toughened plastics confirmed that crazes are formed in ABS polymer[14,15]. These studies revealed that the spherical rubber particles in ABS became spheroidal as a result of craze formation in the adjacent SAN matrix material and that crazes tended to branch in rubber-toughened plastics. These results imply that the presence of rubber particles favours craze initiation and propagation thus bringing about a large

4

number of straight crazes in glassy polymers.

The theories so far proposed as explanation of rubber toughening
have been classified into four categories by Boyer and Keskkula[16]:

(1)   Energy absorption by rubber particles

(2)   Craze initiation by rubber particles

(3)   Rubber particles acting by reinforcement and craze
        termination

(4)   Rubber particles acting as obstacles to crack propagation

Toughness in a rubber toughened plastic therefore depends on
several factors; the amount of the dispersed rubber phase in
the system, the particle size of the dispersed rubber phase, the
adhesion of the rubbery phase to the rigid matrix. Therefore,
the rubber dispersed phase must possess the following properties:

(1)   Some incompatibility with the rigid phase

(2)   The ability to absorb energy

(3)   Good adhesion with the rigid phase

(4)   Optimum particle size and distribution

(5)   A low glass transition temperature, preferable below
        $-50^{o}C$

The adhesion between two phases should be strong and the rubber
should be broken down into small particles without becoming
too finely dispersed to be effective in toughening the rigid

5

polymer. Grafting is an important method for obtaining a strong

bond between rubber particles and the surrounding resin. It is

also necessary to produce and maintain phase separation between

the rubber and rigid polymer in order to make a product that

combines stiffness with toughness.
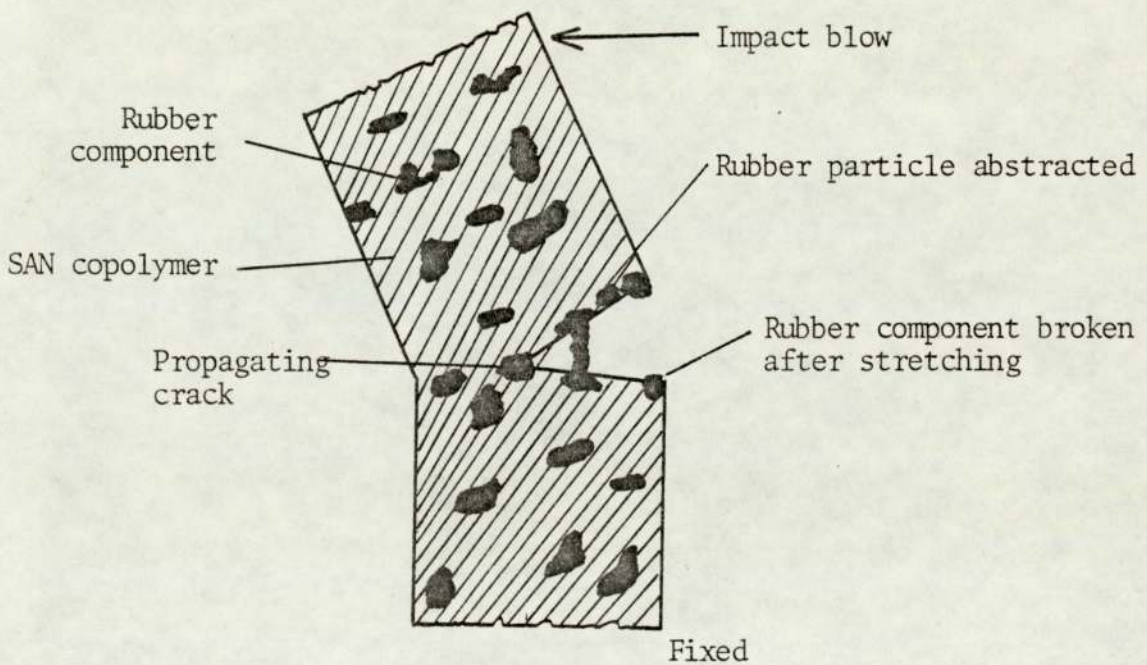
Fig 1.1 A schematic diagram illustrating mechanism of breakage
in an ABS polymer[12]

6

1.3 Mechanical Properties of Toughened Polymers

Rubbers are added to plastics to improve flexibility and impact resistance. Plastics are also added to rubbers to modify their processing characteristics and physical properties.

1.3.a Impact Properties

Impact tests are designed to measure the toughness or the resistance to breakage materials under high velocity of impact conditions. The field of impact is very complex for a number of reasons[17].

(1)   There are a large number of impact tests which all measure somewhat different quantities.

(2)   Tests are made on specimens of various sizes and shapes.

(3)   The specimens are broken under different kinds of stress distributions and under different speeds of impact.

(4)   Variations in the specimens themselves, for example, different behaviours from the surface to the interior and the degree of molecular orientation, make it difficult to obtain reproducible results.

Fig 1.2 shows the change of impact strength with temperature for graft and blend ABS containing the same (20% by weight) amount of rubber[18]. The impact strength of the graft ABS in the useful temperature range is far superior to the polyblend of the same
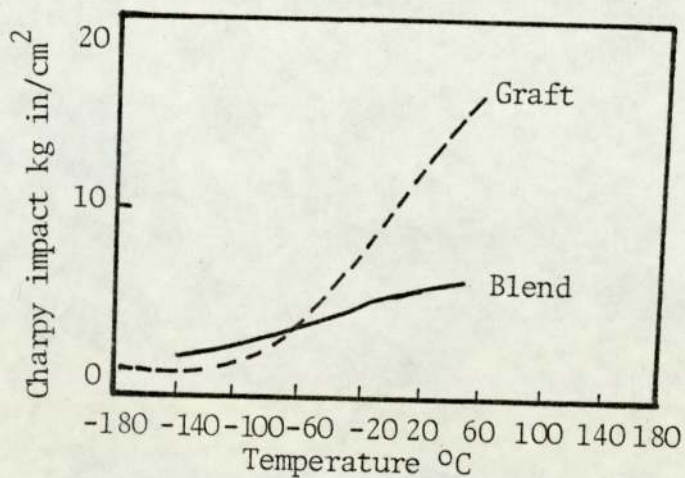
Fig 1.2   Temperature dependence of charpy impact strength for graft
and blend ABS (ref 18)
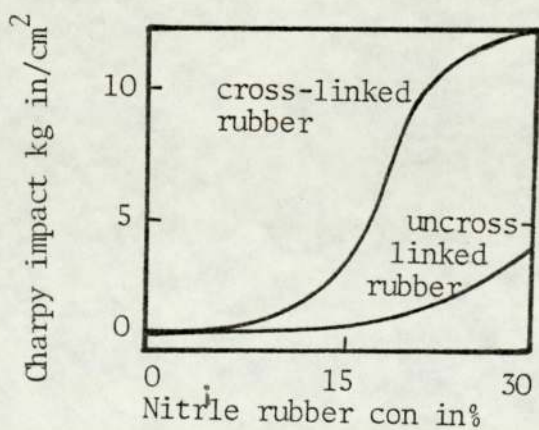
Fig 1.3   Variation in impact strength against concentration of
nitrile rubber in ABS polyblend (Ref 10)

composition. Grafting the SAN glassy phase to the PBD rubbery
phase increases the interfacial strength or adhesion between
the two phases resulting in higher impact strength. Cross-linking
of the rubber phase will increase the amount of energy which can
be absorbed without fracture during impact. Fig 1.3 shows the
effect of cross-linked and uncross-linked rubber on the impact
strength of the ABS polyblend[10,19].

Temperature has a profound influence upon the impact behaviour
of all plastics including rubber-toughened polymers. At very
low temperatures, the rubber phase is hard and glassy and the
rubber-toughened polymer is brittle. At high temperatures,
the rubber is able to relax even in the rapidly forming stress
field ahead of the travelling crack. Fig 1.4 shows the effect
of temperature on the impact strength of high impact
polystyrene (HIPS)[20].

The glass transition temperature (Tg) of rubber has a significant
effect on the impact strength of toughened polymers. Dynamic
mechanical measurements on two HIPS polymers, one based on
polybutadiene and the other on poly(butadiene-co-styrene)[21],
showed Tg at -98 and -16°C respectively for the two rubbers.
The low temperature impact data correlates well with these Tg
values. The impact strength begins to rise at -90°C in the
HIPS containing PBD and at about -20°C in the HIPS containing
copolymer rubber. It is explained that the PBD is able to
control rapid crack growth at temperatures above 10°C whilst
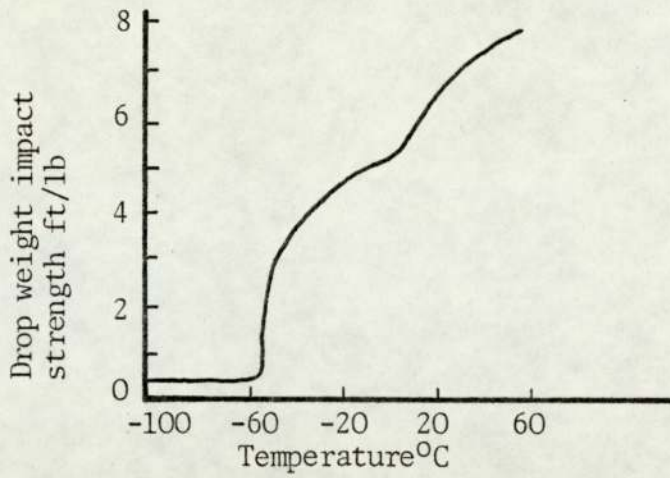
Fig 1.4   Drop weight impact strength of 80   HIPS sheet
           as a function of temperature (ref 20)
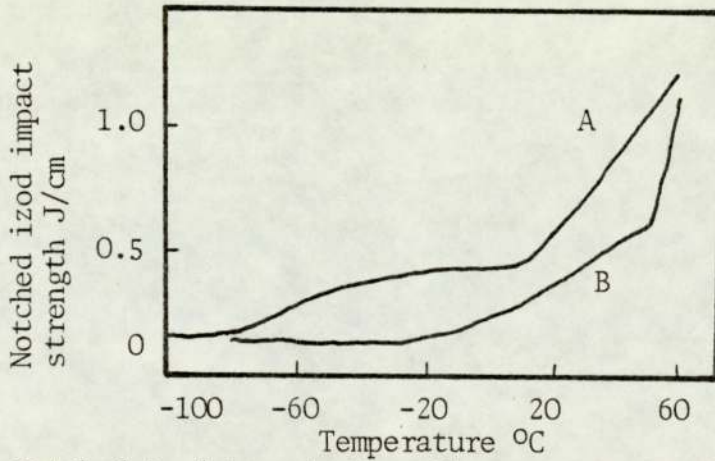
Fig 1.5   Notched izod impact strength over a range of temperatures for
           HIPS polymers. A toughened with PBD, B toughened with BD-CO-S (ref
                                                                           21)
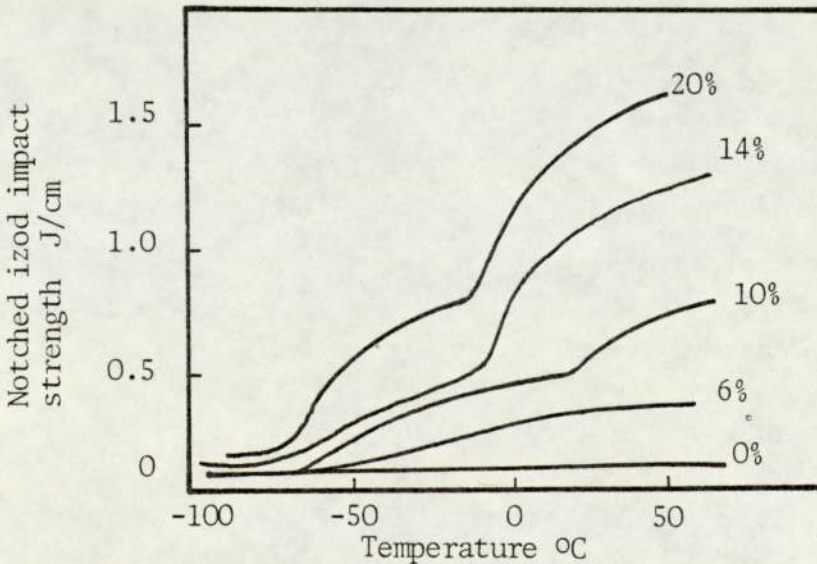
Fig 1.6   Effect of amount of rubber, 6-20% PBD, on the notched izod
           impact strength of ABS (ref 22)

10

poly(butadiene-co-styrene) is ineffective in this respect at temperatures below 50°C, owing to its higher Tg.

The effect of rubber content on impact strength over a range of temperatures is illustrated in Fig 1.6, which compares SAN with a series of ABS polymers containing respectively 6, 10, 14 and 20% of PBD[22].

There are several methods for the measurement of impact strength. The Izod and Charpy impact tests measure the energy required to break the specimen from the loss in kinetic energy of the weight. The falling weight test measures the amount of energy required to break the sheet or plate of material from the weight of the ball and the height from which it is dropped. High speed stress-stain tests, in which the area under a stress-strain curve is proportional to the energy required to break a material, this area should be directly proportional to the impact strength of the plastic at a high enough rate.

1.3.b Dynamic Mechanical Properties

Dynamic mechanical tests measure the response or deformation of a material to periodic or varying forces. Generally the applied force and the resulting deformation both vary simultaneously with time.

Perfectly elastic materials have no mechanical damping. Nearly

11

perfectly elastic materials, such as steel spring or a rubber band, store energy as potential energy when they are stretched. This energy is converted to kinetic energy when the applied load is removed and the material snaps back to its original dimensions. Viscous liquids are examples of the other extreme which cannot store potential energy and all the energy which is to deform them is dissipated as heat, thus they have high damping. High polymers are examples of viscoelastic materials which have the characteristics of both viscous liquids and elastic springs[17]. Viscoelasticity of plastic materials can be represented by the use of a sufficiently elaborate system of spring and dashpot modulus. The dynamic mechanical properties of this model are shown in Fig 1.7. Assume that the viscosity of the dashpots decrease with temperature and the viscosity of the single dashpot η_3 is greater than that of the middle one η_2. At very low temperatures, the viscosity will be so high that the dashpots are frozen and will not respond to a force, so only the single spring E_1 stretches and the damping will be very low. At a higher temperature, the viscosity will have decreased enough for the middle dashpot η_2 in parallel with the second spring E_2 to respond to a stress. Now a stress, initially stretches the single spring but the middle spring and dashpot also will stretch as the stress continues. The middle section lags behind the applied stress, and when the periodic external stress again becomes zero, the middle section will still be partly stretched and will continue to decrease in length. Thus, the stress and strain are not in phase. The motion of the viscous dashpot η_2 dissipates energy into heat and in this temperature interval the damping will be

12
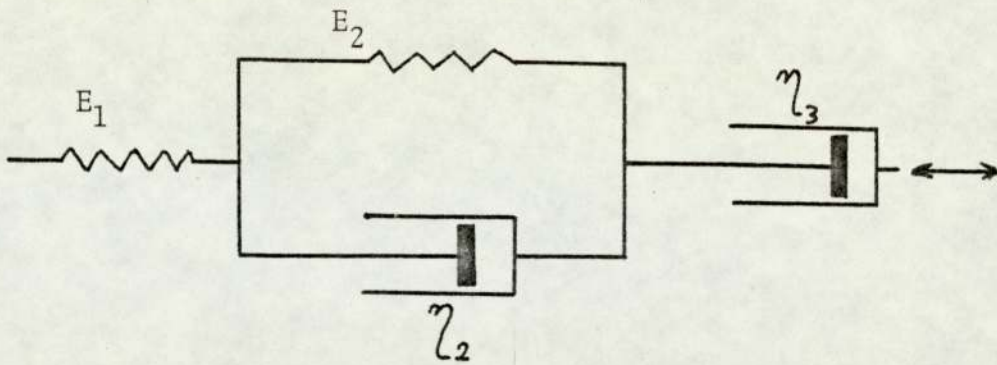
Fig.I.7.Spring and dashpot scheme for representation of viscoelastic behavior.
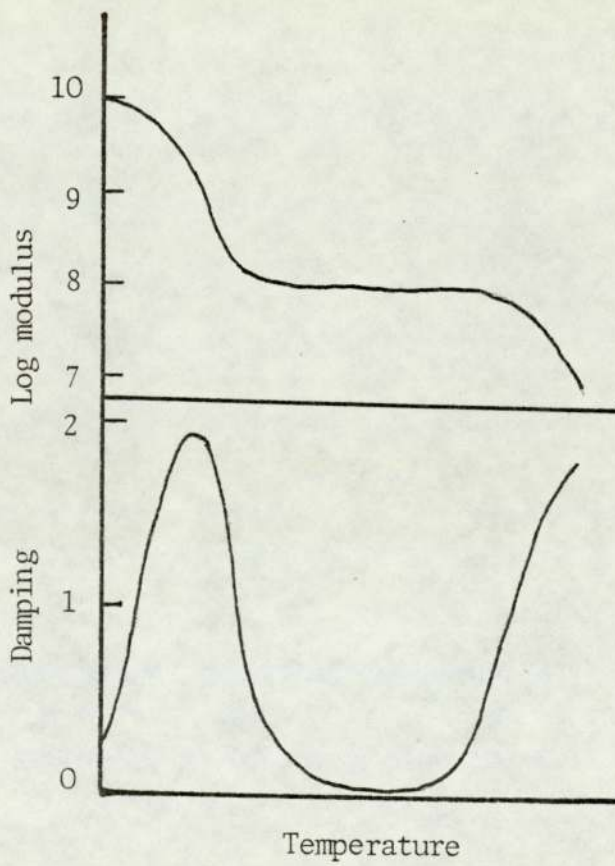
Fig 1.8 Dynamic mechanical properties of a 4-element model as a function of temperature

high. At somewhat higher temperatures the viscosity of the single

dashpot η_3 is still too great for it to respond much to a stress but

the visotisity of the middle dashpot will be very low. Now both springs

readily respond to a stress so the modulus will be lower. The damping

will also be fairly small since the viscosity of the dashpot is too

low to dissipate much energy in spite of its large motion. At still

higher temperatures well above the damping peak the damping can again

increase when the viscosity of the single dashpot has decreased enough

so that it can respond to the external stress. The 4-element model now

behaves similar to a molten polymer with viscosity controlled by molecular

shippage.   Therefore when such materials are deformed, part of the

energy is stored (E') is called the elastic modulus, as potential energy

and part is dissipated (E") is called the imaginary modulus as damping

and the ratio of E"/E' is called the dissipation factor and shown by

tan δ , it will be discussed in detail in Section 2.11.b

There are several methods for measuring the dynamic mechanical

properties of polymers including torsion pendulum, vibrating

reed and cyclic tension tests. Each of these methods consists

in measuring modulus and loss tangent (tan δ) over a range of

temperatures in small-amplitude oscillation. One of the best

instruments which is capable of measuring dynamic mechanical

properties of plastics over a wide range of temperatures is

Rheovibron whose function will be explained in Section 2.11.

The damping (dissipation factor E"/E') goes through a maximum

and then a minimum as the temperature is rasied for a material

such as the polymer shown in Fig 1.9. At low temperatures,

molecular motion of the chain segments is frozen in thus there

is not dissipation of the energy and damping is low. At
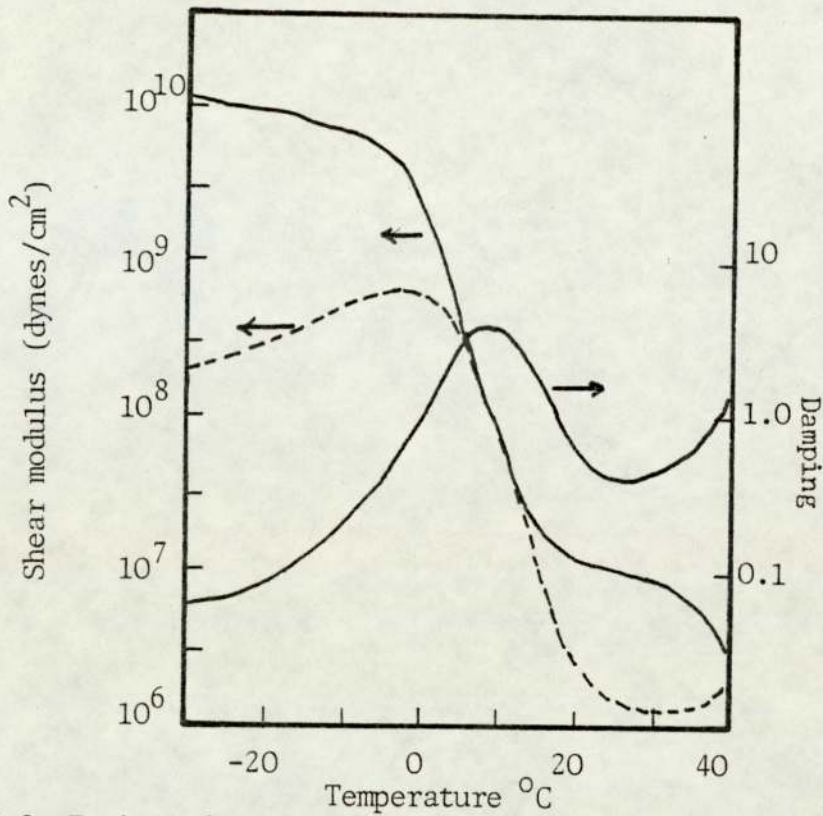
Fig 1.9 Typical dynamic mechanical behaviour of uncross-linked
amorphous polymers. The material is a copolymer of styrene
and butadiene, ref 23
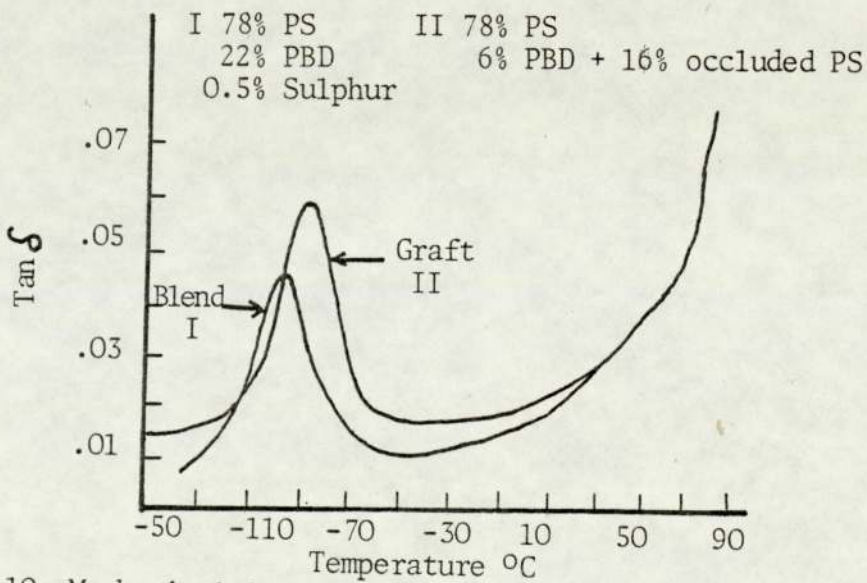
Fig 1.10 Mechanical loss curves of impact polystyrene containing
similar rubber phase volume with different morphologies, ref 22

15

temperatures above the glass transition region, rubber like a
weak spring stores energy without dissipating it into heat, the
damping is low. Thus, if chain segments are completely frozen
in or are completely free to move, damping is low. In the
transition region, the damping is high because some of the
molecular chain segments are free to move while others are not.

Molecular weight in general does not affect the dynamic mechanical
properties of polymers at temperatures below the glass transition
region. The damping above the glass transition is strongly
dependent upon molecular weight, the minimum in damping
decreases as the molecular weight increases due to chain
entanglements which delay the onset of viscous flow. The width
of the damping curve in the neighbourhood of the minimum used
to estimate the distribution in molecular weights. As the ratio
of weight average to number average molecular weight increases,
the damping minimum broadens[23,24]. Cross-links prevent much
of the viscous flow from taking place and damping of highly
cross-linked rubbers is relatively insensitive to temperature
and there is also shift in glass temperature with cross-linking.
Plasticisers lower the temperature of maximum damping in the
same way they lower the glass transition temperature. In order
that a liquid lower   the glass transition, it must be
soluble in the polymer. The amount of lowering of the Tg depends
upon the Tg of the pure plasticiser. If two polymers are
insoluble in one another so that the two phases exist, the
polyblend will have two glass transitions instead of the usual

16

single one. The two transitions occur at nearly the same temperatures as the individual transitions of the pure polymers making up the mixture[25]. The concentration of the components in a polyblend may be estimated from the heights of the damping peaks. The greater the concentration of a polymer, the larger is its damping peak[26-29]. Table 1.1 lists the maximum damping of a rubber as a function of its concentration in a polystyrene polyblend. There are other factors which influence the damping to some extent; the extent of solubility and the size of the particles of the dispersed material. The behaviour of two-phase systems was studied by Matsue[14] in terms of compatibility and molecular interaction between two phases, using both electron microscopy and dynamic mechanical tests. In this study, blends of PVC/PBD and PVC/NBR were studied, the first blend showed a sharp separated peak due to the lack of compatibility between two phases, while the damping peak of NBR disappeared with increasing rubber content in the polyblend which indicates the rubber component is molecularly dissolved in the PVC matrix.

Graft polymers are similar to polyblends in their dynamic behaviour but the loss peak in the graft polymers is considerably greater than that in a blend containing the same concentration of rubber component. This difference is connected with the difference in the volume fraction of the rubber particles in the two polymers. Polystyrene sub-inclusions greatly increases the volume fraction of the rubber phase in

17

Table 1.1   Maximum damping of the rubber phase in polystyrene-
            butadiene/styrene mixtures

Percent Rubber in Polyblend	Maximum Damping
0	0.04
10	0.12
26	0.28
40	0.58

the graft polymer. Wagner and Robeson[30] prepared two HIPS

containing 22% by volume of rubber particles, one was a blend

of polystyrene with 22% polybutadiene and 0.5% sulphur. The

other was a graft polymer containing 6% polybutadiene, the

remaining 16% by volume of rubber phase consisting of

polystyrene-sub-inclusions. The results are shown in Fig 1.10.

The peaks are similar but not identical in area and the loss

tangent maximum is approximately $10^{o}C$ higher in the graft

polymer than in the bulk.

Dynamic mechanical behaviour of ABS was reported[31] using the

Rheovibron, showing two remarkable transitions, one at $115^{o}C$

due to ST-AN copolymer and the other at about $-82^{o}C$ due to the

PBD. The decrease in modulus and the area of the loss peak are

both proportional to the volume fraction of the rubber particles,

which depend in turn upon the amount of rubber added initially

and upon the amount of grafting occurring during polymerisation.

Grafting tends in general to increase the volume fraction of

the rubber and to shift its glass transition to higher

temperatures but there is an important difference between the

two effects[20]: the volume fraction of the rubber depends on

the total weight of grafted chains, whereas the transition

temperature depends on the number of points at which these

chains are attached - a small number of long side-chains has

less effect on the mobility of a rubber molecule than a large

number of short ones. The model which was suggested by Turley[32]

to explain the behaviour of toughened polymers is that the

rubber particles acts as a two-component body having a core of PBD and a shell of graft rubber. A second model was suggested by Bucknall[33] that the HIPS is treated as a two-phase composite containing only polystyrene and PBD, with no distinct region of graft copolymer. The rubber particles are represented as random dispersions of polystyrene-sub-inclusions in a continuous PBD matrix. This model has the advantage of being based on electron microscope studies of morphology and is potentially of considerable value of predicting properties.

It is now generally accepted that a two-phase structure is necessary and a good adhesion between phases is pre-requisite to the dispersed phase toughening action. Good interfacial adhesion is usually achieved by grafting the glassy polymer to the rubber particles. To what extent and the way in which these have to be grafted in order to obtain the maximum toughening efficiency seems to be still one of the points requiring clarification. Ricco[89] has   reported   that the amplitude of the transition $(\tan\ )_{max}$ and the transition temperature decreases as the degree of grafting increases, in a series of ABS resins. Since the weight fraction of PBD was kept constant such a reduction of $(\tan\delta)_{max}$ was interpreted as due to a progressive immobilisation of the rubber particles at least on their outer shells when they are increasingly grafted.

1.4 General Mechanism of Oxidative Degradation of Polymers

In the degradation of a polymer, there is an induction period during which oxygen up-take is slight and build-up of various hydroperoxides is slow[34]. This induction period will vary in length depending on the chemical structure of the polymer, the presence of impurities, antioxidants and the temperature of oxidation. The induction period is followed by an autocatalytic stage in which hydroperoxides formed as the primary product of the oxidation, decompose to produce free radicals. This stage is usually regarded as the process responsible for further rapid oxidation. The following stages can be recognised during auto-oxidation of a polymer[35].

1   Initiation

$$ROOH \longrightarrow RO\cdot + \dot{O}H \tag{1}$$

$$2ROOH \longrightarrow RO\cdot + ROO\cdot + H_2O \tag{2}$$
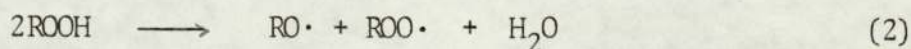
Cleavage of C-C (335 KJ/mole) or C-H (418 KJ/mole) bound in the initiation stage to produce $(R\cdot)$ alkyl radical is dependent on the substitution of the carbon atom[36].

Macromolecular hydroperoxides can decompose homolytically due to thermal energy, uv irradiation and catalysts such as transition metal ions[37]. As oxidation progresses, the bimolecular reaction (2) assumes greater importance.

2   Propagation

$$RO\cdot + RH \longrightarrow ROH + R\cdot \qquad (3)$$

$$ROO\cdot + RH \longrightarrow ROOH + R\cdot \qquad (4)$$

$$R\cdot + O_2 \xrightarrow{\text{fast}} ROO\cdot \xrightarrow{RH} ROOH + R\cdot \qquad (5)$$

$$\dot{O}H + RH \longrightarrow H_2O + R\cdot \qquad (6)$$

3   Termination

$$2R\cdot \longrightarrow R\text{--}R \qquad (7)$$

$$ROO\cdot + R\cdot \longrightarrow ROOR \qquad (8)$$

$$2ROO\cdot \longrightarrow \text{Non-radical products} + O_2 \qquad (9)$$
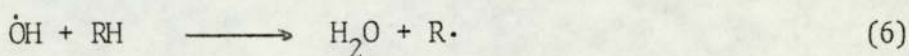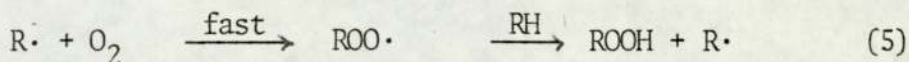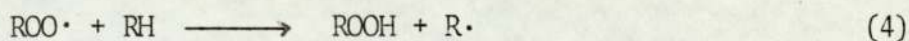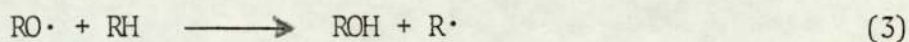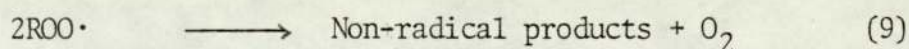
Reaction (9) is the only important one in the termination in
the absence of an effective antioxidant[35].

1.5 Oxidative Degradation of Rubber Toughened Plastics

Most rubber toughened plastics (HIPS, ABS) are based on PBD,
although other diene rubbers are used. Unsaturated rubbers are
not entirely satisfactory as toughening agents, as they are
easily oxidised, especially upon exposure to sunlight, with the
result that the toughened plastics become brittle.

The oxidation of rubber toughened polymers, such as HIPS[39]
and ABS[40-42] has been studied by several groups. They all
reported a decrease in the rubber component of the plastics.

22
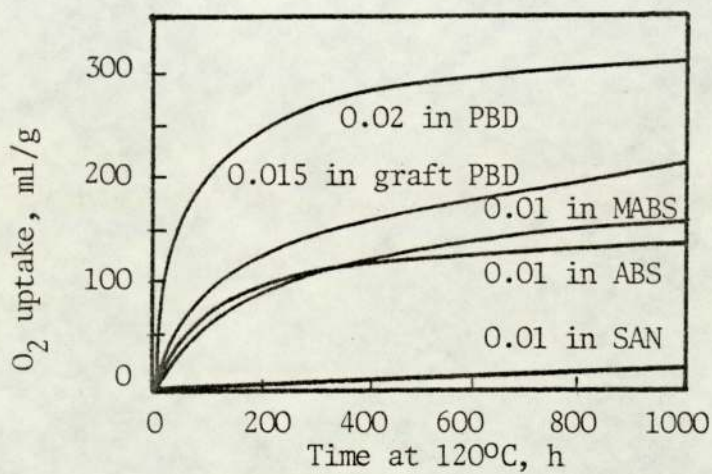
Fig 1.11   Oxygen uptake for PBD, grafted PBD, methacrylonitrile-
butadiene-styrene (MABS), ABS and SAN copolymer (ref 46)

The oxidation of individual constituents in ABS resin was reported[42] to confirm the vulnerability of the rubber component to oxidation (Fig 1.11).

Theoretically,'pure' PBD should not absorb light in the solar wavelength region, the fact that it does is evidence of the presence of absorbing impurities present on the surface and in the bulk of the polymer[46]. Such impurities are formed during the manufacture and/or as a result of high-temperature processing, and the two most important species invoked as photodegradable chromophores in polyolefin systems are carbonyl groups[43] and hydroperoxides[44,45]. Which of these is the most important is an unresolved question in polydienes systems such as PBD, but hydroperoxides have been championed as the major precursor[47]. Thermally produced hydroperoxide, however, was reported by A Scott[48] to be directly responsible for subsequent oxidative reactions in photo-oxidation of HIPS. It was also reported that photo-initiation by carbonyl compounds did not appear to be important under conditions encountered in industrial fabrication operations. The work to date concerning the oxidation of PBD has shown[48] that the two oxidation mechanisms possible (thermal and photo) lead to similar products, and that the mechanism may well be the same. The mechanism of oxidation of trans-1,4-polybutadiene will be discussed in Chapter 3.

1.6 Stabilisation of Polymers

Elastomers and other polymeric hydrocarbon systems are attacked
by oxygen even at room temperature and the reaction is
accelerated by heat, light and the presence of certain
metallic impurities which catalyse the decomposition of
peroxides to form free radicals. Consequently the addition of
an antioxidant is required to minimise oxidative degradation
during fabrication, storage and use. Four types of stabilisers
have been recognised, based on the mechanism of reaction[49]:

(1)   light stabilisers,

(2)   metal deactivators,

(3)   peroxide decomposers; preventive antioxidants, and

(4)   chain-breaking antioxidants.

1.6.a Stabilisation Against Photodegradation

Photostabilisation can be obtained in many ways[50,51]:

(1)   Screening of radiation, in this process the photostabilising
       activity consists of preventing the penetration of uv
       light into the material. Light screens include exterior
       coatings such as paints, protective films, that are
       excluded from within the polymer bulk, and additives,
       notably pigments, that are dispersed through the polymer.
       Carbon blacks which probably owe their efficiency as

25

light stabilisers for polymers to their ability to act
as inner filters for uv radiation and function as an
ultraviolet absorber through energy level transitions in
its polynuclear aromatic structure, and it was also
suggested[77] that carbon blacks act as free radical
scavengers which reduce the propagation of the initial
photo-chemical attack because many of the carbon blacks
contain stable free radicals. The chemical and physical
properties of carbon blacks are dependent upon the nature
of the oxygenated structure on their surface. All
commercial carbon blacks contain oxygen and oxidised
groups such as quinones, phenols, lactones and ether
groups.

(2) Ultraviolet absorbers function by absorbing and
dissipating uv radiation that would otherwise initiate
degradation of the polymer. The photo-physical
processes which an excited molecule A* can undergo fall
under three different categories:

$$A^* \xrightarrow{\text{emisssion}} Ao + h\nu$$

$$A^* \xrightarrow{\text{radiationless conversion}} Ao + heat$$

$$A^* + Bo \xrightarrow{\text{energy transfer}} Ao + B^*$$
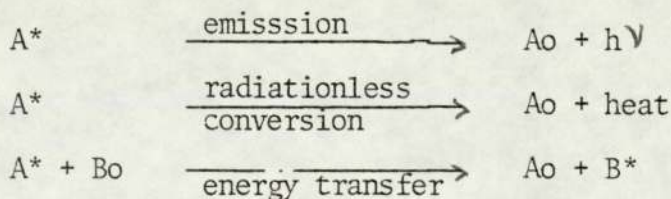
The deactivation of excited states can occur by any of
the photophysical processes outlined above. These are:
radiative processes such as fluorescence ($S_1 - S_o$) and

phosphorescence ($T_1 \longrightarrow S_o$), inter system crossing ($S_1 \leadsto T_1$), internal conversion ($S_1 \leadsto S_o$, $S_2 \leadsto S_1$) and quenching by energy transfer. Each of the above paths could conceivably function as a photostabilisation process. However, it is possible that the acceptor of this energy B* can undergo chemical reactions which is the case in photo-sensitised reactions.

(a)   Radiative processes in general involve the emission of light at longer wavelengths than those of the light absorbed. At first glance fluorescence would seem to offer an ideal mechanism for deactivation. However, it is conceivable that the emitted light would be reabsorbed by the polymer and degradation would occur. Fluorescent compounds are very effective photostabilisers but unfortunately the poor light and thermal stability of the majority results in a gradual decrease in their efficiency. However, one light stable fluorescent compound, 6,13-dichloro-3,10-diphenyl-triphenodioxazine, was found to be an excellent stabiliser for cellulose ester plastics[52] approaching carbon black in effectiveness.

(b)   Internal conversion is the process that converts electronic energy into vibrational energy by a radiationless route without a change in spin multiplicity ($S_1 \leadsto S_o$, $S_2 \leadsto S_1$). It is the major mechanism for photostabilisation in the

27

case of the o-hydroxybenzophenones (I), o-hydroxyphenyl benzotriazoles (II) and salicylates (III).

(I)   (II)   (III)
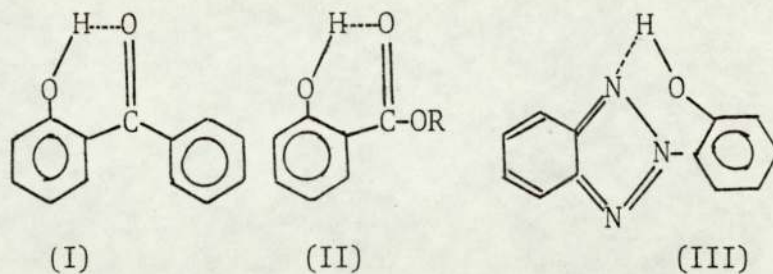
All these compounds have a common structural feature, the inter-molecular hydrogen bond. It is generally accepted that the presence of this structural grouping is responsible for the efficient deactivation of the electronically excited states of the uv absorber.

The photostabilising mechanism of o-hydroxybenzophenones is believed to be a rapid tautomerism of the excited states[53].
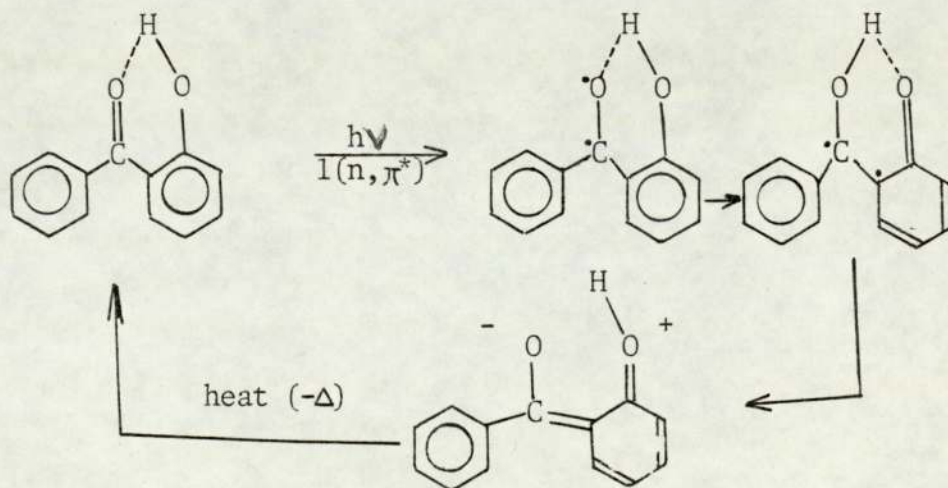
Therefore the rapid tautomerism in the excited state is facilitated by the strong intermolecular hydrogen bond.

Benzotriazoles like o-hydroxybenzophenones may form internal hydrogen bonds. Their photo-stabilisation mechanism is considered to be a rapid tautomerism of the excited states[54].
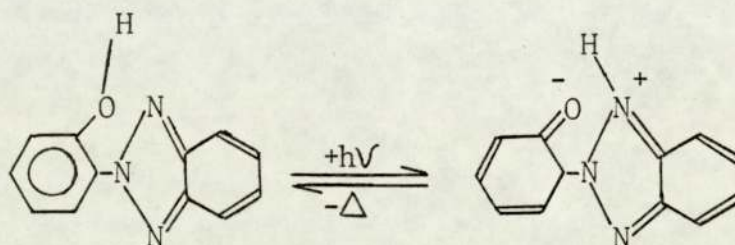
The distribution of a benzotriazole stabiliser (Tinuvin 328) in crystalline polypropylene has been investigated by uv microscopy[55]. The results obtained show that the stabiliser accumulates in the non-crystalline regions and between polypropylene spherulites and is rejected by crystalline regions. These observations are very important for understanding the photostabilisation mechanism of polymers.

1.6.b Stabilisation Against Thermal Degradation

The general mechanism of antioxidant action can be represented in the following sequence of reactions[49,50]:

29

$$\text{ROOH} + \text{AH} \longrightarrow \text{Non-radical products} \quad \begin{array}{l}\text{(peroxide decomposition)}\\\text{(preventive antioxidant)}\end{array}$$

Initiation:

$$\text{nROOH} \longrightarrow \text{RO}^{\cdot}, \text{RO}_2^{\cdot} \ \text{------}$$

$$\text{RH} + \text{O}_2 \longrightarrow \text{R}\cdot + \text{HO}_2 \quad (\text{O}_2 \text{ attack on hydrocarbon})$$

$$\text{AH} + \text{O}_2 \longrightarrow \text{A}\cdot + \text{HO}_2\cdot \quad (\text{O}_2 \text{ attack on antioxidant})$$

Propagation:

(same as uninhibited)

$$\text{RO}_2^{\cdot} + \text{RH} \longrightarrow \text{ROOH} + \text{R}\cdot$$

$$\text{R}^{\cdot} + \text{O}_2 \longrightarrow \text{RO}_2^{\cdot}$$

chain transfer
(with antioxidant)

$$\text{RO}_2^{\cdot} + \text{AH} \longrightarrow \text{ROOH} + \text{A}\cdot$$

$$\text{A}\cdot + \text{RH} \xrightarrow{\ 2\text{O}_2\ } \text{AO}_2\text{H} + \text{RO}_2^{\cdot}$$

Termination:

(by antioxidant)

$$\text{RO}_2^{\cdot} + \text{A}\cdot \longrightarrow \text{RO}_2\text{A}$$

$$2\text{A}\cdot \longrightarrow \text{A-A}$$

(as in uninhibited
autoxidation)

$$2\text{RO}_2^{\cdot} \longrightarrow \text{Non-radical products}$$

$$\text{R}\cdot + \text{RO}_2^{\cdot} \longrightarrow \text{RO}_2\text{R}$$

$$2\text{R}\cdot \longrightarrow \text{R-R}$$
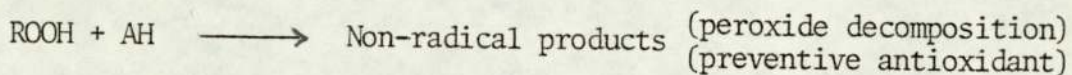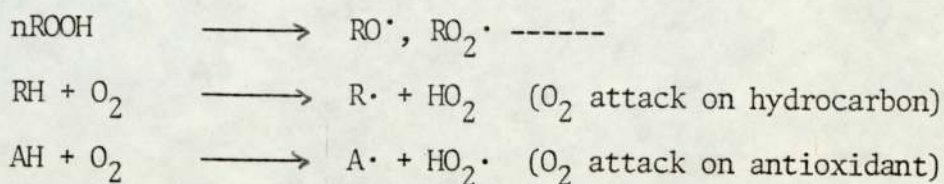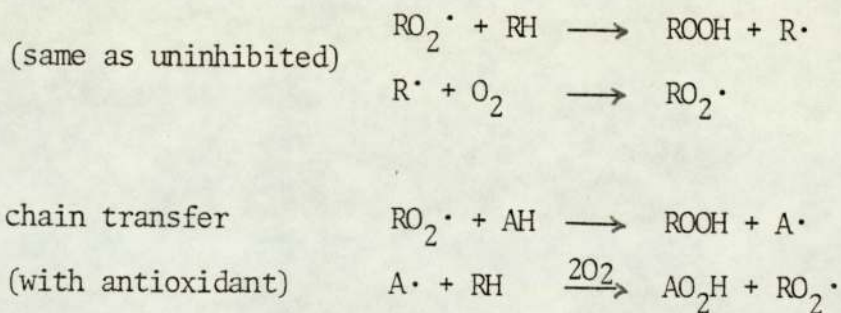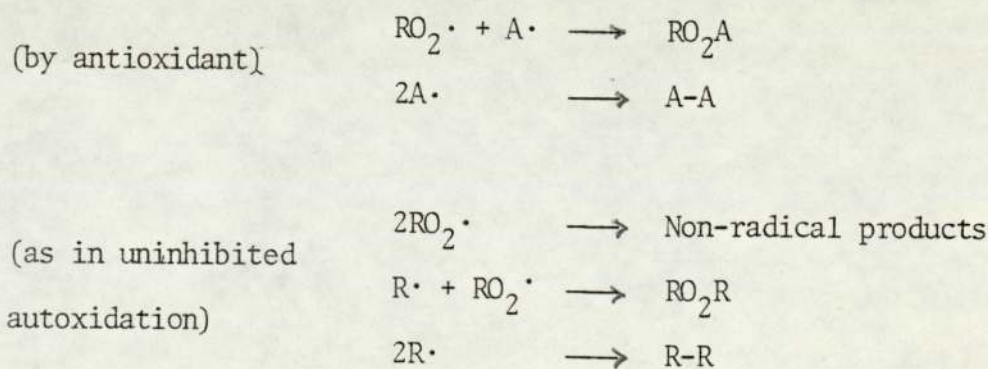
Antioxidants which retard the formation of free radicals in the
initiation step are referred to as preventive antioxidants.

30

Those which interrupt the propagation cycle by reaction with R· or RO_2· free radicals are called chain-breaking antioxidants. The preventive type thus slow the oxidation without changing the mechanism but the chain-breaking type introduces competing reactions so that the mechanism of retarded autoxidation becomes considerably more complex than the uninhibited reaction.

1.6.b.1 Preventive Antioxidants

Hydroperoxides are the principle source of free radicals for the initiation of autoxidation. The decomposition of hydroperoxides is accelerated by heat, light and metal ions capable of undergoing one-electron transfer reaction.

Any material which is capable of slowing the initiation process in some way may be classed as a preventive antioxidant. Stabilisers of this type include: (a) light absorbers, (b) metal deactivators and (c) peroxide decomposers (to non-radical products).

(a)   The function of light absorbers as preventive stabilisers is to reduce the catalytic effect of light upon peroxide decomposition.

(b)   The function of metal-ion deactivators as preventive antioxidants is to counteract the catalytic effect of the metal on hydroperoxide decomposition.

31

$$ROOH + M^{n+} \longrightarrow RO\cdot + M^{(n+1)+} + OH^-$$
$$ROOH + M^{(n+1)+} \longrightarrow RO_2\cdot + M^{n+} + H^+$$
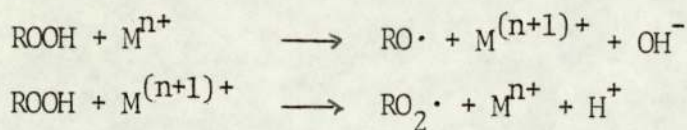
When the metal has two valence states of comparable stability, both reactions will occur and a trace amount of the metal can convert a large amount of hydroperoxide to free radicals.

The inhibition of metal-catalysed autoxidation may be achieved by strongly complexing the metal ion to its maximum co-ordination number or in some cases by stabilising one valence state at the expense of the other[56]. The effectiveness of various ligands as metal-ion deactivators depends in large measure upon the stability of the metal chelate formed. Since the ligand functions as a Lewis acid in the formation of the co-ordination complex, electron-releasing substituents would be expected to increase and electron-attracting substituents to decrease the stability.
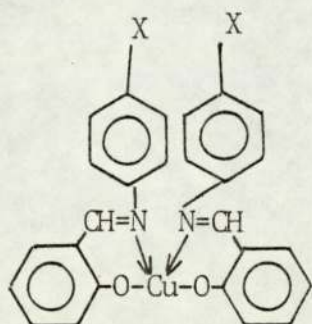
It appears that the metal ion must be co-ordinated to its

maximum in order to prevent complexing with hydroperoxide and the consequent electron-transfer reactions leading to the production of free radicals[57].

(c)   Peroxide decomposers. A variety of organic sulphur, nitrogen and phosphorus compounds are known to accelerate the decomposition of organic hydroperoxides without production of free radicals and thus function as preventive antioxidants. One of the important class of sulphur containing antioxidants is the group of metal complexes derived from dithiocarbamic (I) and dithiophosphoric (II) acids and related thiols such as mercaptobenzthiazole (III) and mercaptobenzimidazole (IV).
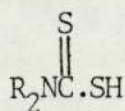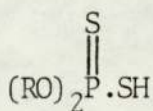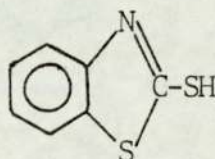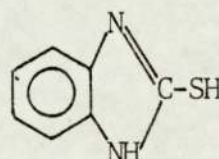
(I)   (II)   (III)   (IV)

It was reported by several reporters[58,59] that it is not the sulphides but rather certain of their oxidation products that function as the active inhibitors of autoxidation. The various possible oxygenated products of the active sulphides and disulphides were checked and it was found that the only active oxygenated products formed by reaction with hydroperoxides are the sulphoxides derived from monosulphides and thiosulphides formed from disulphides. Instability of the sulphoxide or

33

thiolsulphinates appears to be an important requirement for
activity as an inhibitor, and the formation of more reactive
species from further oxidation and decomposition reactions has
been suggested to account for the catalytic nature of the
overall reaction in which many moles of hydroperoxides are
decomposed per mole of sulphur compound.[59]

It was confirmed that the nickel complex (NiDBC), nickel-dibutyl-
dithiocarbamates, function as (i) hydroperoxide decomposer,
(ii) chain-stopper, (iii) and uv screener. Hydroperoxide
decomposition with NiDBC in uv light was investigated, it was
shown that the concentration of CHP reduced to zero by NiDBC
at $29^{\circ}C$ and the products formed were identical to those obtained
thermally at $60^{\circ}C$ indicating the same Lewis acid catalyst (SO_2
or SO_3) must be involved[60].

The formation of sulphur dioxide has been invoked to explain the
antioxidant activity of various sulphur containing antioxidants.
They include the transition metal dithiocarbamates[60-63], the
transition metal dithiophosphates[68], the metal complexes of
mercaptobenzothiazole[68], diaryldisulphides[62] and the
esters of thiodipropionic acid[63-64].

It was reported that the product formed from mercaptobenzthiazole
(MBT) and its zinc complex (XMBT) with hydroperoxides are much
more effective than either MBT or ZMBT. Although both function
as hydroperoxide decomposers, MBT is superior to ZMBT due to

34

the formation of benzthiazole sulphenic acid (BTSO) in addition to the formation of sulphur dioxide[65].

(BTSO)

(ZMBT)   (stable)
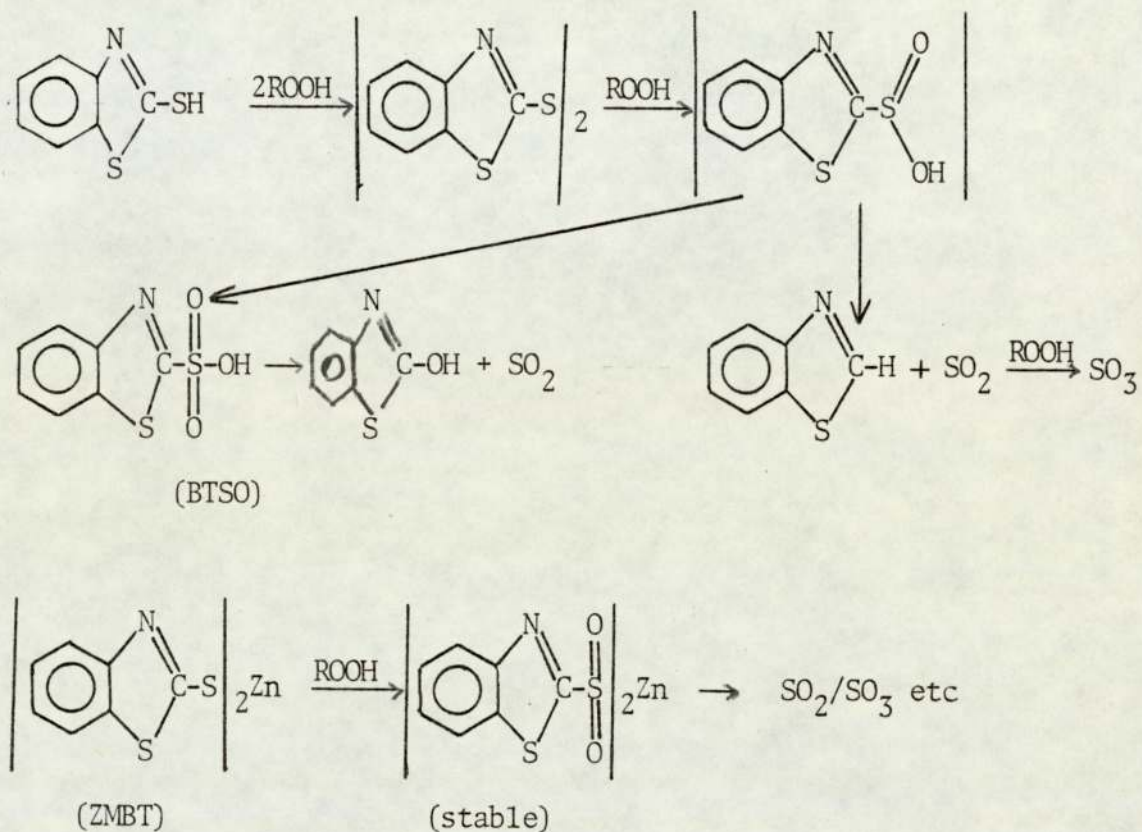
It was reported that the low molecular weight antioxidants with structure (I) in which R is the rubber chain are more reactive than an equimolar mixture of a simple hindered phenol (TBC,II) with the same antioxidant functional group and a non-phenolic sulphide (III)[60,67].
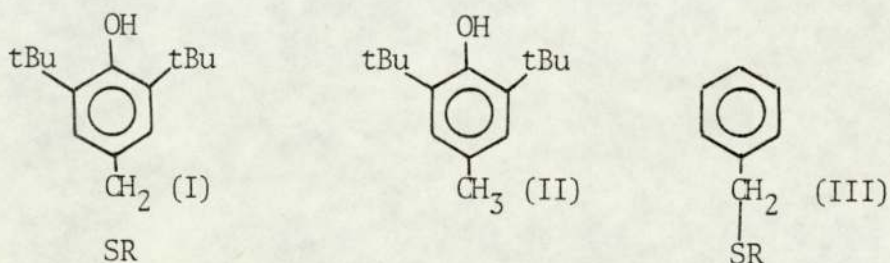
It was suggested that the effectiveness of (I) results from the presence of two antioxidant functions in the same molecule, acting as a hydroperoxide decomposer and chain-stopper, autosynergistic.

1.6.b.2 Chain-Breaking Antioxidants

Consideration of the free radical chain mechanism of autoxidation suggests the use of materials capable of reacting with either R$\cdot$ or RO$_2\cdot$ free radicals to interrupt the propagation cycle and thus retard the oxidation process. Since the concentration of R$\cdot$ is usually negligible compared to RO$_2\cdot$, most antioxidants of this type react with peroxy radical in two ways to terminate the kinetic chain: (a) free radical traps and (b) hydrogen donors.

(a)   Any substance capable of reacting with free radicals to form products that do not reinitiate the oxidation reaction could be considered to function as a free radical trap; such as quinones, many polynuclear hydrocarbons, carbon black and stable dialkyl nitroxyl radicals.

$$(CH_3)_3CNC(CH_3)_3 \quad \text{di-t-butyl nitroxide}$$
$$\overset{|}{O}\cdot$$

$$R'_2NO\cdot \;+\; R\cdot \;\longrightarrow\; R'_2NOR$$
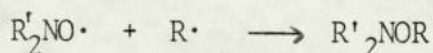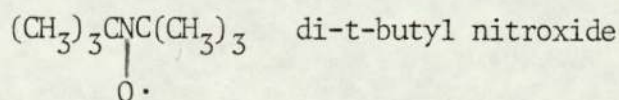
The above reaction must compete with O$_2$ for the R$\cdot$

36

radicals thus the rate of inhibited oxidation is proportional to the partial pressure of oxygen, and exclusively with R· and not RO_2· radicals. Diaryl nitroxyls are more stable than dialkyl nitroxyls and a radical such as 4,4'-dimethyoxydiphenyl nitroxyl reacts with both R· and RO_2·.

$$CH_3O-\langle\bigcirc\rangle-N-\langle\bigcirc\rangle-OCH_3$$
$$\overset{|}{\underset{\cdot}{O}}$$

$$ArO· + RO_2· \longrightarrow RO_2ArO$$
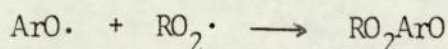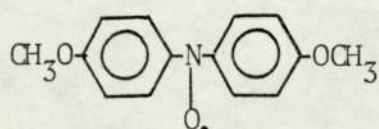
Similarly, the ArO· radicals produced from phenols by hydrogen transfer also function as free-radical traps and thus contribute half of the total antioxidant efficiency observed for the hindered phenols.

(b)   The presence of a reactive N-H or O-H functional group in the diaryl amine and hindered phenol types of antioxidants suggests that they compete with the polymer for the RO_2· radical and thus terminate a kinetic chain by transfer of hydrogen to form RO_2H. The antioxidant radical will then function as a radical trap and terminate a second kinetic chain.

$$RO_2· + \overset{(ArOH)}{AH} \longrightarrow RO_2H + A· (ArO·)$$
$$RO_2· + A· (ArO·) \longrightarrow RO_2A (RO_2ArO)$$

37
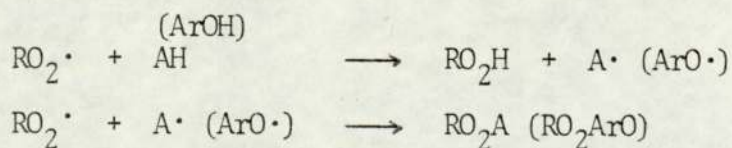
The relation of structure and antioxidant efficiency has been studied for a variety of phenolic antioxidants[56]. Electron releasing substituents (eg methyl, t-butyl and methoxy) markedly increase antioxidant activity, whereas electron withdrawing groups (eg nitro, carboxy and halogen) decrease it. α-branched ortho alkyl groups considerably increase antioxidant activity whereas such groups in the para position decrease activity. Steric protection of the OH group is essential to prevent too rapid consumption of the antioxidant by direct oxidation and to reduce the activity of the derived phenoxyl radical in chain transfer.

1.7 Synergism

When the combined effect of two stabilisers is better than that of either alone at the same concentration, the phenomenon is called synergism. In the opposite case, when the observed effect is weaker 'antagonism' between the components of the mixture is said to occur. Two mechanistically distinct types of synergism have been recognised[56]: homosynergism involving two compounds of unequal activity but operating by the same mechanism and heterosynergism, arising from the co-operative effect of two or more antioxidants acting by different mechanisms. In the latter category, would be combinations of chain-breaking antioxidants with preventive antioxidants of various types. In the case of a combination of two different chain-breaking antioxidants that function by donation of

hydrogen to a peroxy radical, the most likely mechanism would involve transfer of hydrogen from one inhibitor molecule to the radical formed in the reaction of the other inhibitor with a peroxy radical.
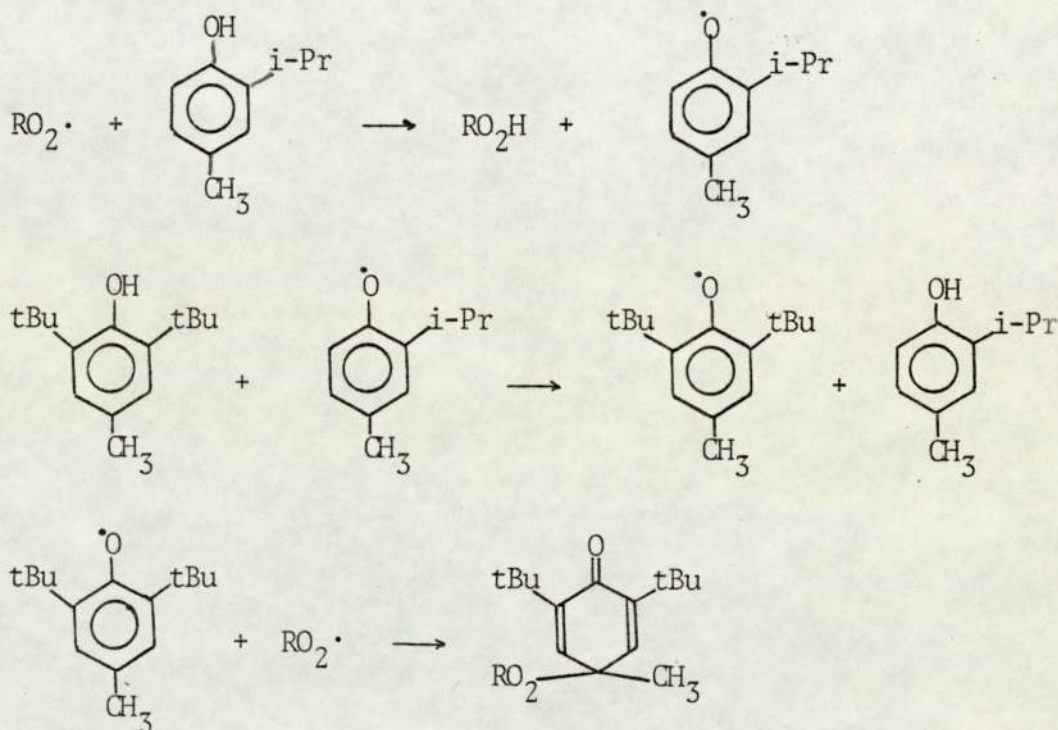
The advantages of such combinations as two phenolic inhibitors differing in the degree of hindrance by bulky ortho substituents or two amine type antioxidants differing in structure and reactivity, or a combination of a secondary diaryl amine with a hindered phenol, is that the more reactive inhibitor will efficiently scavenge any oxy or peroxy radicals formed in the system and yet will not be depleted, since the less efficient hydrogen donor can still serve as a reservoir of hydrogen for regeneration of the more effective chain-breaking antioxidant.

39

The following reactions illustrate regenration of the oxidised
forms by hydrogen transfer from the phosphate ester:

$$RO_2\cdot \;+\; \text{(phenol)} \longrightarrow R'O_2H \;+\; \text{(phenoxy radical)}$$

$$\text{(phenoxy radical)} \;+\; H\text{-}\overset{O}{P}(OR)_2 \longrightarrow \text{(phenol)} \;+\; \cdot\overset{O}{P}(OR)_2$$

$$2\,\text{(quinone)} \;+\; H\text{-}\overset{O}{P}(OR'')_2 \longrightarrow \text{(phenol)} \;+\; \text{(O-}\overset{O}{P}(OR'')_2\text{)}$$
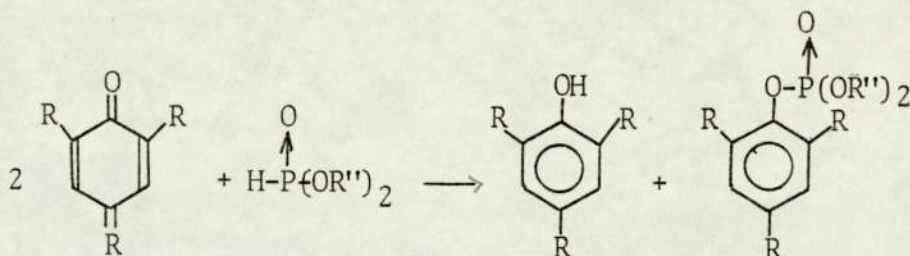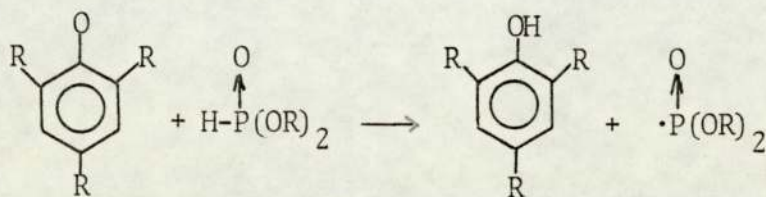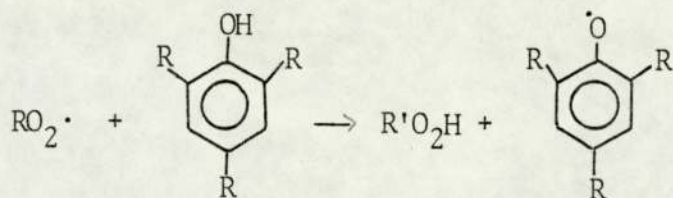
It would appear that a combination of three or more stabilisers
such as uv absorpber, metal deactivator and a peroxide decomposer
give tremendous synergistic effects to a polymer which contains
metal impurities and subject to both photodegradation and
thermal degradation. Autosynergism is probably involved in the
observed effectiveness of certain stabilisers that appear to
have two kinds of antioxidant activity in the same molecule[56-66,67].
Carbon black is also an example of a multifunctional inhibitor
showing evidence of reactivity as a free radical trap and
hydrogen donor, light screen and its interaction with iron and
other metal ions[68].

40

Combination of 2-hydroxybenzophenones as uv absorbers with either chain-breaking antioxidants or peroxide decomposers have been reported to give synergistic effects in PE during photodegradation[56]. Studies of combinations of peroxide decomposers and antioxidants breaking free radical chains show that the optimum ratio of the compounds is different for each combination examined under standard conditions[69].

A strong synergistic effect has been observed in the case of mixtures of uv photostabilisers and organic phosphites, for example, trisnonylphenyl phosphite in combination with different photostabilisers, octylphenylsalicylate and 2-hydroxy-4-n-octoxybenzophenone.

The Object of the Present Work

It is well known that the polybutadiene (PBD) moiety in ABS polymer accelerates its degradation and behaves as a photo-pro- oxidant for SAN copolymer. Photo-oxidation of polybutadiene- modified plastics (HIPS, ABS) leads to cross-linking of the rubber phase accompanied by scission of the graft between rubber and matrix with consequent rapid loss of impact strength[78] and decrease in the height of the loss peak[39].

A primary object of the present study is to study photo and thermal degradation of unstabilised ABS using a variety of techniques to find correlations between impact strength and the height of the loss peak (tanδ) and to correlate these two properties and the unsaturation of polybutadiene. Stabilisers containing thiol group (BHBM, EBHPT) were bound to ABS in latex and their stabilities were studied during photo and thermal degradation using infra-red to measure functional groups[75]. A second object is to bind the above named stabilisers to ABS by latex and powder masterbatch techniques (by processing in a torque rheometer) in order to study the effect of bound stabilisers and their synergistic mixture on the physical and mechanical properties of ABS during photo and thermal degradation.

CHAPTER TWO

EXPERIMENTAL

2.1 Materials

The ABS latex, unstabilised, was supplied by Borg-Warner
Corporation, Holland, as a special experimental grade. It
containing thirty-three parts dry ABS per one-hundred parts
of latex and was claimed to be non-stabilised.

A commercial grade of stabilised ABS (lustrain ABS) polymer was
supplied by Monsanto Corporation.

Chemicals (eg 2,4-dihydroxybenzophenone, ethylene chlorohydrin,
thioglycollic acid, 2,6-di-tert-butyl phenol, tert-butyl alcohol,
epichlorohydrin) for preparation stabilisers were obtained from
Aldrich and Fison Chemicals Limited.

2.2 Sample Preparation

2.2.1 Torque Rheometer

A full charge of 33 g of powder (coagulated ABS latex) and 35 g
of commercial ABS was used in the chamber exposed to air (ram
withdrawn) of the variable RAPRA torque rheometer[39.]. The
samples were processed in a closed chamber (ram down) for 3 mins

at 190°C, at high shear rate (72 rpm). The hot melt was chilled
in water on removal from the rheometer to avoid uncontrolled
thermal oxidation.

2.2.2 Compression Moulding

The appropriate weight (0.5 g) of processed polymer (in a torque
rheometer) was compression moulded between two polished steel
plates at 190°C for 3 mins (1½ mins pre-heating time) to obtain
films of desired thickness (0.075 - 0.1 mm).

2.3 Extrusion

Continuous film was extruded using an 18 mm Betol (Betol
Machinery Limited, Luton, Bedfordshire). A commercial grade of
stabilised ABS (Monsanto) was extruded. Fixed temperature
settings were used throughout all operations. These were as
follows: barrel zone 3 at 220°C, barrel zone 2 at 180°C, barrel
zone 1 at 160°C, die zones 1 and 2 at 220°C. A 10°C temperature
gradient was used on the take-off rollers. The top roller was
set at 60°C and the bottom at 40°C. Take-off speed was fixed
at 2.3 m min^{-1} (7.5 ft/min) and screw speed (approximately 20
rpm) was adjusted to produce various thicknesses of extrudate
ranging from 0.06 to 0.1 mm. The above conditions are
similar to the processing conditions for HIPS[39].

44

2.4 Coagulation and Drying of ABS Latex

Coagulant was made from Borg-Warner ABS latex by adding 1.5 parts of concentrated H_2SO_4 for every 100 parts of ABS, to 500 ml of distilled water. The temperature of the distilled water was raised to $65^{\circ}C$ and ABS latex was added slowly with stirring to give crumbs of coagulum.

The solution was cooled by adding water, then filtered and washed several times with distilled water to free it from excess acid. The crumb was dried in a vacuum oven at $55^{\circ}C$ to a constant weight.

2.5 Solution Casting

Films were cast from solution of polymer in dichloromethane in a vacuum desiccator. Seven pounds of mercury was poured into the well of the desiccator and the polymer solution was poured slowly onto the surface of the mercury avoiding the formation of bubbles. The vacuum was produced by a water jet vacuum line and sealed for up to 3 hours at the end of which the vacuum was reapplied to remove the vapour of the solvent. When all the solvent vapour had been removed from the desiccator and the film was completely dry, it could be easily separated from the surface of the mercury.

2.6 Ultraviolet Exposure Cabinet

Uv irradiation of the samples was carried out in a uv cabinet which comprised a metal cylinder of about 110 cm in outer diameter and having a concentric circular rotating sample drum whose circumference was 15 cm from the periphery of the metal cylinder. Thirty-two tube lamps were mounted on the inside of the cylinder (see below). The rotating arrangement of the samples allows an identical amount of total radiation to fall on every sample. The cylindrical cabinet was opened to the atmosphere on both the lower and upper sides and the circulation of air in the cabinet was ensured by the driven ventilator situated under the rotating frame. The samples were attached separately to cardboard 'window frames' and arranged vertically on a rotary wheel so as to face the lamps all the time. The radiation source consisted of a cylindrical array of 20 watt lamps mounted inside on the wall of the cabinet. 24 lamps, type C (Phillips Actinic blue OS) and 8 lamps, type Al (Westinghouse Sunlamps FS20) were used and these were symmetrically distributed so that the combination was one lamp type Al for every 3 lamps of type C. The spectral distribution of both types of lamps used is shown in Figs 2.1 and 2.2 for the lamp Al and lamp C respectively. The maximum in the relative intensity of the lamp Al is at 317 nm and of the lamp C, 374 nm. The available wavelength distribution with the above combination of lamps was between 290 nm and 500 nm and the radiation intensity Io at the sample surface was I_o=44.3 W/m^2.

46
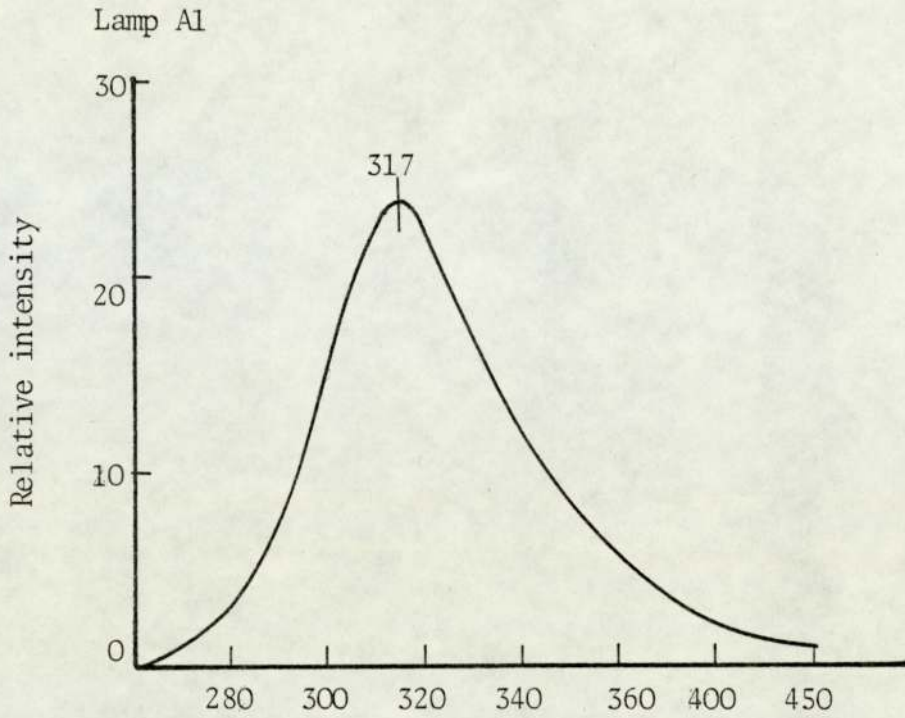
Fig 2.1   Spectral distribution of fluorescent lamp type A1
          (Westinghouse sunlamp FS20)
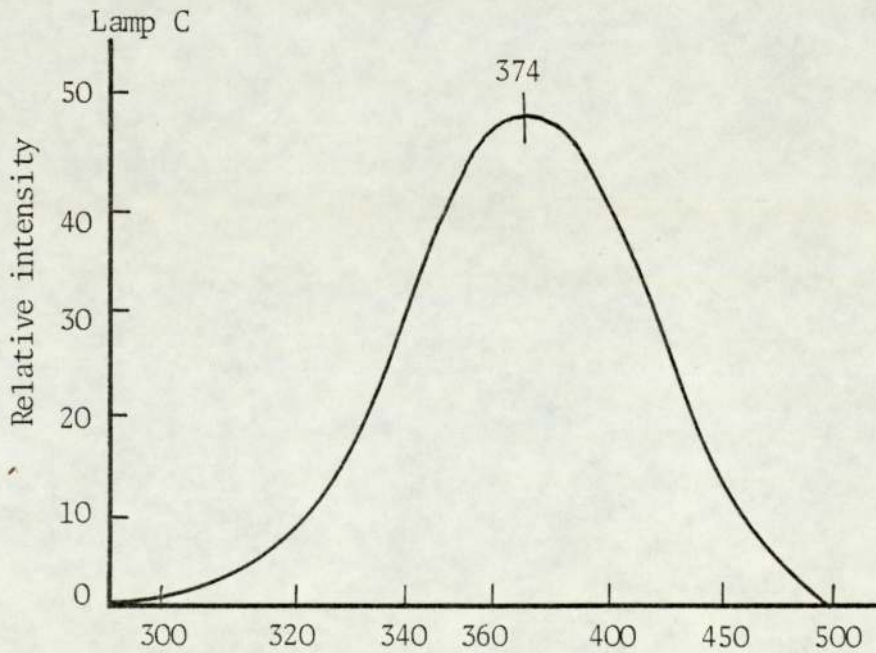
Fig 2.2   Spectral distribution of fluorescent lamp C (Phillips
          Actinic Blue 05)

47

The tubes were replaced in rotation every 2000 hours of exposure.

2.7 Oven Ageing

Films of ABS polymer mounted on cardboard 'window frames' were
suspended in the cavities of a Wallace oven about 10 inches from
the top. These samples were aged in air at 100oC flowing at
½ cu ft per hour. The oxidation degradation was measured by
measuring functional groups by ir, physical and mechanical
properties.

2.8 Calculation of Absorbance of Functional Groups

To minimise errors due to variation in film thickness as well
as errors due to the instrument, a characteristic absorption
peak at 2220 cm^{-1} related to the absorption of C≡N group was
used as reference. This peak remained constant during
irradiation. The growth or decay of observed absorption peaks
(for functional groups) were expressed as indices which were
defined as the ratio of the absorbance of functional group
peaks to that of the reference peak.

$$\text{Index} \ = \ \frac{\text{Absorbance of the functional group}}{\text{Absorbance of reference peak}}$$

The base line technique[71] was used to calculate the absorbance
due to various functional groups. This was done as shown in
Fig 2.3 by drawing a straight line (base line) tangential to

48

Fig 2.3

49
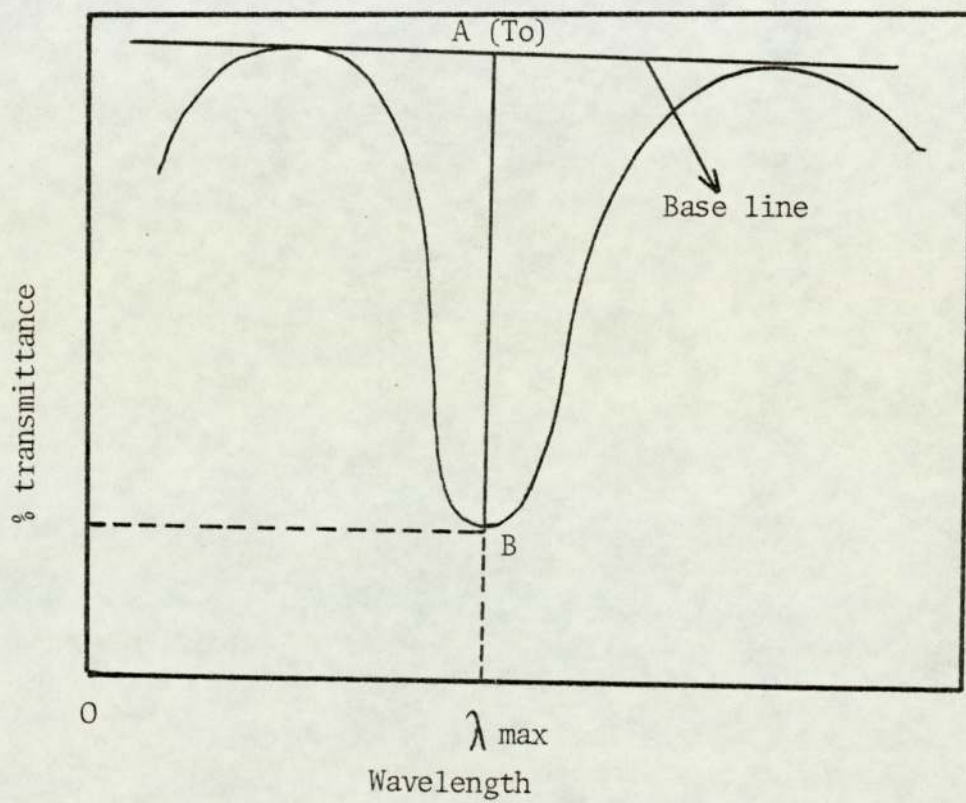
adjacent absorption maxima or shoulders, then erecting a
perpendicular through the analytical wavelength until it
intersects the base line. At 'A' the concentration of the
functional group to be determined is zero and at 'B' there
appears an absorption peak whose height serves to calculate the
concentration. Before putting the sample in, the spectrophoto-
meter was adjusted to read 100% transmission.

2.9 Measurement of Carbonyl, Hydroxyl and 1,4-trans-PBD Absorbances by Infrared Spectroscopy

Infra-red samples were cut and mounted on cardboard with a
'window hole' at the exact position of interception of the ir
beam.

Samples of almost equal thickness were chosen for exposure. The
thickness of the samples ranged from 0.075 to 0.1 mm. Studies
were made by using Perkin Elmer Model 457 Infra-red
spectrometer. Selected peaks were recorded on continuous chart
paper and the peak at 2220 cm^{-1} corresponding to the absorption
of C≡N group was used as the reference. The indices were
defined as the ratio of the absorbance of growing or decaying
peak to that of the reference. Transmittance was converted to
absorbance using a standard table for rapid quantitative
analysis.

50

2.10 Measurement of Impact Strength

The polymer films were cut into thin strips (about 1.5 cm wide) and mounted on cardboard for exposure in the uv cabinet and also for oven ageing. Samples of exactly equal thickness were chosen for replicate impact studies but the thickness of the samples at other exposure times varied between 0.075 and 0.1 mm. The impact strength of the films was measured before and during photo and thermal degradation by means of a small falling weight impact tester. This apparatus enables the measurement of impact tests to be carried out on very small specimens.

This apparatus consisted of a metallic tube (A) fixed to a square steel block (B); this block can be fitted onto another square steel block (C) by means of two pins (D and E). In the middle of (C) there is a round hole on which the film is mounted. The sample is clamped between (B) and (C) before testing. A slit was drilled along the length of the metallic tube and a ruler attached alongside the tube to enable measurement of heights. A pin was moved along the slit to the height required and the weight was introduced into the tube so that it settled on the pin. Then the pin was withdrawn in a quick movement giving free way to the dart-like weight to fall onto the sample. If an adquate weight and height are used, the dart perforated the sample, penetrating into the block (C).

About 20 measurements of the impact strength were made for every
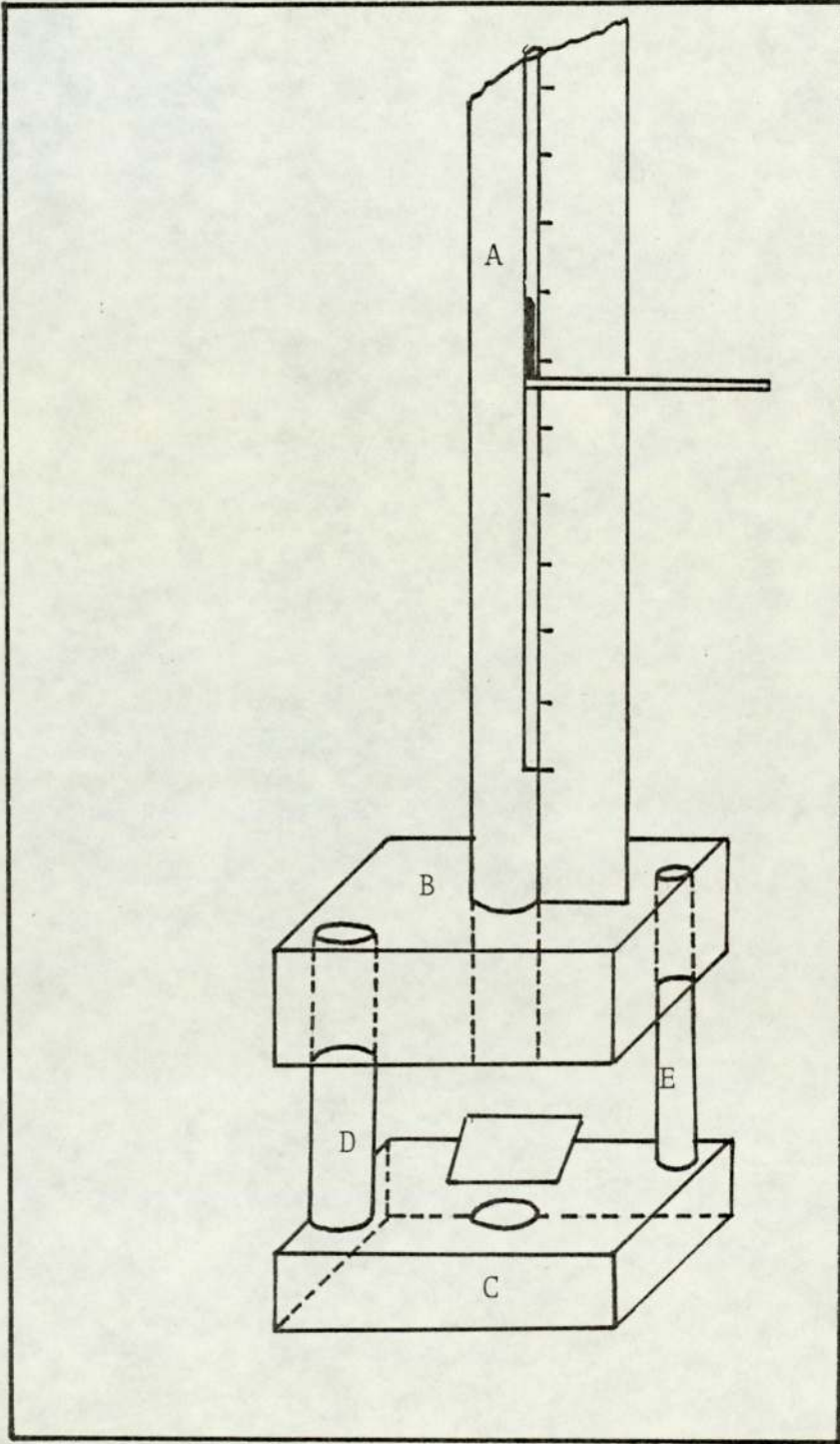
Fig 2.4 Experimental film impact tester

period of degradation. The impact strength of a film was taken as the enrgy required to break the film per unit thickness. Hence the impact strength was calculated in erg/mm.

$$E = \frac{m \times g \times h}{\text{thickness (t)}}$$

where: m = mass of the falling weight (g)

g = 981 cm/sec^2

h = height of the falling weight (cm)

t = thickness of the film (mm)

2.11 Measurement of Dynamic Mechanical Properties

2.11.a Procedure

The Rheovibron model DDVII, Toyo Measuring Instruments Company Limited, (TMI), Tokyo[70], was used at ambient temperature and over a temperature range from -120 up to 0°C. All measurements were made at a frequency of 110 hertz (Hz). Specimens (3 mm x 60 mm) were stamped out using a steel cutter from either compression moulded or extruded film (along the direction of extrusion). The sample chamber was cooled to -120°C fairly quickly, maintaining constant tension in the sample to prevent 'kinking' or fracture. After reaching equilibrium the liquid nitrogen was allowed to boil off and readings were taken as the chamber slowly returned to ambient temperature; the air flow being adjusted as required. For good temperature control, the
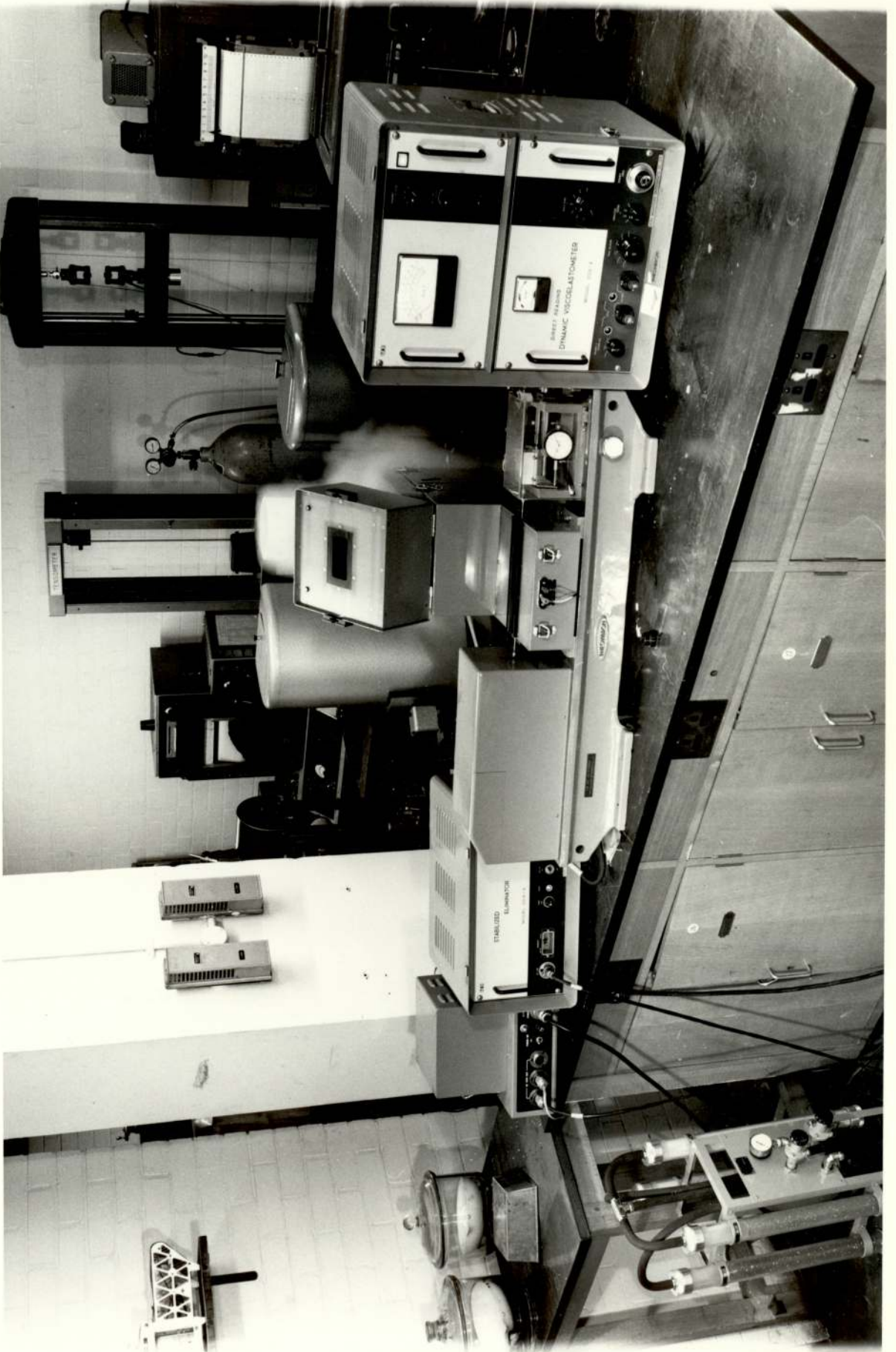
air must be dry and for this purpose it must be passed through the columns containing silica gel and molecular sieves and they must be dried before each measurement.

Readings can also be taken during the cooling operation, but the former method (while the chamber slowly returns to ambient temperature) was found[39] to give more accurate results owing to better temperature control.

The rheovibron istrument was calibrated before each measurement.

2.11.b   Theory and Derivation of Basic Dynamic Equations

The purpose of using the rheovibron is to measure the temperature dependence of the complex modulus and mechanical damping of high polymers at a definite frequency.

Modulus of elasticity is a measure of stress accompanying a unit deformation and for material obeying Hook's law it is the ratio of stress to strain. It also provides a measure of recoverable potential energy. However, not all materials follow Hook's law ideally and the energy utilised in deforming a body is not fully recoverable, a part is always lost as heat. The extent of this energy dissipation, however, varies from material to material.

Mechanical damping is a measure of loss of energy as heat and

is defined by the ratio of the energy dissipated as heat to the energy stored as potential energy. The mechanical damping can be calculated as logarithmic decrement (Δ) which is the logarithmic ratio of amplitudes of two successive damped oscillations (Fig 2.5).

High polymers are the best known examples of the class of material known as viscoelastic having characteristics of both viscous liquids and elastic springs. If a stress is suddenly applied to a polymeric material the resulting strain reaches some value immediately and then decays or relaxes over a period of time.

The sinusoidal experiments involving viscoelastic materials appears to show two stress components, one in phase with the applied strain ($6'$), or parallel to the direction of strain (Fig 2.6) and the other out of phase with the applied strain ($6''$) or perpendicular to the direction of the strain.

The magnitude of the two stresses is given by:

$$6' = E' \times strain \qquad (2.1)$$
$$6'' = E'' \times strain \qquad (2.2)$$

Where: E' and E'' are real and imaginary parts of the complex modulus defined as $E^* = E' + iE''$.

55

$$\triangle = \text{Ln} \ \frac{A1}{A2} \ = \ \text{Ln} \ \frac{A3}{A1}$$

A1 A2 A3 A4

P
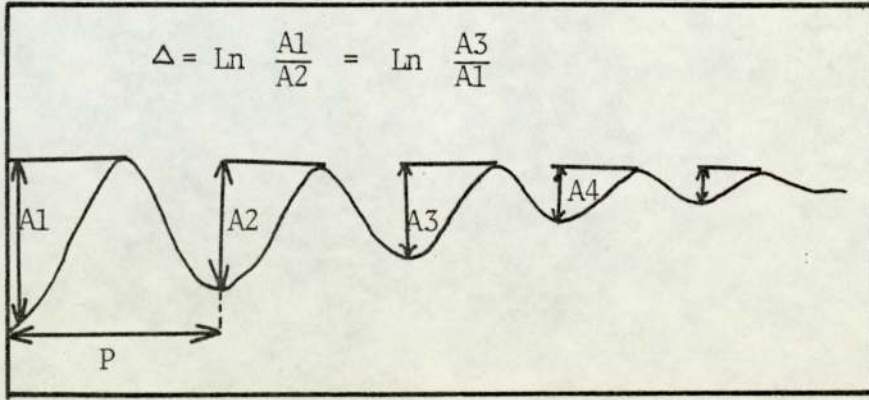
Fig 2.5 Schematic representation of typical damped oscillation curve

$E^* = E' + iE''$

a1

a1-a2

$\sigma^=$

δ

a2

σ'
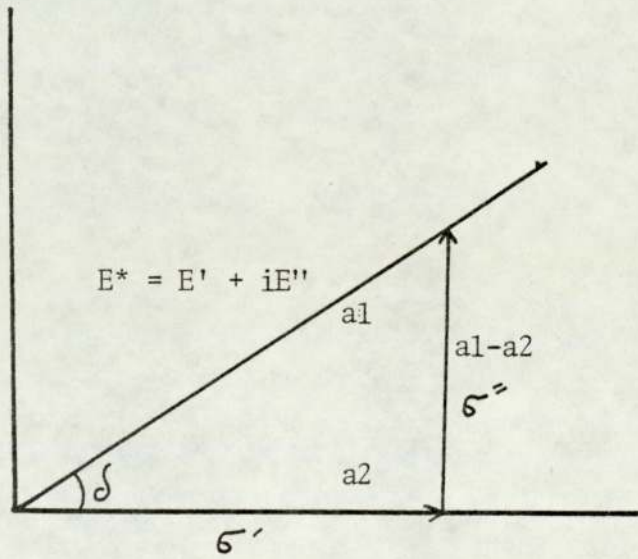
Fig 2.6 Vector diagram

The quantities of E' and E'' are also called storage and loss modulus respectively. The former is related to the stored and recoverable energy and the latter is related to the damping terms which determines the dissipation of energy into heat when the material is deformed.

The equation $E^* = E' + iE''$ can also be expressed in terms of the absolute value of complex modulus of elasticity $\left| E^* \right|$ and phase angle δ between the stress and strain.

$$E^* = E' + iE'' = \frac{\sigma \max}{\varepsilon \max} \tag{2.3}$$

$$\text{where: } E' = \frac{\sigma'}{\varepsilon_0} = \frac{\sigma_0}{\varepsilon_0} \cos \delta = E^* \cos \delta \tag{2.4}$$

$$E'' = \frac{\sigma''}{\varepsilon_0} = \frac{\sigma_0}{\varepsilon_0} \sin \delta = E^* \sin \delta \tag{2.5}$$

The ratio of out-phase modulus to in-phase modulus,

$$\frac{E''}{E'} = \frac{E^* \sin \delta}{E^* \cos \delta}$$

The ratio of E''/E' is called loss tangent, loss factor, dissipation factor or mechanical damping.

$$\frac{E''}{E'} = \tan \delta \tag{2.6}$$

Therefore the mechanical dissipation factor is proportional to the ratio of the energy loss to the energy stored during a cycle

of deformation.

2.11.c Principles involved in the Rheovibron

Both ends of the sample are fixed to transducers, one of which
is a transducer of displacement, ΔL, (Model T-7) and the other
of which is a transducer of generated force, ΔF, (Model T-1).
The specimen is deformed sinusoidally with the help of the
driving device and the sinusoidal stress which is generated at
the other end of the specimen is out of phase with the applied
strain and differing by a phase angle, $\tan \delta$.

To obtain the angle, δ, both the magnitude of the oscillating
displacement, ΔL, and oscillatory force, ΔF, are transformed
into electrical out-put by strain (T-7) and stress (T-1) gauges
respectively specified for strain and stress detection[72,73].

The output voltages of T-1 (stress transducer) and T-7 (strain
transducer) are indicated by vectors $\left| a_1 \right|$ and $\left| a_2 \right|$ respectively,
are adjusted to unity, $\left| a_1 \right| = \left| a_2 \right| = 1$ by attaining full scale
deflection, vector substraction is made by changing the output
circuits of the two gauges. This enables the value of tan
to be read directly from the meter. After the condition of
$\left| a_1 \right| = \left| a_2 \right| = 1$ is satisfied, $\tan \delta$ is given by the equation
(2.7) which it $(\tan \delta)$ can be read directly from the meter.

$$\left| a_1 - a_2 \right| = \sqrt{a^2 + a_2^2 = 2a_1 a_2 \cos \delta}$$

$$= \sqrt{2-2\ \cos\delta}$$
$$= \sqrt{2(1-\cos\delta)}$$
$$= \ 4\ \sin^2 \delta/2$$
$$= 2\ \sin \delta/2$$
$$= \tan \delta \quad (\delta\ \text{being very small}) \tag{2.7}$$

The complex modulus embracing both viscous and elastic components can be calculated from the following equations:

$$\left| E^* \right| = \frac{\sigma\ \text{max}}{\varepsilon\ \text{max}} = \frac{\dfrac{\Delta F}{S}}{\dfrac{\Delta L}{L}} = \frac{\text{force}}{\text{area}} \Big/ \frac{\text{length}}{\text{elongation}} = \frac{\Delta F}{S} \cdot \frac{L}{\Delta L}$$

$$\tag{2.8}$$

where: ΔF = oscillating load or amplitude of tensile force

S = cross-section of sample (cm^2)

L = length of the sample

ΔL = oscillating displacement of the sample of amplitude of elongation

If the supply and output voltages of the transducers T-1 and T-7 are E_1, E_2 and C_1, C_2 respectively, then the relation of ΔF and ΔL can be calculated as follows:

$$\Delta F = \frac{C_1}{E_1 f_1} \quad , \quad \Delta L = \frac{C_2}{E_2 f_2}$$

where f_1 and f_2 are the calibration factors of the transducers T-1 and T-7 respectively.

$$V_F = F_{FO} \cos (wt + \delta)$$

$$V_X = V_{XO} \cos wt$$
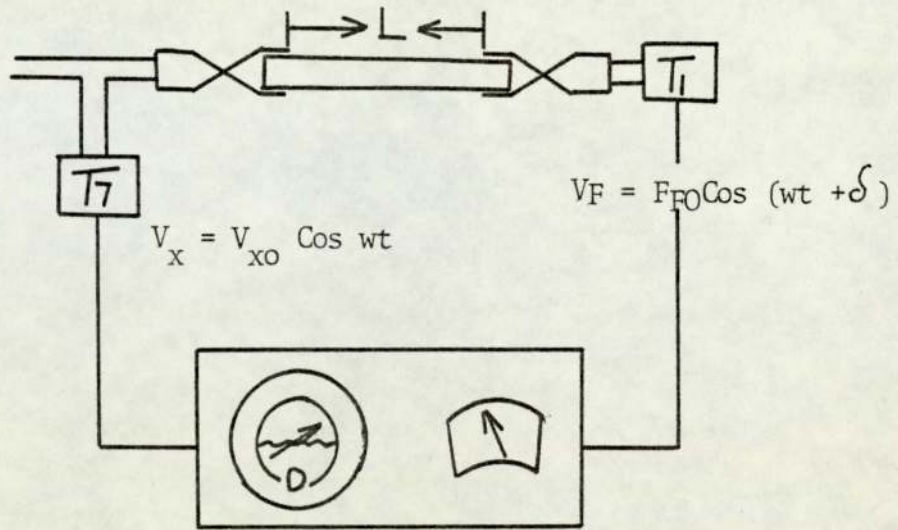
Fig 2.7 Schematic representation of the Rheovibron DDV-II dynamic tensile tester
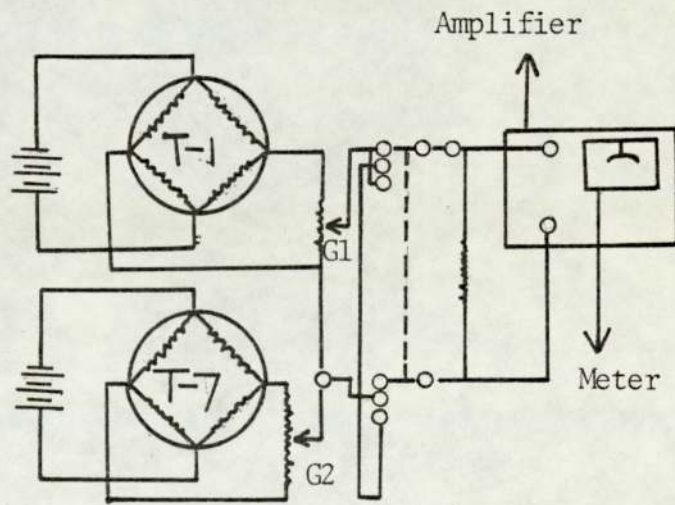
Fig 2.8 General concept of Rheovibron

60

Putting these values in the equation (2.8),

$$\left| E^* \right| = \frac{C_1}{C_2} \cdot \frac{L}{S} \cdot \frac{f_2}{f_1} \cdot \frac{E_2}{E_1} \qquad (2.9)$$

By adjusting the dividers G_1 and G_2, condition $\frac{C_1}{C_2} = \frac{G_2}{G_1}$ is set, since the products of $C_1 G_1 = C_2 G_2$ are made equal at the time of measuring $\tan \delta$ ($\left| a_1 \right| = \left| a_2 \right| = 1$).

Replacing these values in the equation (2.9),

$$\left| E^* \right| = \frac{f_2}{f_1} \cdot \frac{L}{S} \cdot \frac{E_2}{E_1} \cdot \frac{G_2}{G_1} \qquad (2.10)$$

Now $\frac{L f_2}{f_1 S}$ is constant for the sample and transducer used and E_2/E_1 is previously calibrated. Therefore $\left| E^* \right|$ is only dependent on the reading of G_1 and G_2.

Calculation of oscillating load, ΔF

This is obtained from the following equation:

$$F = 10^4 \text{ dynes} \cdot \frac{10^3}{D} \cdot N$$

where: 10^4 dynes = calibration value of T-1 gauge ($\simeq 10$ grm)

D = value of the dynamic force dial at the time of measuring $\tan \delta$

N = the value of the $\tan \delta$ range at the time of measuring $\tan \delta$ and obtained from Table 2.1

61

Table 2.1

Tan δ range or amplitude factor	N or A
0 db	31.6
10	10.0
20	3.16
30	1.0
40	0.316
50	0.1
60	0.0316

<u>Calculation of Oscillating Displacement, $\triangle L$</u>

$$\triangle L = 5 \times 10^{-3} \text{ AN cm}$$

where: 5×10^{-3} cm = calibration value of T-7 gauge

A = the value of the amplitude factor when

measuring tan δ and obtained from Table 2.1

Putting the above values of $\triangle F$ and $\triangle L$ in the equation of complex modulus equation (2.8),

$$\left| E^* \right| = 2 \times \frac{1}{AD} \times \frac{L}{S} \times 10^9 \text{ dynes/cm}^2 \qquad (2.11)$$

Since during the displacement of the sample, there is also a slight displacement in the chuck rod and T-1 rod which give an error in the final L values. To eliminate this, an error constant 'K' is included in the above equation and the final equation of complex modulus of elasticity takes the form,

$$\left| E^* \right| = 2 \times \frac{1}{A(D-K)} \times \frac{L}{S} \times 10^9 \text{ dynes cm}^{-2} \qquad (2.12)$$

where: L = sample length (cm)

S = cross-sectional area (cm^2)

A = value corresponding to amplitude factor selected

(usually A was equal to 1.0)

D = dynamic force reading on dial

K = error factor

2.12   Chemical Synthesis 4-Benzoyl-3-hydroxyphenyl-0-ethyl thioglycollate

The following two stage process was used in the synthesis of this compound[75]:
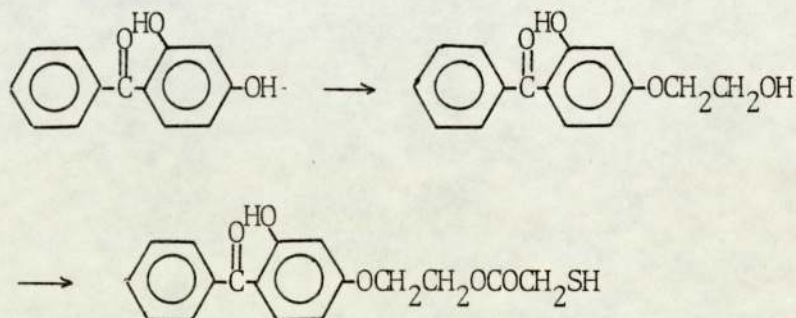
2.12.a   2-Hydroxy-4(β-hydroxy-ethoxy)benzophenone

21.4 g (0.1 M) of 2,4-dihydroxybenzophenone and 0.4 g (0.1 M) of sodium hydroxide were dissolved in 125 ml of distilled water, 8.1 g (0.1 M) of ethylene chlorohydrin were added all at once to the above solution and the mixture was stirred at 90-95°C for 4 hours and then 125 ml of distilled water at 95°C was added to it. The solution was allowed to stand overnight with stirring at room temperature. The next day the precipitate obtained was washed several times with distilled water and mechanical stirring continued during 24 hours. A white powder was obtained, melting point 90°C (literature[75] 92°C) and was used for the next stage without further purification.
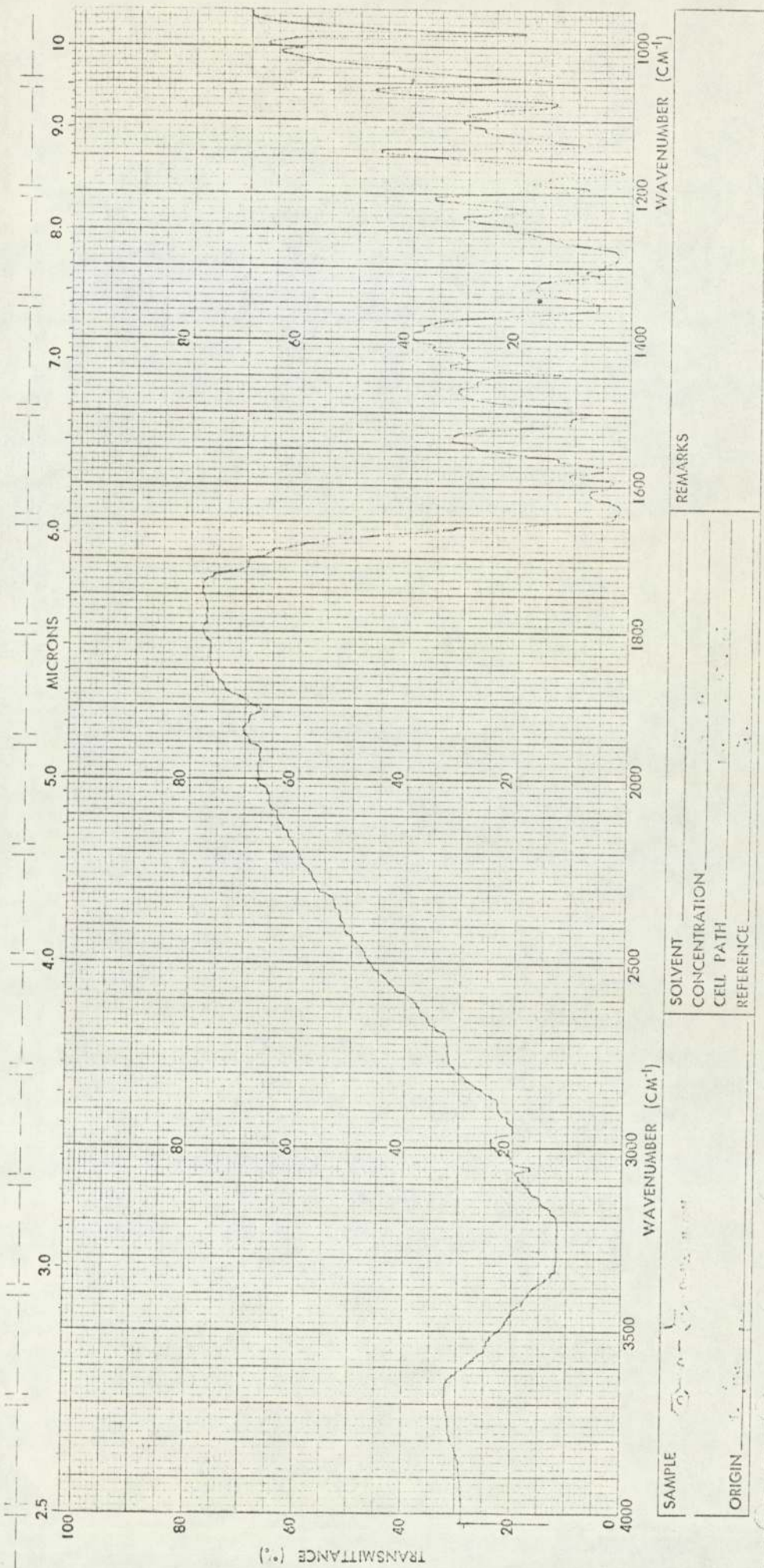
Fig 2.9   Infra-red spectra of 2-hydroxy-4(-hydroxy-ethoxy)benzophenone

65

Ir data

Phenolic hydroxy and alcoholic hydroxy   3500-3100 cm^{-1}

Uv data

Benzophenone group absorption   330 millimicron

2.12.b   4-Benzoyl-3-hydroxyphenyl-O-ethyl thioglcyollate (EBHPT)

25.8 g (0.1 M) of 2-hydroxy-4-(-hydroxy-ethoxy)benzophenone
and 10 g (0.109 M) of thioglycollic acid were dissolved in 200
ml of toluene. 0.5 ml of concentrated sulphuric acid were
added to this solution. The flask was fitted with a Dean and
Stark and a condenser and the solution was refluxed (in an oil
bath at 115°C) until the theoretical amount of water was
removed (6 hours). The solution was washed to neutral pH with
sodium bicarbonate solution and distilled water. It was then
dried with anhydrous magnesium sulphate. Toluene was removed
by rotary evaporation to give a red liquid which gave yellow
crystals in a refrigerator. The melting point of this compound
was found to be 53-54°C (literature[75] 54°C).

Ir data

H-bonded phenolic OH	3400-3200 cm^{-1}
Ester carbonyl	1720 cm^{-1}
Thiol group SH	2550 cm^{-1}
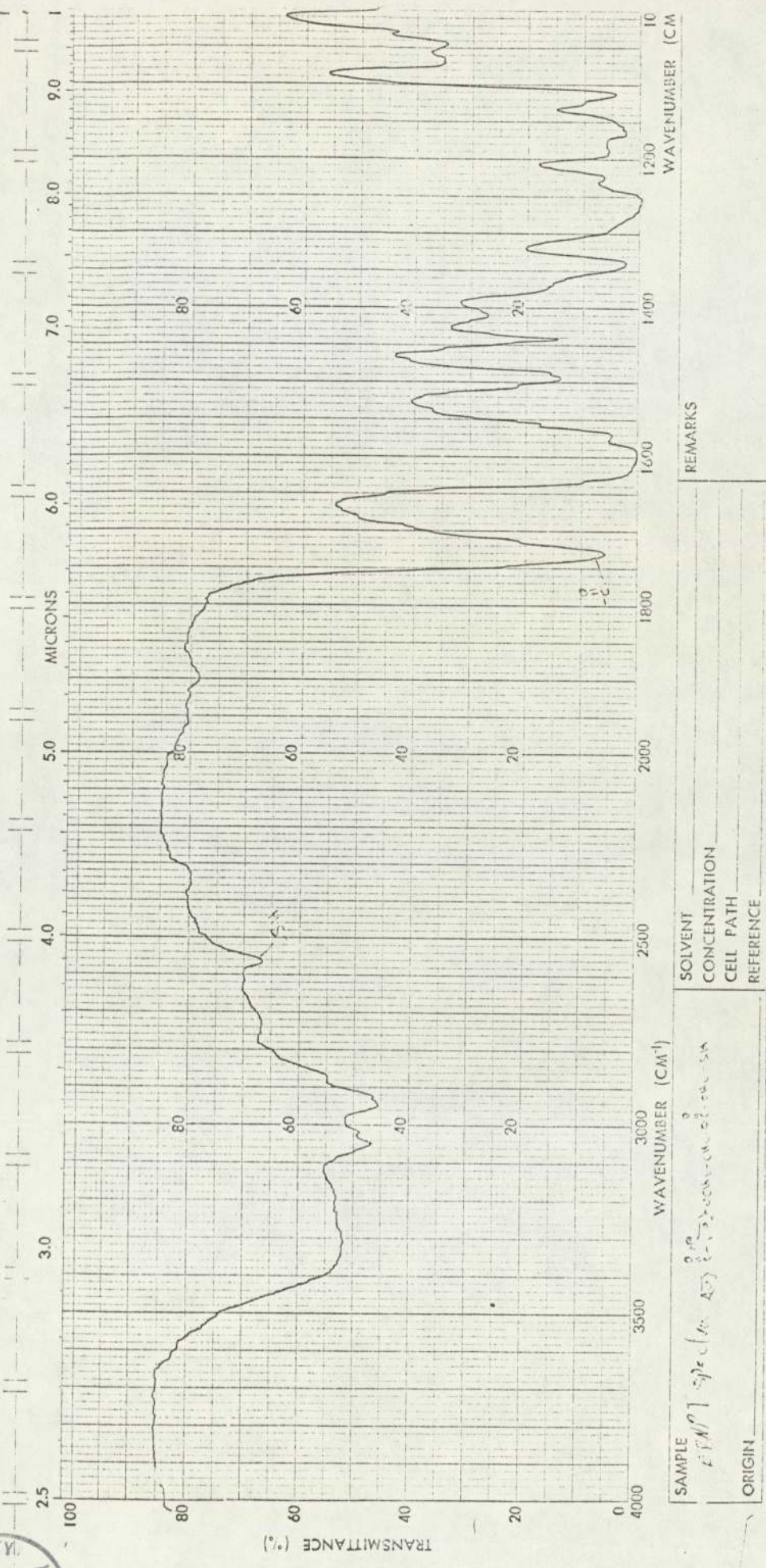
Fig 2.10 Infra-red spectra of EBHPT

Benzophenone group absorption 330 millimicron

2.12.2. 3,5-Di-tert-butyl-4-hydroxybenzyl mercaptan (BHBM)

The following three-stage process was used in the synthesis of this compound:
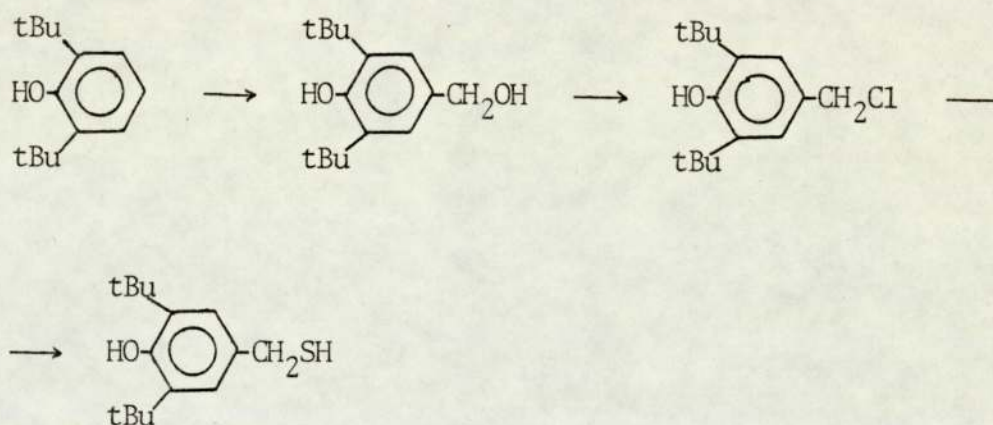
2.12.2.a 3,5-Di-tert-butyl-4-hydroxybenzyl alcohol

53.5 ml (0.140 M) of paraformaldehyde (7.5% solution of para-formaldehyde in tert butyl alcohol), 50 ml (0.128 M) of 2,6-di-tert-butyl phenol (500 g in 1000 ml of tert-butyl alcohol) and 14 ml of potassium tert-butoxide (50 g in 1000 ml of tert-butyl alcohol) were mixed at 20°C and stirred under nitrogen atmosphere for 30 mins.

The mixture was then poured into excess ice-water and two layers

68

were formed, the upper organic layer solidifying. This mixture
was left to stand almost 24 hours, then filtered and poured into
a beaker containing n-hexane, stirred thoroughly and broken the
large pieces into the powder. It was washed several times with
hexane until all the impurities were dissolved in the hexane and
the white powder was filtered and dried in a vacuum oven at
30-40°C. Melting point 137°C. $\left(Literature^{75} \ 137^{\circ c} \right)$.

Ir data

        Free phenolic OH $3620-3640 \ cm^{-1}$

2.12.2.b 3,5-Di-tert-butyl-4-hydroxybenzyl chloride

2 Mole of 3,5-di-tert-butyl-4-hydroxybenzyl alcohol with 500 ml
of toluene stirred for 15 mins, 600 ml of 30% HCl was added
and the reaction was continued for 3 hours at 25°C. The clear
solution was separated into two layers, then the temperature
raised to 45°C for one hour.

The organic layer was separated from water layer and washed
several times with water and dried over calcium chloride.

The toluene is removed under reduced pressure and the obtained
benzyl chloride was used in the next stage for preparation of
BHBM.

2.12.2.c 3,5-Di-tert-butyl-4-hydroxybenzyl mercaptan (BHBM)

5.8 g of magnesium hydroxide powder was taken in a 1000 ml round
bottomed flask and 200 ml of dimethyl formamide (DMF) was added
to it. The mixture was stirred at room temperature for 15 mins
and then H_2S gas was passed into the mixture for 30 mins until
a deep blue colour was obtained showing that Mg $(OH)_2$ solution
was saturated to H_2S. 22.5 g of 3,5-di-tert-butyl-4-hydroxy-
benzyl chloride was dissolved in 500 ml of technical grade
hexane fraction and was added slowly to the mixture. At this
stage the rate of addition of benzyl chloride solution and
H_2S must be controlled in such a way as to prevent the formation
of yellow coloured sulphides. After the addition of the benzyl
chloride solution was finished, the mixture was allowed to
stand for one hour with stirring and was then poured into the
ice-water. The mixture was washed thoroughly severaly times
with ether and the organic layers were collected.

The organic layer was dried over magnesium sulphate for 24 hours,
filtered and then the solvent was evaporated using a rotary
evaporator. The product was vacuum distilled and the fraction
which distilled at 128-131°C at 1.0 mm pressure was collected.
Yield 70%. Mp 28°C (literature 28°C), Bp 120°C at 1.0 mm
of Hg pressure.
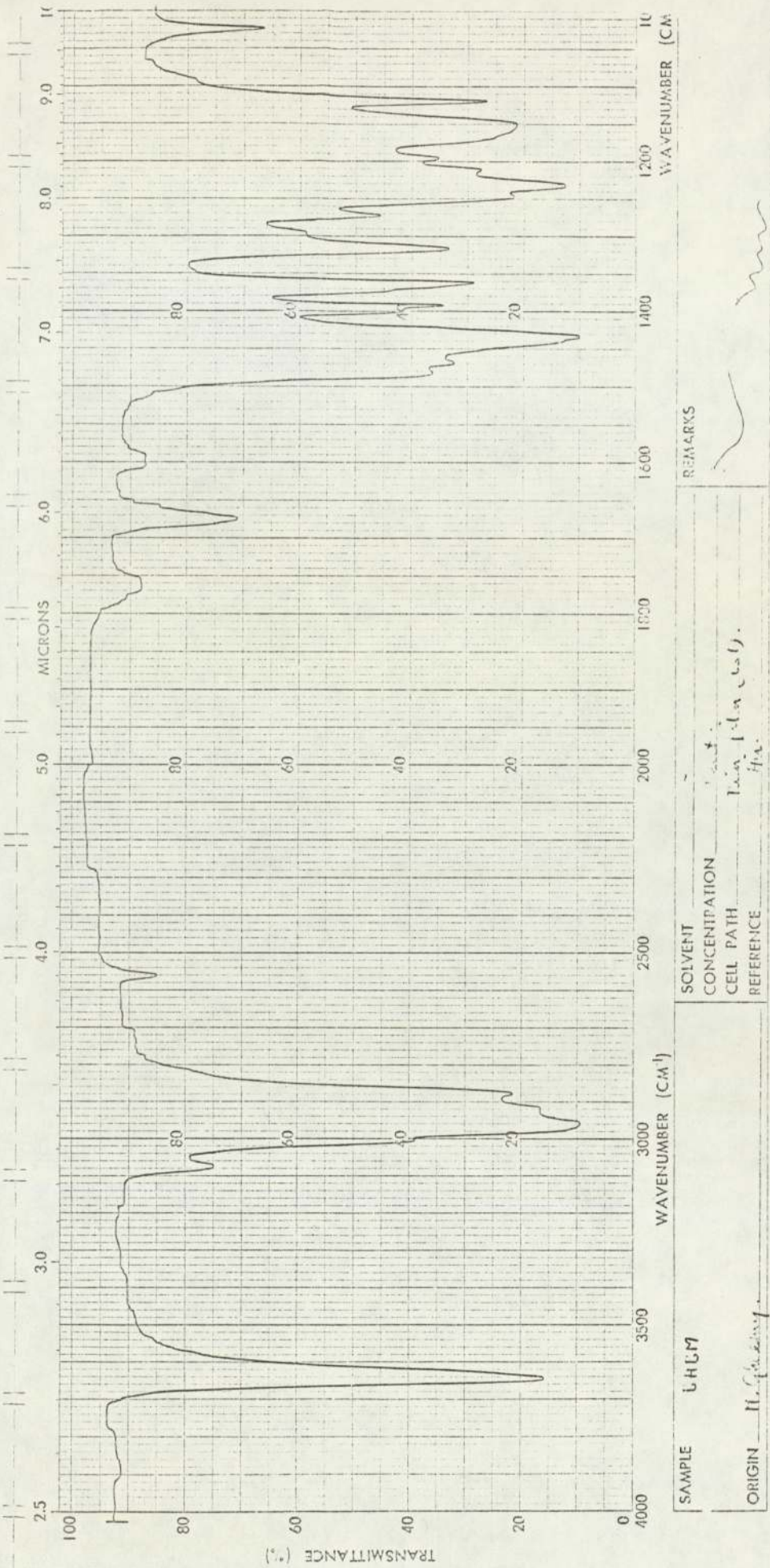
Fig 2.11 Infra-red spectra of BHBM

71

<u>Ir data</u>

| Phenolic OH group | 3640 cm^{-1} |
| SH group | 2560 cm^{-1} |

2.13   4-Benzoyl-3-hydroxyphenyl-O-propane-2ol mercaptan

The following two-stage process was used in the synthesis of
this compound:
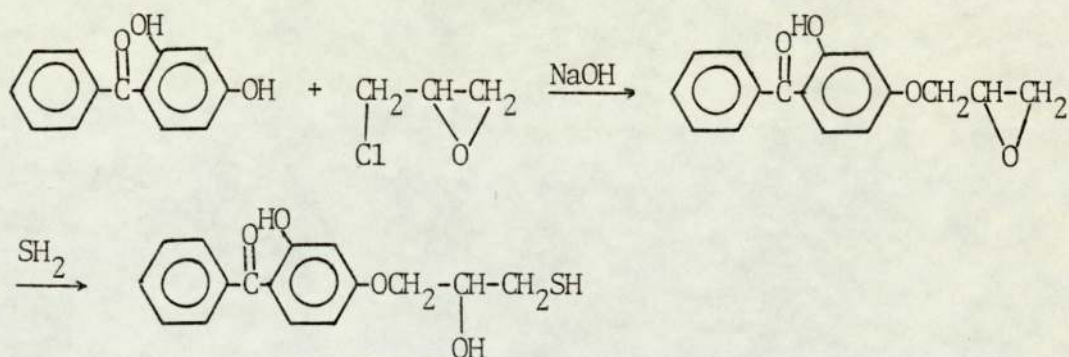
2.13.a   2-Hydroxy-4-(1,2-propyleneoxide)benzophenone

0.1 mole (21.4 g) of 2,4-dihydroxybenzophenone and 1 mole (78 ml)
of epichlorohydrin were mixed in a three-necked flask which is
connected to a dropping funnel, Dean and Stark apparatus and
thermometer. The mixture was heated to 119°C with stirring by
means of a magnetic stirrer. When the epichlorohydrin started
to reflux 40% aequeous sodium hydroxide (0.1 mole) was slowly
added from a dropping funnel to the mixture during a period of
2½ hours. The amount of the water must be maintained less than

0.5% throughout the reaction to obtain a high yield of the product. This is achieved by distilling off the water as an azeotrope with epichlorohydrin and returning the epichlorhydrin to the reactor after separation of the water.

Heating was continued for an addition 30 mins after all the caustic had been added. The reaction mixture was then subjected to rotary evaporator for removal of unreacted epichlorohydrin. In order to separate salt from the crude product, approximately 500 ml of toluene was added with stirring and the mixture was filtered, the salt cake being washed with additional toluene and the washing combined with the filtrate. The mixture was then subjected to the rotary evaporator and finally to the vacuum pump with a cold trap in between for removal of toluene. The resulting product is a viscous brown-orange coloured liquid.

The molar ratio of epichlorohydrin to the 2,4-dihydroxybenzo-phenone (EP/B) was studied by measuring molecular weight of the products by mass spectrometer. If the molar ratio of EP/B is less than 10/1 (eg 4/1) the molecular weight of the product is high, > 300, and it does not give thiol compound in the second stage, probably because of this reaction:
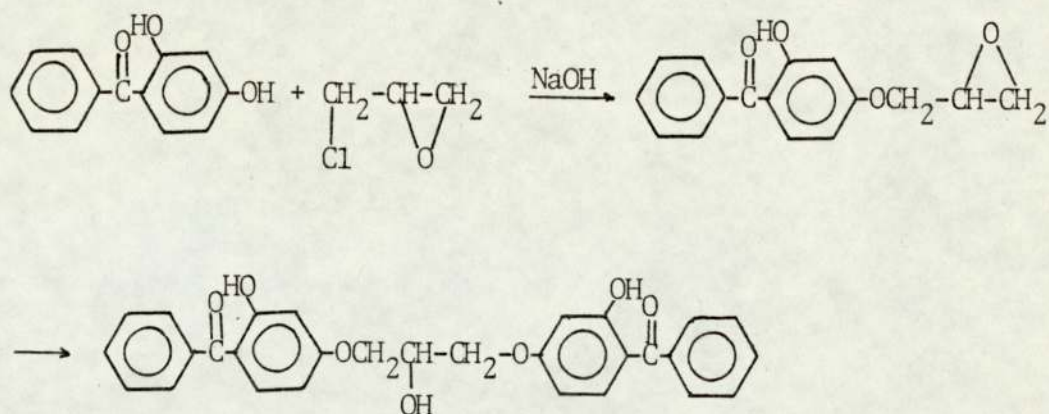
If the molar ratio of EP/B is higher than 10/1 (eg 20/1) the molecular weight of the product is high, 300, but the compound which is produced in the second stage shows an SH group at 2556 cm^{-1} of infra-red region. The high molecular weight product for molar ratio of EP/B = 20/1 could be due to polymerisation of epichlorohydrin in the presence of catalyst along the chain.

However, at molar ratio of EP/B = 10/1, the major part of the product had a molecular weight of 270 equal to molecular weight of 2-hydroxy-4-(1,2-propyleneoxide)benzophenone and some high molecular weight product. This compound was used, after attempted purification in the second stage for the preparation of thiol compound.

2.13.b 4-Benzoyl-3-hydroxphenyl-0-propane-2-ol mercaptan

Into a flask fitted with a separating funnel and gas inlet, weighed 3.3 g (0.05 mole) KOH dissolved in 100 ml of ethylalcohol. H$_2$S was passed into the solution until it was saturated. Then

27.0 g (0.1 mole) of the above compound (epoxide) dissolved in
100 ml of tetrahydrofuran (THF) was allowed to drop into the
saturated solution within a period of about 150 mins, H_2S gas
being passed at the same time.

After the addition of the resin solution, the passage of H_2S
gas was continued for a further 30-45 mins. The reaction
temperature was maintained at $20^{\circ}C$ throughout this reaction.

Thereafter the KOH was neutralised with 50 ml of 2 N H_2SO_4 and
N_2 gas was passed into the reaction flask to remove unreacted
H_2S gas. The reaction mixture was extracted twice with 200 ml
of benzene. The benzene layer was dried and concentrated giving
a brown-orange viscous liquid containing an -SH group at 2556
cm^{-1} and broad band of -OH group at 3500-3300 cm^{-1} absorbance
in the uv region at 330 millimicron related to the benzophenone
group. The yeild is not high because of impurities from the
first stage. Therefore it is recommended that some
modifications to be made to the first stage process in future
for preparation of this compound.

2.14 Preparation of Sodium Salt of 4-benzyl-3-hydroxyphenyl-O-ethyl thioglycollate (EBHPT)

2 g of EBHPT was dissolved in equal mole gram of sodium
hydroxide in cold distilled water. 2 g of EBHPT was weighed
inside a beaker with almost 100 ml of distilled water and

75

0.240 g of sodium hydroxide was slowly added to it with stirring to avoid formation of white precipitant. This precipitant may be the initial alcohol which is formed during hydrolysis of EBHPT. After preparation, this orange solution, the pH was adjusted to 9.0-9.5 by titration with dilute acetic acid. This mixture was used for grafting of EBHPT to the rubber backbone of ABS polymer.

2.15 Preparation of Stripped ABS Latex

The latex was stripped to remove residual styrene monomers which may interfere[75] with masterbatch formation due to consuming the initiator radicals.

A 2-necked flask fitted with a stirrer was connected to a vacuum pump, via a liquid nitrogen trap through a tube with a small bore (0.5 mm). The flask was immersed in a water bath and the temperature was raised slowly within an hour to around $60^{o}C$. The latex was stirred at around 30 rpm during this period. It was found that 600 ml of ABS latex (containing approximately 200 gm dry ABS) could be stripped when the temperature was allowed to rise to $60^{o}C$ in 50 mins. About 50 ml of distilled water was added to the latex before stripping, to compensate for what is lost during the operation.

2.16 Extraction of Bound Stabilised ABS

Refluxing hexane was employed to extract ABS in the form of
powder. Whatman paper thimbles were used to place the powder in
the Soxhlet. Extraction was usually carried out, for ABS in the
form of powder, for at least 48 hours, allowing 10-15 minute
intervals for each filling of the Soxhlet with condensed hexane.

Hexane was also employed to extract ABS films, thickness range,
0.25 mm (0.01 in). Films with low thickness (0.075-0.1 mm)
were also extracted with hexane but because of the penetration
of solvent into the film it became opaque which was not suitable
for ultraviolet and infra-red spectroscopy. Therefore,
somewhat thicker films (0.25 mm, 0.01 in) were extracted for a
longer period and then they were pressed down using compression
moulding machine at $180^{o}C$ for 3 mins, $1\frac{1}{2}$ mins pre-heating to the
desired thickness (0.075-0.1 mm) (the thickness which was used
to study photo and thermal degradation of ABS). The opacity
disappeared during pressing.

The extraction was switched off after a certain time, a piece
of film was pressed down to the desired thickness and was used
to determine the absorbance of functional group by infra-red
(OH group) and uv (benzophenone group). This technique was
used to find the optimum time of extraction of films. It was
found that 96 hours (4 days) extraction was enough for films
of thickness 0.25 mm (0.01 in) (for details, see Chapter 5,

Sections 5.2.a and 5.3.b).

2.17 Quantitative Determination of 4-benzoyl-3-hydroxyphenyl-O-ethyl thioglycollate (EBHPT)

It was suggested[7.5] that 2-hydroxybenzophenone derivatives in
chloroform solution show an absorption maximum in the uv region
of 300-350 millimicrons. This absorption was used in the
estimation of these derivatives. Hexane extracts of ABS were
evaporated and the residue was dissolved in benzene, and any
residual polymer was removed by adding absolute alcohol. The
solution was filtered and the filtrate was used to obtain a
uv spectrum using benzene/absolute alcohol as the blank. The
concentration of the stabiliser was read off using a calibration
curve.

The calibration curve was made by preparation of different
concentration of EBHPT in benzene. These solutions were used to
obtain the uv spectra. A calibration curve was plotted of the
absorption maximum at 330 millimicrons against the corresponding
weight of EBHPT.

2.18 Modification of the Technique of Bound EBHPT Estimation

The technique which described in the Section 2.17 for estimation
of bound EBHPT is indirect since it measures the amount of
EBHPT in the hexane extract.

It was decided to attempt to estimate the percentage of bound
stabiliser (EBHPT) directly on the polymer film using the EBHPT
uv absorption at 325-330 nm. ABS masterbatch in the form of
powder was extracted and diluted to a lower concentration in
the torque rheometer and compression moulded was used to obtain
the uv spectrum using unstabilised ABS film as the blank.
The amount of stabiliser was read off using a calibration curve.

ABS in the form of film was extracted (Section 2.16) and
pressed to the desired thickness. (For high concentrations of
EBHPT it was diluted to the lower concentration in the torque
rheometer and compression moulded.) The films so obtained were
used for uv spectrophotometric measurements using unstabilised
ABS film as the blank.

The calibration curve was made by processing unstabilised ABS
powder with different amounts of EBHPT in the torque rheometer.
Samples were made into films by compression moulding and these
films again used to obtain the uv spectra using unstabilised ABS
film as the blank. Films with standard thickness of 0.075 mm
were used and the calibration curve was obtained by plotting the
maximum absorption at 330 millimicron against the corresponding
weight of the EBHPT (Fig 4.1).

2.19 Chemical Determination of Bound 3,5-di-tert-butyl-4-hydroxy-benzyl mercaptan (BHBM)

Metcalf and Tomlinson's method of colourimetric determination of phenolic antioxidants was used in these estimations[75,76]. This procedure involves oxidation of antioxidants (A) under controlled conditions with ferric ions followed by the reaction

$$A\ reduced\ +\ Fe^{+3}\ \longrightarrow\ A\ oxidised\ +\ Fe^{+2}$$
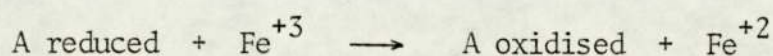
of Fe^{+2} ions produced with 2,2'-bipyridyl to form a coloured complex the intensity of which is proportional to the concentration of the antioxidant.

Procedure

10 g of ABS (containing approximately 1 phr of antioxidant) was thoroughly extracted with 150 ml of Analar hexane. The extract was rotary evaporated and the residue was dissolved in 25 ml of Analar toluene. 25-30 ml of absolute ethanol was added to precipitate any residual polymer. The solution was filtered and the filtrate made up to 100 ml with absolute ethanol.

Two dry 10 ml volumetric flasks painted with several layers of black paint were immersed and clamped in a thermostatted ($25 \pm 5^{\circ}$C) water bath. 10 ml of the filtrate was pippetted to one and 10 ml of 25/75 (v/v) toluene/EtOH solution to the other. 0.5 ml

of dipyridyl solution (0.5% solution in absolute ethanol) and 1.0 ml of $FeCl_3$/EtOH solution (0.2% solution of $FeCl_3$, 6 H_2O in absolute ethanol) were added to the two flasks which were allowed to stand at $25^{\circ}C$ for about an hour. The optical density of the solution was measured against the blank using spectometer cell, using wavelength at visible region 520 millimicron.

Calibration curve was made by making a solution of 0.03 g BHBM with 25/75 (v/v) toluene/EtOH into a 100 ml volumetric flask. Varying amounts of this solution was then diluted to 100 ml with toluene/EtOH (25/75) solution and dipyridyl and $FeCl_3$ solutions were added according to the above procedure and the optical densities for the corresponding antioxidant concentrations determined. It was attempted to plot the optical density against the corresponding weight of the BHBM. The results were so scattered that attempts were made to find another technique for estimation of bound BHBM (see below).

2.20   Modification of the Technique of Bound BHBM Estimation

Several problems were encountered with the procedure described in Section 2.19:

(a)   The coloured complex is very sensitive to light causing great difficulty in the preparation of the solutions and causing uncertainty as to the optical density corresponding to the concentration of BHBM.

(b)   Because of the very high absorptivity of the coloured
        complex at 520 nm, the solution must be very dilute
        and preparation of such solutions led to substantial errors.

(c)   The above is an indirect method since it measures the
        amount of BHBM in hexane extract which is subtracted from
        the initial amount of BHBM to obtain the amount of BHBM
        bonded to the polymer[75].

(d)   During emulsion reaction of BHBM with ABS latex or during
        processing of BHBM with ABS powder in the torque
        rheometer in the presence of air, there is the possibility
        that some of the BHBM is oxidised through the OH group
        to give quinonoid products and these products are not
        included in this technique of estimation and are therefore
        ignored.

In view of the above difficulties, attempts were made to find
another technique for estimation of bound BHBM in ABS. The
infra-red technique was used to measure the OH group of BHBM.
Compression moulded films of ABS containing different amounts
of BHBM did not show an absorption at 3640 cm^{-1} related to the
phenolic OH group, but they showed a broad peak from 3620-3300
cm^{-1} due to the overlap of the absorption of the phenolic OH
group and alcoholic groups which was formed in the polymer
during compression moulding. Because of this difficulty, the
extracted ABS films were solution cast (procedure in Section 2.16)

82

and the cast films showed a sharp absorption at 3640 cm^{-1}.

The calibration curve was made by dissolving unstabilised ABS powder with different amounts of BHBM in dichloromethane according to the procedure described in Section 2.5. The calibration curve was made using the cast films to obtain ir spectrum.   The calibration curve was obtained by plotting the indices of OH group against the corresponding weight of the BHBM (see Fig 5.1).

2.21 Masterbatch Technique

Conventional stabilisers are added either in the latex stage or during the processing of a polymer. An obvious implication of the adduct formation reaction of BHBM and EBHPT with the commercial material is the escalation of the cost of manufacture of the polymer. Therefore, for any future commercial application of this process, such an increase in the cost should be justified by its performance.

The cost of the process can be kept to a minimum if higher than normal amounts of stabilisers can be reacted with a given amount of polymer to form a 'masterbatch' which can be diluted at a later stage. Masterbatching of a product is only successful if the performance of the diluted material remains more or less unchanged at the same concentration in the polymer.

It was found earlier[75] that the performance of the masterbatch adducts when diluted with unstabilised ABS latex to obtain stabiliser concentration for normal applications of the polymer were comparable to those reacted individually at similar concentration. Therefore the masterbatch technique appeared to be a convenient and cheap way of introducing bound antioxidants into rubber (procedure, Section 4.2.1.c).

CHAPTER THREE

CORRELATION BETWEEN IMPACT STRENGTH AND DYNAMIC MECHANICAL
PROPERTIES OF ABS DURING OXIDATIVE DEGRADATION

3.1 Results

Photodegradation of unstabilised and commercial stabilised ABS
was carried out by measuring changes in the functional groups
(-OH, C=O, 1,4- C=C) using infra-red spectrometry, impact
strength changes using weight falling tester and dynamic
mechanical property change by means of rheovibron.

3.2 Infra-red Spectra of ABS Polymer

The following absorption bonds in the infra-red spectra of ABS
were assigned with the help of published data[40,79,80]. Table 3.1.

3.3 Photo-oxidation of Unstabilised and Commercial Stabilised ABS

Compression moulded films of unstabilised ABS and commercial
stabilised ABS, and extruded films of commercial stabilised
ABS were exposed to uv irradiation at ambient temperature and
the change in the concentration of functional groups were
monitored by infra-red spectrometry. Typical infra-red spectra
of compression moulded and extruded films of photo-oxidised
ABS are shown in Figs 3.1 and 3.2. The development of carbonyl

85
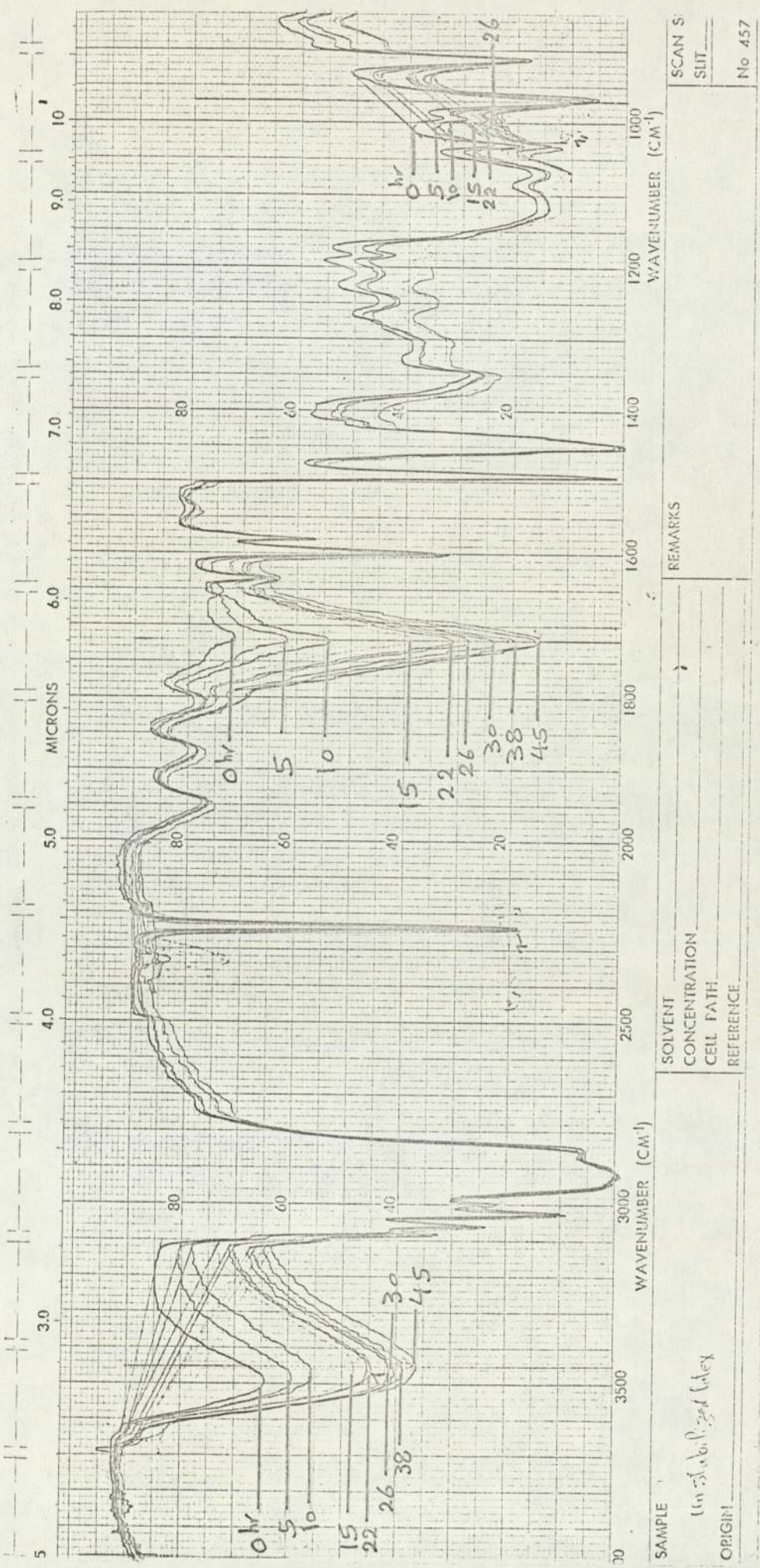
Fig 3.1 Compression moulded film of unstabilised ABS (Borg-Warner latex) subjected to uv irradiation
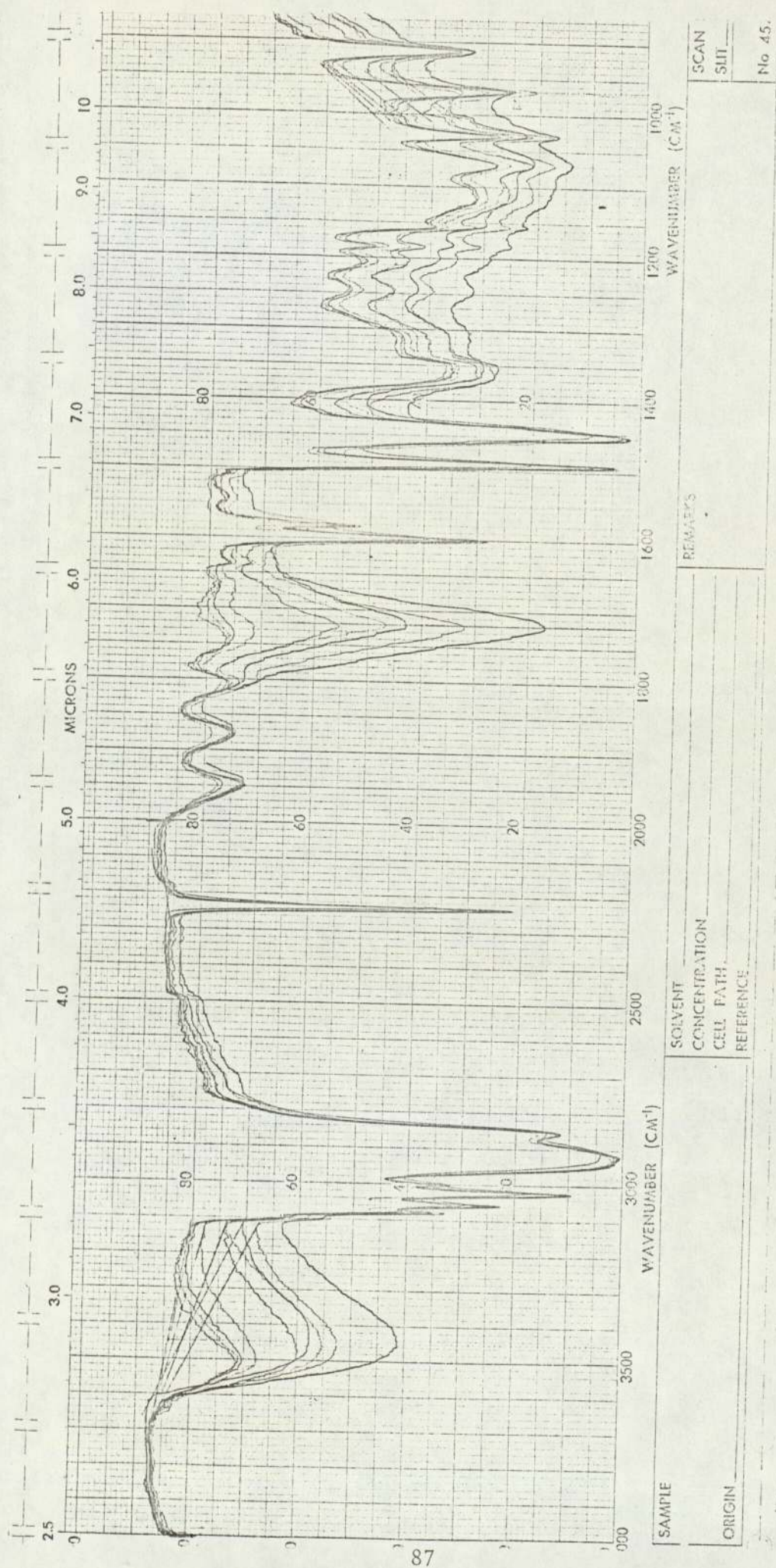
Fig 3.2 Compression moulded film of commercial stabilised ABS (Monsanto) subjected to uv irradiation
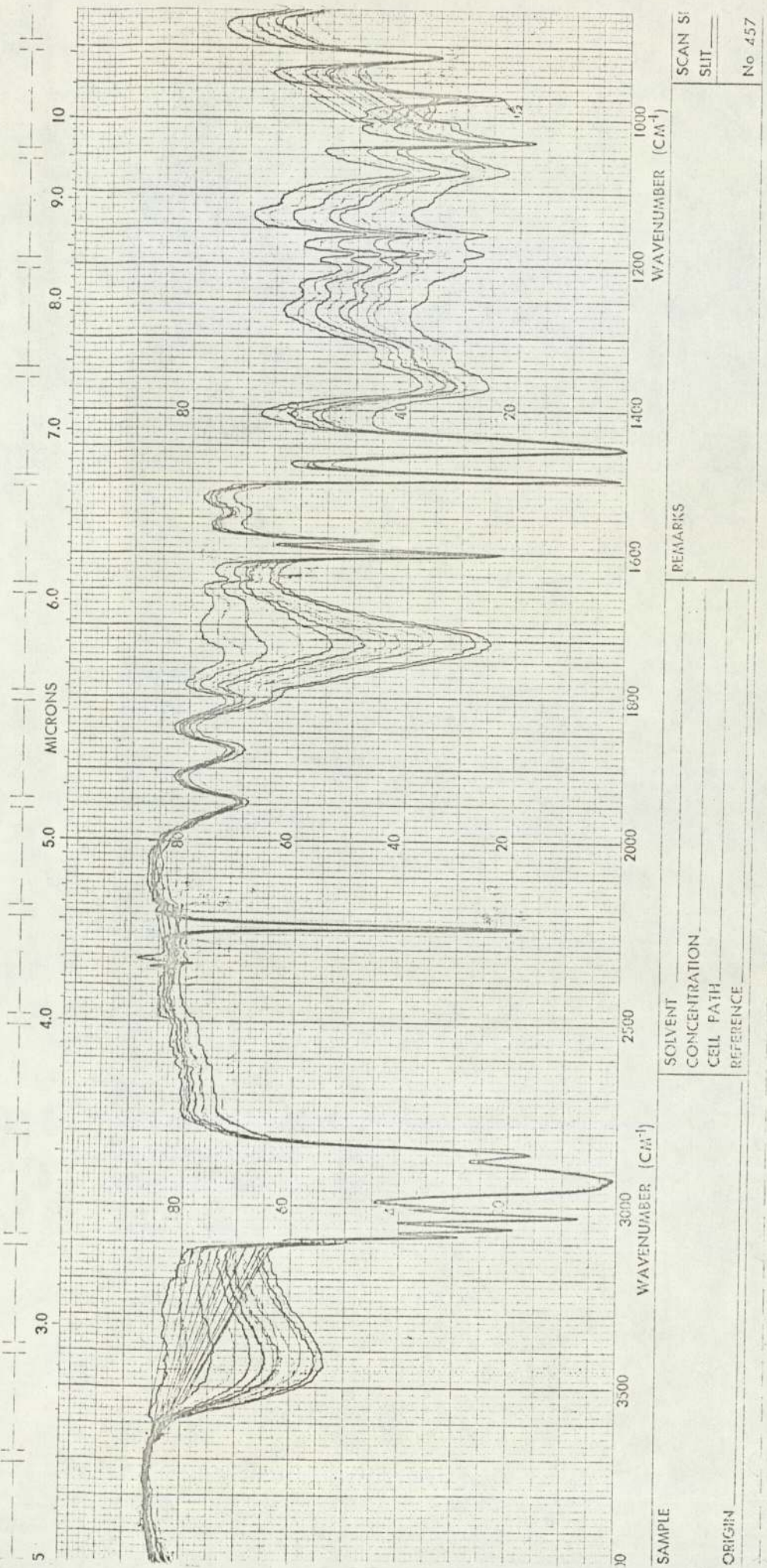
Fig 3.2 Extrudate film of commercial stabilised ABS (Monsanto)

Table 3.1   Ir group frequencies in ABS

Polymer	Absorption band, cm^{-1}	Assignment
Unoxidised	3060	C-H stretching of phenol group
	3015	C-H stretching of phenol group
	2920	CH_2
	2850	CH_2
	2220	CN
	1950,1870,1810,3 peaks	Mono-sub of phenyl group
	1638	cis-1,4- C=C
	1600,1580	phenyl group
	1500	CH_2, phenyl group
	1450	CH_2, phenyl group
	1360-1160	C-H bending, CH_2, phenyl group
	1120,1070,1030	phenyl group
	965	trans-1,4- C=C
	912	1,2-butadiene, phenyl group
	845	Tri-sub, C=C
	760,700	Mono-sub of phenyl group
Oxidised	3450	OH stretching
	1720	C=O stretching

Fig 3.3 Photo-oxidation of unstabilised ABS (Borg-Warner latex) compression moulded film
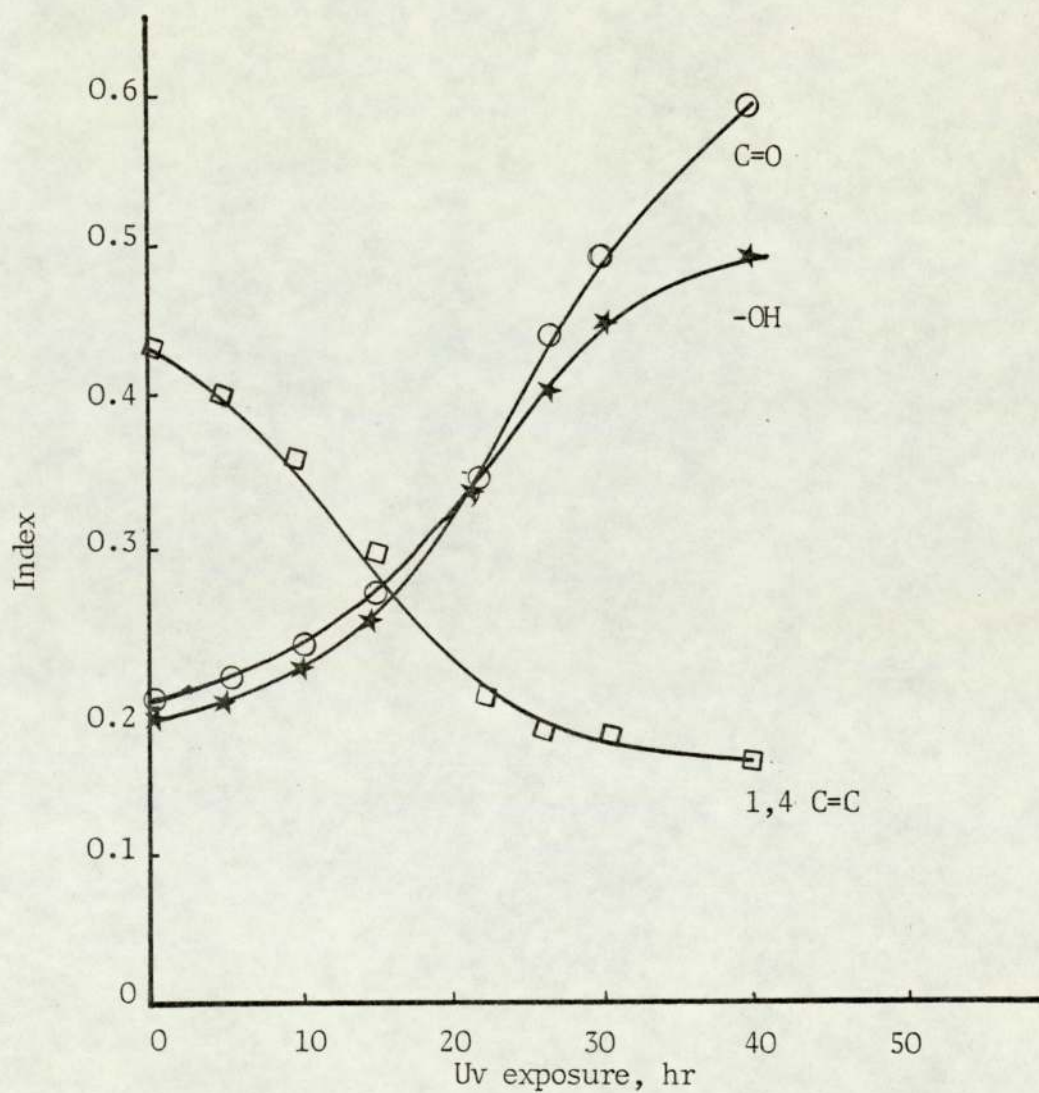
Fig 3.4 Photo-oxidation of commercial stabilised ABS (Monsanto) compression moulded film

91
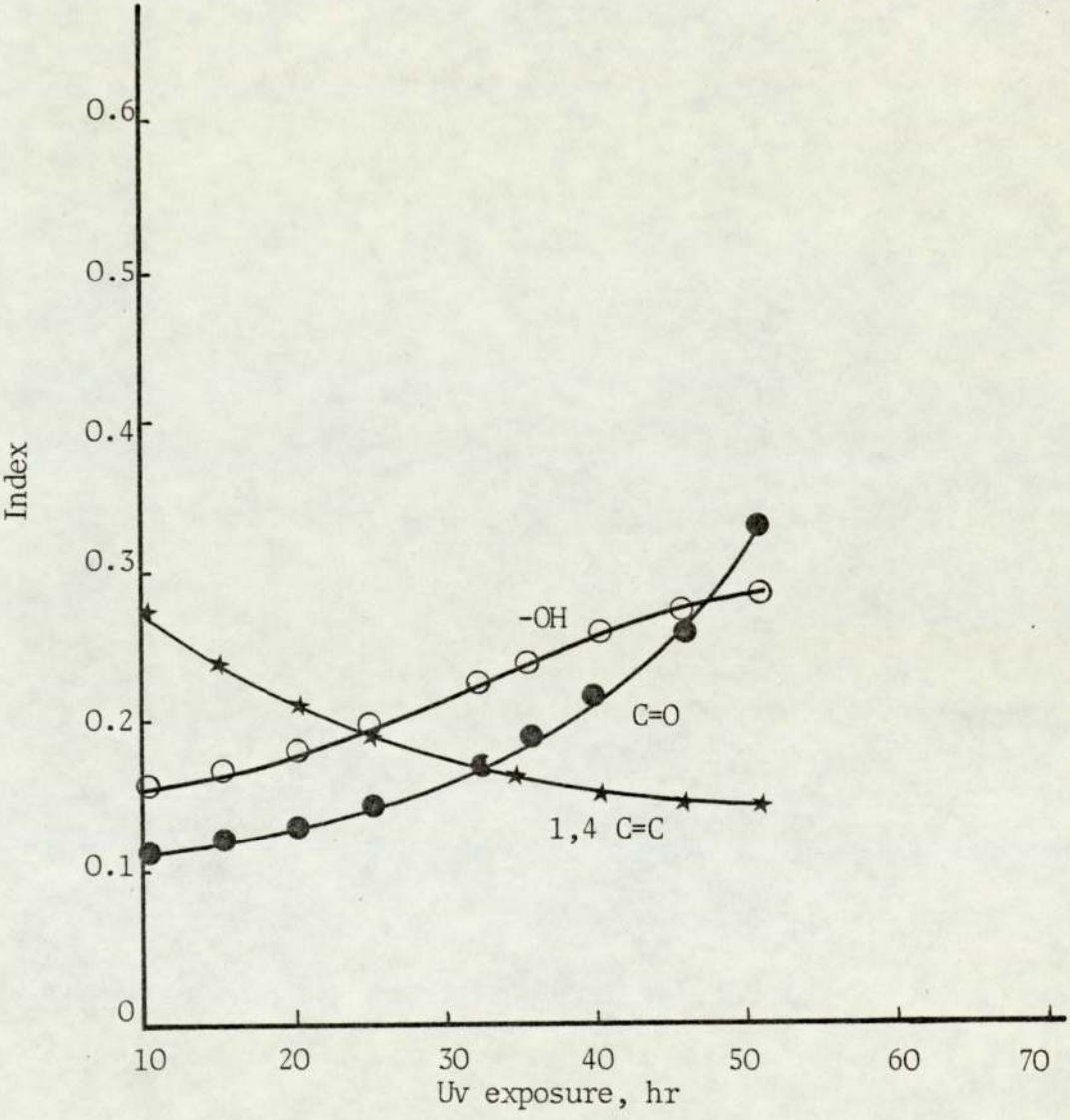
Fig 3.5 Photo-oxidation of commercial stabilised ABS
         (Monsanto) extrudate film
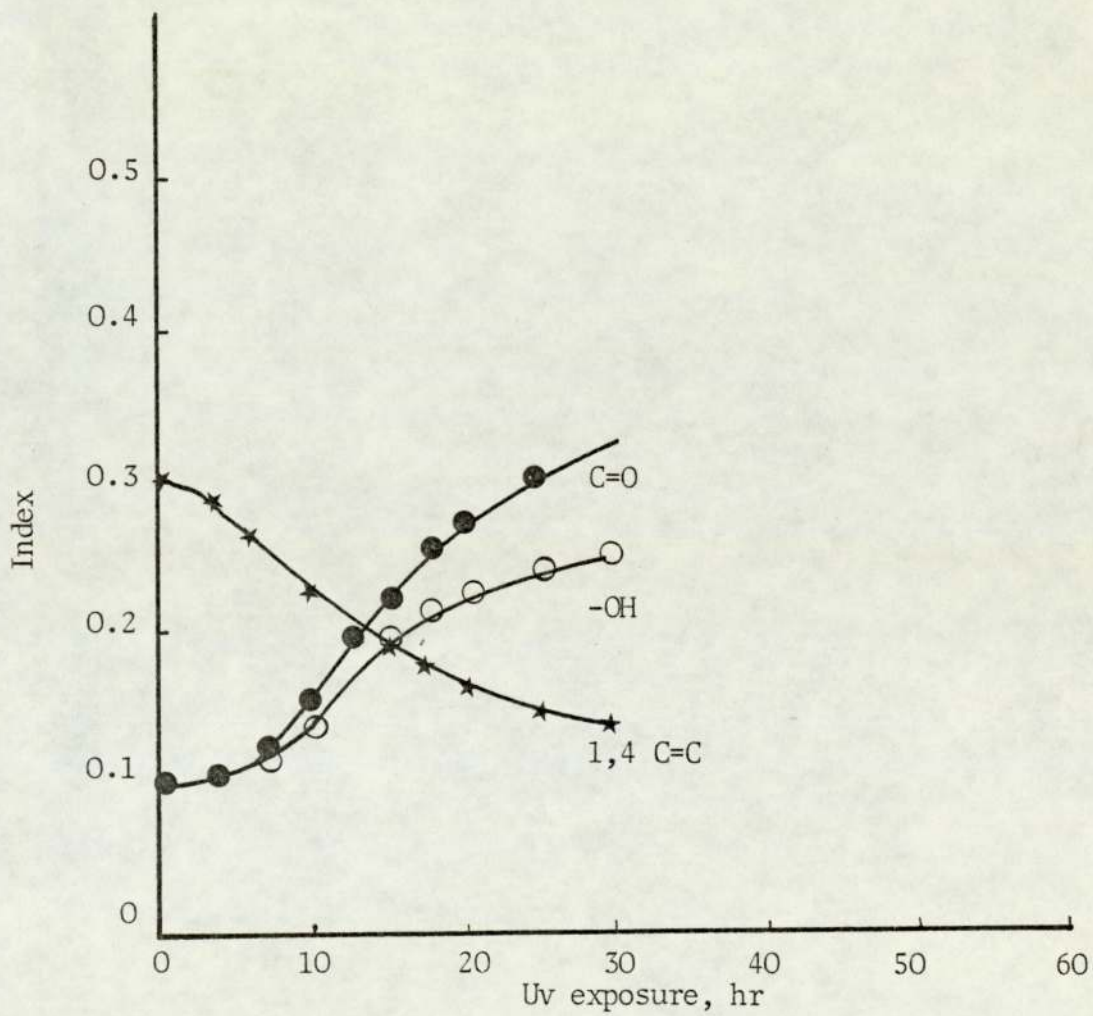
and hydroxyl centred around 1720 cm^{-1} and 3450 cm^{-1} and the decay of trans-1,4 C=C absorption at 965 cm^{-1} are shown for unstabilised and commercial stabilised ABS in Figs 3.3, 3.4 and 3.5 respectively. In the case of unstabilised ABS (Fig 3.3) the change in functional groups (-OH, C=O, 1,4 C=C) did not show an induction period. However, in the case of commercial stabilised ABS (Figs 3.4,3.5) the functional groups showed between 3-5 hours induction period.

The complex band in the carbonyl region is centred around 1720 cm^{-1}, the shoulders were assigned as follows[75]:

Table 3.2

1670-1685 cm^{-1}	unsaturated ketone
1690 cm^{-1}	unsaturated aldehyde
1705-1700 cm^{-1}	carboxylic acid group
1720 cm^{-1}	saturated carbonyl group
1735 cm^{-1}	ester carbonyl group

The vinyl absorption at 912 cm^{-1} was not taken into account in the quantitative analysis by infra-red, due to the fact that it overlaps with an absorption of the phenyl group. No change in the nitrile or phenyl absorption was observed. The exposure of the films to the uv light was interrupted frequently for infra-red spectroscopy.

3.4   Impact Properties

Compression moulded films of unstabilised ABS and commercial
stabilised ABS, and extruded films of commercial stabilised ABS
were exposed to uv irradiation at ambient temperature and the
change in the impact strength was measured by the falling weight
tester. The falling weight test uses a spherical ball striker
attached to a load carrying device to which the weight can be
attached. The striker assembly slides freely in vertical guides
and is released from a height to strike centrally on the
specimen which is supported on the base of the equipment (see
Fig 2.4). This procedure was repeated using at least twenty
samples of exactly the same thickness for each period of
exposure to uv light, in order to obtain the weight and the
height at which the first sign of a break in the specimen occurs.

The change in the impact strengths of the photo-oxidised films
of ABS are shown in Fig 3.6. The impact strength change of unstabilised
ABS did not show an induction period and reached the lowest
value in 15 hours. The impact strength of commercial stabilised
ABS showed about 5 hours induction period and reached the lowest
value in 14-16 hours.

In all cases, the impact strength decreased sharply to the
lowest value during exposure to uv light and then almost remained
constant until the samples became completely brittle.

94

Fig 3.6   Changes in the impact strength of ABS during
           photo-oxidation

○   unstabilised ABS
     (compression moulded film)

●   Monsanto ABS
     (extrudate film)

✶   Monsanto ABS
     (compression moulded film)
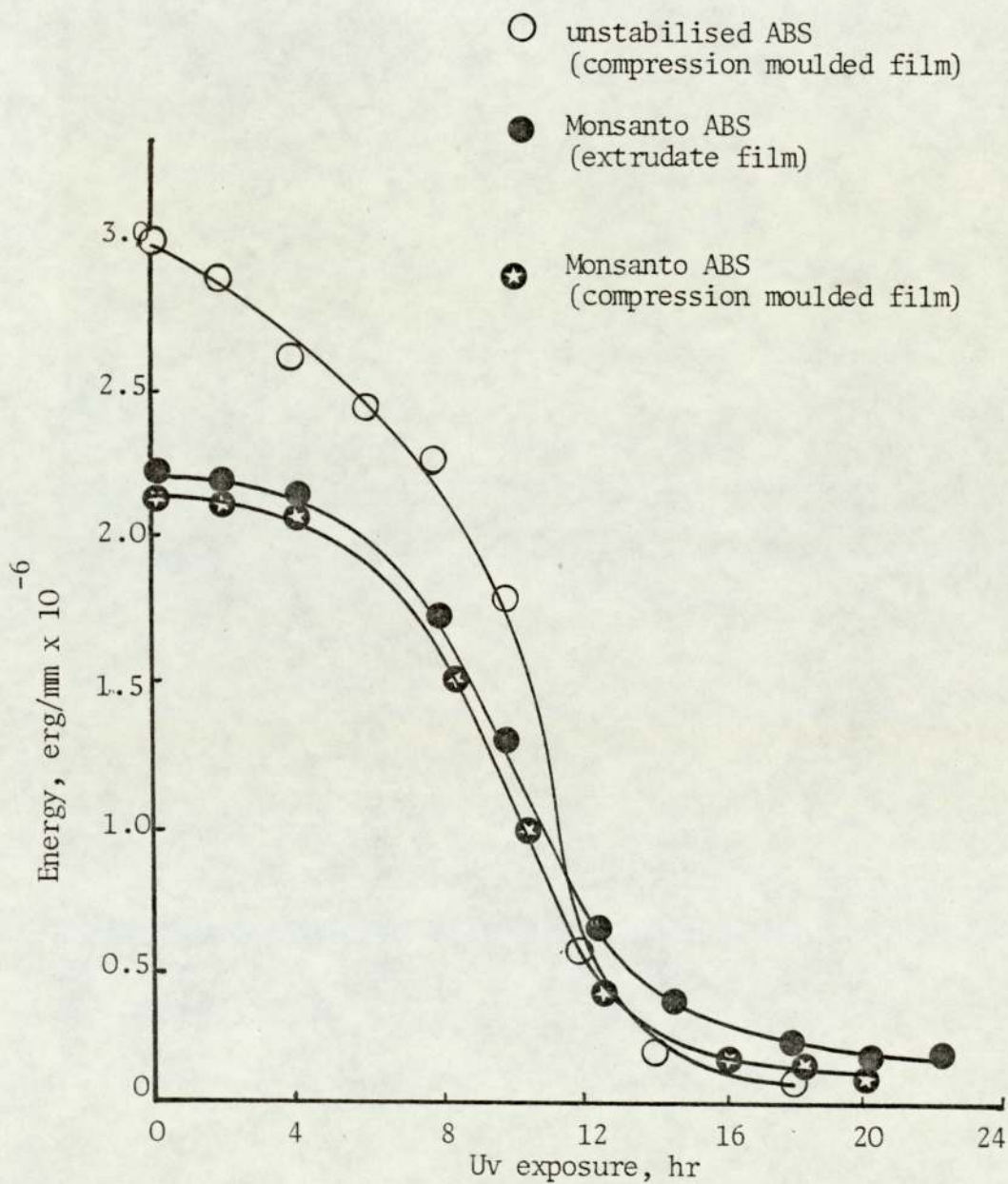
3.5 Dynamic Mechanical Properties

Compression moulded and extruded films of commercial stabilised ABS and compression moulded film of unstabilised ABS (thickness 0.075 mm) were exposed to the uv light and the changes in damping and complex modulus was measured at ambient temperature by rheovibron. Only one sample was used throughout the photo-oxidation and it was prepared according to the procedure which was given in Section 2.11.a. The results are shown in Figs 3.7, 3.8 and 3.9. The readings at ambient temperature (20°C) were recorded at least 5 times due to the scatter result, for each period of exposure to uv light. Generally, there were more scatter readings during the initial period of uv exposure. Tan δ measured at 20°C for unstabilised ABS did not show an induction period and increased to a maximum in 18 hours exposure and then started to decrease to the lowest value in 26 hours exposure which corresponds to the maximum complex modulus (E*). The commercial stabilised samples showed 6-8 hours induction periods and reached the maximum value in 16-18 hours, for compression moulded and extruded films respectively. The tan δ at 20°C decreased to the lowest value in 22-25 hours corresponding to the maximum value of complex modulus (E*). The complex modulus (E*) was calculated using equation 2.11 (Section 2.11.c). Tan δ at 20°C increased again but at a much slower rate to a minimum value. The rapid linear rise in complex modulus at 20°C corresponded to the maximum in tan δ (20°C) and the maximum in complex modulus corresponded to the minimum value of tan δ. The

96

Fig 3.7 Effect of photo-oxidation on impact strength and dynamic mechanical properties of compression moulded films of unstabilised ABS

Maximum height of tan δ at -80°C and tan δ at 20°C

Energy, erg/mm x 10⁻⁶

E*

Tan δ at 20°C

Tan δ at -80°C

Energy

Uv exposure, hr
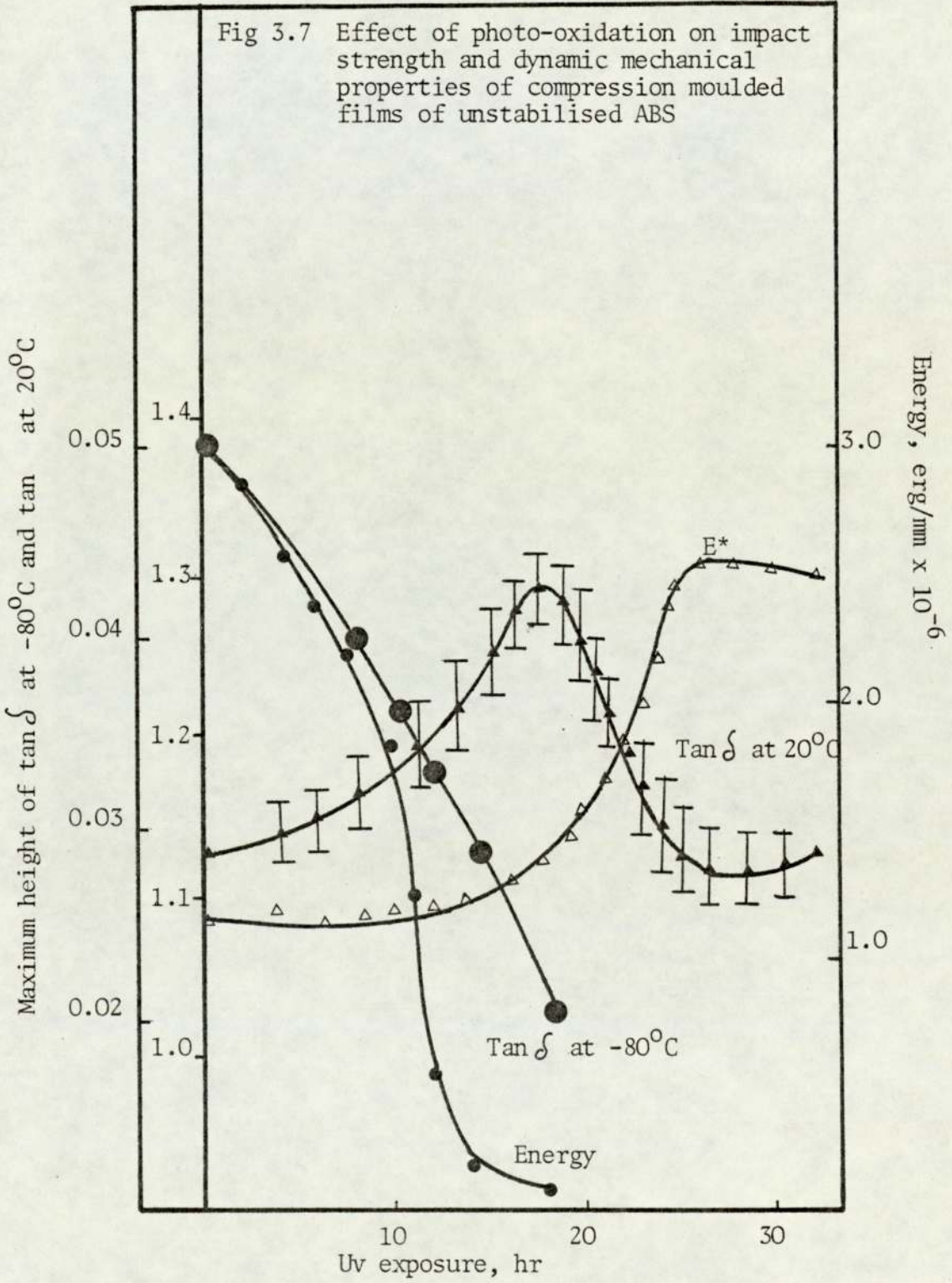
Fig 3.8   Effect of photo-oxidation on impact
strength and dynamic mechanical
properties of compression moulded
films of Monsanto ABS

98
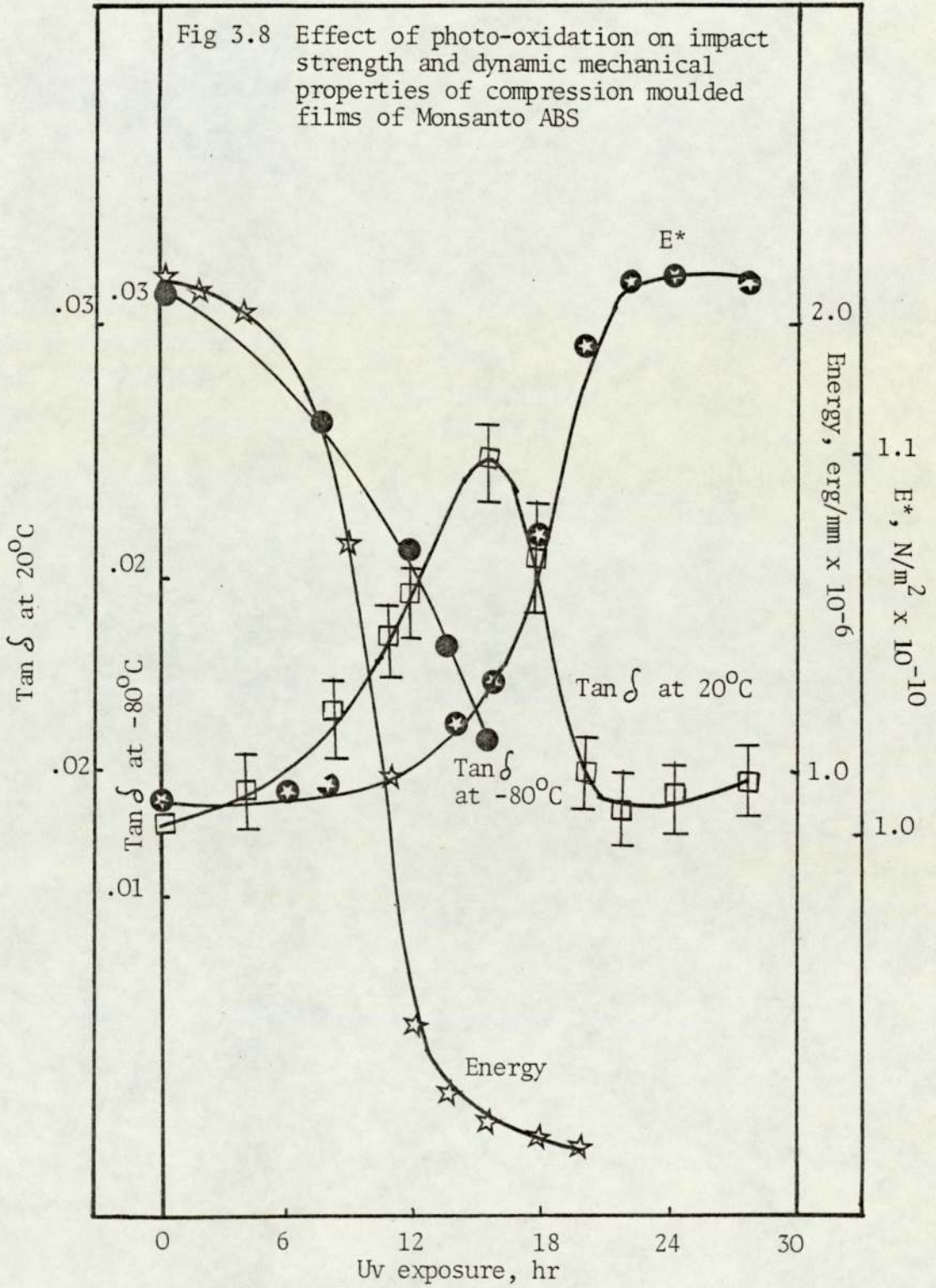
Fig 3.9   Effect of photo-oxidation on impact
          strength and dynamic mechanical
          properties of extrudate films of
          Monsanto ABS

Tan δ at 20°C

Tan δ at -80°C

Tan δ at
-80°C

Tan δ at
20°C

E*

Energy

Energy, erg/mm x 10⁻⁶

E*, N/m² x 10¹⁰

.03

.03

.02

.02

.01

1.2

2.0

1.1

1.0

1.0

0   6   12   18   24   30

Uv exposure, hr

99
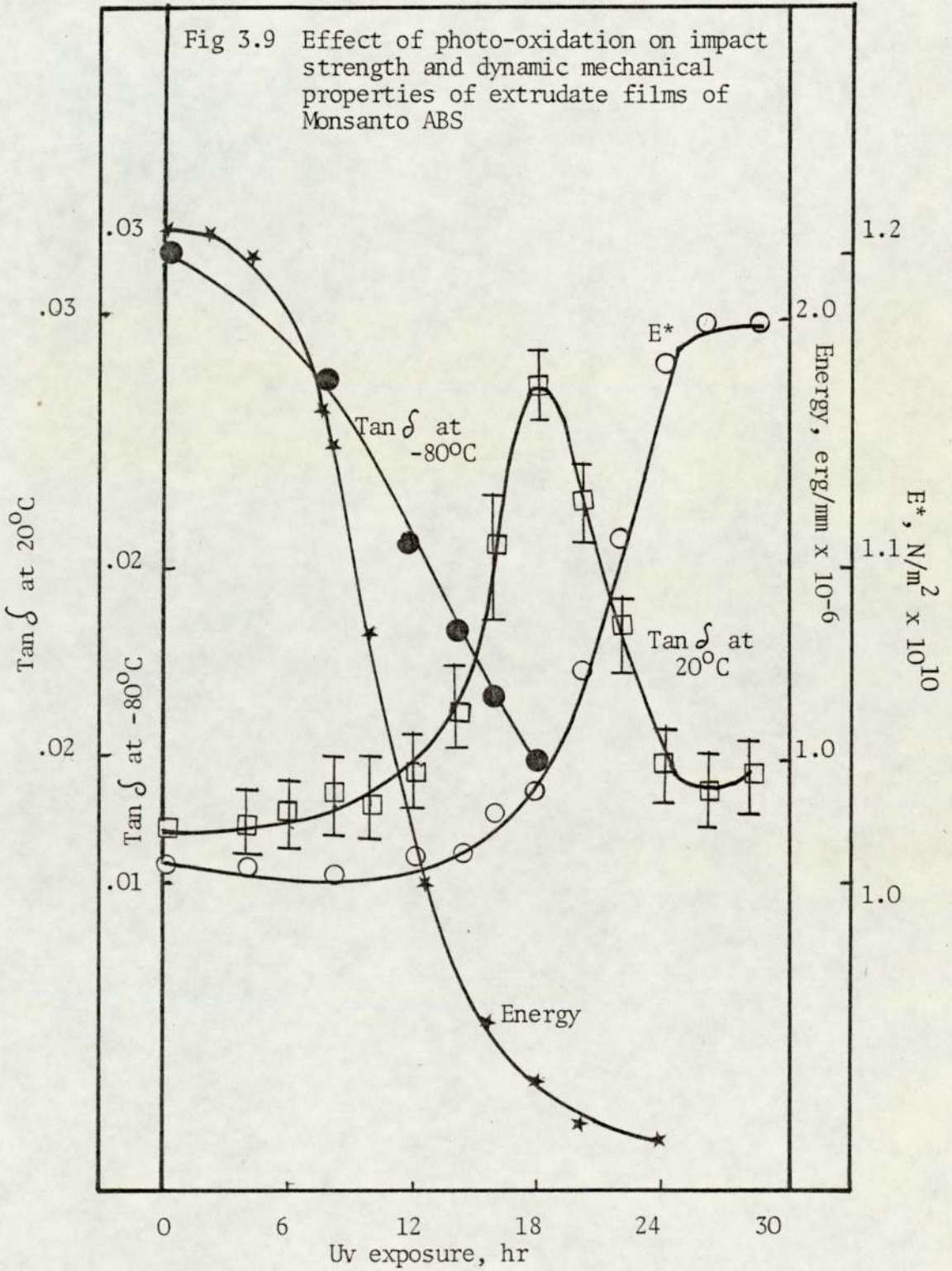
complex modulus (E*) started to decrease very slowly which corresponded to the slow increase in tan δ at 20°C.

The low temperature dynamic-mechanical properties of compression moulded film of unstabilised ABS is shown in Fig 3.10. Samples of thickness 0.075 mm (0.003 in) were stamped out using a steel cutter (see Section 2.11.a). The sample was subjected to the uv exposure and it was frequently interrupted to measure the dynamic mechanical properties at low temperature. The same smaple was used throughout measuring low temperature (- 80°C) dynamic mechanical properties during photo-oxidation. The cold chamber of rheovibron and the specimen were cooled down to -120°C with liquid nitrogen (see Section 2.11.a) and the readings were taken on the rheovibron from -120 to 0°C. The region between -120°C to -110°C was completely flat for unexposed film (control) and then tan δ started to increase to a maximum of 0.05 at -82°C. The height of the peak rapidly diminished during exposure to uv light and after 18 hours it was almost extinct (Fig 3.10). Similarly the width of the peak increased and the apex shifted to higher temperatures during uv irradiation and thus the flat region from -120°C increased during uv exposure. Consequently, the area under the damping curve was reduced. A change was also apparent in the plateau region above -50°C. During photo-oxidation, tan δ in this region (-50°C) increased. However, when the destruction of the tan δ peak around -80°C was complete, tan δ at -50°C dropped sharply. It was not necessary to review the whole spectrum from -120°C to +120°C

Fig 3.10 Changes in tan peak at -80°C, compression moulded film of unstabilised ABS (numbers on spectra represent hours of exposure to uv light)

101
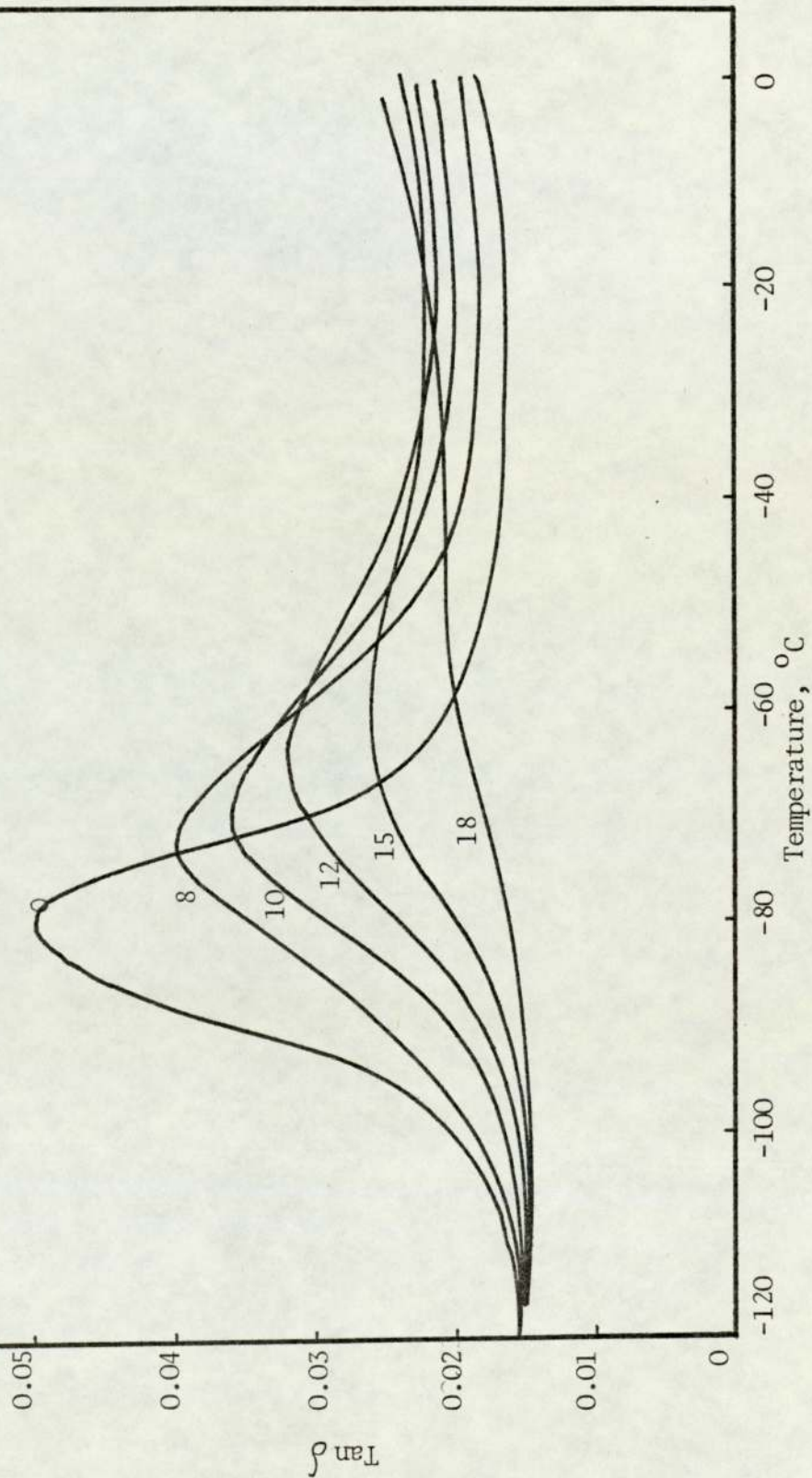
Fig 3.11 Changes in tan peak at -80°C, compression moulded film of Monsanto ABS (numbers on spectra represent hours of exposure to uv)
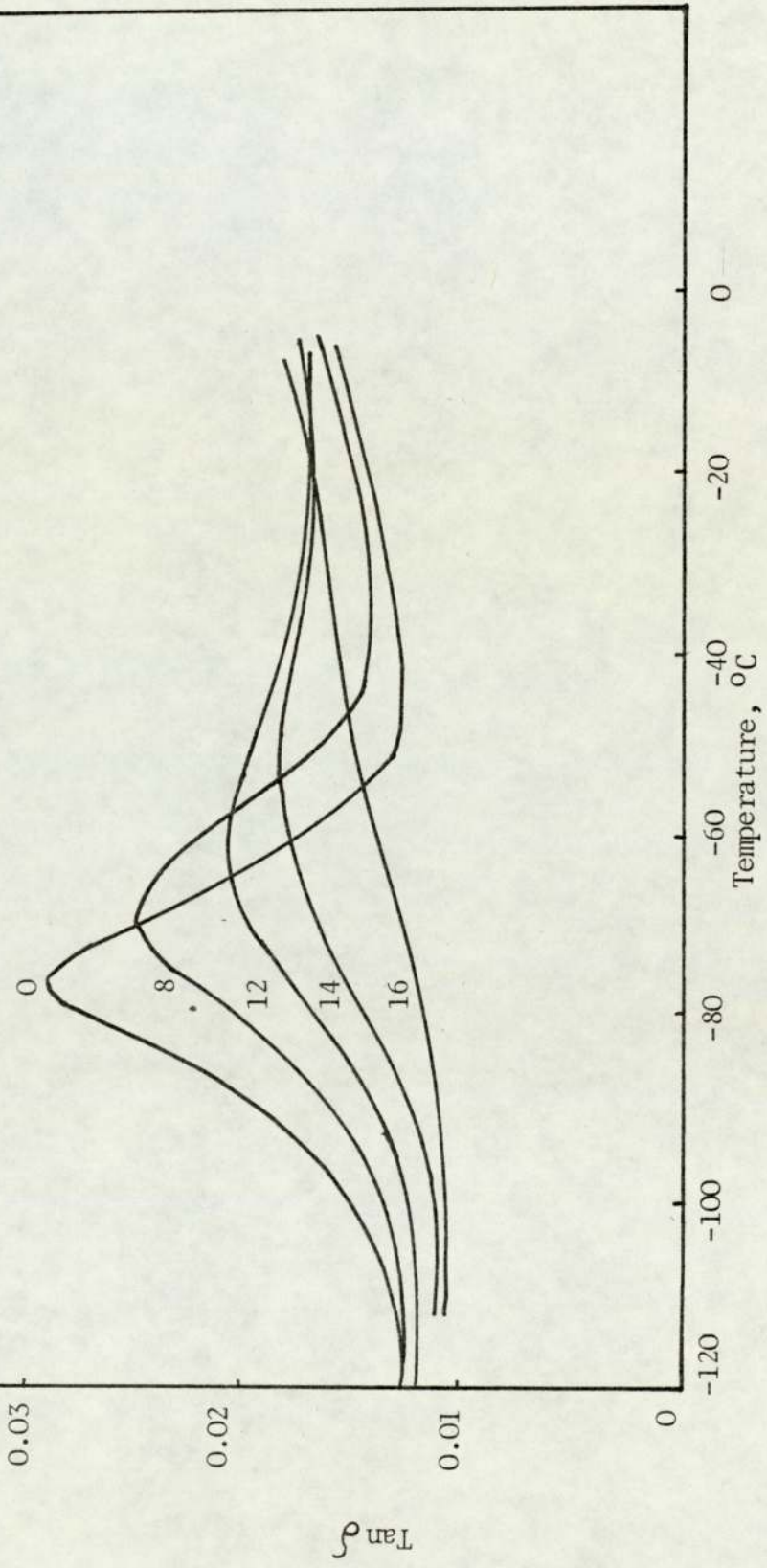
Fig 3.12 Changes in tan peak at -80ºC, extrudate film of Monsanto ABS (numbers on spectra represent hours of exposure to uv)

103
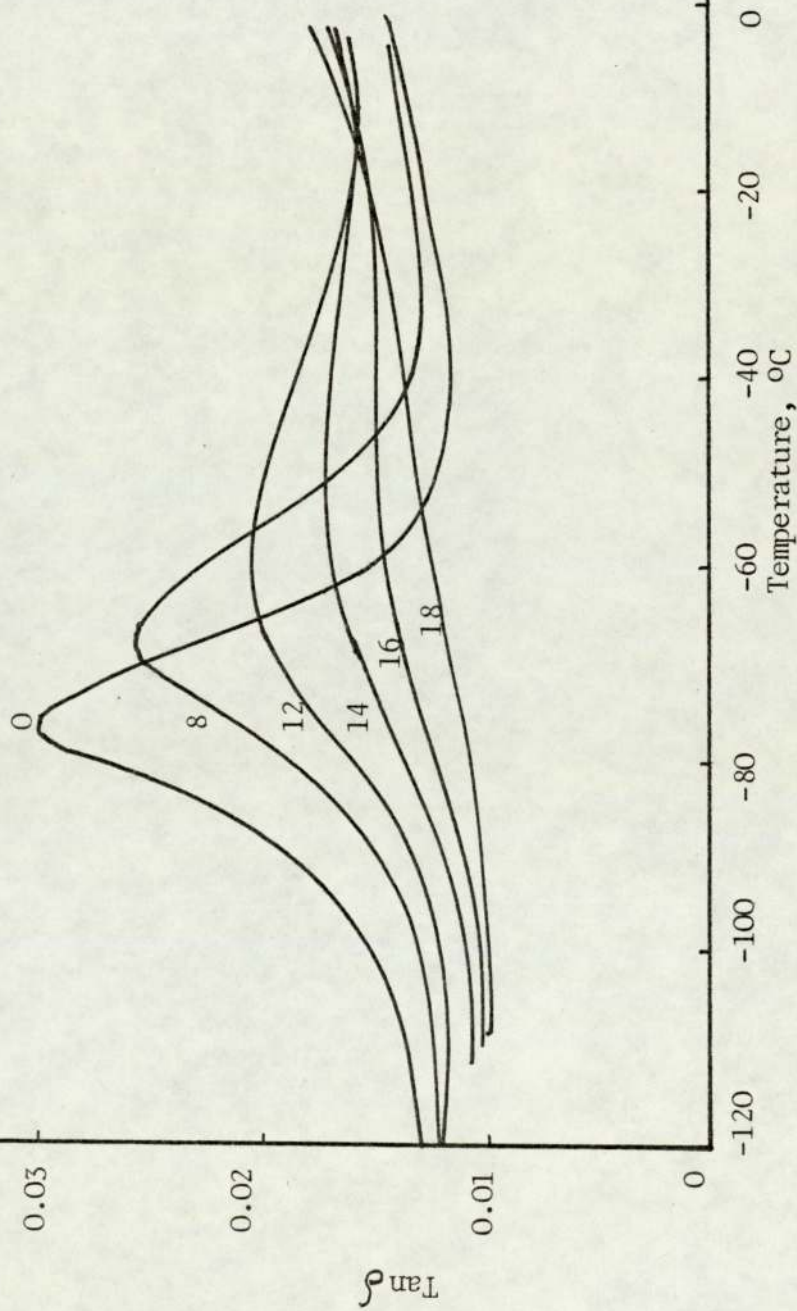
each time since only the rubber component in ABS is responsible
for the photodegradation of ABS leading to the deterioration of
its physical properties.

Similar results were obtained for commercial stabilised ABS
which are shown in Figs 3.11 and 3.12. The specimens were cut
from the compression moulded and extruded sheets. Tan δ reached
the maximum (0.028, 0.03) at -78°C and -80°C; the tan δ peaks
disappeared after 16 and 18 hours exposure to uv light for
compression moulded and extruded specimens respectively. The
plateau regions at lower and higher temperatures than the
rubber transition were similar to the unstabilised ABS. However
the length of the plateau region before the transition increased
and also tan δ at -50°C increased during uv exposure. The
width of the peaks increased and the apex shifted to higher
temperatures during uv irradiation.

3.6 Discussion

Infra-red spectroscopy is a useful non-destructive method which
can be used to follow degradation of a polymer film by measuring
changes in the functional groups. Examination of thin films by
transmission spectroscopy permits the course of the degradation
reaction to be followed without damage and the same area of the
film can be used repeatedly for test.

It can be seen from the infra-red spectra of unstabilised ABS

(Fig 3.1) that the absorptions at 3450 cm^{-1}, 1720 cm^{-1} and 965 cm^{-1} change during uv irradiation due to the increase in the hydroxyl and carbonyl group concentrations and decrease in the trans-1,4-polybutadiene concentration respectively. Fig 3.3 shows the changes in the functional group concentration against time of exposure to uv light for unstabilised ABS. This data shows that during the first 20 hours of exposure, only the unsaturation due to polybutadiene is affected. The decrease in the unsaturation is accompanied by an increase in the hydroxyl and carbonyl groups. The unstabilised ABS films did not show an induction period and a slow increase in the hydroxyl and carbonyl group concentration was followed by a rapid rise. Similarly, a slow decrease in unsaturation was followed by rapid decrease after 5 hours exposure. The commercial stabilised ABS showed similar results (Figs 3.4 and 3.5). The changes in the concentration of functional groups showed short induction periods due to the presence of commercial stabiliser.

Similar changes in the PBD component were observed by Scott et al[39] in HIPS and Fernando et al[75] in ABS. The log of the absorbance ratios of OH, C=O and trans-1,4-PBD to the nitrile (C≡N) group was plotted against time of exposure to uv light, (Fig 3.13). Under constant incident light intensity, trans-1,4-polybutadiene unsaturation is destroyed at a rate proportional to its concentration[81]. This can also be seen in Figs 3.14 and 3.15 which compare the destruction of 1.4-unsaturation of ABS films containing different concentrations of unsaturation.

Fig 3.13   Photo-oxidation of unstabilised ABS, log of indices
(C=O, OH, 1,4-C=C) against time of irradiation

106
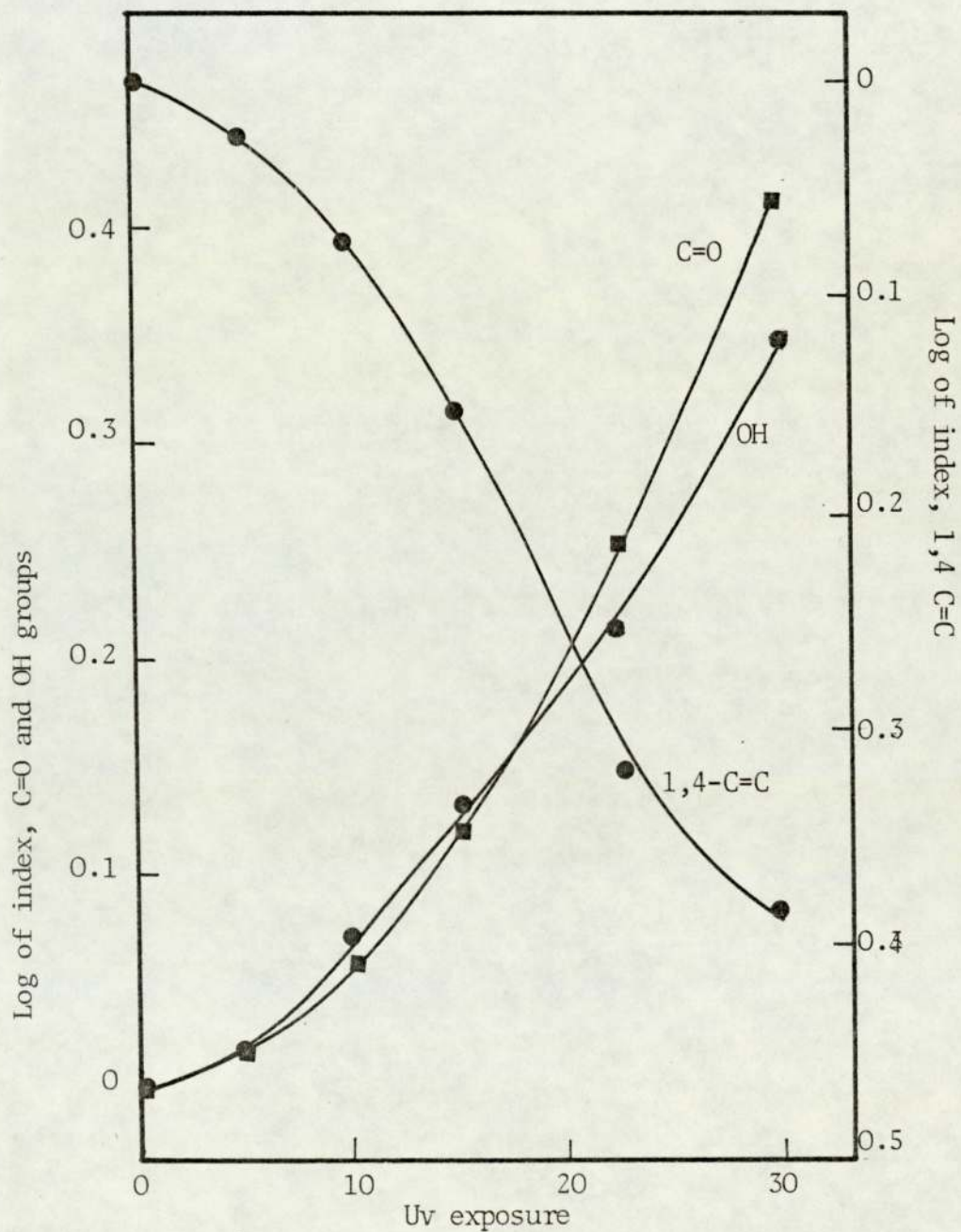
A similar result can also be seen in Fig 3.6 for impact strength decay during exposure to uv light. The impact test is a destructive test and errors occur due to specimen-to-specimen variation but these can be eliminated to some extent by repeating the test at least 15-20 times for each exposure to uv light.

There is a general agreement[75,82,83] that the polybutadiene component of ABS is the only moiety which is affected during exposure to uv light and that its destruction is accompanied by a rapid loss of physical properties such as impact strength. The degree of chemical degradation necessary to cause failure in the ABS films is slight since the unstabilised sample after 15 hours exposure to uv light loses 90% of its impact strength but only 30% of the intensity of its diene group concentration by infra-red spectroscopy. After 7 hours additional exposure to uv light, impact strength remained relatively unchanged whereas the diene concentration as measured by infra-red decreased to about 50% of its original value. It seems clear that the loss in toughness is due to an embrittlement in the surface. Oxidation starts from the surface of the film and the weight falling tester, the weight strikes on the surface of the film at a high speed and cracks propagate from the brittle surface of the film to the inner part of the film which there is still some rubber. Therefore, because of the fast crack formation in the surface of the film which in turn initiates crack propagation throughout the polymer film, a rapid loss in the impact strength is observed during the early stages of

Fig 3.14   Changes in the concentration of trans-1,4-PBD
component of ABS during photo-oxidation

☐   Unstabilised ABS, compression moulded film

●   Monsanto ABS, extrudate film

✪   Monsanto ABS, compression moulded film
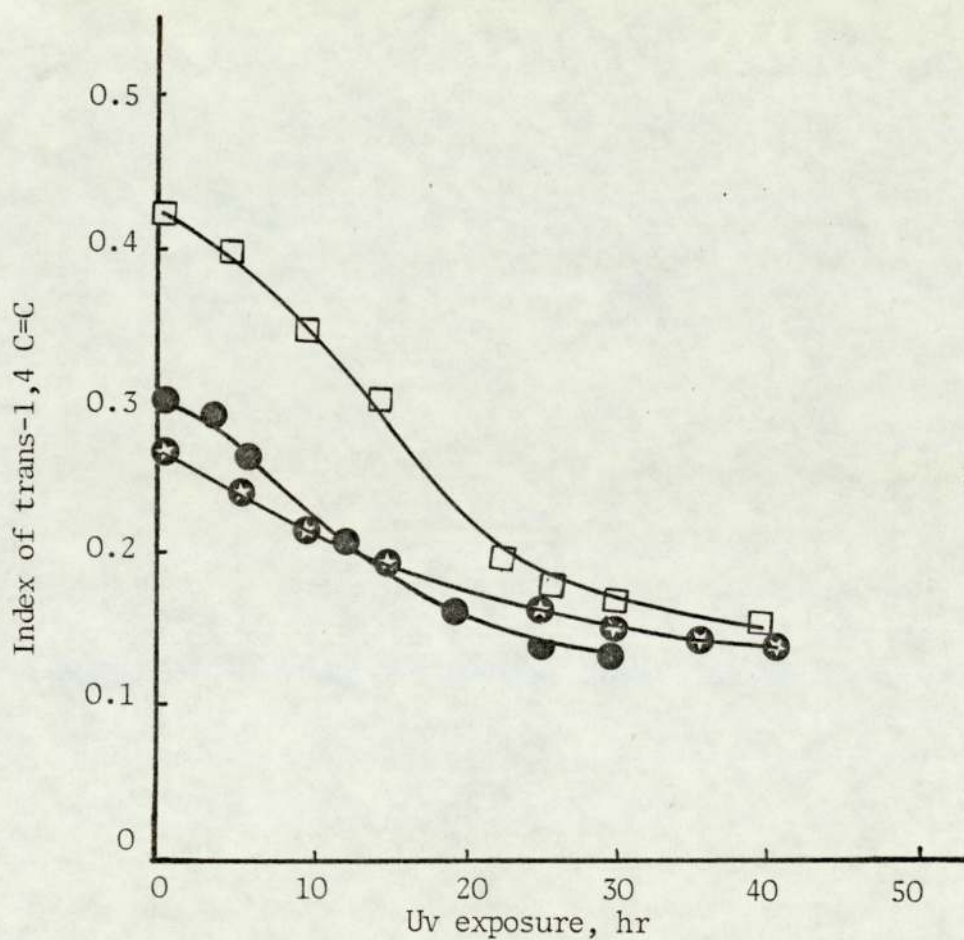
Fig 3.15 Rates of decrease of trans-1,4-PBD unsaturation
during photo-oxidation are compared

● Unstabilised ABS,
compression moulded film

■ Monsanto ABS,
extrudate film

▲ Monsanto ABS,
compression moulded film

Log I_t/I_0 trans-1,4- C=C

Uv exposure, hr
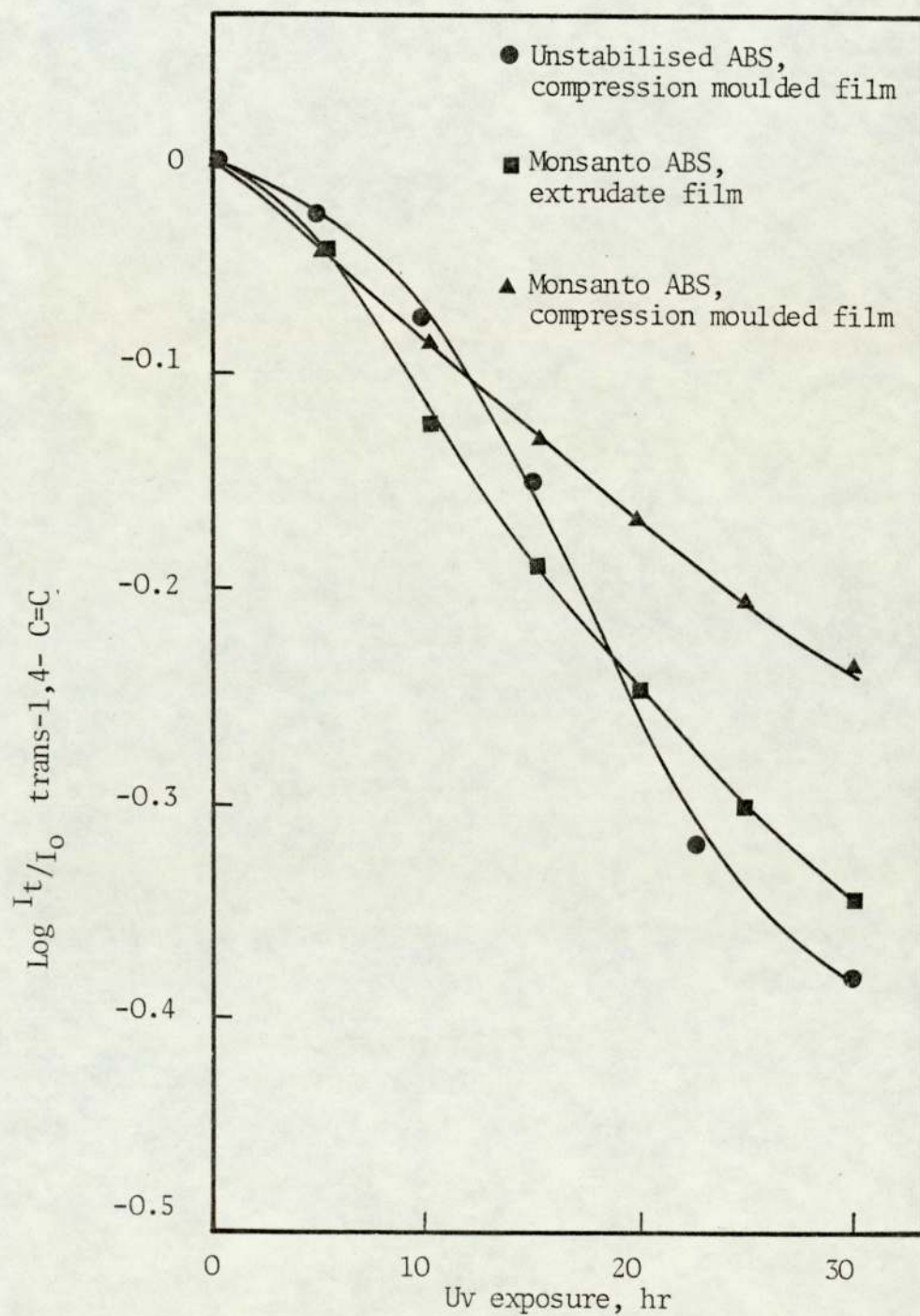
photodegradation. In spite of the difference in rate, similarity in the shape of the decay of rubber unsaturation and loss of toughness (Figs 3.17, 3.18 and 3.19) confirms the relationship between the loss of the elastic properties of the rubber and loss of the impact strength of ABS polymer during photodegradation. However, the loss of impact strength of ABS films on uv irradiation was initially faster and rapidly reached a limiting value (see Fig 3.6).

Compatibility of the rubber in the matrix is the primary pre-requisite for improved polyblend toughness. The directed scission of the grafted chains reduces the bonding between the phases, destroying the compatibility of the rubber in the matrix and this was suggested to be the reason for ABS loosing its toughness during artificial weathering[83]. As in the case of polybutadiene modified polystyrene, rapid photo-oxidation of the rubber phase appears to be the main cause of the rapid loss of toughness[84]. However, the photo-oxidation behaviour of ABS polymer could not be related merely to chain scission of the matrix since the extent of molecular weight reduction was small in the initial stages of the exposure[83]. The fast cross-linking of the polybutadiene phase contributes to the drastic loss of elasticity and energy absorbing properties. The cross-linking reaction was followed by Scott et al[85] by measuring gel formation and cross-link density. Gel formation, like hydroperoxide formation[86] showed no induction period and rose to a maximum. It was suggested that the initially formed

gel is peroxidic in nature and subsequently photolysis of peroxy gel leads to chain scission of the graft between polybutadiene and polystyrene.

Dynamic mechanical measurements have also been used to study structural changes in ABS during photo-oxidation. Dynamic mechanical properties were measured by means of the rheovibron and only one sample was used throughout photo-oxidation measurements. The damping behaviour of ABS films during photo-oxidation are shown in Figs 3.7, 3.8 and 3.9. The results were scattered at room temperature so at least five readings were taken for each period of exposure to uv light. This behavior (change in damping at room temperature) of ABS during photo-degradation can be explained by the theory of polymer elasticity. At early stages of the photo-oxidation, the molecular segments are free to move (elastic) and damping is low, as the photo-oxidation proceeds the number of the free molecular segments decrease due to cross-linking. Therefore part of the molecular segments are free to move and others are not, damping is high because some of the energy will be dissipated as heat. After the maximum damping, cumulative cross-linking takes place and damping decreases rapidly to a minimum. This cumulative cross-linking also corresponds to the rapid rise in the complex modulus. The damping behaviour at room temperature can also be explained from the chnages in the whole spectrum from -130 to +120°C. It was reported by Scott et al[39] that the main transition of HIPS, Tg of polystyrene shifted to the lower

Fig 3.16 Decrease in the maximum height of tan   peak at -80°C
          are shown against time of irradiation

■   Unstabilised ABS, compression moulded film

●   Monsanto ABS, extrudate film

▲   Monsanto ABS, compression moulded film

112
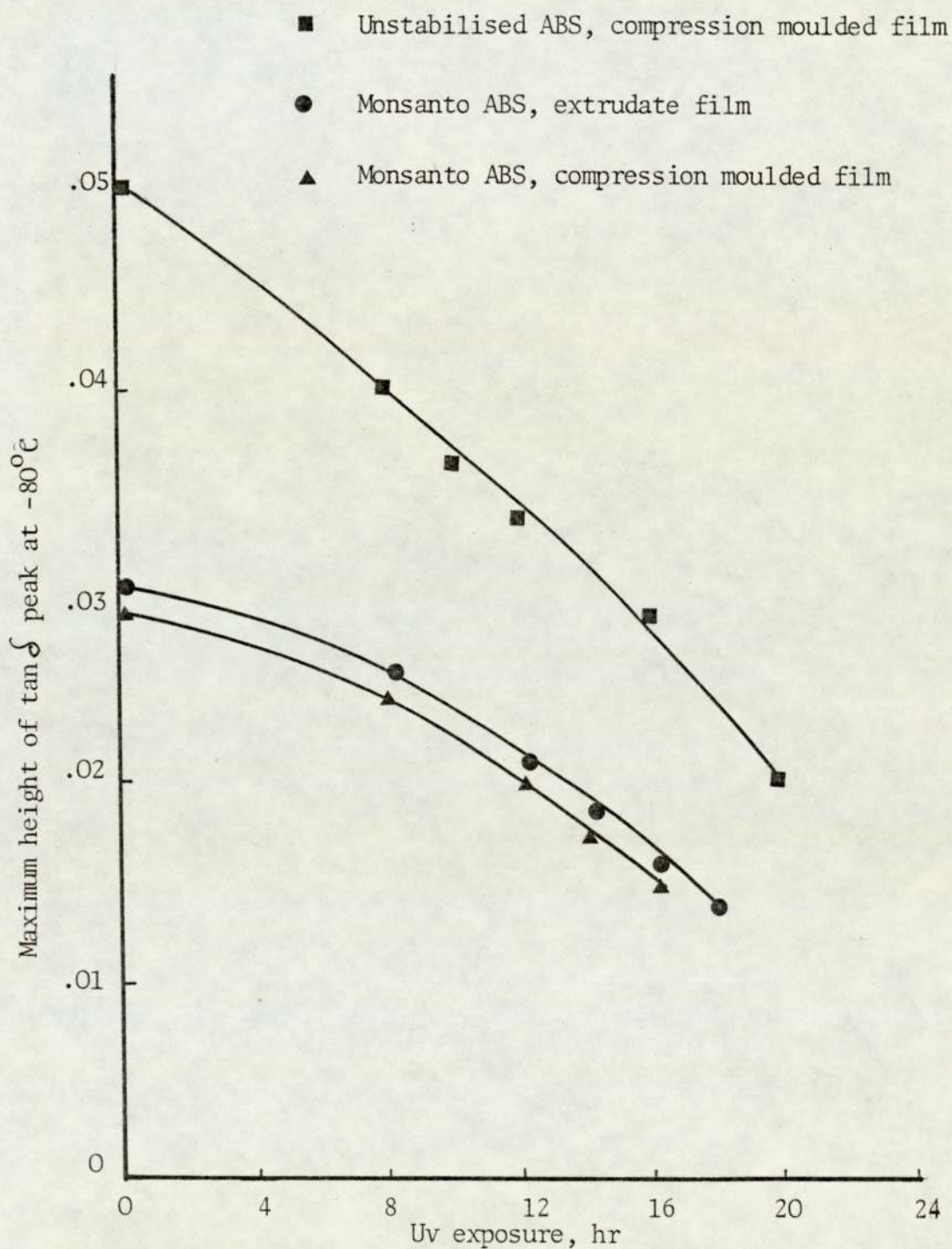
temperatures during photo-oxidation. When the low temperature damping peak disappeared the shoulder of the main transition shifted to $+50^{\circ}$C. The changes in damping at room temperature could be due to the shift of main transition to the lower temperature which might be due to plasticisation of SAN copolymer by rubber components which were separated from the matrix because of the chain-scission.

The complex modulus continues to increase until embrittlement point is reached which corresponds to the minimum $\tan\delta$. The complex modulus falls off slowly while the damping peak rises gradually, chain scission in the highly degraded polymer is likely to become predominant at this stage. The behaviour of impact strength and damping at 20°C during photo-oxidation are compared in Figs 3.7, 3.8 and 3.9. The impact strength has its lowest value when the damping reaches its maximum. This is consistent with the view that photodegradation starts from the surface of the film and is accompanied by cross-linking. Because of the surface cross-linked polymer crack propagation is very fast and causes a rapid failure throughout the polymer bulk. Thus the impact strength reaches its lowest value before the complex modulus reaches its maximum value. The low temperature damping of ABS films was measured by rheovibron. The temperature of the transition from a rubber to a glass (Tg) arises from segmental motion of molecular chains of PBD in ABS. The results of low temperature damping of ABS films during photo-oxidation are given in Figs 3.10, 3.11 and 3.12 for unstabilised ABS and

Fig 3.17 Changes in trans-1,4-C=C, impact strength and maximum
height of tan δ at -80°C for unstabilised ABS, compression
moulded film, are compared during photo-oxidation
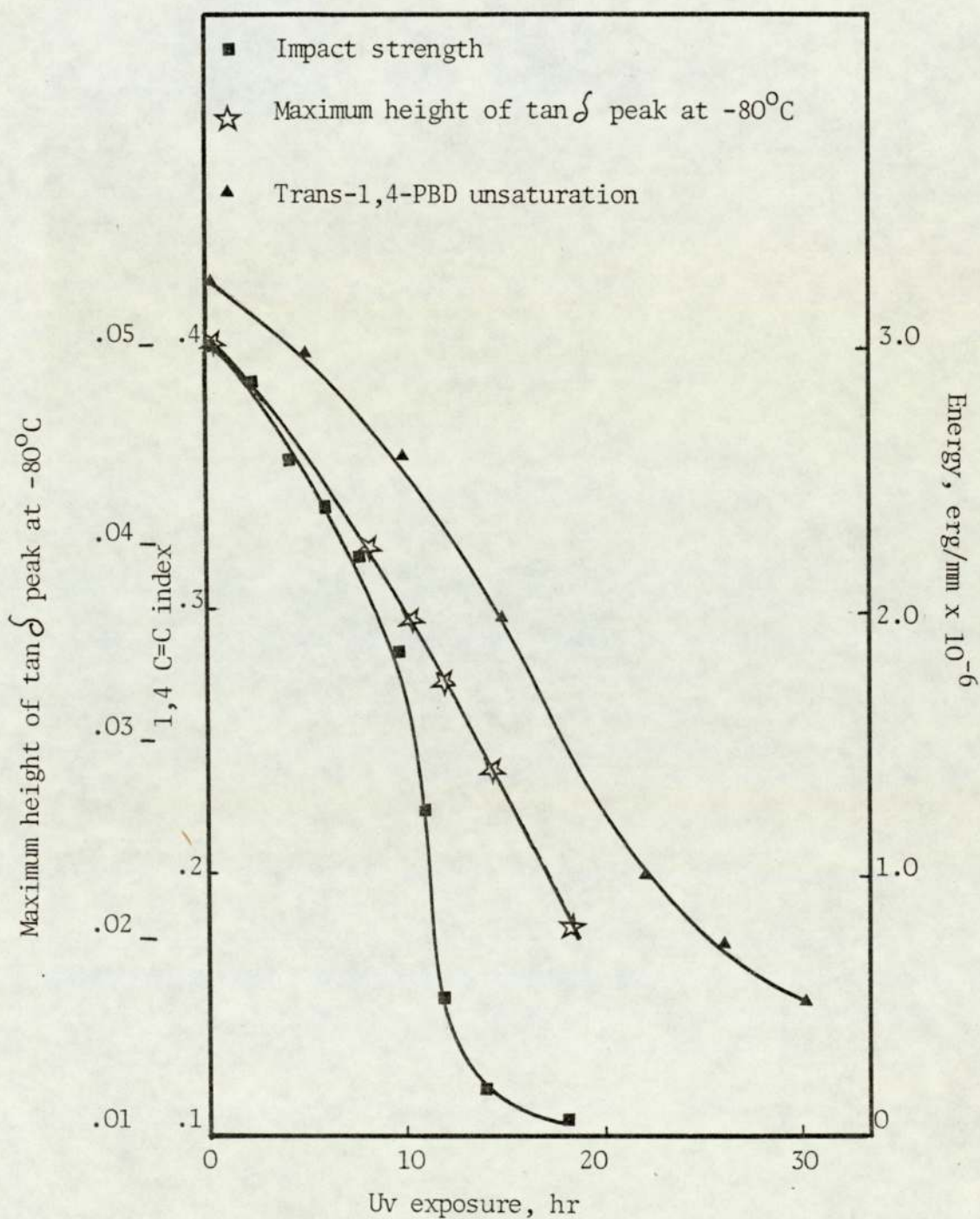
commercial stabilised ABS respectively. During the extrusion
of ABS the extrudate (see Section 2.3) was quench cooled from
+220 to +50°C. Under these conditions, segments of chains
aligned by drawing of the extrudate onto the rollers will become
'frozen' in the direction of the extrusion. Consequently
samples cut in this direction will consist of a prepondance of
segments orientated parallel to the length of the sample[39].

The extruded films have a higher impact strength (Fig 3.6) and
damping peak (Figs 3.11 and 3.12) than the compression moulded
films which may be related to the higher rubber content
remaining after processing in the extruded films, (Figs 3.14
and 3.15). The degree of degradation occurring during
extrusion seems to be less than that occurring during processing
in the torque rheometer followed by compression moulding.
Another factor which must be discussed is the crystallisation
of polybutadiene component of ABS during cooling to below
Tg. However, it was reported[39,87] that the presence of
grafted chains of butadiene in rubber modified polymers will
reduce the possiblity of rearrangement of segments to form
crystallites. For measurement of the low temperature damping
only one sample was used throughout the film exposure to uv
light and only one reading was taken every 2°C change in
temperature. The curves shown in Figs 3.10, 3.11 and 3.12 are
a representation of the rubber peak that exists as a separate
phase in ABS; the temperature is approximately the Tg of the
PBD[31,88-90].The height of the loss peak is proportional to

Fig 3.18 Changes in trans-1,4 C=C impact strength and maximum height of tan δ at -80°C for Monsanto ABS, compression mouldef film are compared during photo-oxidation
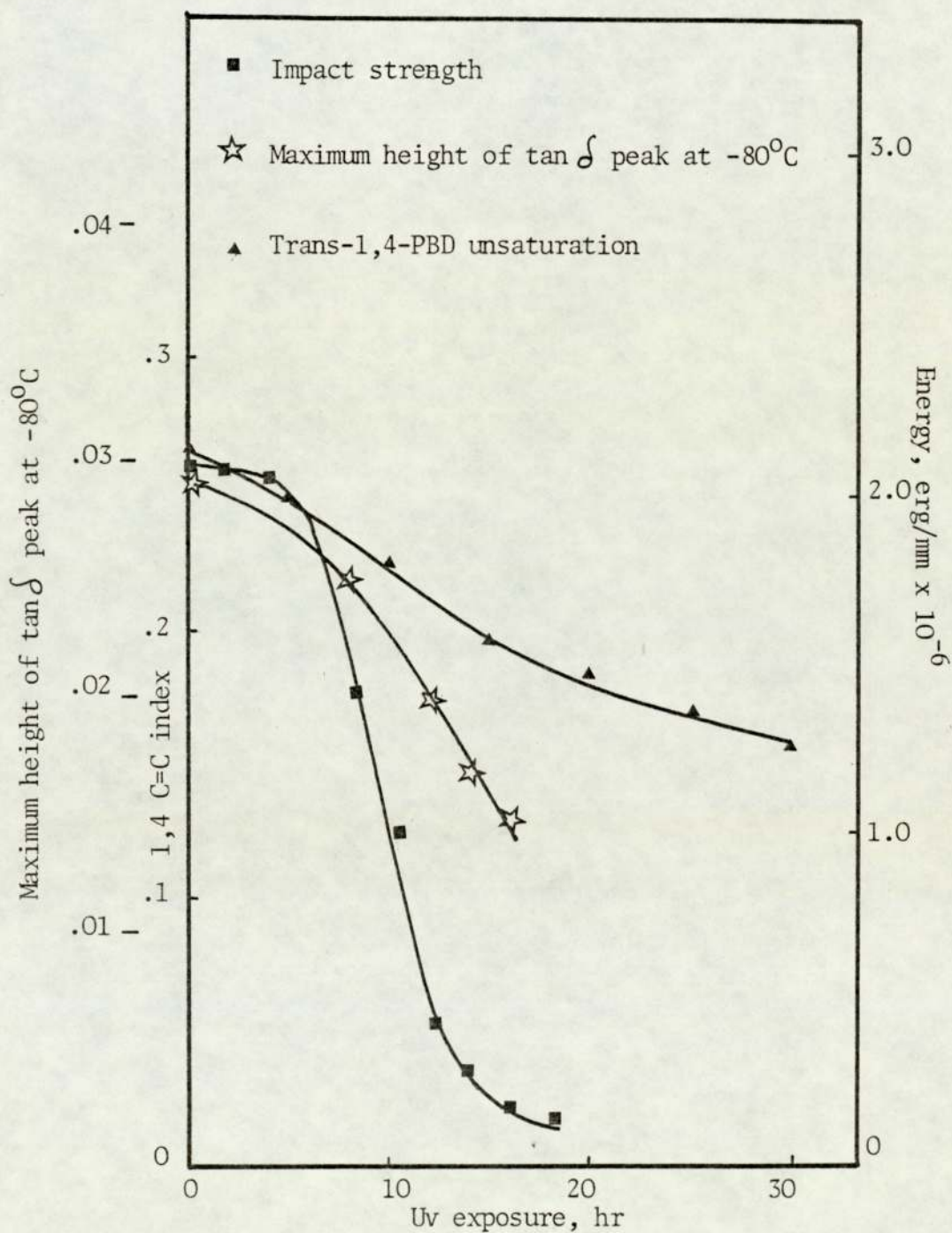
the amount of rubber present[23]. Exposure of ABS films to uv irradiation has the effect of reducing the concentration of rubber to zero. Reduction in the concentration of rubber during photo-oxidation is therefore accompanied by a decrease in the height of the low temperature damping peak. The damping at low temperature (Tg of PBD) goes through a maximum and then a minimum for a material containing rubber component such as ABS polymer. At low temperatures, there is no molecular motion of the chain segments (stiff spring) because _ the chain segments are completely frozen in, damping is low. At temperatures above the glass transition region, the chain segments are completely free to move (elastic material), damping is low. In the transition region, the damping is high because some of the molecular chain segments are free to move while others are not. Thus every time a stressed, frozen-in-segment becomes free to move, its excess energy is dissipated as heat. It is character-istic of the transition region that only part of the molecular segments are free to move. The low temperature damping (tanδ) cannot be measured when the concentration of rubber is very low (approaching zero) because the sample is brittle at low temperature. The shift of the rubber peak (at low temperature) to higher temperatures during expousre to uv light is consistent with extensive cross-linking in the PBD phase in ABS. The broadening of the damping peak indicates an increase in the molecular weight distribution of the PBD as a result of cross-linking. The increase of the damping above Tg is suggested to be a result of a further decrease in the molecular weight

117

Fig 3.19

Fig 3.19   Changes in trans-1,4-C=C impact strength and maximum
            height of tan δ at -80°C for Monsanto ABS extrudate
            film are compared during photo-oxidation

118
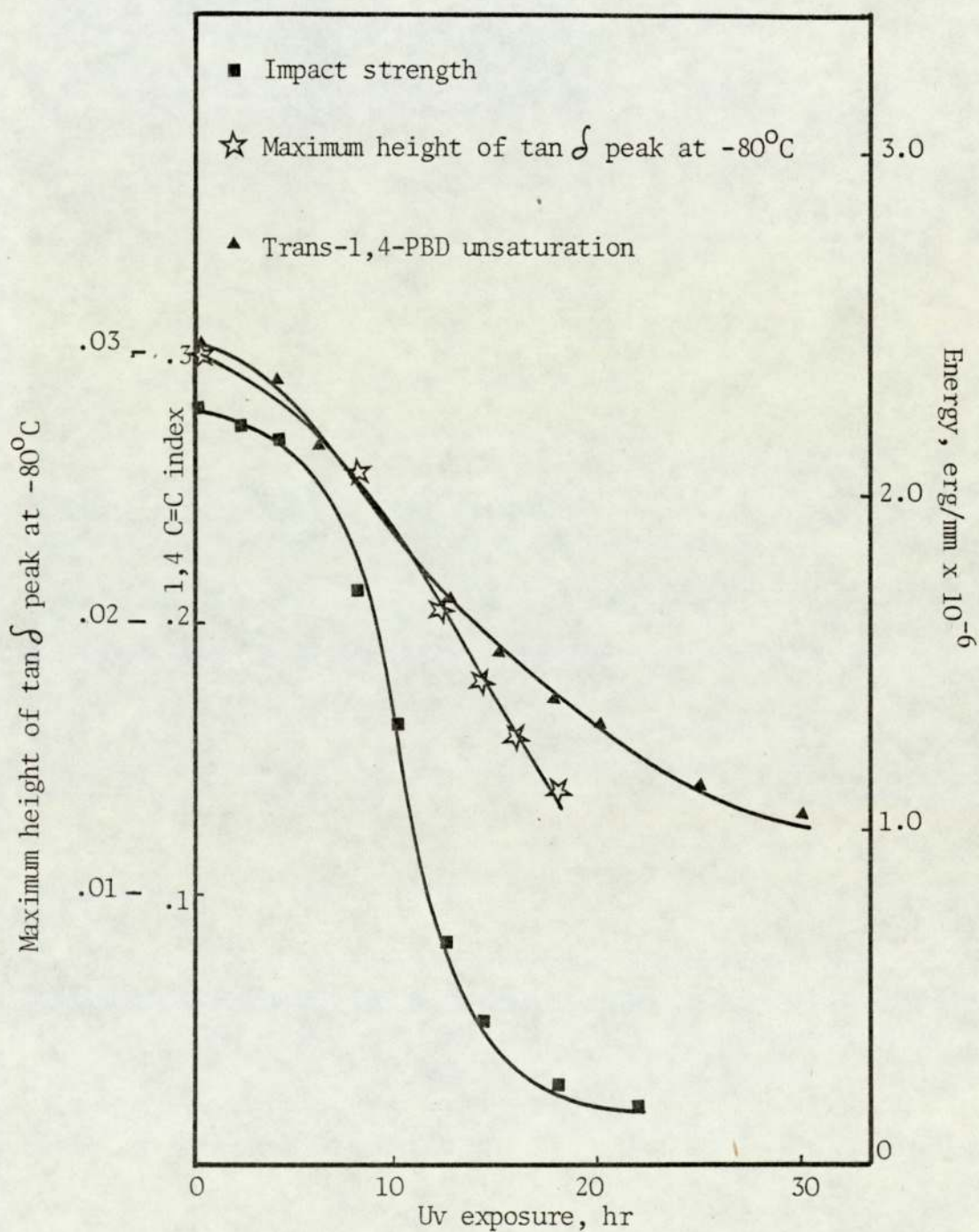
of the polymer[91]. The maximum height of low temperature

damping peak were plotted against time of exposure (Fig 3.16).

The height of the damping peak reduced to its lowest value after

18 hours exposure to uv light for unstabilised ABS film, which

corresponds to the maximum tan δ at 20°C and the lowest value of

impact strength. At the same time by comparing the loss of

unsaturation in PBD, impact strength and the maximum height of

damping peak at low temperature, (Figs 3.17, 3.18 and 3.19) it

can be seen that after 10 hours exposure, only 20% of

unsaturation and tan δ are lost whilst at the same time, about

50% of impact strength is lost. It may be concluded from these

observations that unsaturation and tan δ related to bulk properties

of polymers whereas impact strength is a formation of surface

properties.

The mechanism of photodegradation of ABS has been examined by

several workers[40,42,92-94,81]. Oxygen absorption of ABS

samples has been studied under 3650 A° light, in oxygen at 50°C

the initial oxidation was reported to be very important for ABS

resins since they were brittle by the time they consumed 10 cc

of oxygen per gram of compound[94]. It has been reported[40,75,95]

that the decrease of trans-1,4-polybutadiene structure was due

to the photolysis or dissociation of the C-C bond of α-methylene

of the poly-trans-1,4-butadiene structure.

In the present work, the olefinic band at 965 cm^{-1} disappeared

very rapidly after an auto-accelerating period while the hydroxyl

and the carbonyl bands grew in a similar mode (see Figs 3.3, 3.4 and 3.5). The hydroxyl peak reached a maximum on disappearance of the double bonds whilst saturated carbonyl continued to grow. First order plots (Figs 3.13, 3.15) showed that the rate of disappearance of trans-1,4-butadiene unsaturation in ABS is comparable with that of hydroxyl formation. On the other hand, the carbonyl formation was considerably slower, consistent with the observation that in PBD modified polystyrene carbonyl compounds are secondary breakdown products of hydroperoxide[86]. ABS undergoes considerable changes during processing, particularly loss of unsaturtion[83]. A large carbonyl peak developed during processing, centred at 1710 cm^{-1} with a shoulder at 1730-1740 cm^{-1}. Consequently, this film photo-oxidised with almost no induction period.

The function of PBD in the photo-oxidation of rubber modified polystyrene has been discussed in some detail[48,84-86]. The present results, together with the previous work lead to the following conclusions:

(1)   The rubber segment is the initial point of attack of oxygen, giving rise to allylic hydroperoxides.

(2)   The rubber component acts as a photo-activator for the photo-oxidation.

(3)   Photolysis of hydroperoxides leads to cross-linking of the rubber component by addition of alkoxy radicals to 1,2-PB groups and conjugated carbonyl formed by alkoxy

radical breakdown.

(4)   Cross-linking destroys the elastomeric properties of the rubber phase with loss of the impact resistance of the polymer and damping peak at low temperature.

(5)   Thermal processing activates polybutadiene modified polymers to photo-oxidation by introducing photo-sensitising hydroperoxides into the polymer.

Therefore the mechanism of photo-oxidation of rubber modified polystyrene which was suggested by Scott et al[39,84] is consistent with the discussed results. This mechanism is given in Scheme 1.

3.7 Correlations between Rubber Content, Damping Peak and Impact Strength of Unsatabilised ABS during Photodegradation

The maximum value of $\tan \delta$ at low temperature during uv exposure of unstabilised and commercial stabilised ABS plotted together with the loss of impact strength and tran-1,4-PBD against time of exposure in Figs 3.17, 3.18 and 3.19. All the specimens were exposed to uv light under identical conditions. $\tan \delta$ decreases from the onset of exposure to uv light and begins to level out after 18 hours exposure (Fig 3.17) but does not fall to zero. It is clear that the initial rate of decay of trans-1,4-polybutadiene is similar to rate of disappearance of the $\tan \delta$ peak. (After 30 hours uv exposure, trans-1,4-polybutadiene levels out and indicates less decrease.) The rate of disappearance

121

Scheme 1   Mechanism of photo-oxidation of unstabilised ABS

Grafted styrene-acrylonitrile copolymer to
butadiene rubber

Abstraction of tert allylic
hydrogen by alkoxy radical

Alkyl radical (stabilised
by resonance)

Peroxy radical

Tert allylic hydroperoxide

Alkoxy radical

Allylic alcohol (3400 cm^{-1})

Conjugated ketone (1685 cm^{-1}) (separation of SAN + PBD
chains)

$\xrightarrow[\text{(b)}]{\beta\text{-scission}}$

$CH=CH_2$ $\quad \dot{C}H_2$

$+$

O $\quad CH=CH$

C

SAN
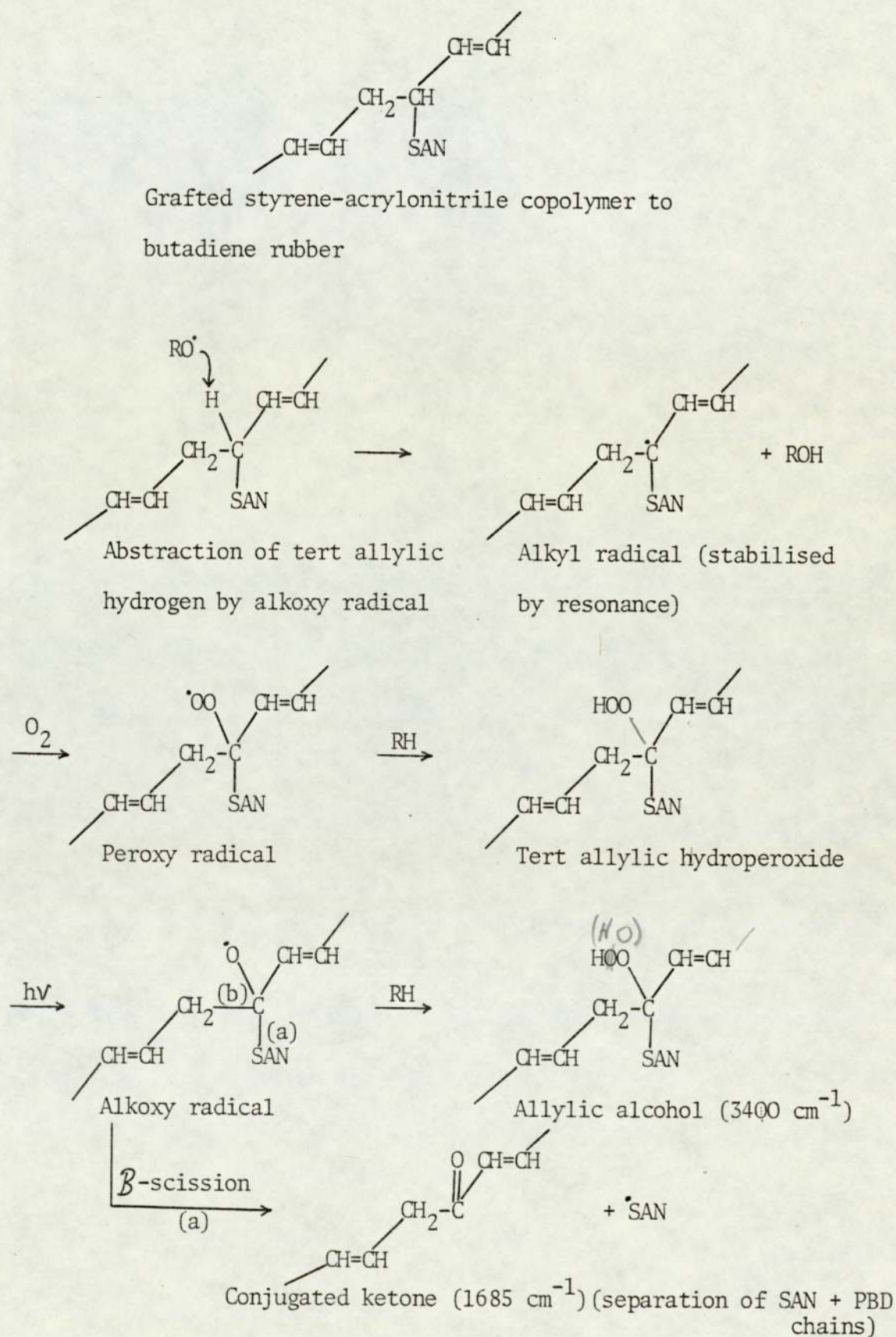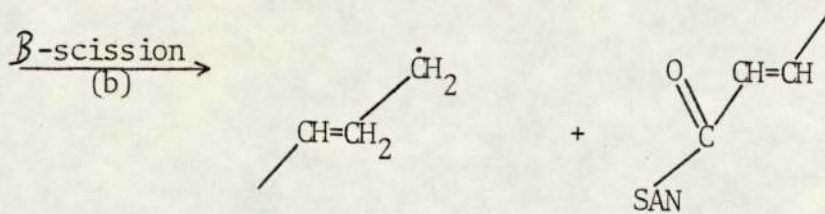
Formation of peroxidic gel:

$\dot{O}O$ $\quad CH=CH$

CH_2-C

$CH=CH$ $\quad SAN$

Peroxy radical

$\xrightarrow[R'CH=CH_2]{1,2-PB}$

$R'\dot{C}HCH_2OO$ $\quad CH=CH$

CH_2-C

$CH=CH$ $\quad SAN$

$\xrightarrow{O_2/RH}$

OOH

$R'CHCH_2OO - CH=CH$

CH_2-C

$CH=CH$ $\quad SAN$

$+ R^{\cdot}$

Peroxy gel (cross link)

$\downarrow h\nu$

$\dot{O}$ $\quad CH=CH$

CH_2-C

$CH=CH$ $\quad SAN$ (RO·) alkoxy radical

$\downarrow$

O $\quad CH=CH$

CH_2-C

$CH=CH$

$+ \dot{S}AN$

123

Formation of ether gel:

CH=CH

CH$_2$-C O CH=CH

‖
O

+

ċH$_2$-C Ȯ CH=CH

CH=CH SAN

$\xrightarrow{O_2/RH}$

OOH

O CH-CH

CH$_2$-C O CH=CH
‖
O

CH=CH CH$_2$-C

CH=CH SAN

+ R·

Ether gel (cross-link)

or

Ȯ CH=CH

CH$_2$-C SAN

CH=CH

+

CH=CH

CH-Ċ
|
CH=CH SAN

$\longrightarrow$

SAN CH=CH

CH$_2$-C

CH=CH O CH=CH

CH$_2$-C

CH=CH SAN

Ether gel (cross-link)

124

of the low temperature peak and decay of trans-1,4-polybutadiene
is similar to the loss of impact strength in the early stages
of uv exposure but impact resistance drops more sharply in
further irradiation. The reason seems to be the effect of
brittle surface of the films on the rate of crack propagation
in the whole polymer system and also to differences to the
techniques of measurements. Impact strength is a high speed
measurement on the surface of the film, viscoelastic properties
are measured at very low strain in the bulk of the polymer in
the linear region and in the infra-red measurements, specimens
are under no stress. Figs 3.7, 3.8 and 3.9 show correlation
between the maximum value of $\tan\delta$ at -80°C and $\tan\delta$ at
ambient temperature during exposure to uv light. It is observed
that $\tan\delta$ at 20°C reaches its maximum at the same time that the
damping peak height at -80°C drops to its lowest level. (The
temperature at which this peak occurs shifts during uv
irradiation, however, it is the maximum value of $\tan\delta$ for each
curve that is referred to in the figures). The maximum in tan
at 20°C also corresponds to the lowest value of impact strength
(see Figs 3.7. 3.8 and 3.9).

An attempt was made to correlate impact strength and trans-1,4-
polybutadiene unsaturation (Fig 3.20). The maximum value of
$\tan\delta$ at low temperature and trans-1,4-polybutadiene
unsaturation (Fig 3.21) and impact strength and maximum value
of $\tan\delta$ at low temperature (Fig 3.22).

125

Fig 3.20 Correlation curves between impact strength and trans-1,4-PBD unsaturation of ABS during photodegradation

■ Unstabilised ABS, compression moulded films

★ Monsanto ABS, compression moulded films

● Monsanto ABS, Extrudate film.
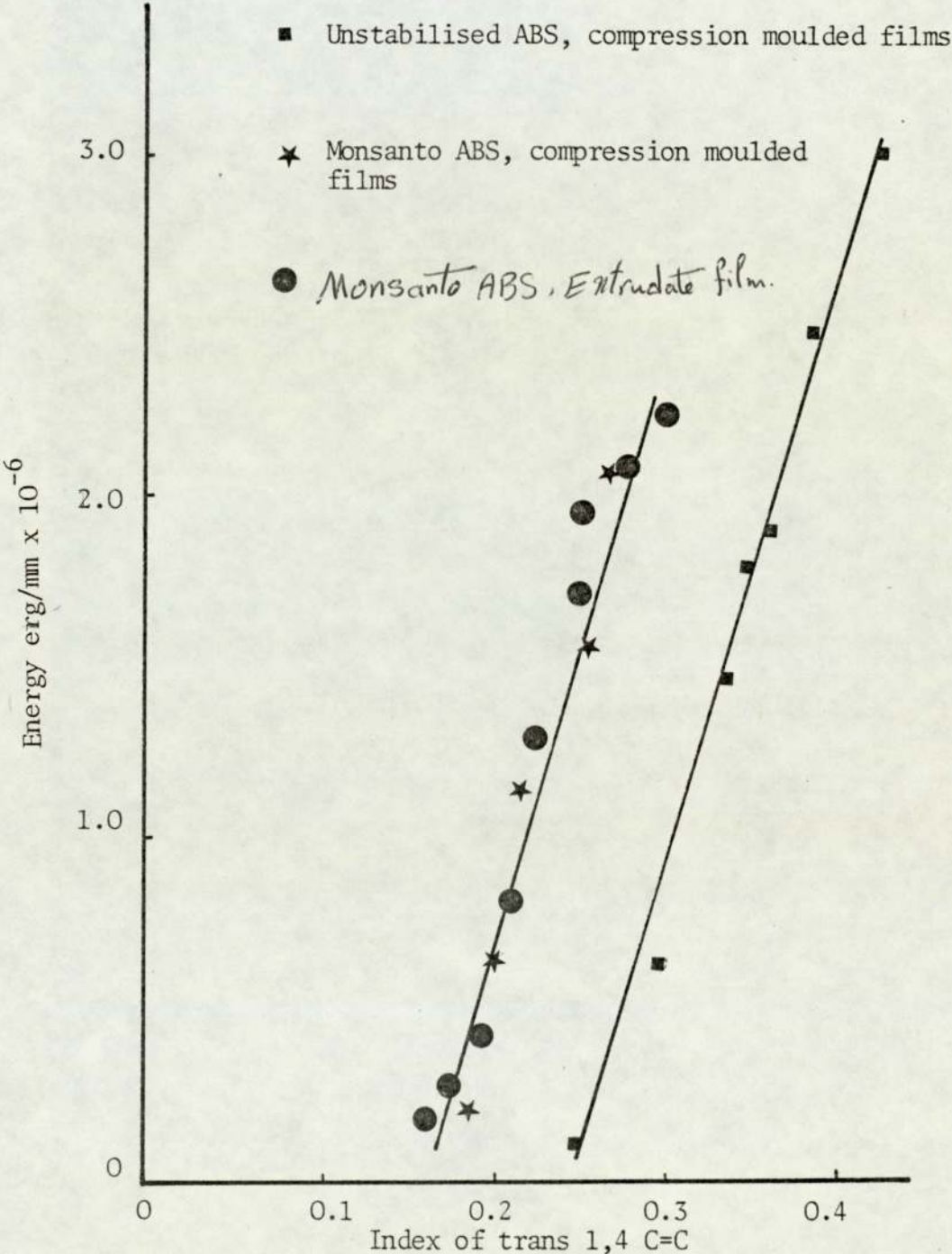
It has been previously reported[96] that the area under the damping peak is directly proportional to the concentration of the rubber component and the greater the drop in modulus in the rubber transition region, the greater is the toughening component. It was found that the falling weight impact strength correlated well with toughness as measured by high speed[97] (8000 in/min) test and with the toughness (integrated stress-strain curve) obtained on an Instron at its highest cross-head speed[98] (0.333 in/sec). It has also been reported[27,88,99] that the magnitude of the rubber peak (damping peak at transition temperature) is related to both the quantity of rubber present and the impact strength of the rubber modified polymer.

Linear relationships (Figs 3.20, 3.21 and 3.22) exist between the maximum value of tan δ at low temperature, impact strength and rubber concentration in the polymer during photo-oxidation. These results indicate that the damping properties at low temperature and impact strength are related to the toughening agent, rubber, in the rubber-modified ABS and that because of destruction of rubber during photo-oxidation, these two properties are also destroyed. Therefore, Fig 3.20 shows that, for ABS having a particular composition, morphology and method of preparation, the damping peak can provide an indication of the rubber concentration during photo-oxidation and vice-versa. The correlation shown in Fig 3.22 indicates that within these same limitations, the dynamic properties also provide an

Fig 3.21   Correlation curves between trans-1,4-PBD unsaturation
            and maximum height of tan δ peak at -80°C of ABS during
            photodegradation

Trans-1,4 C=C unstabilised ABS

● Unstabilised ABS compression moulded film

■ Monsanto ABS, extrudate film

✫ Monsanto ABS compression moulded film

Maximum height of tan δ peak at -80°C Monsanto ABS

Maximum height of tan δ peak at -80°C unstabilised ABS

Index of trans-1,4 C=C Monsanto ABS

128
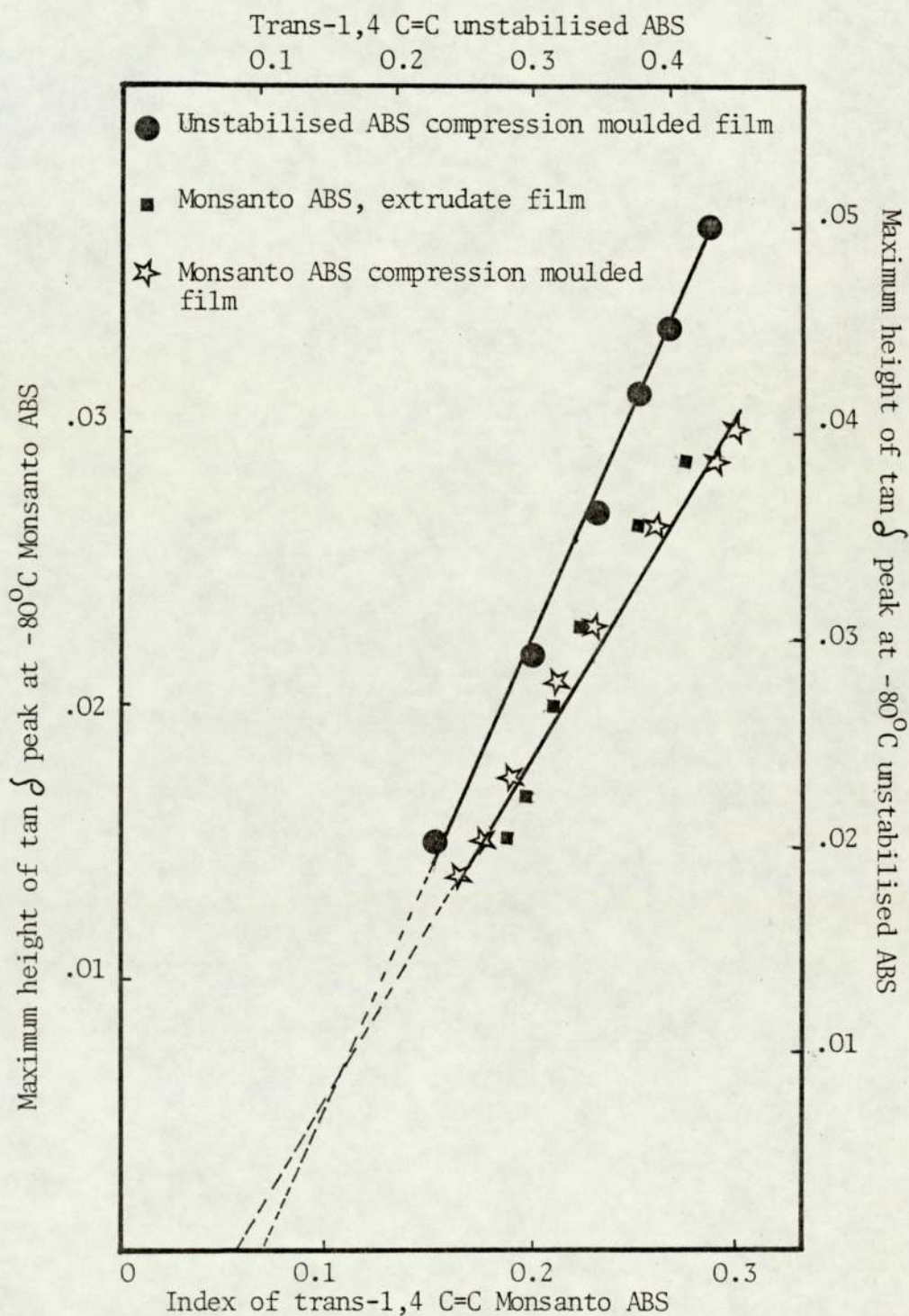
indication of impact strength during photo-oxidation.

Non-destructive testing has become increasingly useful for
obtaining information about the influence of factors such as
molecular composition and molecular weight upon mechanical
properties. In a destructive test (impact test) the amount of
information available is limited because once an impact test
piece is broken no more information can be obtained on that
sample. Dynamic elastic results may be quoted to $\pm$ 5% with
confidence, an accuracy which is not normally associated with
standard destructive tests, particularly during degradation,
where other factors such as cross-linking are involved. The
sample is not broken and repeat results can readily be obtained.
This feature represents another advantage of non-destructive
testing of the rheovibron type.

If a plastic is being subjected to environmental ageing, then,
to carry out destructive tests at intervals requires a large
stock of samples to be aged simultaneously in order to enable
the required number to be broken at each test. The advantage
of using a non-destructive test for routine testing has a clear
advantage. It is important to note that although polymers
generally show strain-dependence and non-linearity in their
mechanical properties, such effects are not apparent at the
low levels of strain at which dynamic mechanical experiments
are carried out. As a result of this work on ABS polymer, it
appears that a linear relationship exists between impact strength

Fig 3.22 Correlation curves between impact strength and maximum
height of tan δ peak at -80°C for ABS during photodegradation

■ Unstabilised ABS compression moulded film

✶ Monsanto ABS compression moulded film

◎ Monsanto ABS extrudate film
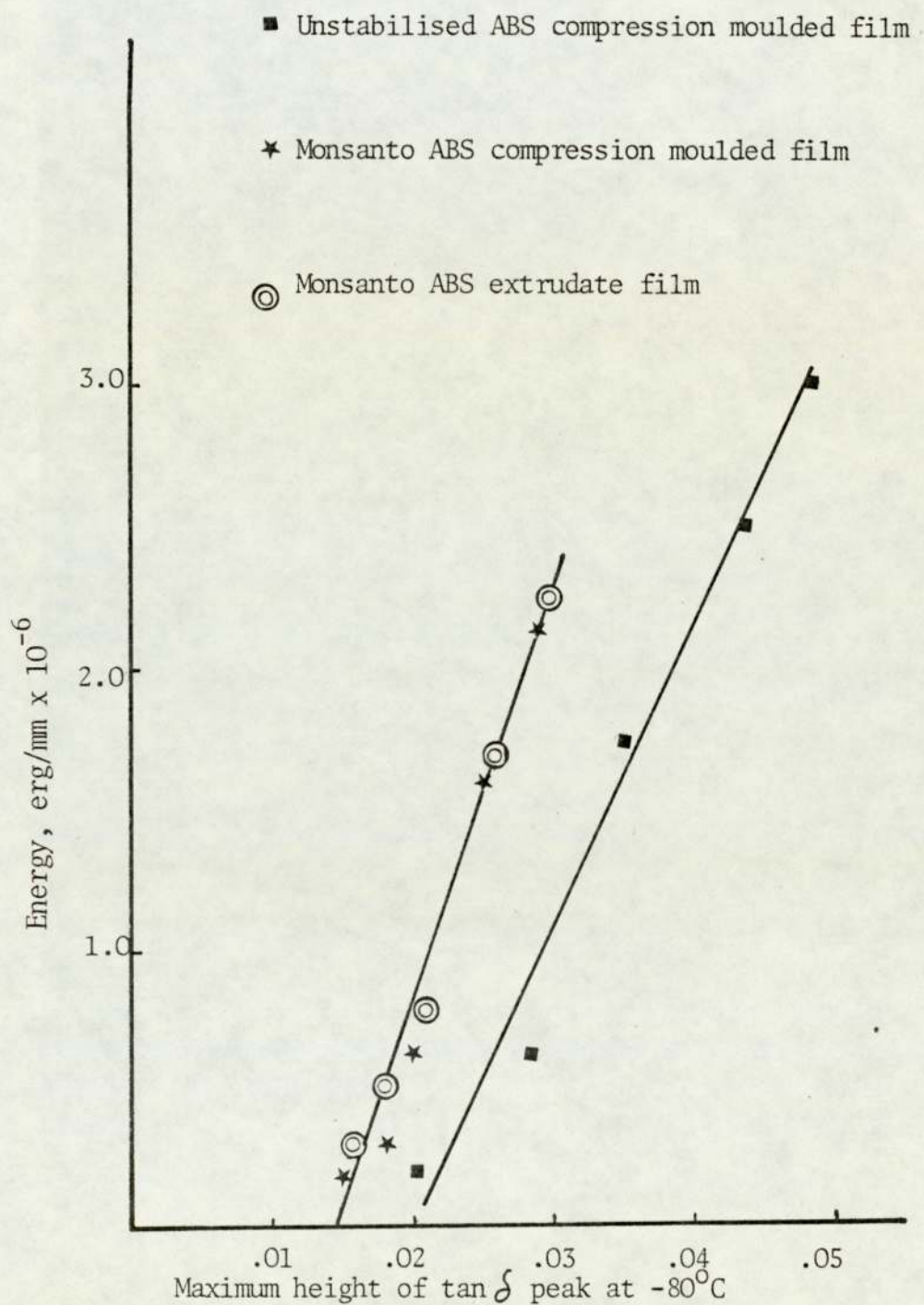
and dynamic mechanical properties at low strains.

3.8 Thermal-oxidative Degradation of Unstabilised ABS

Compression moulded unstabilised ABS films were oven aged at
$100^{\circ}C$ in air and the changes in the concentration of functional
groups were monitored by infra-red spectroscopy, impact strength
by falling weight tester and low temperature damping by
rheovibron viscoelastometer.

3.8.a Infra-red Measurements

The carbonyl and hydroxyl groups showed an induction period of
4-5 hours at $100^{\circ}C$ in an air oven. The rapid development of
these, after the induction period was quite similar to that
observed on photo-oxidation. The decay of trans-1,4-polybutadiene
absorption also showed an induction period of about 4 hours. No
changes in the absorption bands of nitrile and phenyl group
were observed during this period of ageing. The changes in the
functional groups (C=O, -OH, 1,4 C=C) are shown as ratios to
the absorption of nitrile (C≡N) group at 2220 cm^{-1}, against
time of heating (Fig 3.23).

3.8.b Impact Strength Measurements

The impact strengths of unstabilised ABS films of identical
thicknesses were measured during oven ageing at $100^{\circ}C$ in air by

Fig 3.23 Thermal oxidation of unstabilised ABS, heating temperature 100°C in air

132
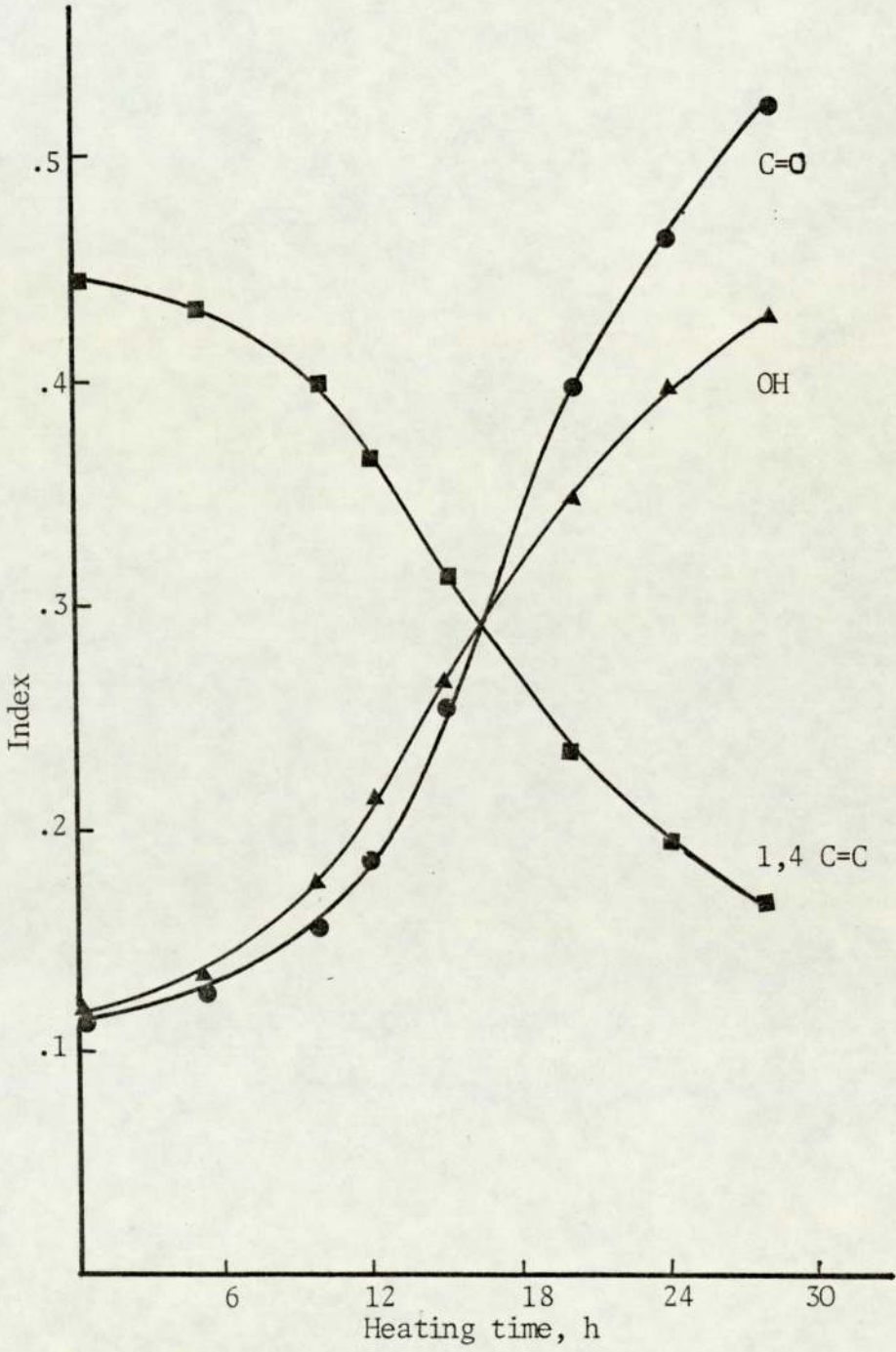
falling weight impact tester. The impact strength showed an induction period about 4 hours, then a sharp fall and reached the lowest value after 18 hours of ageing (Fig 3.25).

3.8.c Measurement of Low Temperature Damping

The change in the height of low temperature damping at $-80^{\circ}C$, was measured by rheovibron during oven ageing at $100^{\circ}C$ in air. Only one sample was used throughout the measurement with thickness identical to those which were used for infra-red and impact strength (0.075 mm). The ageing of this sample was interrupted frequently for low temperature damping measurements. The method used was similar to that used for photo-oxidation. The temperature range was from -120 to $0^{\circ}C$ and the reading of $\tan \delta$ was carried out while the temperature of sample was allowed to rise to $0^{\circ}C$. As can be seen in Fig 3.24 the change in the height of $\tan \delta$ and shift to higher temperature during thermal oxidation is similar to that observed during photo-oxidation. After 20 hours heating, $\tan \delta$ levelled out with more ageing there was no change in height and samples could not normally be further tested at low temperature after 20 hours ageing due to the fracture.

3.8.d Discussion

During the ageing of ABS at $100^{\circ}C$ the nitrile and phenyl absorbances did not change but oxidative products containing

133
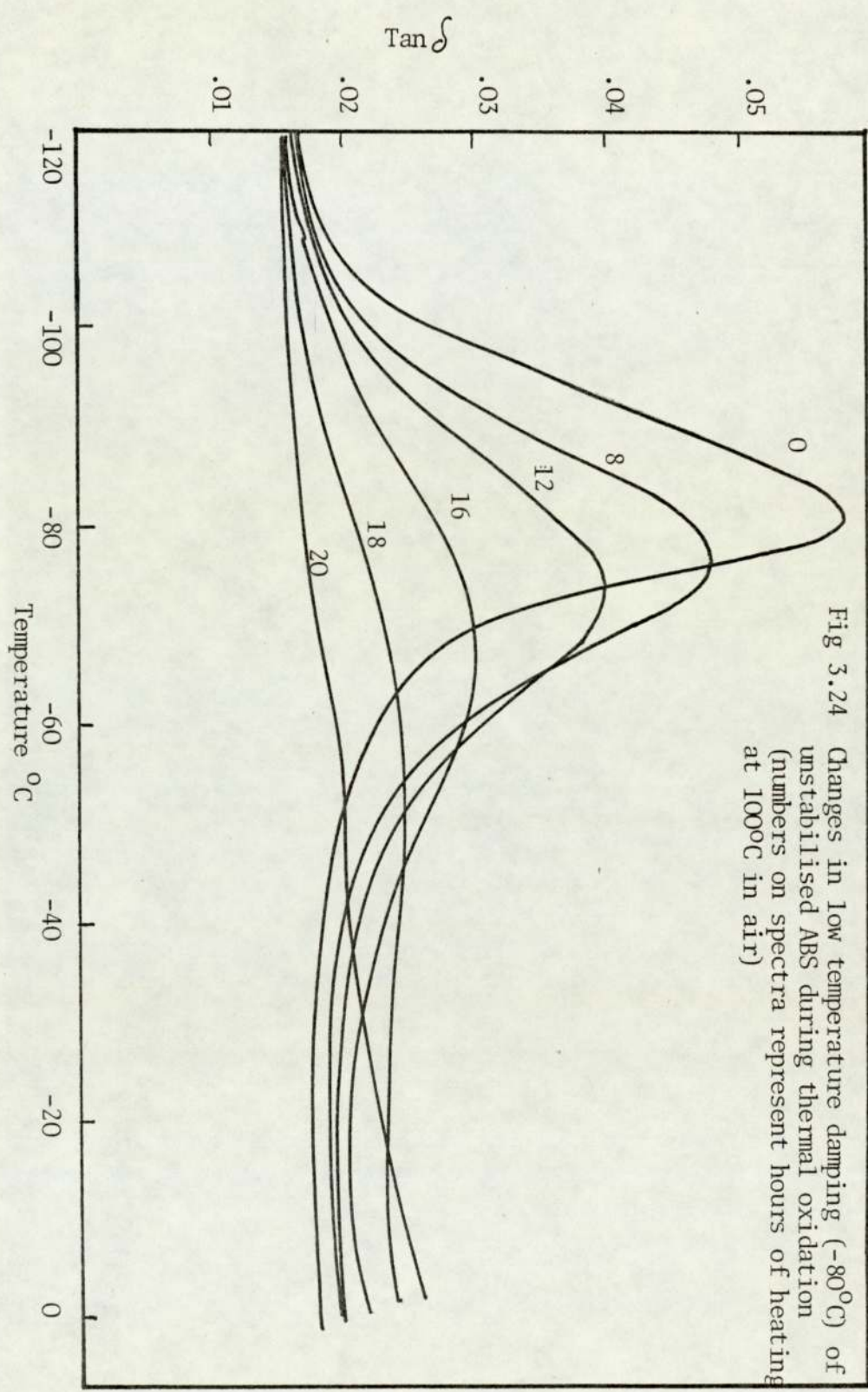
Fig 3.24 Changes in low temperature damping (-80°C) of
unstabilised ABS during thermal oxidation
(numbers on spectra represent hours of heating
at 100°C in air)

134

hydroxyl and carbonyl groups were produced rapidly and the butadiene content decreased at a similar rate. It was observed that the physical properties, such as impact strength of the ABS polymer aged at $100^{\circ}C$ in air show conspicuous deterioration. The effects are recognised to be due mainly to chemical changes brought about through thermo chemical reactions occurring primarily on the surface of the polymer. The surface changes in the film have a striking effect on the impact strength of the bulk polymer. Comparison of impact strength with trans-1,4-polybutadiene during thermal ageing show that after 18 hours oxidation only 44% of unsaturation disappeared whilst at the same time 86% of impact strength is lost (Fig 3.25). Shimada and Kabuki[41] reported that the initiation process occurring in ABS during thermal oxidation involves the formation of hydroperoxides induced by radical formation and the subsequent degradation process are initiated by the decomposition of hydroperoxides.

The formation of hydroperoxide in HIPS was determined iodometrically by Scott et al[39] on oven ageing. They found that the initial concentration of hydroperoxide increased linearly without an induction period and reached a maximum concentration. With further heating the hydroperoxide concentration fell at a similar rate to that of its formation. With the decay of hydroperoxides after attaining a maximum concentration, the other functional groups, OH and carbonyl, begins to develop rapidly. It is generally believed that the same radical chain

135

Fig 3.25 Impact strength, trans-1,4 C=C and maximum height of
tan   peak at -80ºC of unstabilised ABS are shown
against time of heating

■ Impact strength

● Maximum height of tan δ peak at -80°C

▲ Trans 1,4-PBD unsaturation

136
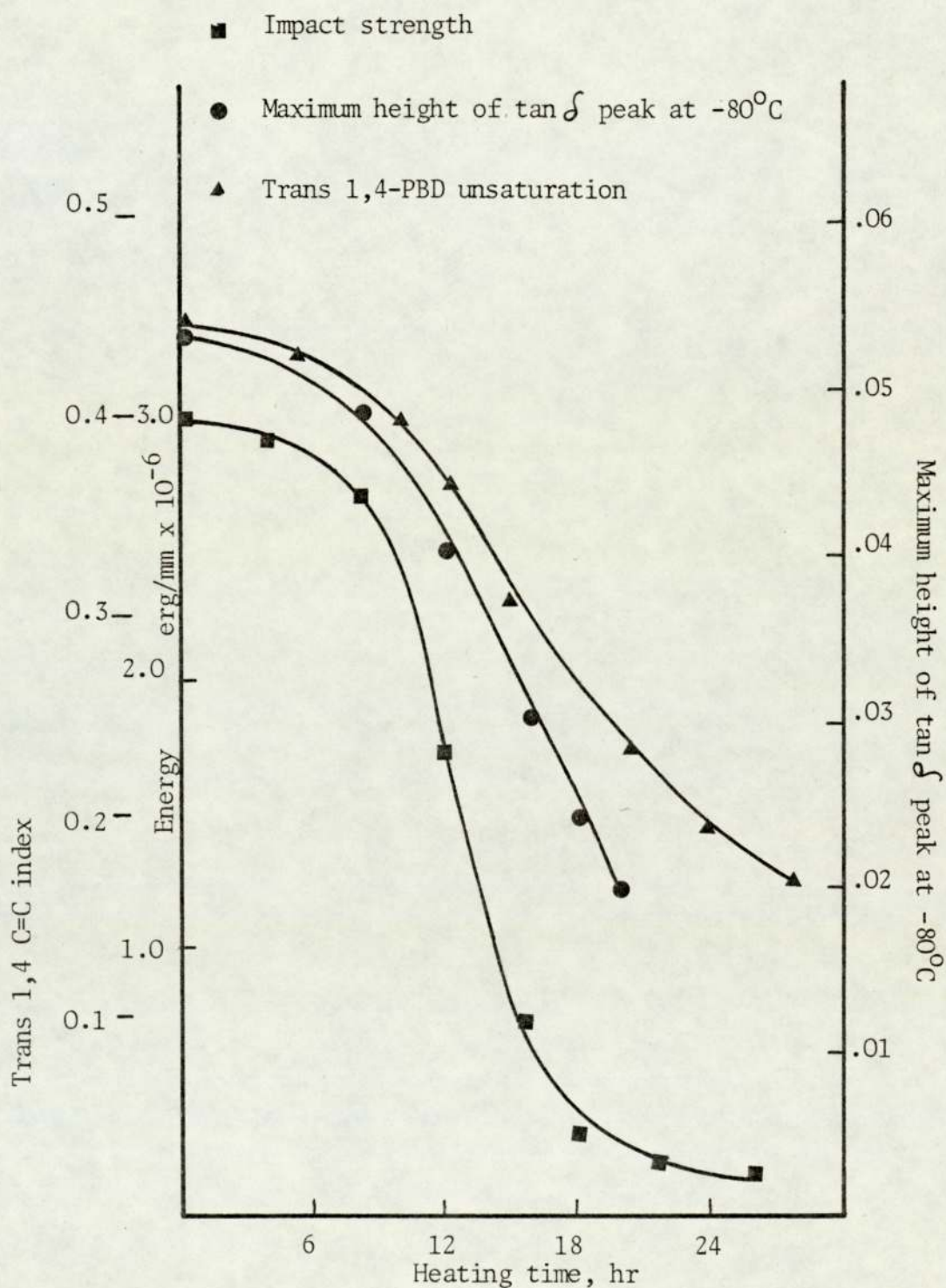
reactions occur in both photo and thermal oxidative degradation[42,39]. Consequently, ABS which has had a prior thermal oxidative treatment will contain hydroperoxides which undergo heating conditions produce active alkoxy and hydroxyl radicals capable of hydrogen abstraction. Hydrogen abstraction will occur at an α-methylenic position producing an allylic alkyl radical which behaves as photo-oxidation. Impact strength and low temperature damping changes occurring during thermal oxidation suggest an initial formation of gel similar to that formed in photo-oxidation. According to Scott et al[39] the maximum gel is formed before the maximum hydroperoxide concentration, only alkylperoxy radicals will be available in these early stages before homolysis of hydroperoxide yields a supply of alkoxy radicals for possible ether linkages. Carbon-carbon cross-linking is unlikely when the supply of oxygen is high. These results, the shift of damping peak to higher temperatures and sharp decrease in impact strength due to the effect of cross-linking on the rate of crack propagation, is consistent with results obtained on photo-oxidation and the results of HIPS[39] and therefore the same mechanism was suggested for photo-oxidation can also be suggested for thermal oxidation.

3.8.e Correlation between Impact Strength and Maximum Height of Tan δ at Low Temperature During Thermal Oxidation

The height of tan δ at -80°C decreases slowly in the initial

137

Fig 3.26   Correlation curve between impact strength and maximum
            height of tan δ peak at -80ºC for unstabilised ABS
            during thermal oxidation
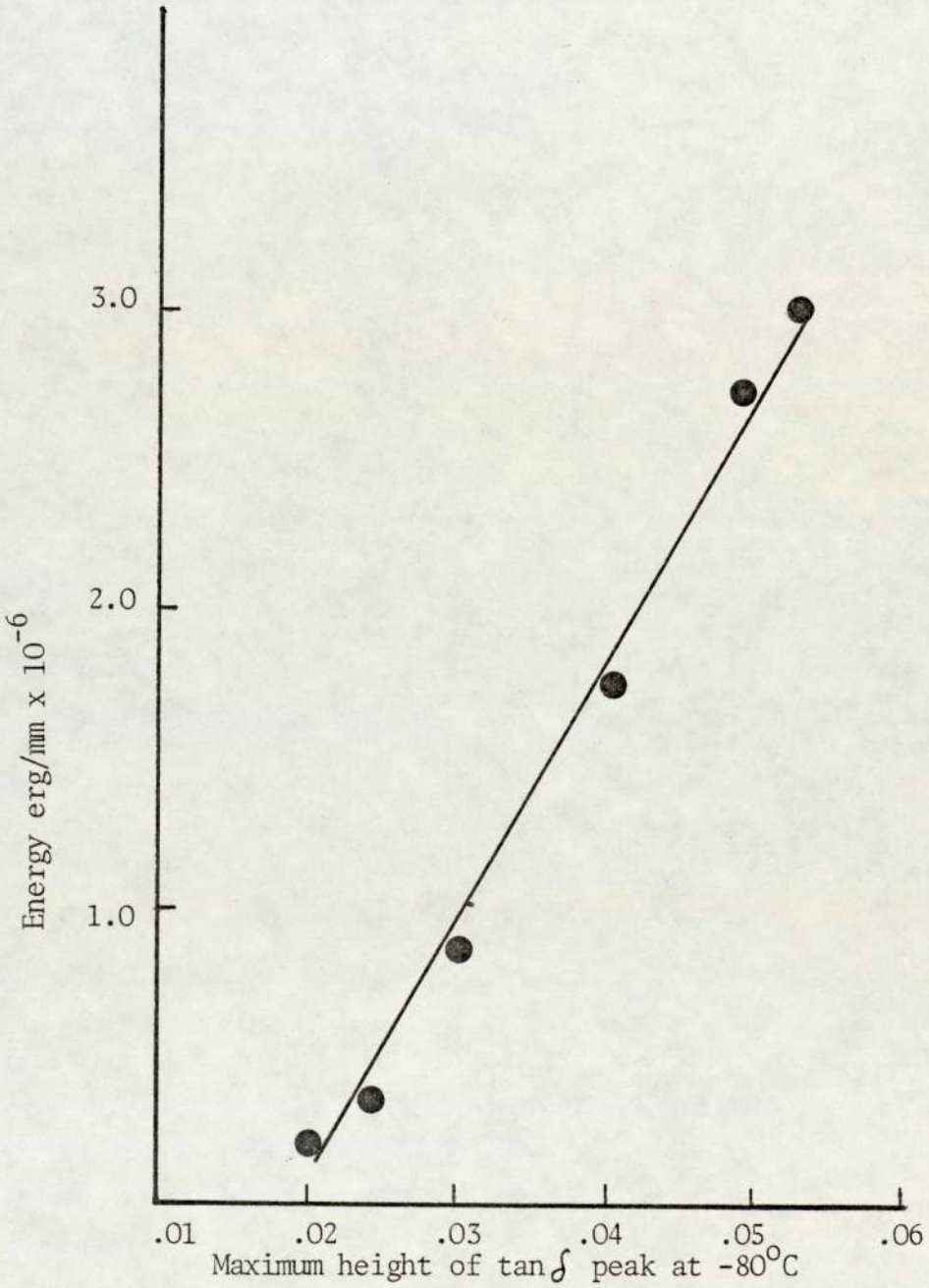
stage of thermal oxidation, very much similar to the decrease

in trans-1,4-PBD but decreases faster in the later stage of

oxidation, so that after 18 hours ageing, 44% of unsaturation had

disappeared whilst at the same time 56% height of damping and

86% impact strength are lost. Thus the loss of impact strength

after 18 hours is almost twice the loss of unsaturation because

the impact changes reflect chemical and hence physical changes

in the surface of the polymer where degradation is most

severe whereas transmission ir spectroscopy measures changes

through the bulk of the polymer. The decrease in the height

of damping peak at low temperature was plotted against time of

heating (Fig 3.25). Tan δ reaches its minimum value (0.02)

after 20 hours of heating. Similarly, to photo-oxidation, there

is a linear relationship between impact strength and the height

of the low temperature tan δ at which is shown in Fig 3.26.

This result indicates that the damping property at low

temperature and impact strength are related to the toughening

agent, PBD, in ABS which determines the course of oxidative

degradation in both thermal and photo-oxidation.

CHAPTER FOUR

THE FREE RADICAL ADDITION OF THIOL COMPOUND TO ABS LATEX

4.1 Free Radical Addition of Thiols to Unsaturated Compounds

The anti-Markovnikov's rule was independently discovered by
several workers. Kharasch and Mayo discovered[102] that the mode
of addition of hydrogen bromide to the carbon-carbon double bonds
is determined by the presence or absence of peroxides. They found
that if peroxides are carefully excluded from the reaction
system the addition of HBr to alkenes follows Markovnikov's
rule. On the other hand, if peroxides are not excluded or are
deliberately put into the reaction, HBr adds to alkenes in the
reverse direction.

$$CH_3-\overset{\overset{\displaystyle CH_3}{|}}{C}=CH_2 \quad \xrightarrow{\text{HBr}}$$

Isobutylene

no peroxide

$$CH_3-\overset{\overset{\displaystyle CH_3}{|}}{\underset{\underset{\displaystyle Br}{|}}{C}}-CH_3 \quad \text{Markovnikov addition}$$

tert-butyl bromide

peroxide

$$CH_3-\overset{\overset{\displaystyle CH_3}{|}}{\underset{\underset{\displaystyle H}{|}}{C}}-CH_2Br \quad \text{Anti-Markovnikov addition}$$

isobutylene bromide
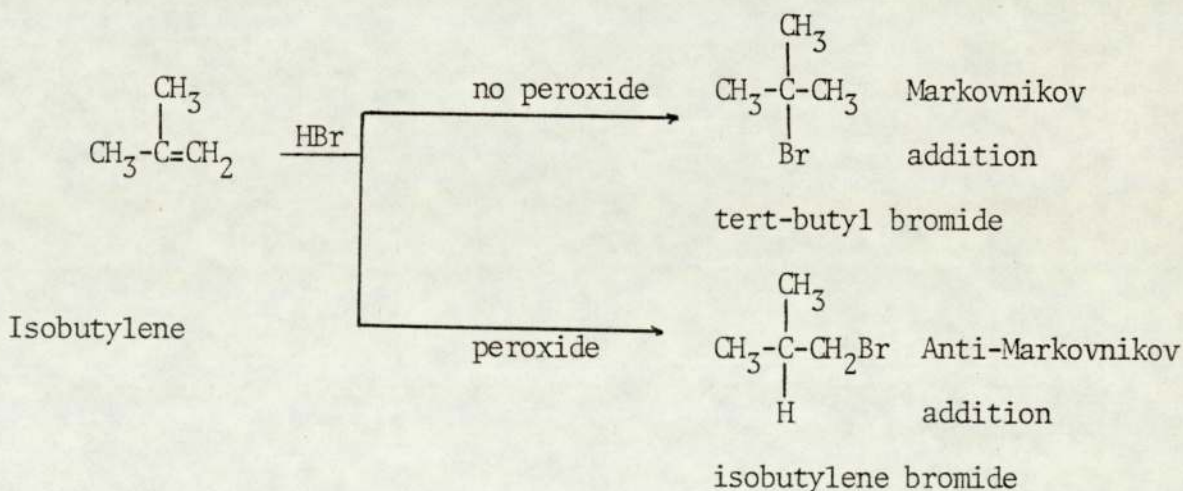
The addition of thiols to unsaturated compounds by Posner[100]
and its much later formulation as a free radical chain reaction[101]
has been the subject of many reviews. Kharasch and Mayo[102]

proposed that anti-Markovnikov addition takes place by a free

radical mechanism. Peroxides initiate the free-radical

reaction, in their absence, addition follows the usual ionic

(Markovnikov) path.

(1)   peroxides $\longrightarrow$ Rad·   ⎤ chain-initiating

(2)   Rad + H:Br $\longrightarrow$ Rad:H + Br· ⎦ steps

(3)   Br· + -C=C- $\longrightarrow$ $-\overset{|}{C}-\overset{·}{\underset{|}{C}}-$

                                         Br   chain-propagating

(4) $-\overset{|}{C}-\overset{·}{\underset{|}{C}}-$ + H:Br $\longrightarrow$ $-\overset{|}{\underset{|}{C}}-\overset{|}{\underset{|}{C}}-$ + Br·   steps

       Br   Br H
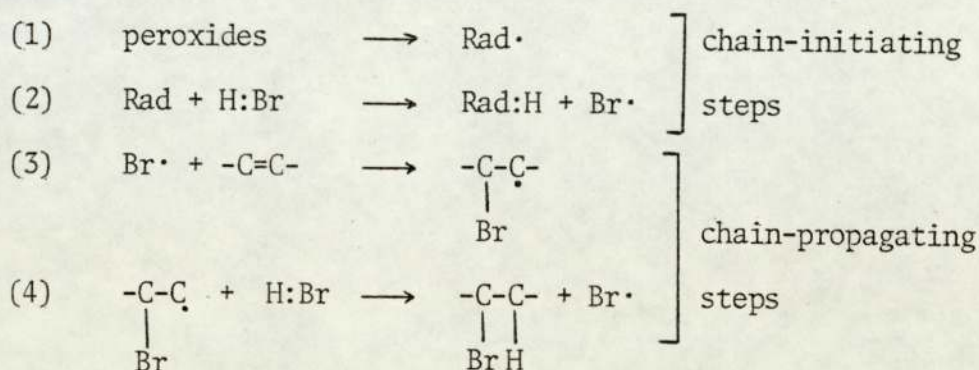
The fact that a very small concentration of inhibitor, eg

hydroquinone, can prevent the change in orientation supports

the above mechanism. These additions were originally

initiated either by exposure to uv irradiation or by addition

of chemical initiators.

4.1.a Mechanism of Addition of Thiols

The free radical addition of thiols to double bonds is a typical

chain reaction, the initiator being alkyl thiyl or aryl thiyl

radicals, which subsequently add to unsaturated substrates to

form a carbon radical, the second stage being usually reversible.

141

$$\text{RSH} \xrightarrow[\text{X·}]{\text{initiator}} \text{RS· + HX}$$

$$\text{RS· + C=C} \rightleftharpoons \text{RS-C-C·}$$
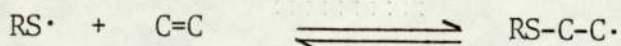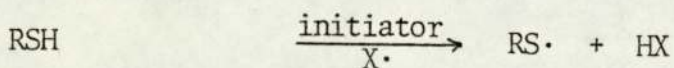
The carbon radical then reacts with a thiol molecule to give the final product and a new thiyl radical, thus propagating the radical chain.

$$\text{RS-C-C· + RSH} \longrightarrow \text{RS-C-C-H + RS·}$$
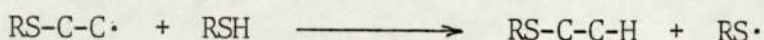
Both the addition of the thiyl radicals and the hydrogen transfer are normally exothermic with the result that the overall reaction is fast and has kinetic chain lengths between a few hundred to several thousand[103].

Hydrogen transfer is generally the rate determining step. Since this involves the cleavage of an S-H bond, its rate is strongly influenced by the structure of the thiol to be added. Thus, aromatic thiols are better chain transfer agents than aliphatic thiols since in the former case, the energy required to break the S-H bond is lowered by resonance stabilisation of the thiyl radical formed[104].
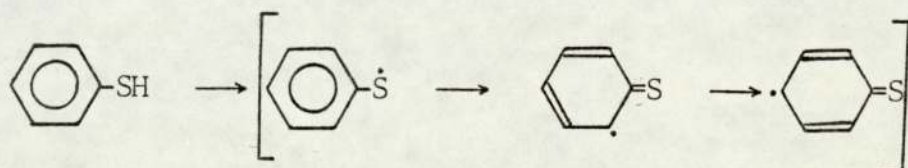
The rate of the hydrogen transfer influences all the variables that depend on the lifetime of the intermediate carbon radical

142

such as:

(1)   the degree of reversibility of the primary reaction
        (carbon radical formation),

(2)   the stereochemical course of the overall reaction,

(3)   possible rearrangements of the intermediate carbon radical,

(4)   the extent of telomerisation, and

(5)   the chain termination reactions.

The termination steps may yield various products[104].

$$\underset{\underset{\overset{|}{H}\;\overset{|}{H}}{}}{\overset{\overset{H\;\;H}{|\;\;|}}{RS-C-C\cdot}} \;+\; RS\cdot \;\longrightarrow\; RS-CH_2-CH_2-SR$$

vicinal bis (thio ether)

$$2RS\cdot \;\longrightarrow\; RSSR$$

$$2\underset{\underset{\overset{|}{H}\;\overset{|}{H}}{}}{\overset{\overset{H\;\;H}{|\;\;|}}{RS-C-C\cdot}} \;\longrightarrow\; RS-CH_2-CH_2-CH_2-CH_2-SR$$

(dimer)
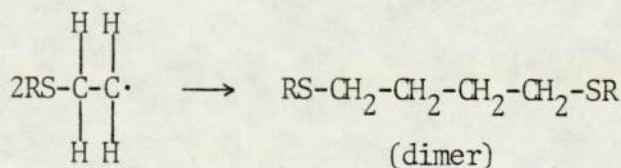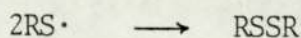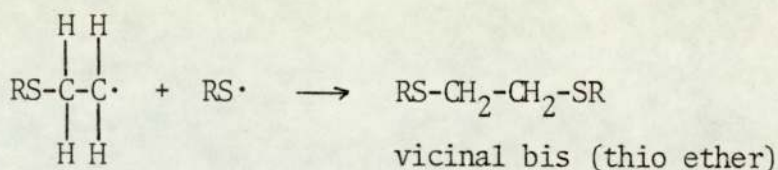
Simple thiol adducts with polymers, in general follow the same
reaction mechanism. Though various polymers containing
olefinic double bonds undoubtedly react with thiols under
appropriate conditions, the present discussion will be limited
to diene homopolymers and copolymers including natural rubber,
emulsion polymerised polyisoprene, copolymers of butadiene with

143

styrene and acrylonitrile.

4.1.b Addition of Alkane Thiols to Polymers

The higher alkane thiols have been extensively used as chain
transfer agents (modifiers) in emulsion polymerisation with
monomers such as butadiene, styrene, acrylonitrile and
chloroprene etc. The transfer reaction represents a competition
between the transfer agent and telomerisation of carbon radical.
Telomerisation occurs when on an average the intermediate
carbon-radical reacts more rapidly with the unsaturate substrate
than by hydrogen abstraction with the chain transfering thiol.
It was reported[105] that the disappearance of alkyl mercaptan
in butadiene emulsion polymerisation depends upon the alkyl chain
length. For mercaptans having chain lengths up to C_{10} the rate
of disappearance is virtually independent of molecular weight.
It was concluded that when the alkyl chain length exceeds 10
carbon atoms, the transfer of mercaptan from monomer droplets
through the aqueous phase to the reaction loci becomes the rate
controlling process. Additional support for this view comes
from the observation that the rate of consumption of n-alkyl
mercaptans having alkyl groups larger than C_{10} can be increased
by raising the pH of the aqueous phase. It appears that in the
case of mercaptan of high molecular weight, diffusion of mercaptan
through the aqueous phase is supplemented by diffusion of
mercaptide ions. These ions by appropriate shift in equilibrium
are presumably able to make the corresponding mercaptan

144

available for free radical addition reactions.

$$RS^- + H_2O \rightleftharpoons RSH + OH^-$$
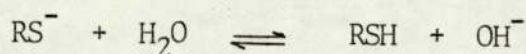
It was also reported that the amount of branching in the mercaptan molecule is an important factor in determining diffusion rate and that the shorter is the longest linear sequence of atoms in the molecule (as in (1)) the faster the rate of diffusion.

$$
\begin{array}{c}
CH_3(CH_2)_3 \\
\hspace{2em} \diagdown \\
\hspace{3em} CH(CH_2)_3SH \hspace{4em} CH_3(CH_2)_{11}SH \\
\hspace{2em} \diagup \\
CH_3(CH_2)_3 \hspace{2em} (I) \hspace{6em} (II)
\end{array}
$$
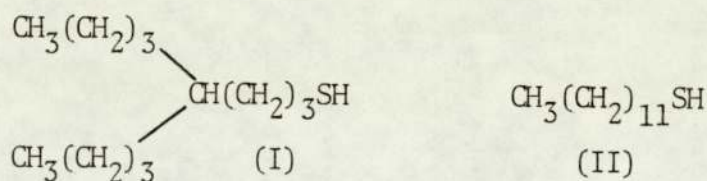
Fryling[106] observed that the presence of oxygen during adduct formation of alkane thiols with SBR caused cleavage of polymeric chains resulting in low molecular weight 'spray' products. The following mechanism for the formation of these products in the presence of oxygen has been suggested. The hydroperoxides formed in oxygen is decomposed by reactions similar to that during oxidative degradation of polymers yielding low molecular weight products.

$$RS \cdot \ + \ R'CH=CHR'' \quad \longrightarrow \quad R'CH-\overset{\cdot}{C}HR''$$
$$\underset{\qquad\qquad\qquad SR}{}$$

$$R'CH-\overset{\cdot}{C}HR'' \qquad \longrightarrow \qquad R'CH-CHR''$$
$$\underset{SR}{\big|} \qquad\qquad\qquad\qquad \underset{SR \ \ OO\cdot}{\big|\quad\big|}$$

$$R'-CH-CHR'' \ + \ RSH \quad \longrightarrow \quad R'-CH-CHR'' \ + \ RS\cdot$$
$$\underset{SR \ \ OO.}{\big|\quad\big|} \qquad\qquad\qquad\qquad \underset{SR \ \ OOH}{\big|\quad\big|}$$
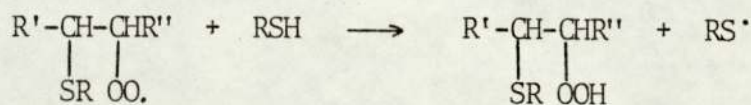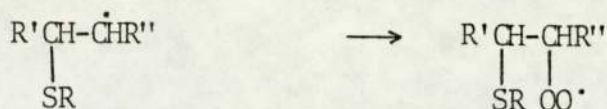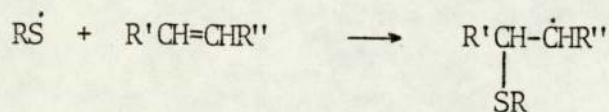
Subsequent reactions which give rise to breakdown products have been discussed in Chapter 3.

4.1.c Modification of Olefinic Polymers with Stabilisers Containing Thiol Group

In aggressive environments, the volatility of antioxidants is more important than their intrinsic activity. It was recognised that for an oxidatively sensitive plastic such as polypropylene all the most effective antioxidants have a high molecular weight and low volatility[107]. Three factors affect antioxidant performance[108]. The first is the intrinsic activity of the antioxidant functional group on a molar basis. The second factor is the compatibility or solubility of the antioxidant in the polymer. The third factor which is dominant in an open system is the volatility of the antioxidant. A potential solution to the problem of antioxidant loss from plastic and rubbers is to bind the antioxidants chemically to the polymers. The effect

146

achieved by chemically grafted of antioxidant I with polypropylene
is much superior to that obtained by using a homopolymer of I.

HO-⬡-CH₂OC-CH=CH₂   (I)
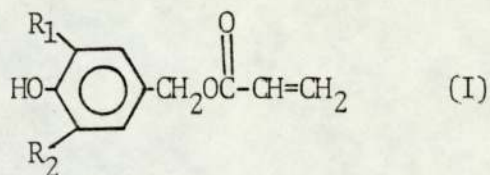
Bonding the 2,4-di-hydroxybenzophenone derivative (4-benzyl-3-
hydroxyphenyl acrylate) by terpolymerisation system to ABS
polymer was reported[109] to solve the problems of compatibility,
dispersability and extractability of the stabiliser. Mayer and
his co-workers have reported[109] that an aromatic amine
antioxidant (II) containing a vinyl group can be copolymerised
with nitrile-butadiene-rubber (NBR) to give a bound antioxidant
which effectively resists extraction by solvents.

⬡-N-⬡-N-C-C=CH₂   (II)
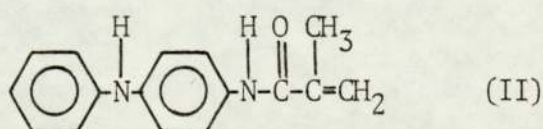
In general, it is inconvenient and hence expensive to incorporate
antioxidants into the rubber molecule during manufacture. Simple
phenols can rarely be made to react with rubbers to give high
yields of bound antioxidants. Furthermore, the concentration
achievable is also limited by side reactions and although
concentrations of bound antioxidants in the region of 2-3% can
be readily achieved, the process is less suitable for the
preparation of latex antioxidant masterbatches. Thiol-containing

147

antioxidants such as 3,5-di-tert-butyl-4-hydroxybenzyl mercaptan (BHBM, III) can however be made to react to much higher conversions (70-80%) than the corresponding alcohol (maximum 20%) since they undergo facile addition to the double bond in rubber in the presence of free radicals[110].

(III)
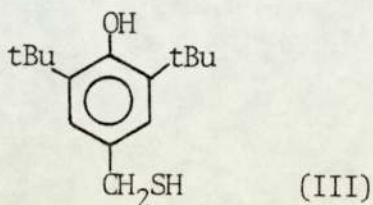
The use of tert-butyl hydroperoxide-polyamine redox system has been shown to increase the yields of adduct formation with natural rubber and lower the temperature of the reaction considerably. Furthermore, a mercapto derivative of 2-hydroxy benzophenone (IV) was added across the double bonds of PBD in latex using $K_2S_2O_8$ as initiator[111], and the double bonds of PBD component in ABS latex using cumene hydroperoxide (CHP) as the initiator[75].

(IV)
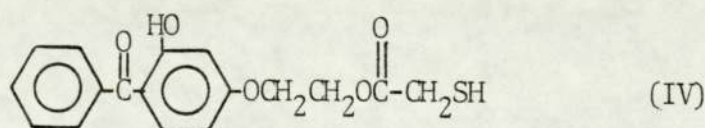
The reaction is a typical radical chain process of the type described above and is terminated by reaction of the thiyl radical (AS·) with other radicals in the systems[115,116].

148

$$
\begin{array}{ccc}
\underset{\displaystyle -\overset{\displaystyle CH_3}{\underset{\displaystyle |}{C}}=CH-CH_2}{} + AS^\bullet & \longrightarrow & -\overset{\displaystyle CH_3}{\underset{\displaystyle \underset{\displaystyle |}{\overset{\bullet}{C}}}{}}-\overset{}{\underset{\displaystyle \underset{\displaystyle |}{SA}}{CH}}-CH_2-
\end{array}
$$

$$
AS^\bullet + -\overset{CH_3}{\underset{H}{\underset{|}{\overset{|}{C}}}}-\overset{}{\underset{SA}{\underset{|}{CH}}}-CH_2- \qquad \xleftarrow{\;ASH\;} \qquad
\begin{array}{c}
-\overset{CH_3\; SA}{\underset{|\quad |}{C}}-CH-CH_2- \\
-\overset{}{\underset{CH_3\; SA}{\underset{|\quad\;|}{C}}}-CH-CH_2-
\end{array}
$$

$$2AS^\bullet \longrightarrow ASSA$$

The sulphur containing byproducts are themselves powerful
antioxidants. Latex products containing bound antioxidants
exhibit exceptional stability when used in applications where
loss of antioxidant by volatilisation or by leaching may occur.
A major advantage of the thiol-based bound antioxidant system
is that it can be used conveniently for the preparation of
high concentration latex masterbatches which can be used as
additives. This is convenient and cheap way of introducing
bound antioxidants into polymers.

Synergism between sulphur compounds (eg the thiodipropionate
ester) and chain breaking antioxidants (phenols and amines) has
been well studied in plastics[112,113]. The adduct reaction
of thiol antioxidants to rubbers gives rise to an auto-
synergistic antioxidant owing to the presence of both a
hydroperoxide decomposer (the monosulphide, A) and a chain-
breaking function (phenolic (B) or amine) in the same molecule (V).

149

$$
\begin{array}{c}
\underset{|}{\text{CH}_3} \\[2pt]
-\text{CH}_2-\text{CH}-\text{CH}-\text{CH}_2- \\[2pt]
\underset{|}{} \\[2pt]
\text{S(A)} \\[2pt]
\underset{|}{} \\[2pt]
\text{CH}_2
\end{array}
\qquad \text{(V)}
$$

tBu   tBu

OH(B)

It is not surprising then that this structure is considerably more effective as a thermal antioxidant than either a phenol or a sulphide alone. Synergistic effects were also observed when these two stabilisers (III, IV) were combined[75]. When the three functions, chain-breaking antioxidant, peroxide decomposer and uv stabiliser, are all present in bound form, a synergistic uv stabilising effect is obtained.

The addition reaction can be attempted during the following stages:

(a)   graft copolymerisation of ABS, or

(b)   on the finished ABS latex.

There are several side reactions which take place during the graft copolymerisation of ABS[75]. The extent of such reactions will depend on a number of factors including the rate of the addition reaction, reactivity ratios of the monomers, rates of diffusion of the monomers and the thiols through the aqueous

phase, etc. On the other hand, the reactions of thiol stabilisers with ABS in latex should proceed without much interference due to the decrease in the probabilities of side reactions as a result of:

(a)   the reduction in number of allylic hydrogen sites due to graft formation, and

(b)   steric hinderance at the tertiary allylic hydrogen sites for the abstraction of hydrogen by RS· radicals.

Therefore EBHPT which is an effective uv stabiliser when chemically bound was investigated in the present study.

4.2   Attempted Masterbatch Formation of EBHPT with ABS in Latex

Attempts were made to bind three concentrations of EBHPT (10, 20 and 30%) in ABS latex. Borg-Warner ABS latex (no antioxidant) was used using the formulation given in Table 4.1, adapted from Fernando's work[75] who prepared 8% masterbatch from EBHPT in ABS latex.

4.2.1.a   Attempted Masterbatch Formulation of 10% EBHPT (10 pph)

The following formulation was used for EBHPT masterbatch formulation:

Table 4.1

ABS latex (stripped latex containing 30% dry ABS)	330 ml
Sodium salt of EBHPT (preparation of Section 2.13)	200 ml
Cumene hydroperoxide (CHP)	0.8 g
Glucose (in 10 ml of water)	2 g
Fe^{+2}/TSPP solution	8 ml
Reaction temperature	$50^{o}C$
Reaction time	5 h
Atmosphere	N_2

The latex was stripped (see Section 2.14) to remove residual monomers which may interfere with masterbatch formation due to consuming the initiator radicals. The sodium salt of EBHPT solution was made (see Section 2.13) with great care to obtain an orange-brown colour solution and the pH of the resulting mixture was adjusted to 9.0-9.5 by dilute acetic acid, and then added to the ABS latex at once. The glucose solution and

TSPP/Fe^{+2} solution were also added to the ABS latex before the start of the reaction. The reaction vessel was heated in a water bath and the temperature was raised slowly to 50°C under a nitrogen atmosphere. CHP was slowly added to the reaction mixture (after the temperature had reached 50°C) during the first half of the reaction. The latex was acid coagulated in the ambient temperature, dried in a vacuum oven at 50°C to constant weight. The material was extracted in a Soxhlet with hot hexane (48 hours) for estimation of bound stabiliser content. The estimation of bound uv stabiliser was made using a calibration curve (Fig 4.1), which was prepared according to the method given in Section 2.18.

4.2.1.b Results

The percentage of bound uv stabiliser (EBHPT) estimated directly on the film (thickness 0.003") using the uv spectrometric method was 58-60%. Because of the high concentration of EBHPT in the original sample (10% masterbatch) and high absorptivity, the 10% masterbatch was diluted to one percent to allow the uv absorbance to be measured.

4.2.1.c Dilution of Masterbatches to Lower Concentration

Dilution of 10% masterbatch was carried out in two different ways.

153

Fig 4.1 Calibration curve for EBHPT

154
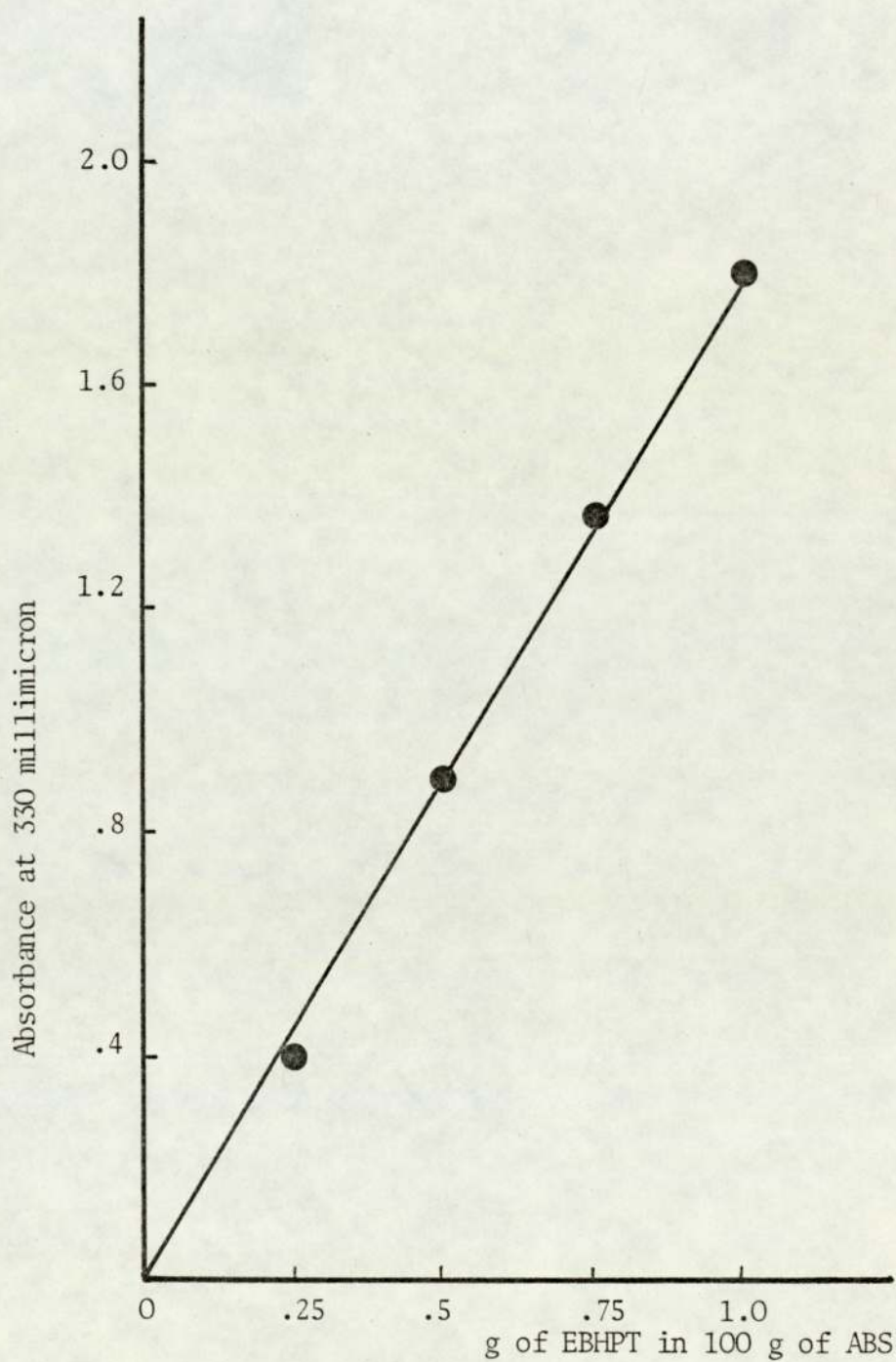
(a)   Dilution was made immediately after the reaction by
        mixing the masterbatch with unstabilised ABS latex.
        Calculation for the dilution of the masterbatch in the
        solution was made on the basis of the initial amount of
        EBHPT (ie 10 pph). Therefore for making 1% bound uv
        stabiliser, 10 ml of masterbatch was diluted with 90 ml
        of unstabilised latex and mechanically stirred for 15
        mins. Dilution was made before extraction, then
        coagulated, dried and extracted.

(b)   Dilution was carried out in the solid stage, after
        coagulation of adduct latex. Dilutions in the solid stage
        were made before and after extraction on the basis of
        10 pph of EBHPT to be compared with the diluted product
        made by the solution process. To make 1% bound uv
        stabiliser, 10 g of masterbatch (10%) and 90 g of unstabilised
        latex were mixed in the melt in the torque rheometer.

        190°C, 3 min in torque rheometer.

4.2.2 Attempted Masterbatch Formation of 20 and 30% EBHPT

The formulation which was used for 10% masterbatch of EBHPT
(Table 4.1) was also used for 20 and 30% masterbatch of EBHPT
in latex except that the amount of initiator (CHP) was
investigated in order to find the appropriate amount of CHP for
both cases.

155

4.2.2.a Procedure

Time, temperature and redox system were kept constant while the amount of initiator was changed over a wide range to find the amount of CHP which gave the maximum percentage of bound uv stabiliser. The result of this investigation is given in Fig 4.2. It was found that 0.8 g of CHP is the optimum amount of initiator to obtain maximum bonding from 20 and 30 g of EBHPT for 100 g of dry ABS or 330 ml of ABS latex.

The adduct latex was acid coagulated, dried in a vacuum oven at $50^{\circ}C$ to a constant weight and then extracted in a Soxhlet with hot hexane for 50 hours for estimation of bound stabiliser content.

4.2.2.b Results

The maximum percentage of bound uv stabiliser obtained is 70% for 20 g of EBHPT and 82% for 30 g of EBBPT in 330 ml of ABS latex. The estimation of bound uv stabiliser was made on 1% samples from 20, and 30% masterbatches. The masterbatches were diluted to 1% at solution and solid stages. The actual concentrations of EBHPT in 1% samples made from masterbatches after extraction are given in Table 4.2.

Therefore as it is seen in Fig 4.3, the percentage of bound uv stabiliser (EBHPT) increased as the amount of EBHPT increased

156

Table 4.2

Masterbatch pph conc	Dilution at solution stage, ml	Dilution at solid stage, g	Conc of EBHPT before extraction, pph	Conc of EBHPT after extraction, pph
10	33 + 297	10 + 90	1	0.6
20	16.5 + 313.50	5 + 95	1	0.7
30	11.0 + 319.0	3.33 + 96.67	1	0.82

Fig 4.2 Dependence of the adduct reaction on the concentration
of initiator

★ 20% masterbatch of EBHPT

□ 30% masterbatch of EBHPT

Percentage of bound EBHPT

g of CHP per 330 ml of latex
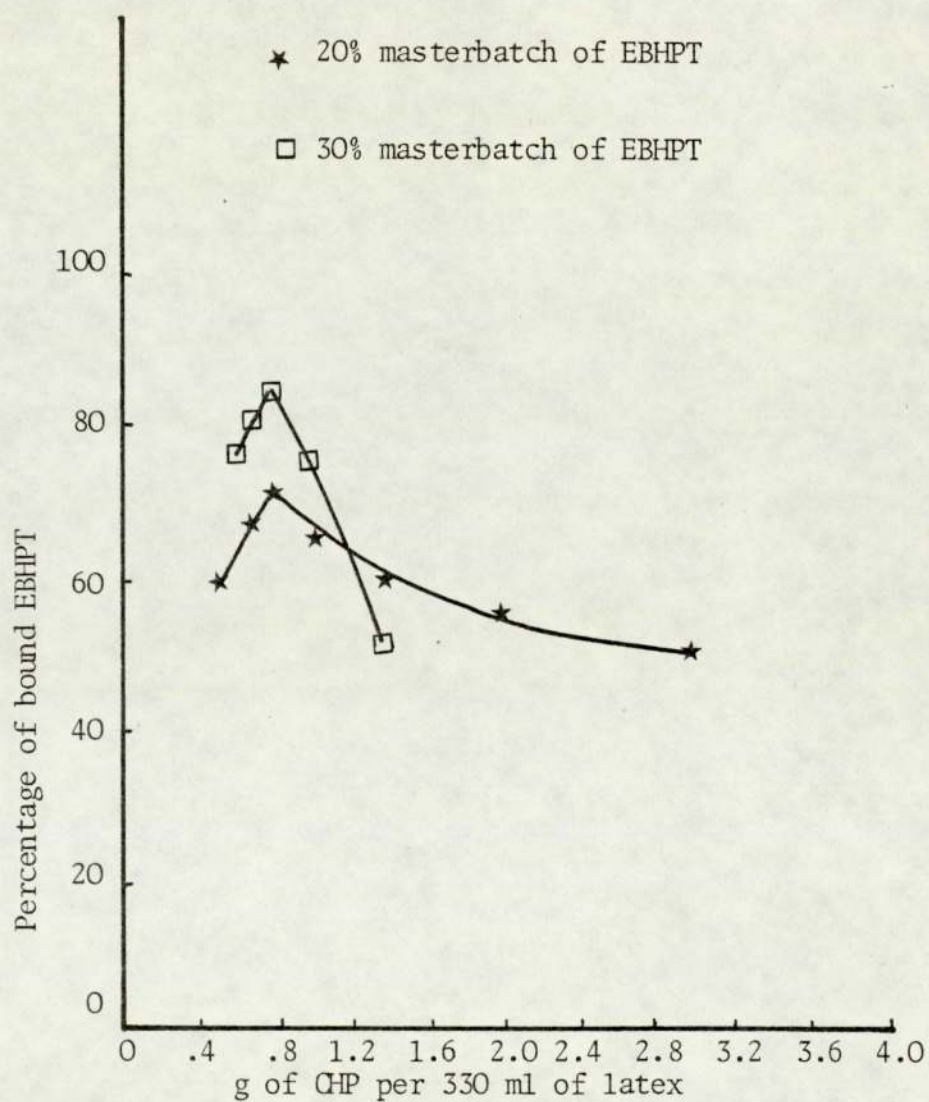
under the same condition (0.8 g of CHP for all concentrations of EBHPT).

4.2.3 Discussion

A major advantage of the thiol-based bound stabiliser system is that it can be used conveniently for the preparation of high concentration latex masterbatches which can be used as additives. This is convenient and cheap way of introducing bound antioxidants into rubber and rubber-modified polymers.

The masterbatches were diluted to the lower concentration at the latex stage and mechanically stirred for 15 mins to obtain uniform dispersion of stabiliser. The inhomogenity is due to the difference in the density of the adduct ABS. On coagulation the coagulum usually floats to the surface. If the densities of coagulum in the stabiliser is different from that of unmodified coagulum, the crumb may take up different positions giving ambiguous results for the final product. Such an ambiguity can be relieved by homogenisation of:

(a)   the latex blend on mechanical stirring, and

(b)   the dry ABS by processing in the melt state.

When ABS latex was used as the substrate for the adduct reaction the sodium salt of EBHPT gave better yields than its emulsion[75]. These results were correlated to the work carried out by

159

Fig 4.3 Percentages of bound of EBHPT are shown against amount
         of EBHPT used in 330 ml latex (100 g of dry ABS) for
         emulsion bounding
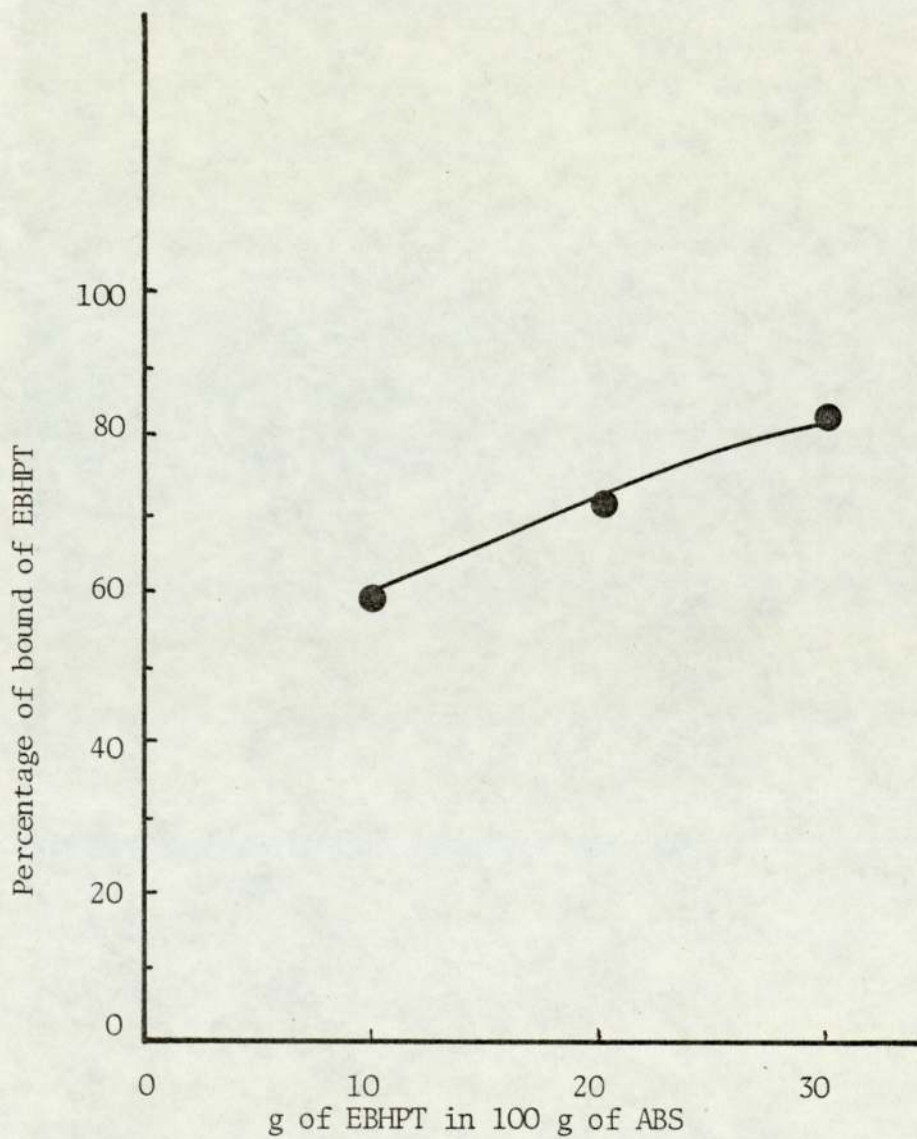
Smith[114] on the influence of pH upon the rate of disappearance of high molecular weight alkyl mercaptan chain transfer agents in emulsion polymerisation. The acid dissociation constant of thiols are in the range of 10-11.

$$RS^- + H_2O \rightleftharpoons RSH + OH^-$$
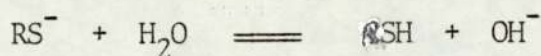
The RS⁻ anion in equilibrium below a pH of 11 offers very little more resistance to diffusion through the aqueous phase than the thiol itself having diffused through the aqueous phase, the change on the anion could help the radical to penetrate the electrical double layer surrounding the polymer latex particle. As long as the pH remains below the acid dissociation constant of the thiol, the shift in the equilibrium can produce thiol SH necessary for formation of free radicals RS˙ for the adduct reactions.

It was reported by Fernando et al[75] that the less polar monomer, styrene, which exists as unreacted monomer in ABS latex must be excluded during the adduct formation (BHBM) reaction. It was found that the styrene monomer inhibits the adduct formation reaction due to the reaction with the initiator which leads to the formation of polystyrene. It was also reported[115] that removing styrene monomers by stripping the ABS latex helps to obtain a higher percentage of bound stabiliser with EBHPT. In an investigation for finding the mechanism of antioxidant activity with hydroperoxides by Husbands et al[65],

161

it was reported that two products are responsible for antioxidant behaviour, namely sulphonic acid and inorganic acids (SO_3, H_2SO_4) formed by the decomposition of the unstable intermediate sulphinic acid. At low hydroperoxides to sulphur compounds, disulphide is the exclusive product formed from the sulphur compound. This product consumes hydroperoxide by further oxidation (scheme 4.1). On the other hand, in the presence of excess hydroperoxide, sulphur compound is converted to the sulphonic acid which is a powerful antioxidant which catalyses the decomposition of cumene hydroperoxide to phenol and acetone.

Scheme 4.1

$$RSH \xrightarrow[\text{(a)}]{ROOH} RSSR \xrightarrow[\text{(b)}]{ROOH} R-S\overset{O}{\underset{OH}{\diagup}}$$

(d) ROOH   (c)

$$R-\overset{O}{\underset{O}{\overset{\|}{S}}}-OH \qquad RH + SO_2$$

$$ROH + SO_2 \longrightarrow SO_3 \ (H_2SO_4)$$

$$RSSR \xrightarrow{ROOH} R-\overset{O}{\overset{\|}{S}}-S-R$$

    ROOH

$$R\overset{O}{\overset{\|}{S}}\cdot + RS^{\cdot} \qquad \text{Further oxidation products}$$
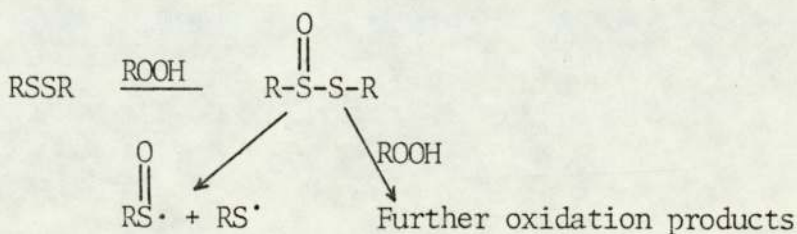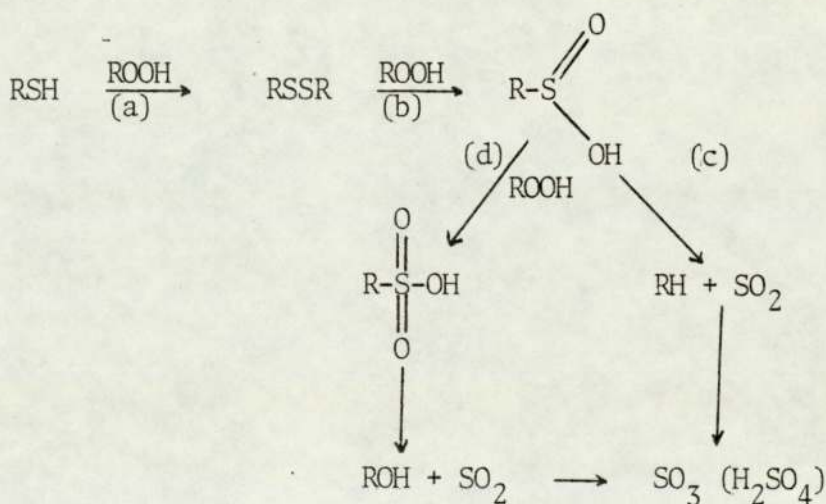
(a)   in the presence of low concentration of hydroperoxide

(b)   in the presence of excess hydroperoxide

162

Sulphur dioxide is a powerful hydroperoxide decomposer which leads to the formation of sulphur trioxide which is a true catalyst for the ionic decomposition of hydroperoxides.

The decomposition of cumene hydroperoxide in the presence of EBHPT was studied by Fernando et al[75]. The Glc decomposition products in the presence of the thiol compounds including EBHPT showed a Lewis acid catalysed process leading to the formation of phenol and acetone (in the presence of excess hydroperoxide).
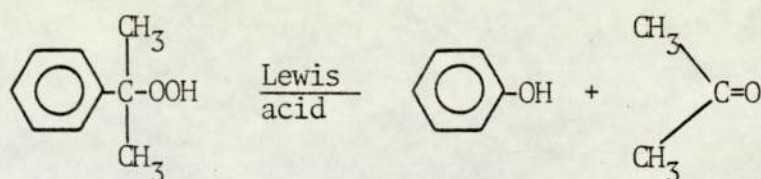
Analysis for antioxidant derivatives after the decomposition reaction showed that the major products are lacking the hetero-atom, sulphur of the original compound. The loss of sulphur suggests that SO_2 may be involved in a Lewis acid catalysed decomposition of hydroperoxides by sulphur compounds. The above suggestions can be well correlated with the results obtained above 0.8 g of CHP (Fig 4.1). The extent of side reactions which take place above 0.8 g CHP depend upon the amount of thiol compounds used. These observations show that the rate of decrease of percentage of bound uv stabiliser above 0.8 g of CHP for 30 g of EBHPT is higher than that of 20 g of EBHPT. This result is consistent with the result obtained by Fernando[75].

163

He showed that for 1 g of thiol (BHBM or EBHPT) the percentage of bonding is at maximum and constant in the range of 0.6 to 0.8 parts of CHP per 100 parts of ABS. Further increase in the amount of CHP decreased the extent of adduct formation but at a slower rate. These results suggest that the rate of decrease of adduct formation above 0.8 parts of CHP is proportional to the amount of EBHPT.

4.3 Photo-oxidation of Stabilised ABS

Compression moulded ABS films containing different amounts of bound uv stabiliser were photo-oxidised under identical conditions. These concentrations of EBHPT were made from 10, 20 and 30% masterbatches in the solution and solid stages. The changes in the functional groups, impact strength and dynamic mechanical property of stabilised ABS were measured during photodegradation.

4.3.a Infra-red Measurements

The infra-red measurements of the functional groups ($C=O$, 1,4 $C=C$) are plotted against time of exposure for diluted samples made from masterbatches in the solution and solid stages and are shown in Figs 4.4, 4.5, 4.6 and 4.7. The functional groups show induction periods proportional to the concentration of uv stabiliser. The induction periods and embrittlement times are given in Table 4.3.

164

Fig 4.4 Development of carbonyl functional group on uv exposure of ABS pressed film, masterbatches were diluted at latex stage (refer Tables 4.2 and 4.3)
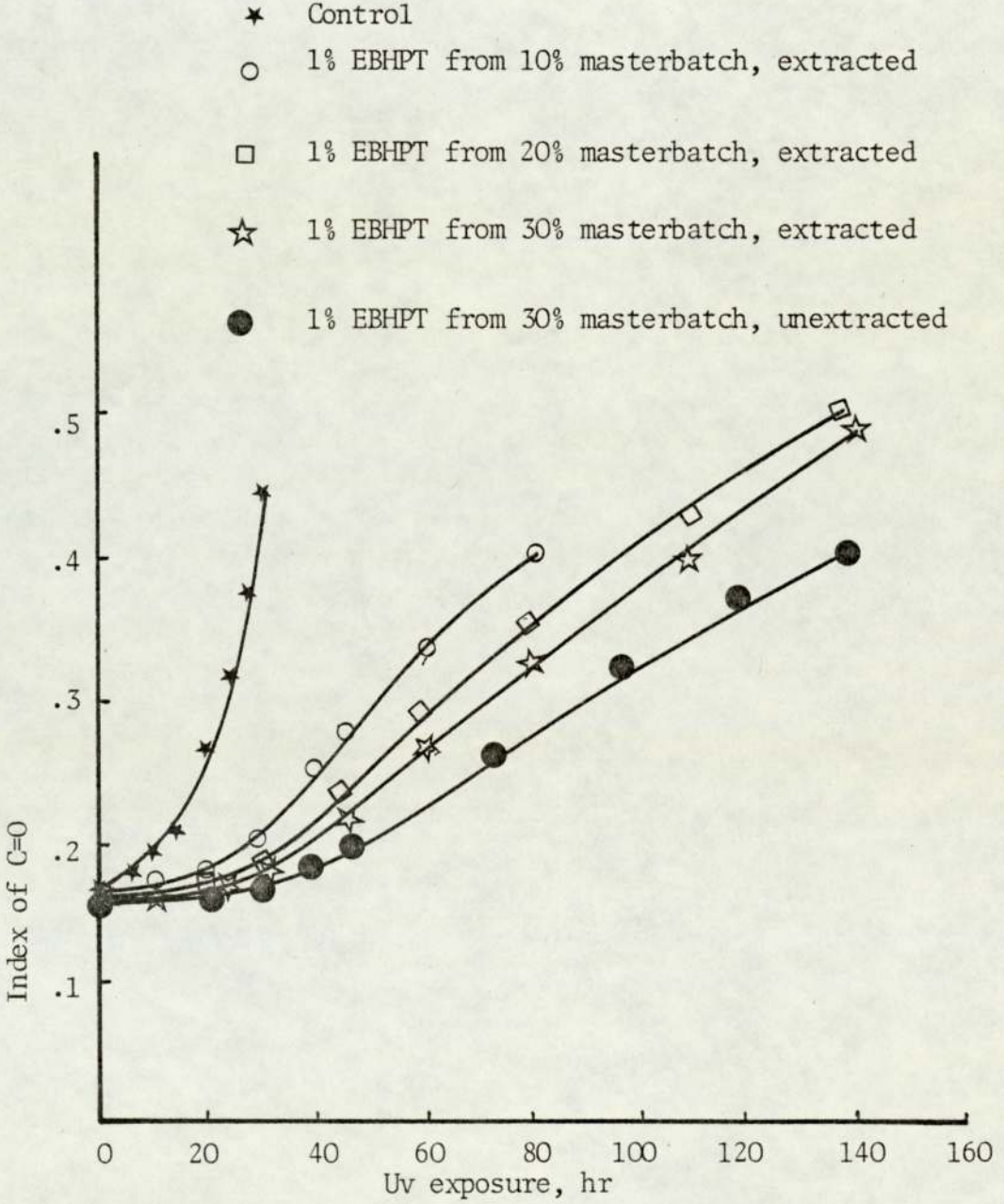
* Control
○ 1% EBHPT from 10% masterbatch, extracted
□ 1% EBHPT from 20% masterbatch, extracted
☆ 1% EBHPT from 30% masterbatch, extracted
● 1% EBHPT from 30% masterbatch, unextracted

165

Fig 4.5 Decay of trans-1,4-PBD unsaturation on uv exposure of ABS pressed films, masterbatches were diluted at latex stage (refer Tables 4.2 and 4.3)

★ Control (Borg-Warner latex)

○ 1% EBHPT from 10% masterbatch, extracted

□ 1% EBHPT from 20% masterbatch, extracted

☆ 1% EBHPT from 30% masterbatch, extracted

● 1% EBHPT from 30% masterbatch, unextracted
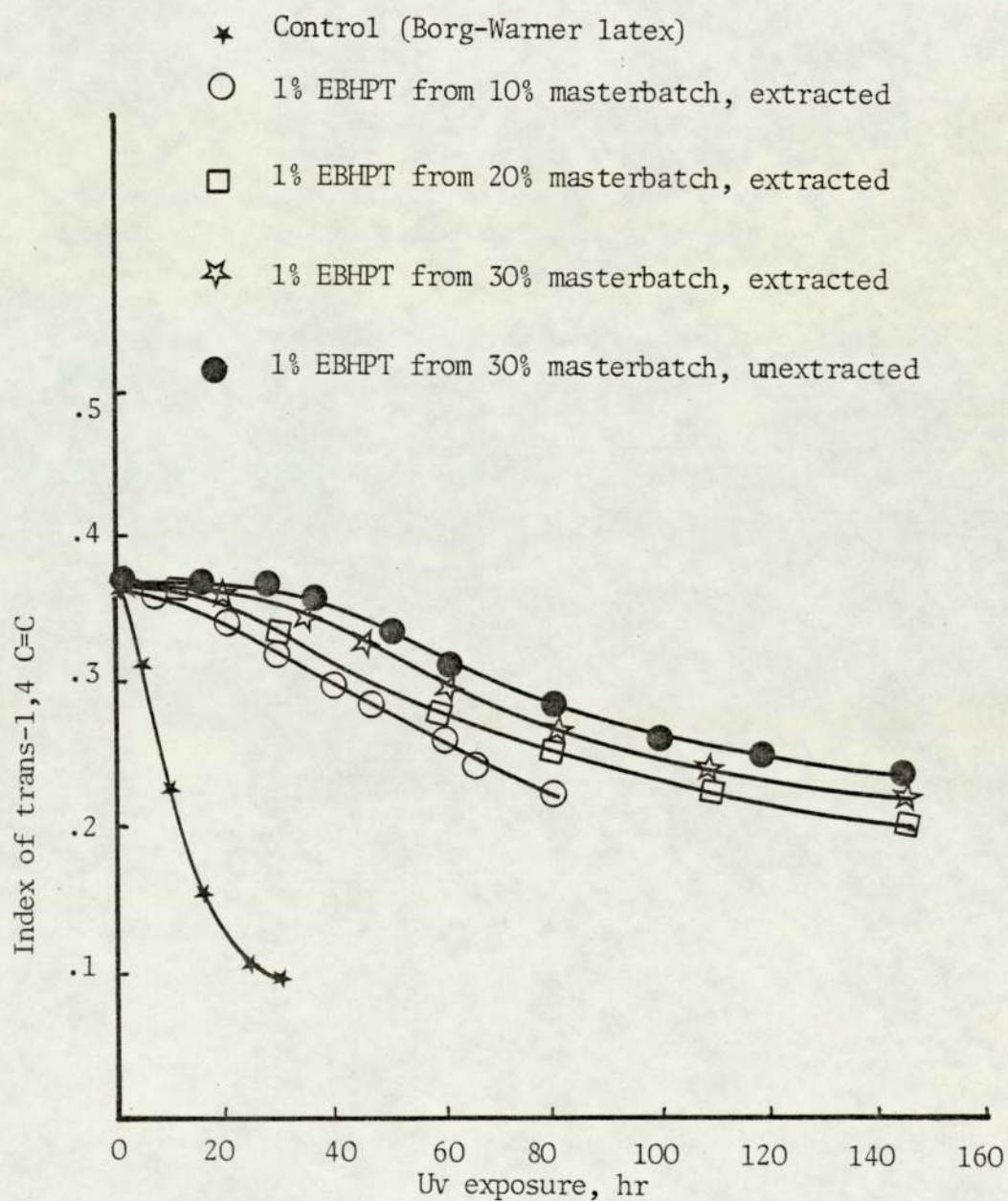
Table 4.3   Concentration of EBHPT before and after extraction in the adducts made from masterbatches
their induction periods and embrittlement times.

Conc of Masterbatch pph	Conc of dilute before extraction, pph	Conc of dilute after extraction, pph	Induction periods after extraction, h	Embrittlement time after extraction, h
10	1	0.60	16	52
20	1	0.70	20	60
30	1	0.82	28-30	72
*Unextracted	1	-	40	88-92
Control	-	-	0-2	25

* only one unextracted sample (1%) was made from 30% masterbatch of EBHPT

167

Fig 4.6 Development of carbonyl functional group on exposure of ABS pressed films, masterbatches were diluted at solid stage (refer Tables 4.2 and 4.3)

★ Control (Borg-Warner latex)

○ 1% EBHPT from 10% masterbatch, extracted

□ 1% EBHPT from 20% masterbatch, extracted

✩ 1% EBHPT from 30% masterbatch, extracted

● 1% EBHPT from 30% masterbatch, unextracted
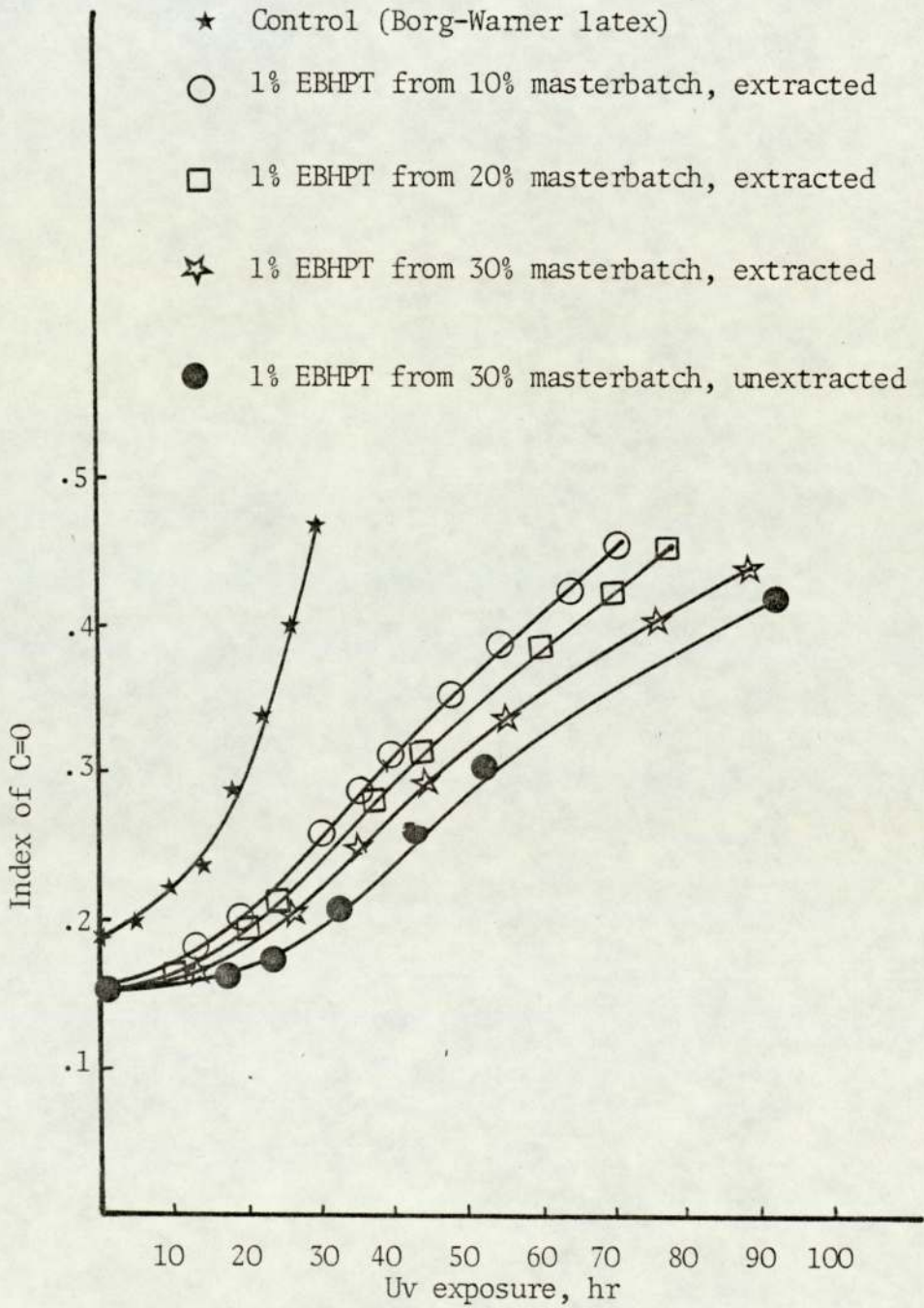
Fig 4.7   Decay of trans-1,4-PBD unsaturation on exposure of ABS
pressed films, masterbatches were diluted at solid stages
(refer Tables 4.2 and 4.3)

★ Control (Borg-Warner latex)

○ 1% EBHPT from 10% masterbatch, extracted

□ 1% EBHPT from 20% masterbatch, extracted

☆ 1% EBHPT from 30% masterbatch, extracted

● 1% EBHPT from 30% masterbatch, unextracted

Trans 1,4 C=C

Uv exposure, hr

169
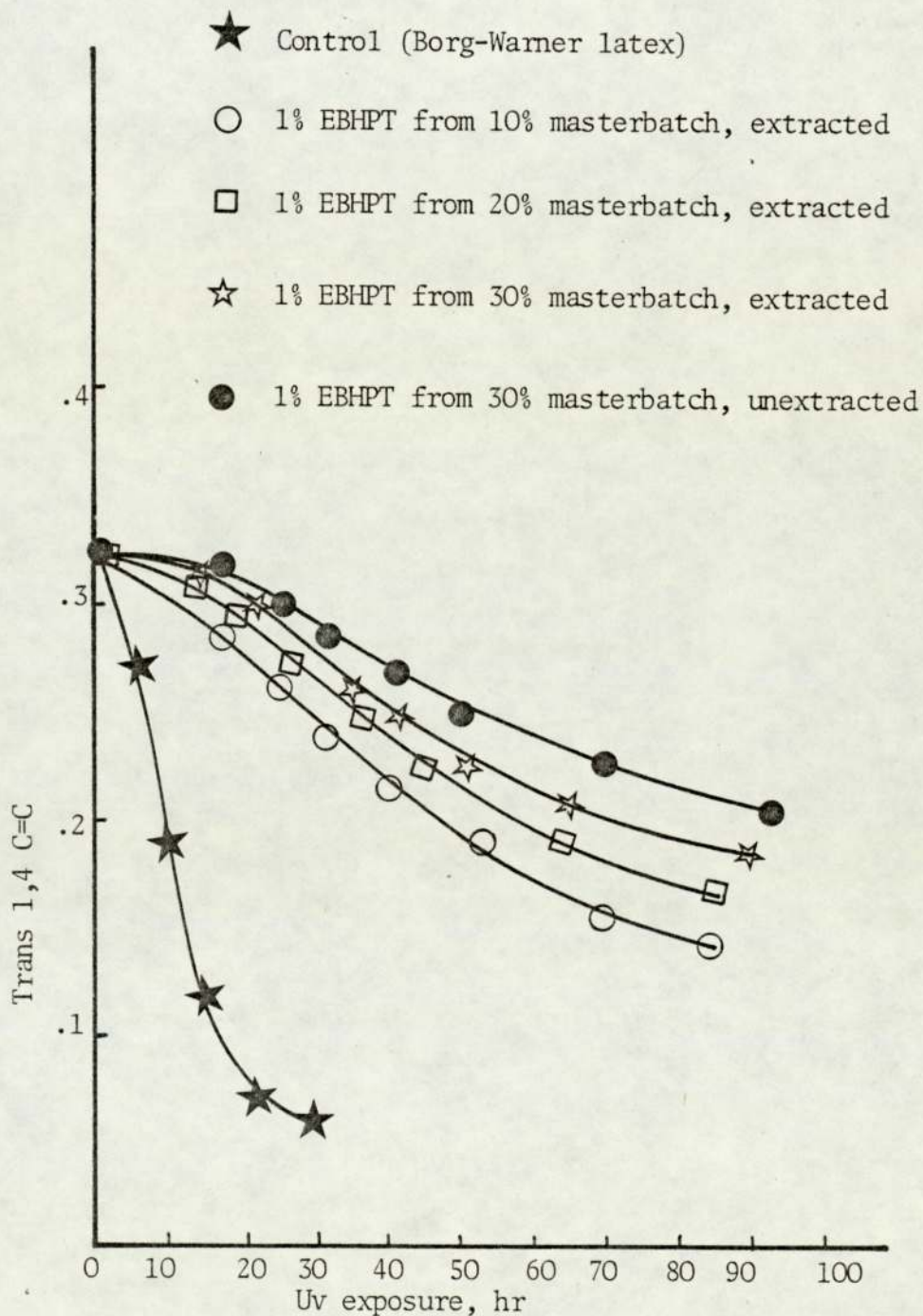
4.3.b Impact Measurement

The impact measurements of ABS samples containing bound uv
stabiliser were carried out during exposure to uv light. The
results are shown in Figs 4.8 and 4.9 for the diluted samples
made from different masterbatches at latex and solid stages.
All ABS samples containing different concentrations of uv
stabiliser show induction periods proportional to the amount of
EBHPT and their impact strengths drop sharply at the lowest value.

4.3.c Measurement of Dynamic Mechanical Properties

Dynamic mechanical properties of stabilised ABS samples were
measured at the Tg of rubber component. Only one sample from
each concentration of uv stabiliser was used throughout the
measurement. The samples were exposed to uv light under
identical conditions. The results are shown only for one
unextracted sample and three extracted samples made at solution
stages from the masterbatches (Figs 4.10, 4.11, 4.12 and 4.13).
The thicknesses of films which were used for low temperature
damping measurements were identical (0.075 mm). The dynamic
spectra of the specimens were observed from $-120 - 0^{\circ}C$. Tanδ
at $-80^{\circ}C$ reached the maximum 0.05 almost for all unexposed
samples and then started to decrease during uv irradiation.
Figs 4.14, 4.15 and 4.16 show changes in tan δ peak at $-80^{\circ}C$
for three extracted samples made at solid stages from the masterbatches.

170

Fig 4.8 Decay of impact resistance on uv exposure of ABS pressed films, masterbatches were diluted at latex stages
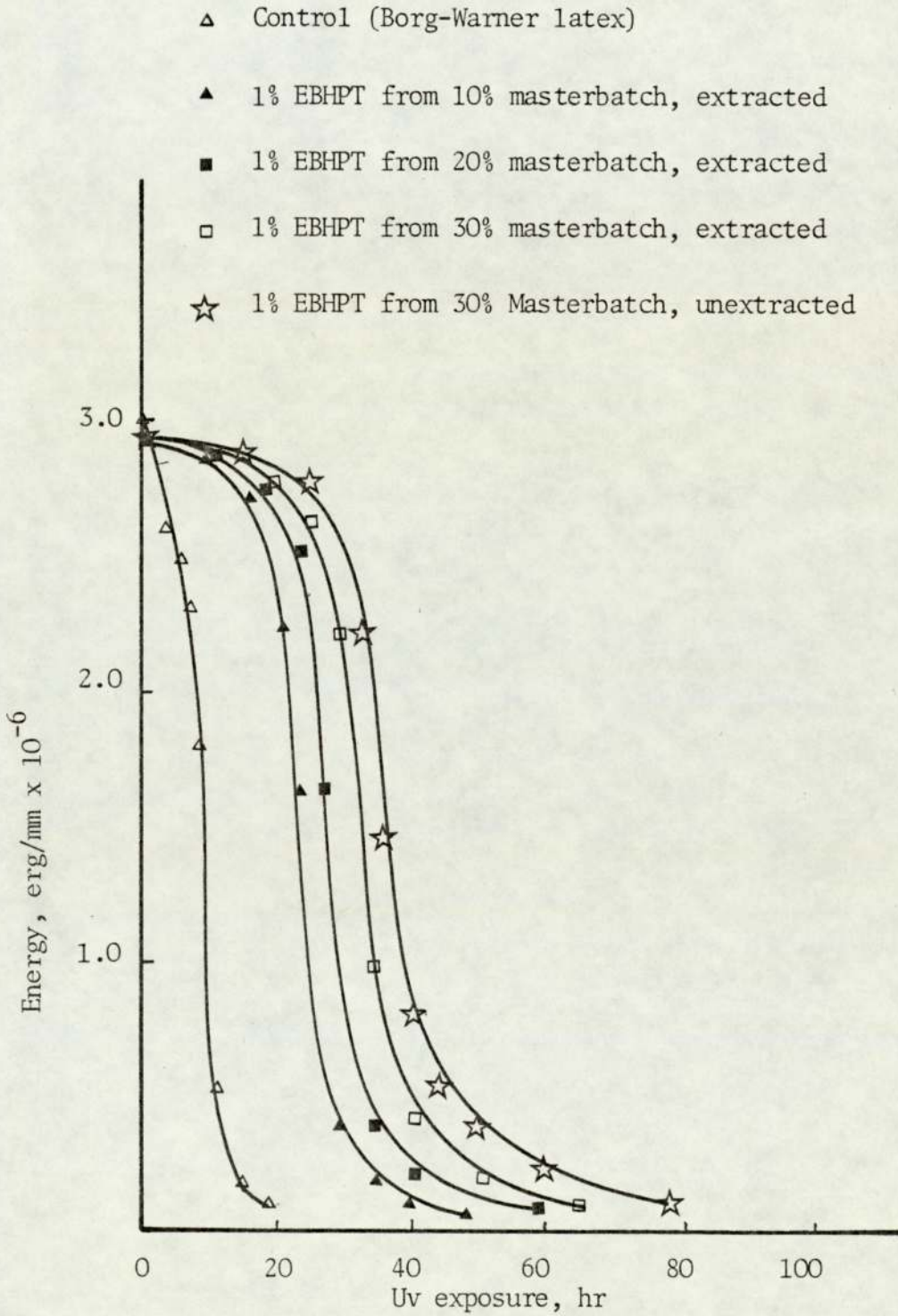
△ Control (Borg-Warner latex)

▲ 1% EBHPT from 10% masterbatch, extracted

■ 1% EBHPT from 20% masterbatch, extracted

□ 1% EBHPT from 30% masterbatch, extracted

☆ 1% EBHPT from 30% Masterbatch, unextracted

Fig 4.9   Decay of impact resistance on uv exposure of ABS pressed films, masterbatches were diluted at solid stages

●   Control (Borg-Warner latex)

□   1% EBHPT from 10% masterbatch, extracted

■   1% EBHPT from 20% masterbatch, extracted

▫   1% EBHPT from 30% masterbatch, extracted

☆   1% EBHPT from 30% masterbatch, unextracted

172
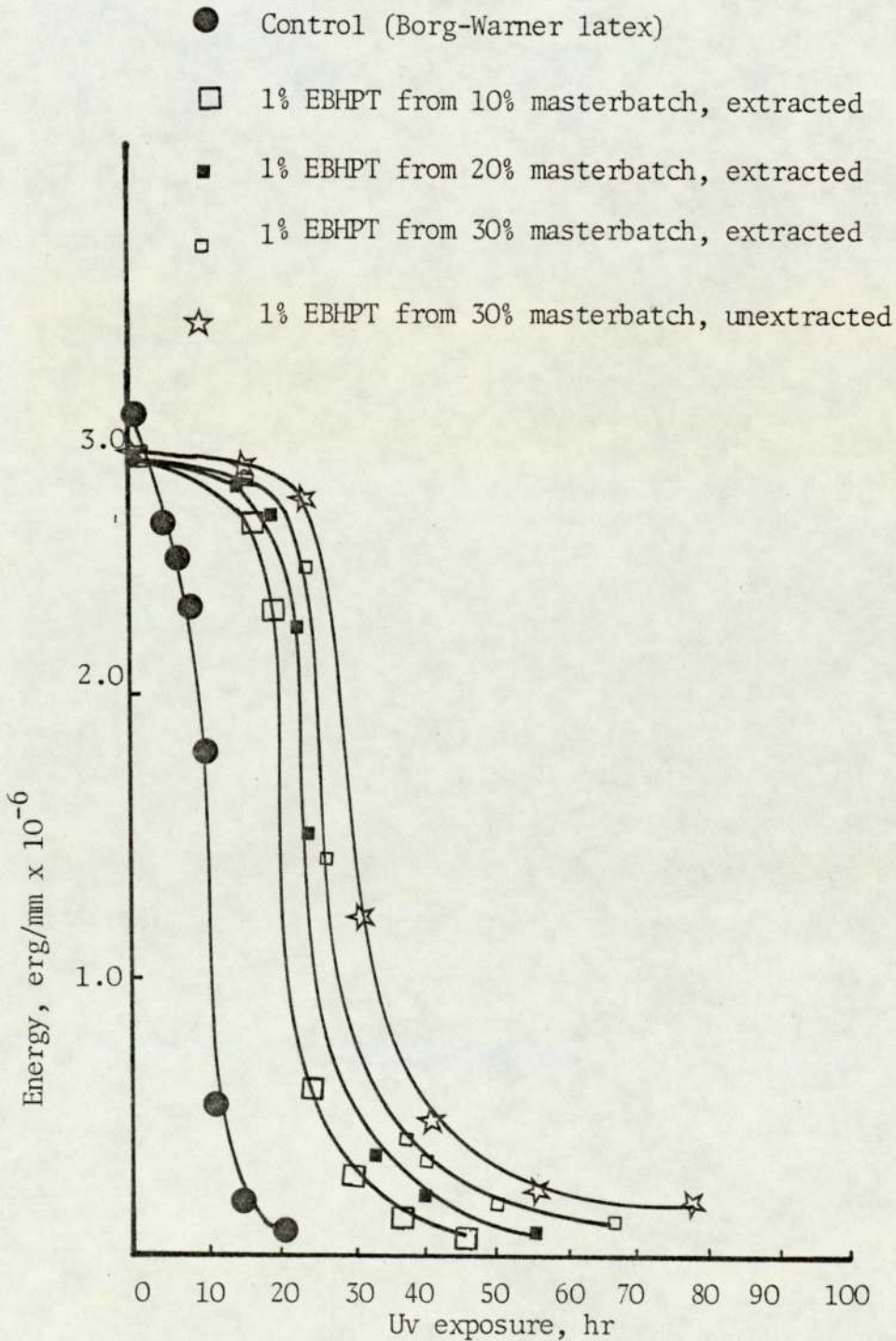
4.4   Discussion

The rubber component of polybutadiene-modified plastics is very susceptible to oxidation. Photo-oxidation leads to cross-linking, as discussed in Chapter 3, of the rubber phase accompanied by scission of the graft between rubber and matrix with consequent loss of impact strength. Conventional light stabilisers afford some protection to ABS polymer during exposure to uv light but are not very effective. This is illustrated in Table 4.4 for some typical uv absorbers[75] and they are compared with the results which were obtained from EBHPT.

As can be seem from Table 4.4, EBHPT gives better stability than the conventional stabilisers and in addition to that it is bound chemically to the rubber component of ABS polymer and in contrast to the additives, it is not lost by volatilisation and solvent leaching. The essential requirements of an effective uv stabiliser are as follows:

(1)   it should be retained in the polymer during its lifetime,

(2)   it should be extremely photo-stable, and

(3)   it must be capable of harmlessly disposing of the absorbed uv energy.

The major mechanism of photostabilisation by uv absorbers is said to the the dissipation of electronic energy into vibrational

173

Fig 4.10 Effect of photo-oxidation on low temperature damping (-80°C) of ABS film containing 1% EBHPT made from 30% masterbatch, unextracted (numbers on spectra represent hours of uv irradiation)

Fig 4.11 Effect of photo-oxidation on low temperature damping (-80°C) of ABS film containing 1% EBHPT made from 30% masterbatch at latex stage extracted

175
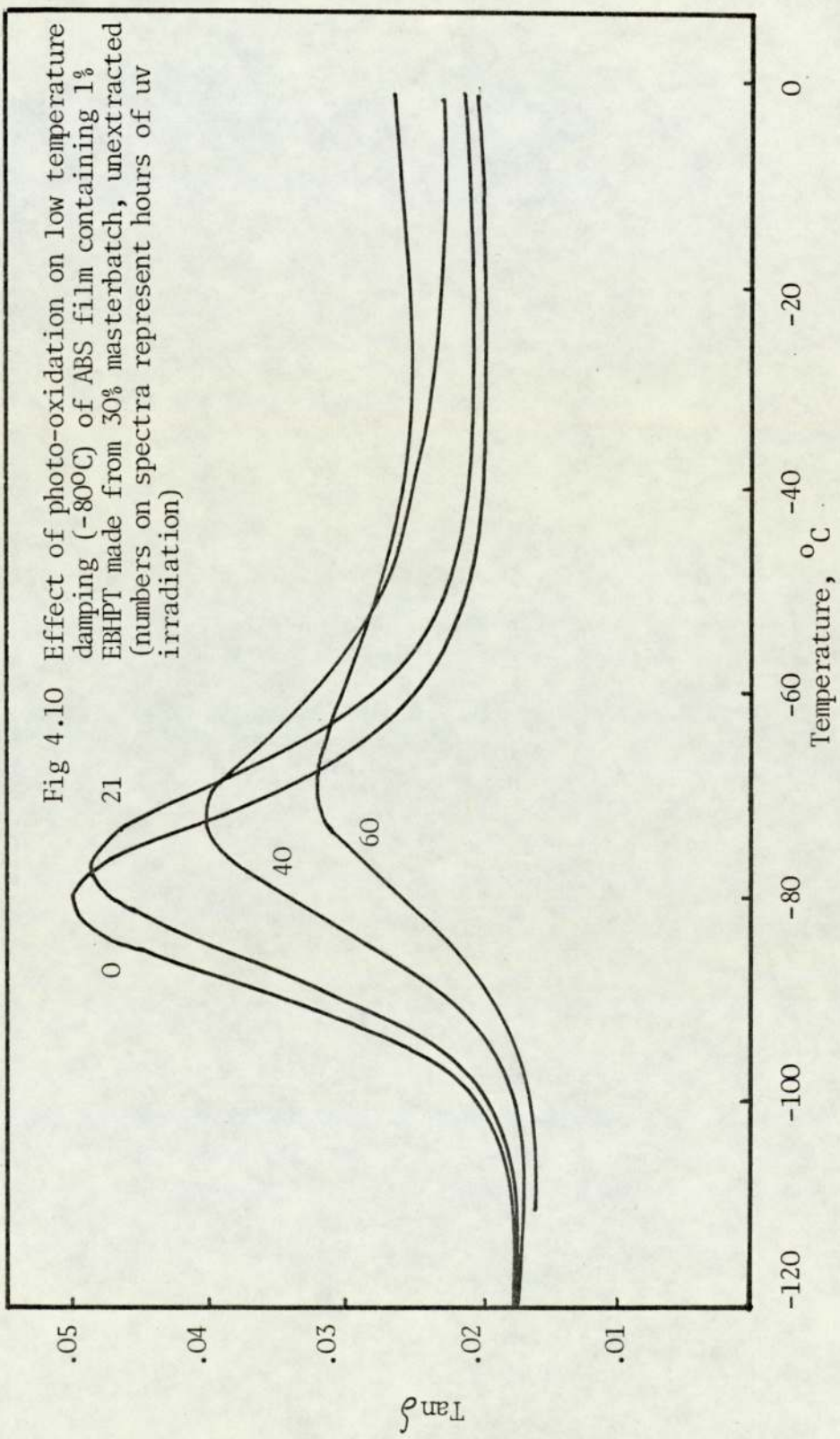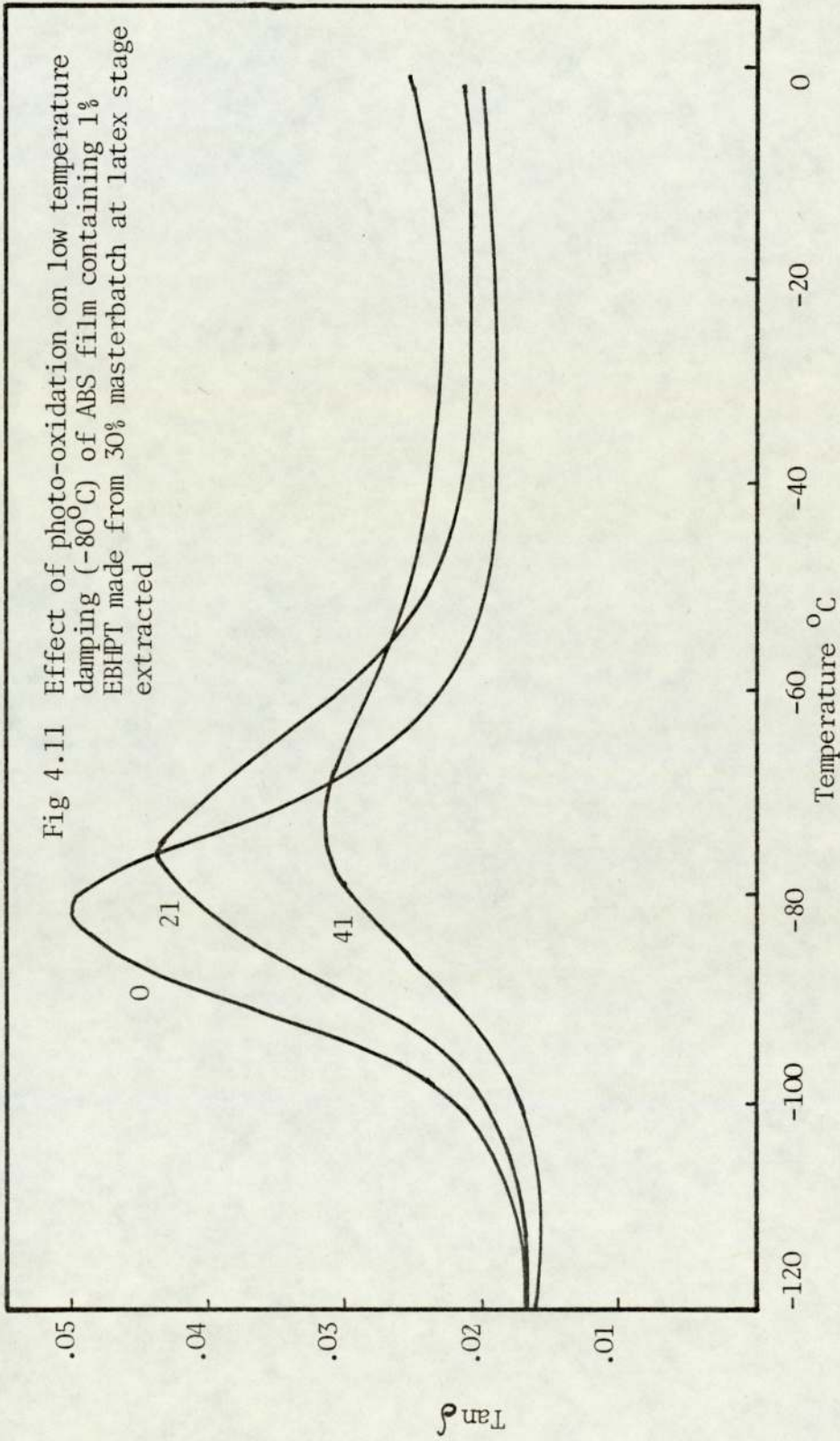
Table 4.4 Comparison stability of ABS containing commercial uv stabilisers as additive and ABS containing bound uv stabiliser (EBHPT)

Reference	Uv Stabiliser	Induction period, h	Embrittlement time, h	Concentration mole/100 g ABS
Ref 75	UV531	10	35	3.06×10^{-3}
Additives	Tinuvin P	12	40	3.06×10^{-3}
	Tinuvin 770	16	37	3.06×10^{-3}
Uv bound stabiliser *	EBHPT	40	88-92	3.06×10^{-3} unextracted
	EBHPT	28-30	72	2.47×10^{-3} extracted
Control	-	0-2	25	-

* These samples were made from 30% masterbatch of EBHPT

176

Fig 4.12 Effect of photo-oxidation on low temperature damping (-80°C) of ABS film containing 1% EBHPT made from 20% masterbatch at latex stage, extracted

177
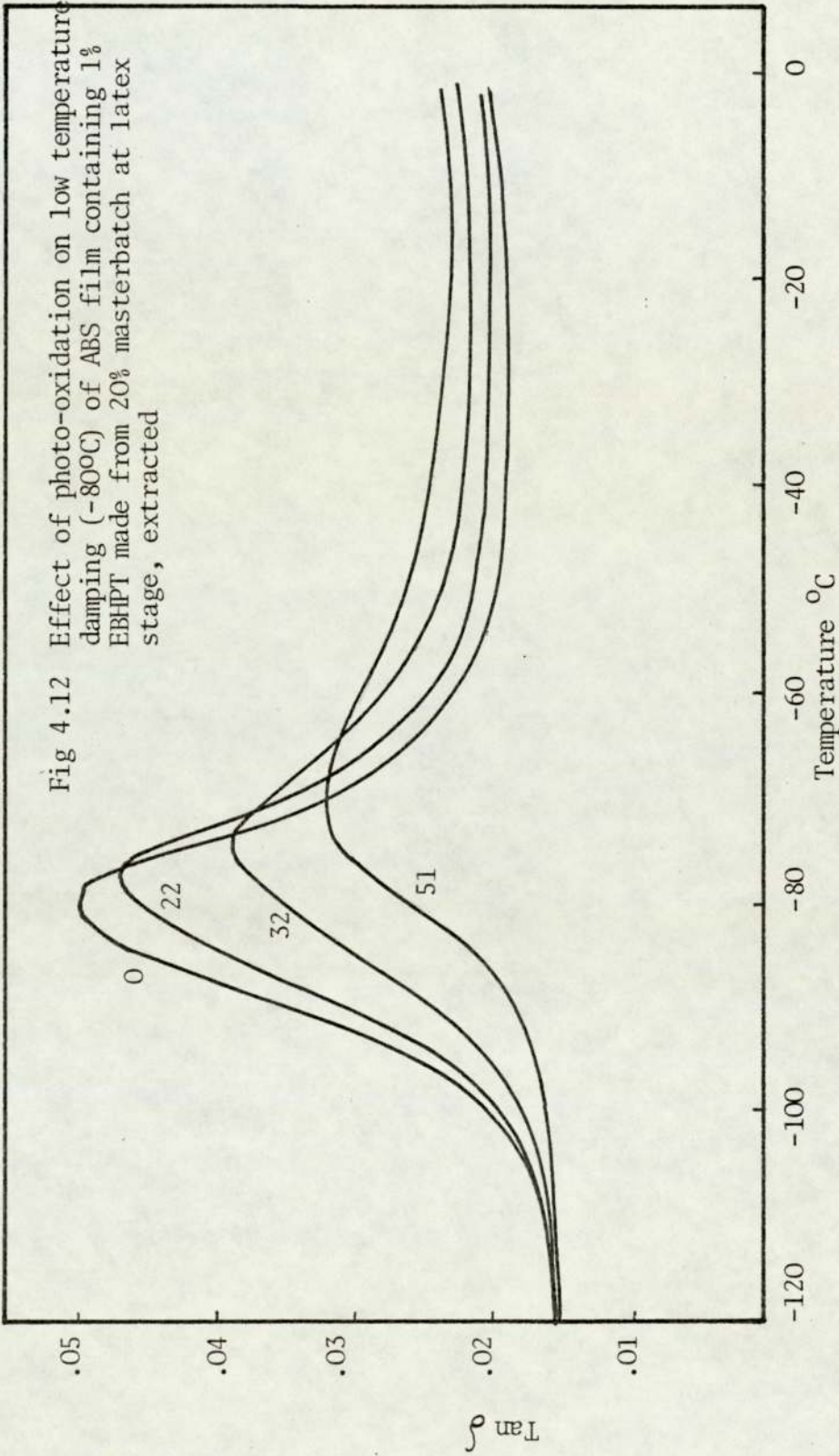
Fig 4.12 Effect of photo-oxidation on low temperature damping (-80°C) of ABS containing 1% EBHPT made from 30% masterbatch at latex stage, extracted

178
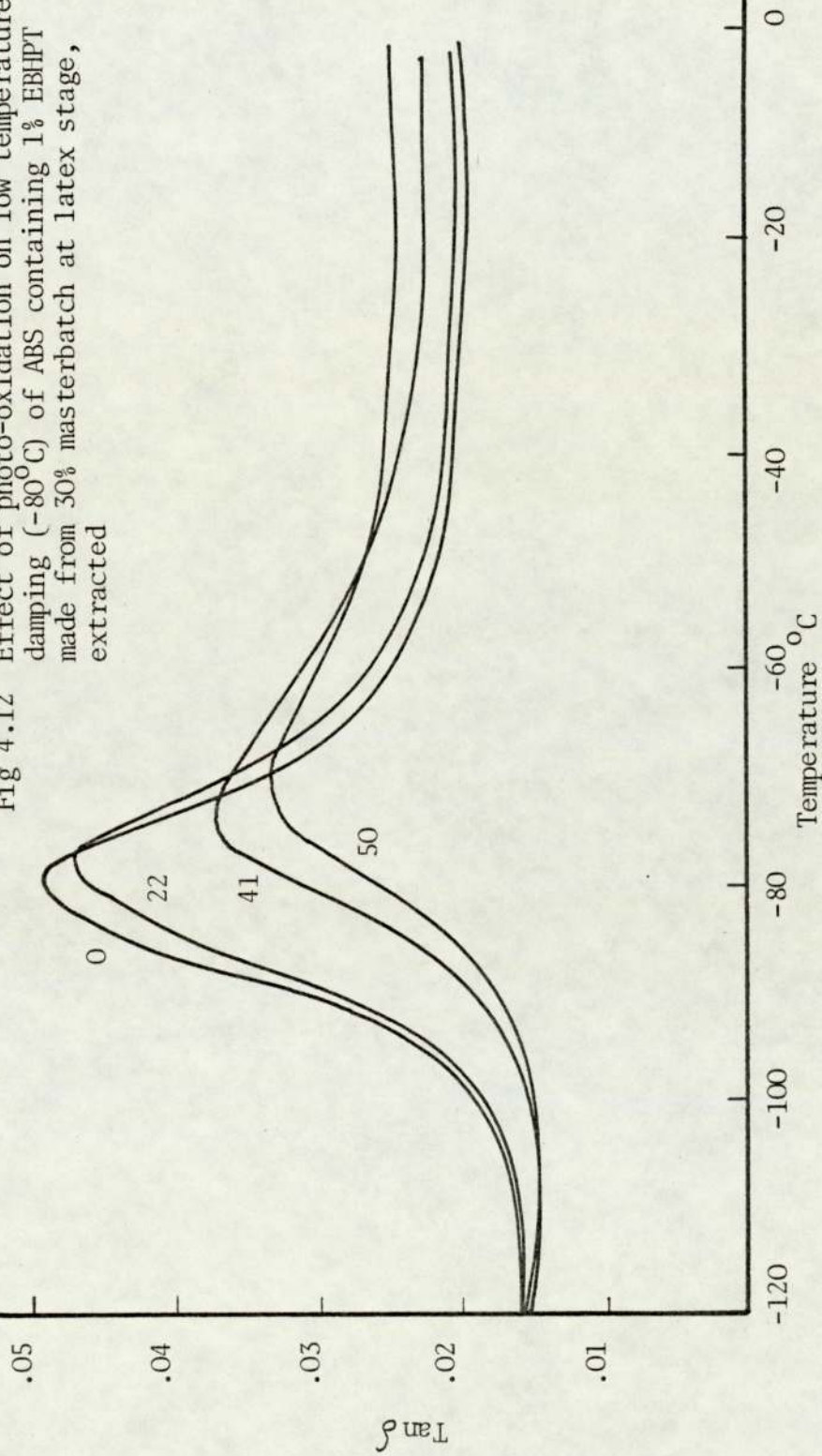
energy through a radiationless route called internal conversion. This is facilitated by the rapid tautomerism in the excited state of the molecule due to the presence of a strong inter-molecular hydrogen bond, in 2-hydroxybenzophenones.
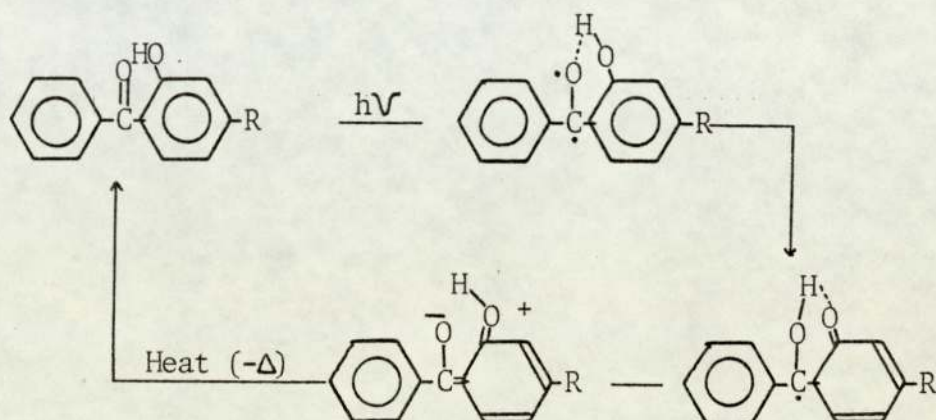
The enhanced activity of the sulphur derivative of 2-hydroxybenzo phenone EBHPT over the other stabilisers, given in Table 4.4, could be due to its additional hydroperoxide decomposing ability. The changes in the functional groups (C=O, C=C) were measured by infra-red are shown in Figs 4.4, 4.5, 4.6 and 4.7, for samples made from masterbatches in the latex and solid stages. Samples made from masterbatches in the latex stages (latex blending) by mechanical stirring gave somewhat better stability over samples made by solid blending during processing in the torque rheometer. This could be due to the loss of some stabilised ABS coagulum (powder) during addition into the chamber of torque rheometer and also during processing. It was also observed that the stability among the specimens made by solid blending is not quite uniform whilst such a result was not

Fig 4.14 Effect of photo-oxidation on low temperature damping (-80°C) of ABS film containing 1% EBHPT made from 10% masterbatch at solid stage, extracted

Temperature °C

Tan δ

180

Fig 4.15 Effect of photo-oxidation on low temperature damping (-80°C) of ABS film containing 1% EBHPT made from 20% masterbatch at solid stage, extracted

181
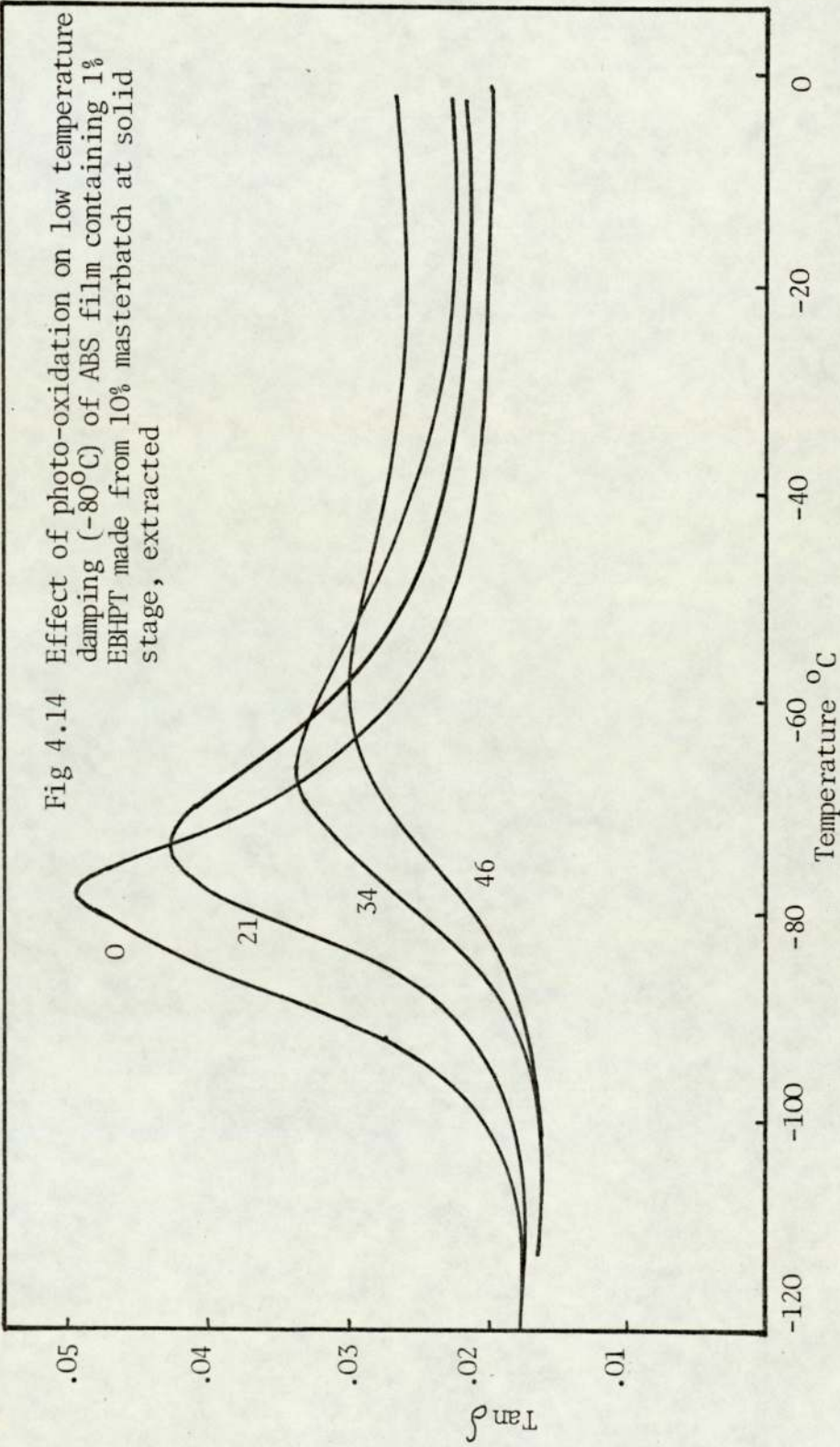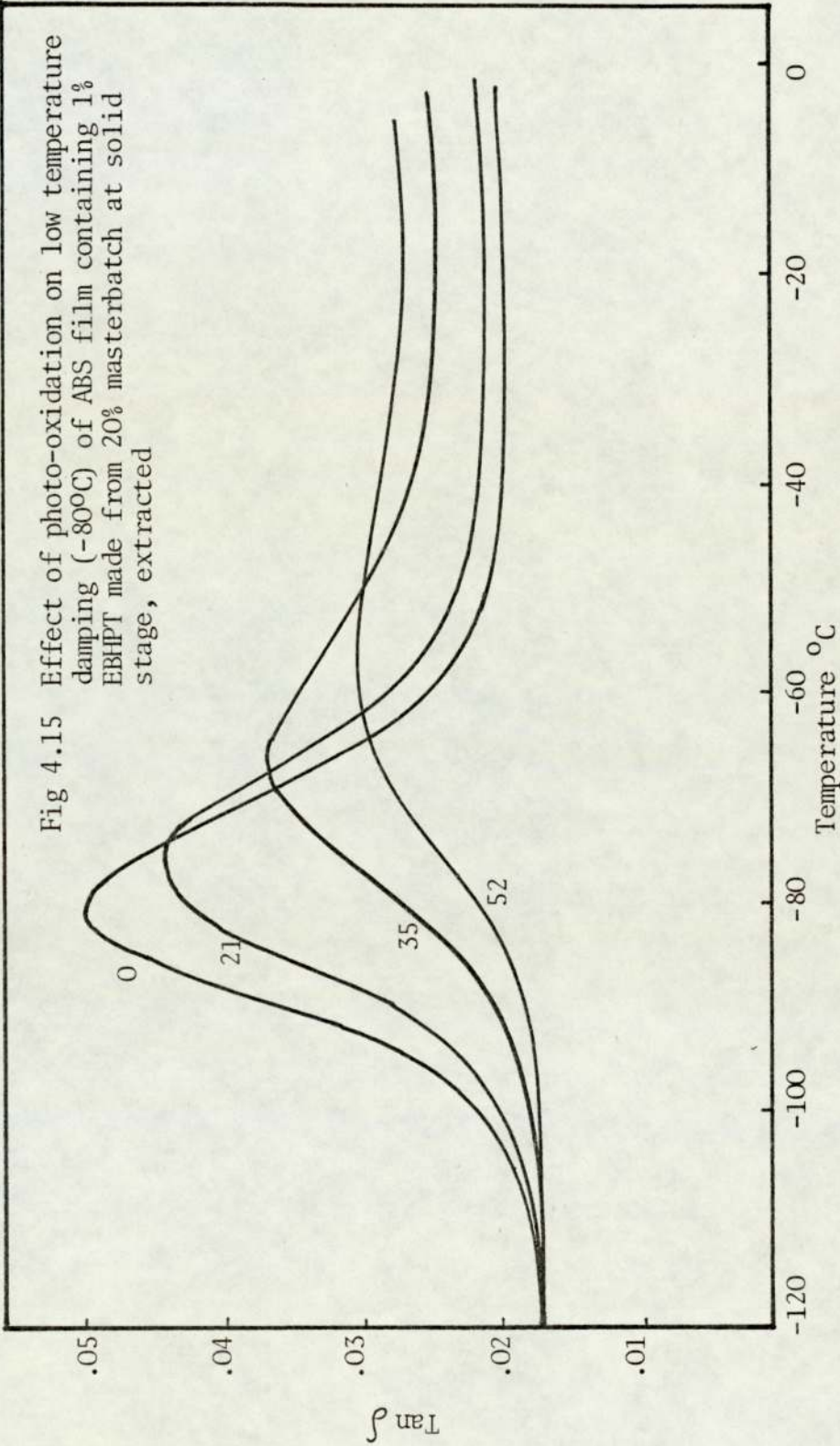
observed for specimens made by latex blending.

Impact measurements carried out by weight falling tester, similarly show a rapid decrease immediately after induction period. The reason for this is that the impact changes reflect chemical and hence physical changes in the surface of the polymer where degradation is most severe whereas transmission ir spectroscopy measures changes through the bulk of the polymer. Comparison of the impact strength of unstabilised ABS with the impact behaviour of stabilised ABS containing 0.8 pph of EBHPT shows that under the same conditions the time to 40% loss of energy to break has been increased from 8 hours to 35 hours (Figs 4.8 and 4.9).

Low temperature damping curves were measured for all samples containing different concentrations of bound uv stabiliser. The rate of decrease in the height of $\tan \delta$ at low temperature depends upon the concentration of bound uv stabiliser. ABS samples containing higher concentration of bound uv stabiliser show slower decrease in the height of damping peak during exposure to uv light. One of the advantages of the masterbatch technique is the preparation of bound uv stabiliser at high concentration which can then be used as an additive for commercial polymer. Preparation of bound stabiliser at high concentration is accompanied by saturation of some double bonds of the rubber component which is accompanied by partial loss of useful mechanical properties (see Chapter 5). However, using a

Fig 4.16 Effect of photo-oxidation on low temperature
damping (-80°C) of ABS film containing 1% EBHPT
made from 30% masterbatch at solid stage,
extracted
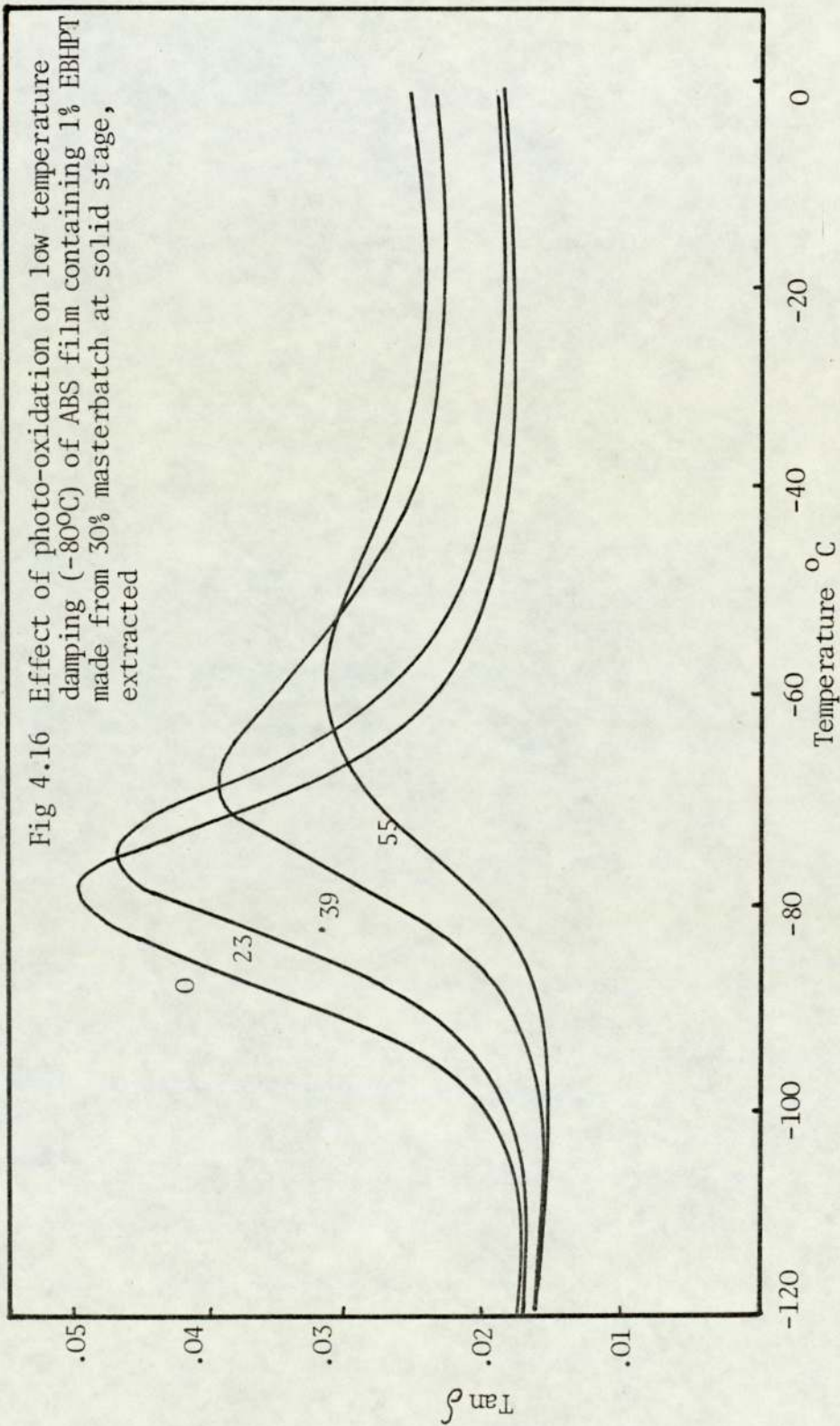
Fig 4.17 Decay of height of tan δ peak at -80°C on uv exposure of ABS pressed films, masterbatches were diluted at latex stage

■ Control (Borg-Warner latex)

✪ 1% EBHPT from 10% masterbatch, extracted

□ 1% EBHPT from 20% masterbatch, extracted

● 1% EBHPT from 30% masterbatch, extracted

▲ 1% EBHPT from 30% masterbatch, unextracted
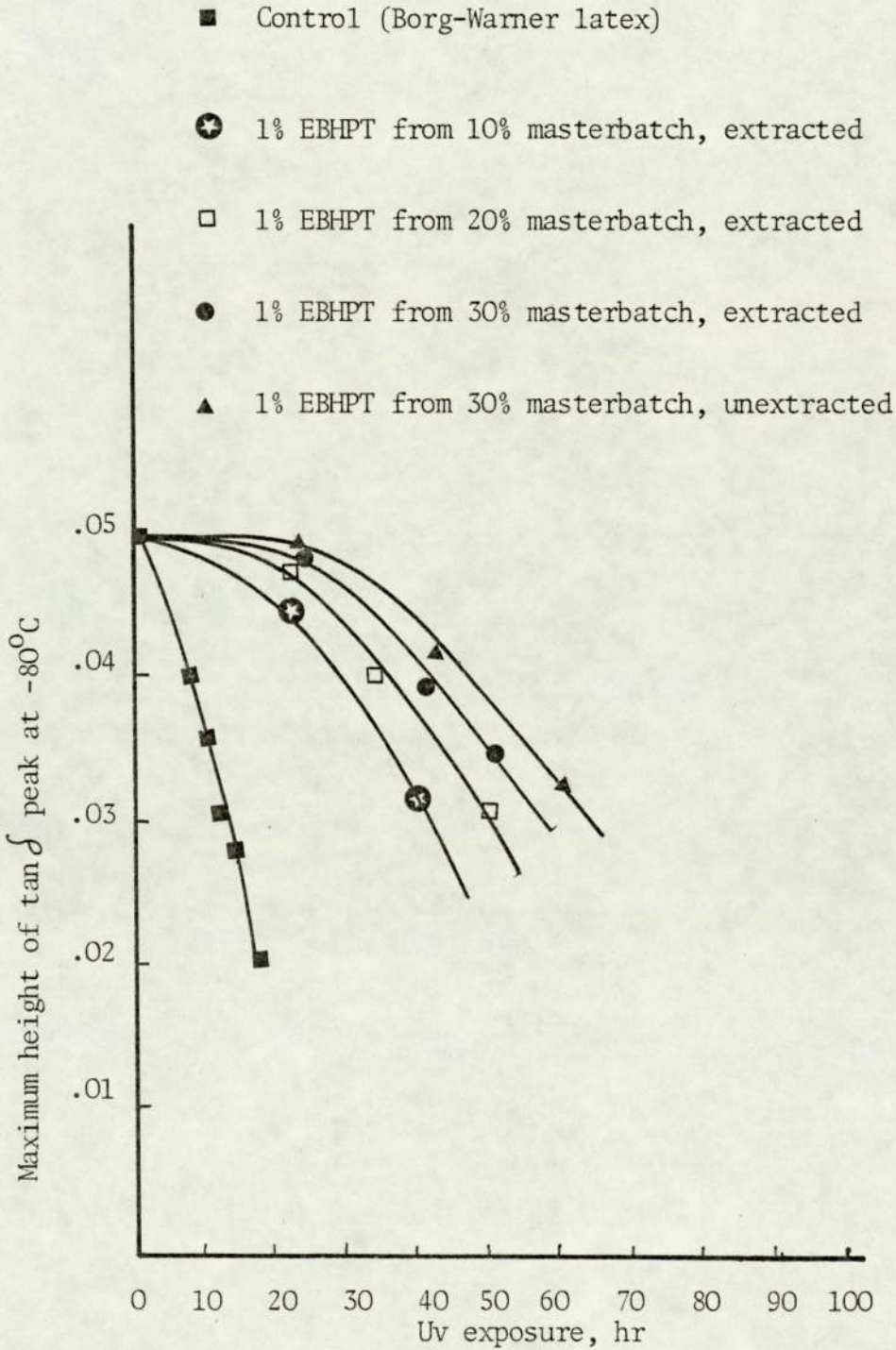
masterbatch containing a high concentration of uv bound stabiliser as an additive for unstabilised ABS does not change the mechanical properties of the ABS to which it is added. It is seen from Figs 4.8 and 4.9 that the initial impact strengths of stabilised ABS and from Figs 4.10 - 4.16 that the height of damping peak at -80°C for unirradiated samples are quite high and identical in magnitude to that of unstabilised ABS. The whole dynamic spectra of stabilised ABS films from $-120 - 0^\circ$C are similar to the dynamic spectra of unstabilised ABS film and no unusual behaviour was observed due to the presence of 1 pph EBHPT. The damping peak for stabilised ABS appeared at -80°C (Tg of rubber) which is again similar to that of unstabilised ABS.

The maximum height of tan δ at low temperature were plotted against time of exposure for all samples containing different concentration of bound uv stabiliser, (Figs 4.17 and 4.18). Comparison of the maximum heights of the low temperature damping peak of unstabilised ABS with the damping behaviour of the stabilised ABS containing 0.8 pph of EBHPT shows that under identical conditions the time to 36% loss of the damping peak has been increased from 12 hours to 50 hours.

4.5   Attempted Masterbatch Formation of BHBM with ABS in Latex

Attempts were made to bind BHBM to ABS latex at different concentrations (1% and 10%). Borg-Warner ABS latex was used using the formulation[75] given in Table 4.5.

185

Fig 4.18   Decay of tan δ peak at -80°C on uv exposure of ABS pressed films, masterbatches were diluted at solid stage

■   Control (Borg-Warner Latex)

●   1% EBHPT from 10% masterbatch, extracted

□   1% EBHPT from 20% masterbatch, extracted

●   1% EBHPT from 30% masterbatch, extracted

▲   1% EBHPT from 30% masterbatch, unextracted

186
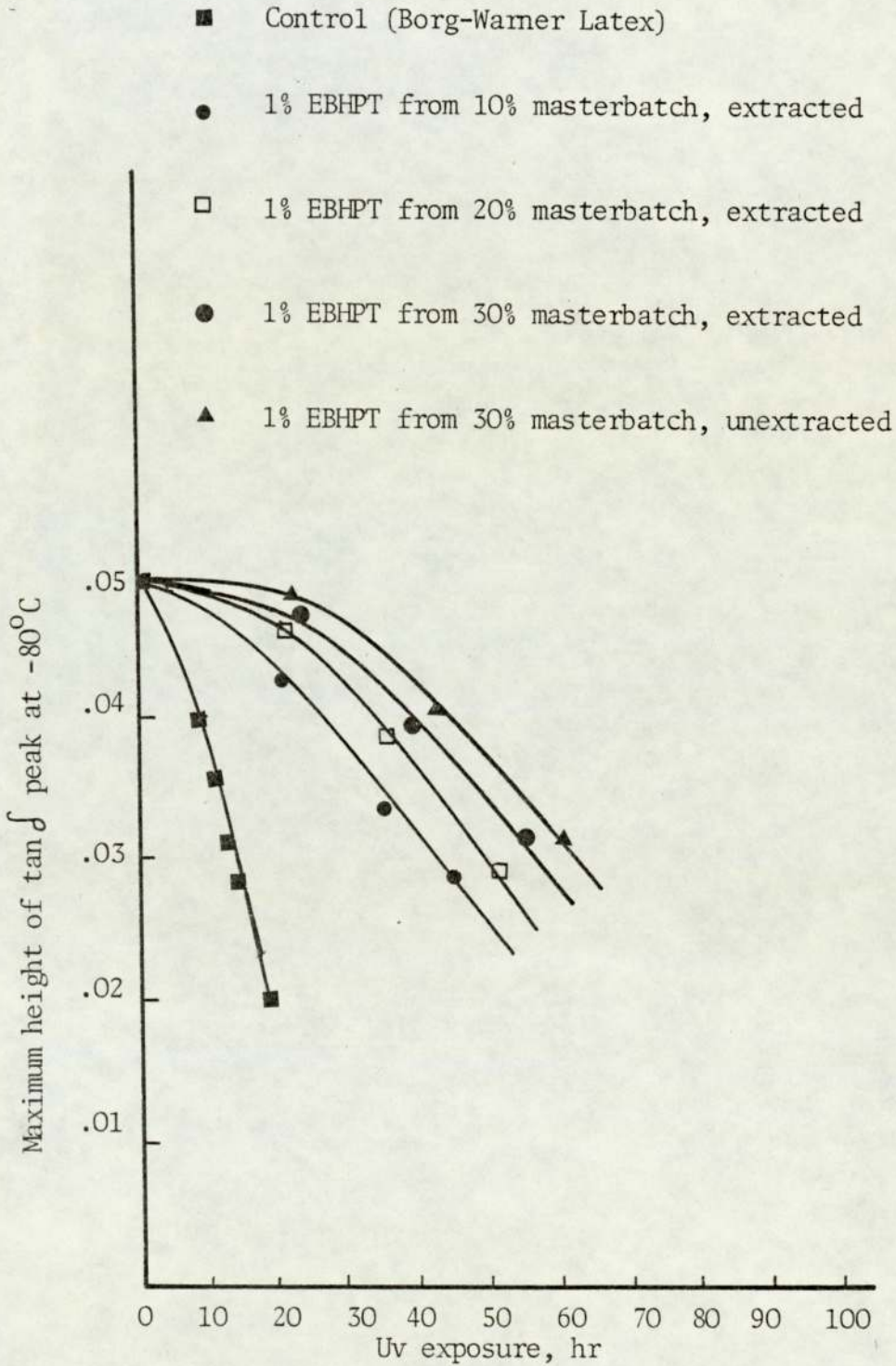
Table 4.5

ABS latex (stripped latex)	330 ml
Antioxidant emulsion (Section 4.5.A)	100 ml
Cumene Hydroperoxide	0.8 g
Fe^{2+}/TSPP solution	8 ml
Glucose (g in 10 ml of water)	2
Time	3 hours
Temperature	$60^{o}C$
Atmosphere	N_2

4.5.A Preparation of Antioxidant Emulsions

Emulsions of BHBM were prepared[75] by melting 1 g of stearic acid with the required weight of BHBM in a water bath at 70-75°C. This mixture was slowly added to 50 ml of warm (50°C) distilled water purged with nitrogen containing 0.140 g of NaOH. The mixture was vigorously stirred and was quickly cooled in a cooling bath. The emulsion was shaken mechanically and warmed in hot water (50°C) before addition to the reaction mixture.

4.5.B Procedure for Adduct Formation

The ABS latex and the antioxidant emulsion were purged with nitrogen prior to the reaction. The redox system was added to the ABS latex and the temperature of the mixture was raised to 60°C in a water bath under nitrogen atmosphere. The initiator (CHP) and BHBM emulsion were added in aliquots (4 aliquots) within the first half of the reaction.

The latex was acid coagulated, dried in a vacuum oven at 50°C to constant weight. The material was extracted in a soxhlet with hot hexane for 48 hours. The estimation of bound BHBM was made by using calibration curve (Fig 5.2) and this was correlated with the stability of polymer films during oven ageing at 100°C in air.

4.5.C Results

Compression moulded polymer films were used to measure the stability of the adducts in a Wallace oven at $100^{\circ}C$. The embrittlement time and changes in the functional group concentration were measured as shown in Figs 4.19 and 4.20. The formulation given in Table 4.5 was used to produce different concentrations of bound BHBM, the results were not reproducible and sometimes there was no antioxidant bound at all. Only twice for 10 g of BHBM and about three times for 1 g of BHBM were similar results obtained. The changes in the concentration of functional groups (C=O; 1,4 C=C) of these polymers are shown against time of heating in Figs 4.19 and 4.20.

4.5.D Discussion

The formulation which was used to bind BHBM to ABS in latex was first reported by Fernando[75]. The redox system and initiator (CHP) were the same as for grafting EBHPT to ABS in latex. The ABS latex (Borg-Warner ABS) was stripped, sometimes for 24 hours, to remove the styrene monomer according to Fernando's procedure. The BHBM emulsions were prepared with great care to prevent oxidation and when oxidation did occur the emulsion was yellow. The grafting results were not reproducible and only 2-3 times similar results were obtained from more than thirty attempts. The reason could be the oxidation of BHBM through OH groups. The radicals of cumene hydroperoxide (hydroxyl radical)

189

Fig 4.19 Development of carbonyl functional group on heating (100°C) of ABS pressed films containing bound BHBM

□   1% BHBM from 10% masterbatch, extracted

△   1% BHBM, extracted

O   Control (Borg-Warner)
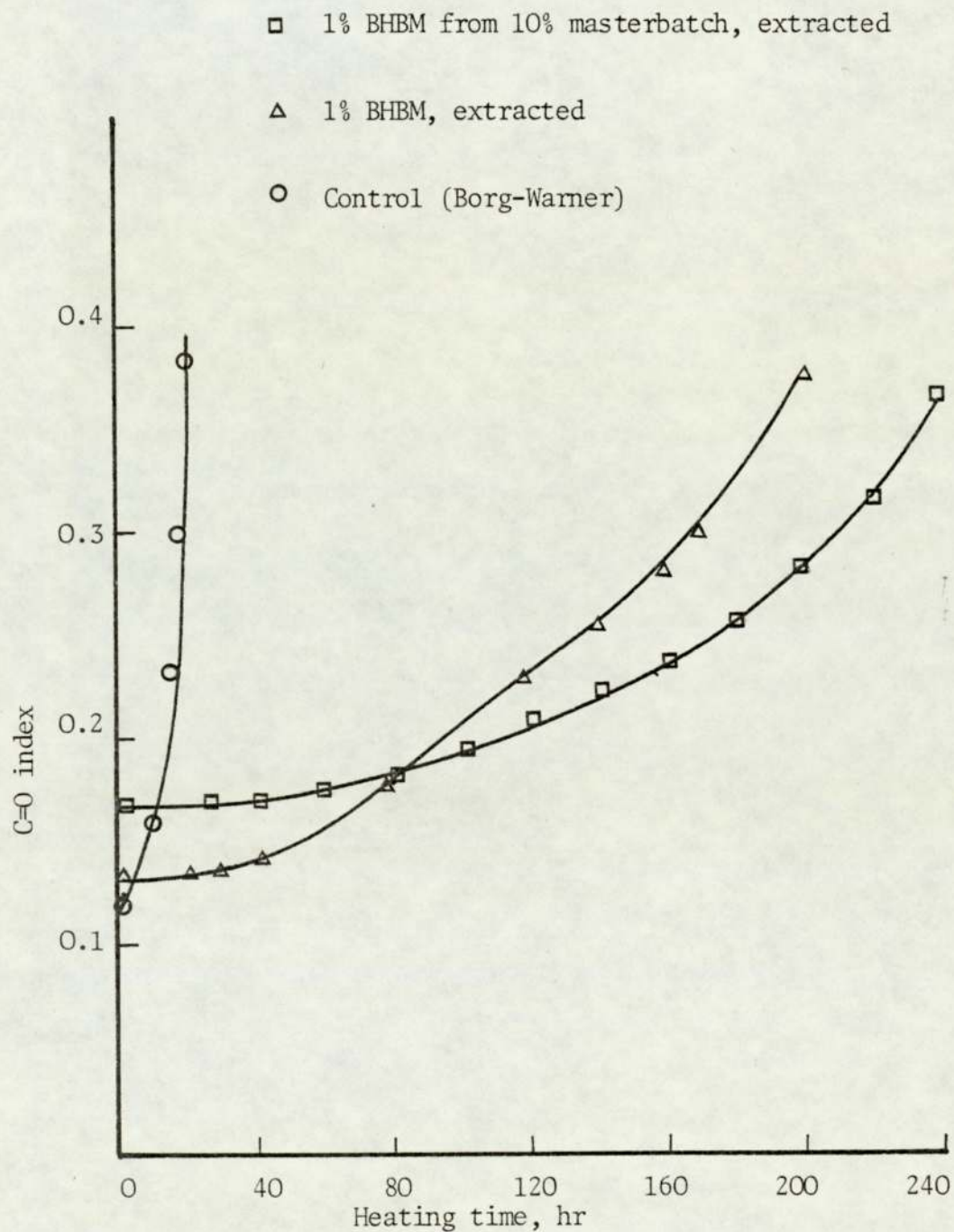
Fig 4.20 Decay of trans-1,4-PBD unsaturation on heating of ABS
        pressed films containing bound BHBM

□   1% BHBM from 10% masterbatch, extracted

△   1% BHBM, extracted

○   Control (Borg-Warner)

191
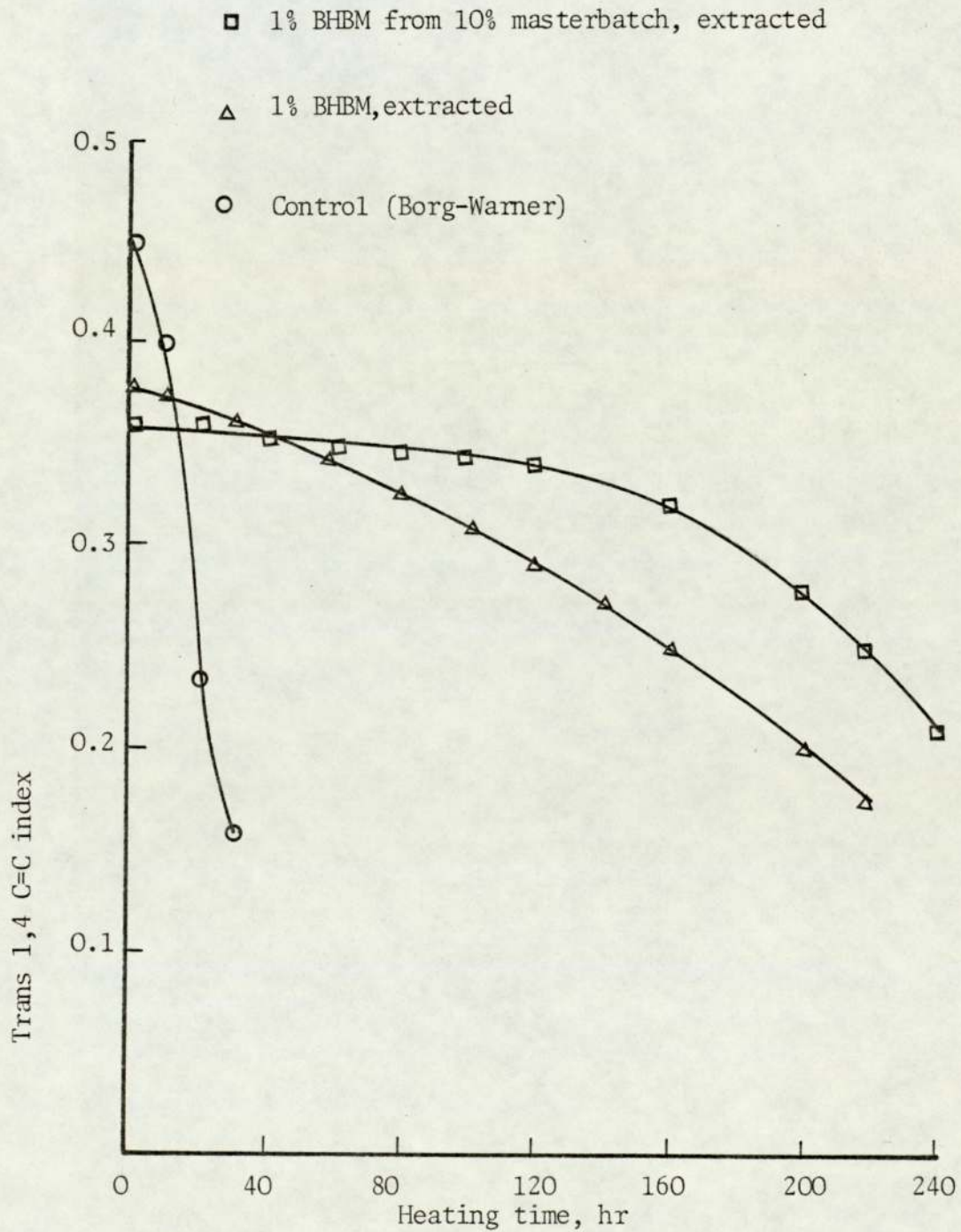
can readily hydrogen abstract from the phenolic group of BHBM[75].
Once the phenoxy radical is formed it can undergo further
reactions leading to the formation of quinones[67].
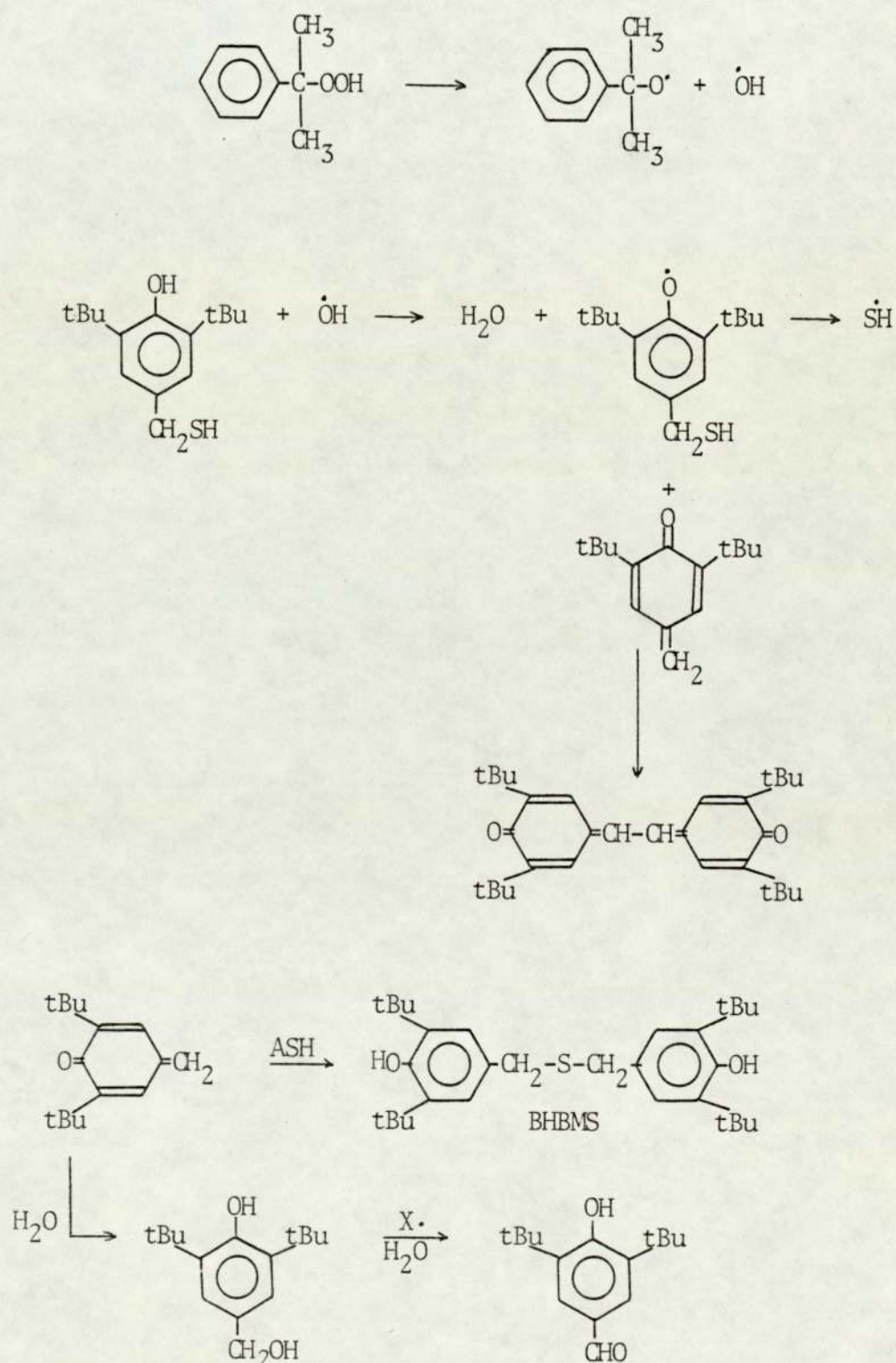
The ABS latex became yellow during grafting, and for higher concentrations of BHBM (10%) the colour was deep yellow. The yellow colour of ABS latex was almost certainly due to the formation of quinones and subsequent stiblenequinone[67].

The Borg-Warner latex was supposed to be free of antioxidant but the ABS latex which was used for BHBM adduct formation after solvent casting showed an induction period of 60 hours to carbonyl formation in the infra-red during thermal oxidation, confirming that the latex contained some kind of commercial thermal stabiliser. The nature of the antioxidant was not known but it seems likely that it was a phosphite ester since the latter are known to interfere with redox reactions involving hydroperoxides due to their ability to destroy hydroperoxides.

Due to shortage of time and because of the much greater potential of the mechanochemical masterbatch procedure (see Chapter 5) the latex process was not followed up further but it is relevant to note that ABS latex containing only a small amount of a phenolic antioxidant obtained from another ABS manufacturer has been successfully reacted with BHBM under the above conditions[141].

CHAPTER FIVE

THE FREE RADICAL ADDITION OF THIOL COMPOUNDS TO ABS BY A
MECHANOCHEMICAL PROCEDURE

5.1 Introduction

The formation of free radicals in uncured rubbers during milling
and mastication processes has been inferred by a number of
workers from the rheological changes in the polymer[118] and from
the chemical reactions which can be initiated in the rubbers
under conditions of shear[119-122]. More recently, direct
evidence has been found for macro-radical formation by ESR
spectroscopy. The free radicals have been trapped by freezing
the masticated polymer in liquid nitrogen below the glass
transition temperature[123] and their reaction with stable-free
radicals previously introduced into the system[124,125] has
been followed. Similar effects have been found during the
milling of vulcanised rubbers[123] and in the presence of
oxygen, the radicals were characterised as alkylperoxy radicals.

It has been reported[125] that the initial chain scission
process gives rise to alkylperoxy radicals which in the presence
of excess hydrogalvinoxyl (I) are converted to hydroperoxides
with the formation of the alkoxy radical.

$$\text{(tBu)(tBu) } O=\!\!\!\langle\rangle\!\!=CH\!-\!\langle\rangle\!-OH \text{ (tBu)(tBu)}$$

(I)

$$-\overset{\overset{\displaystyle CH_3}{|}}{C}=CH-CH_2CH_2-\overset{\overset{\displaystyle CH_3}{|}}{C}=CH-CH_2 \longrightarrow \overset{\overset{\displaystyle CH_3}{|}}{C}=CH-\overset{\displaystyle \cdot}{C}H_2 + \overset{\displaystyle \cdot}{C}H_2-\overset{\overset{\displaystyle CH_3}{|}}{C}=CH-CH_2$$

(R·)

$$R\cdot \; + \; O_2 \; \longrightarrow \; ROO^{\cdot} \; \xrightarrow{\;GH\;} \; G\cdot \; + \; ROOH$$
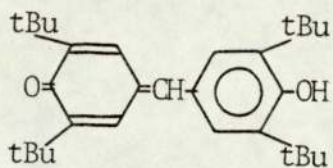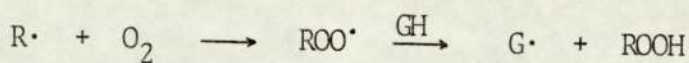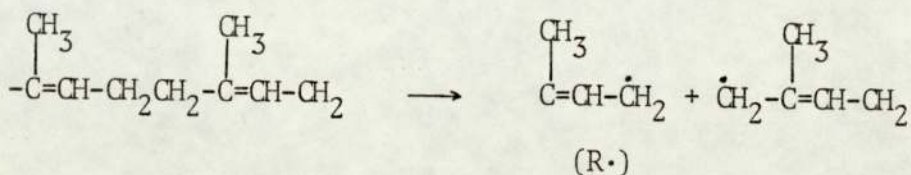
It was suggested however that the disappearance of galvinoxyl may involve either addition to the activated double bond (under stress) or attack at a weakened C-C single bond.

Therefore, the free radicals formed in the scission of the molecular chains of a polymer can react in several ways; reaction with oxygen to form alkylperoxy radicals, reaction with other radicals present in the mixture and reaction with the double bonds of the rubber.

5.2 Attempted Adduct Formation with Stabilisers Containing Thiol Groups during Mechanochemical Process

The uv stabilisers such as 4-benzoyl-3-hydroxyphenol-O-ethyl thioglcyoolate (EBHPT) and 4-benzoyl-3-hydroxy-O-propane-2-ol mercaptan (I), and thermal stabilisers, such as 3,5-di-tert-butyl-

4-hydroxybenzyl mercaptan (BHBM) and 3,5-di-tert-butyl-4-hydroxy-
benzyl carboxy methyl sulphide (BTGA) were used for adduct
formation with ABS (Borg-Warner) during processing in the torque
rheometer.
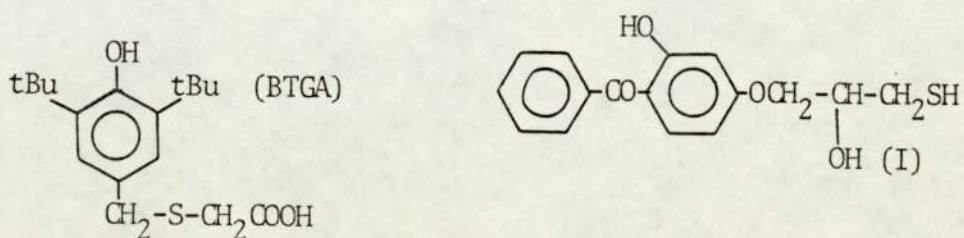
5.2.a Procedure

The mechanochemical reaction carried out using the prototype
RAPRA torque rheometer which is essentially a small mixing
chamber, containing mixing screws contra-rotating at different
speeds. It has good temperature control, and a continuous
readout is provided of both melt temperature and the torque
changes during mixing. The chamber may be operated either open
to the atmosphere or sealed by a pneumatic ram. A full charge
of 35 g of compounded polymer (35 g was the total weight of
polymer and thiol) was processed for 3 mins at various
temperatures with the chamber closed to the atmosphere. A
minimum mixing time of 3 mins was required to ensure complete
gelation of the polymer. An investigation was made to find out
the optimum temperature for obtaining the maximum bound stabiliser
of ABS powder with 5 g of BHBM and EBHPT separately. For this
purpose, a range of temperatures from 80 to 190°C was chosen.

On completion of mixing, the polymer was rapidly removed and quenched in cold water to prevent further thermal oxidation. The material was cold pressed and then compression moulded at 170°C for 3 mins ($1\frac{1}{2}$ mix without pressure and $1\frac{1}{2}$ mins under pressure) into sheets of thickness 0.20 mm to 0.25 mm using a special grade of cellophane as mould release agent. These polymer sheets were hot soxhlet extracted with hexane. It was found that 4-5 days continuous extraction under nitrogen was enough to remove all non-bound EBHPT and in the case of BHBM, about 3 days extraction under nitrogen was enough. This was done by measuring the amount of non-bounded EBHPT and BHBM in the extracts after periods of extraction. Fig 5.1 shows that the absorbances of OH group (by ir) of BHBM and benzo-phenone group (by uv) of EBHPT levelled out after mentioned times of extraction.

5.2.b Estimation of Bound Stabilisers

The polymer sheets became opaque during extraction and could not therefore be used in infra-red and uv spectrsocopy for estimation of bound stabiliser. In the case of polymer film containing EBHPT, the opaque sheets were cut into small pieces and compression moulded at 180°C for 3 mins ($1\frac{1}{2}$ mins without pressure and $1\frac{1}{2}$ mins under pressure) into a clear film of thickness 0.087 mm which were used for uv spectroscopy for estimation of bound uv stabiliser using calibration curve (Fig 4.1). In the case of polymer film containing BHBM, the opaque

197
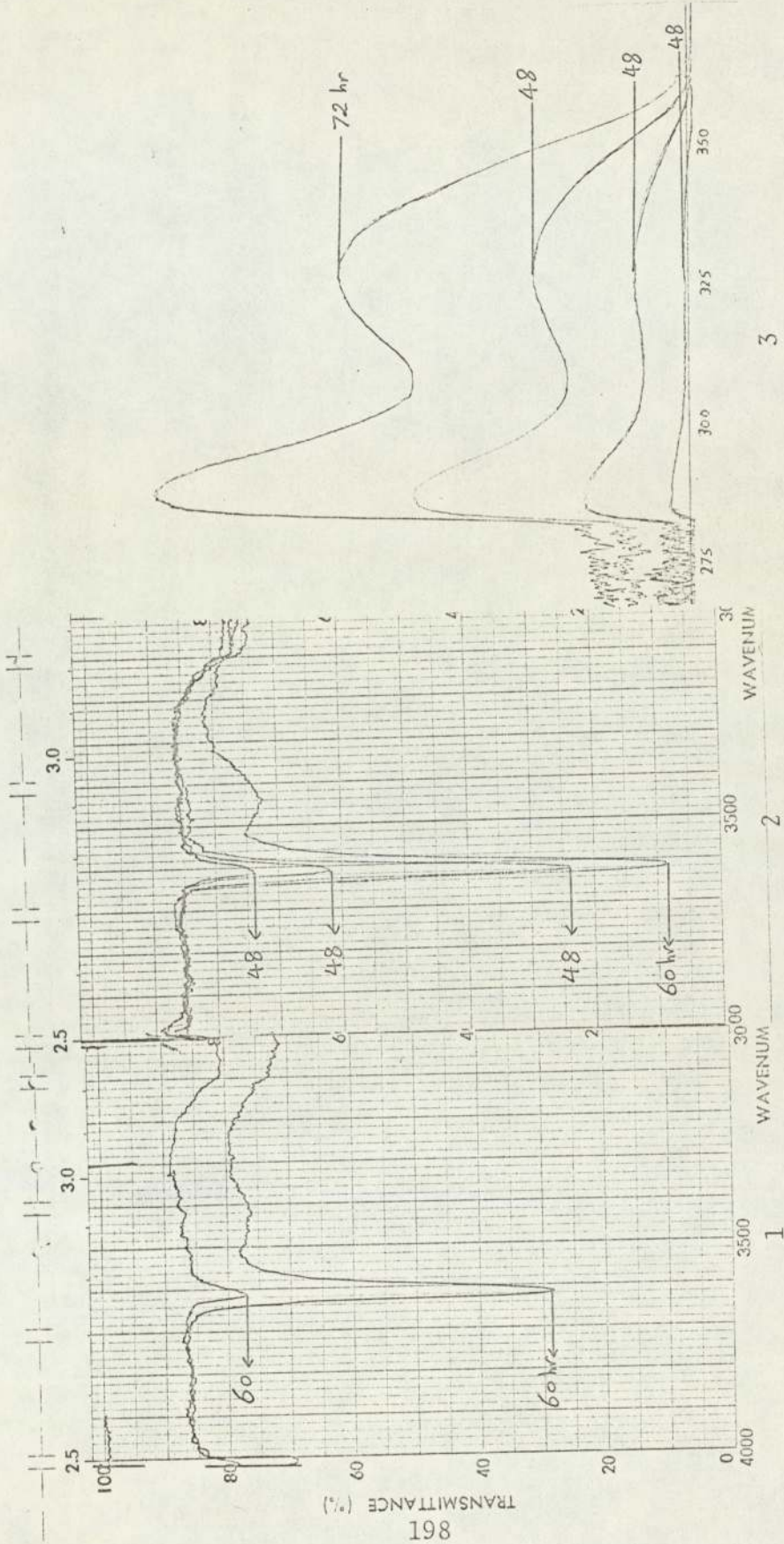
Fig 5.1 Infra-red and uv spectra measurements of OH groups of BHBM and benzophenone ring of EBHPT in extracts

1 10% BHBM - 2 20% BHBM - 3 20% EBHPT

1 10% BHBM - 2 20% BHBM - 3 20% EBHPT

198

Fig 5.2 Calibration curve for BHBM made by measuring absorbance of OH group of BHBM in ABS cast films

199
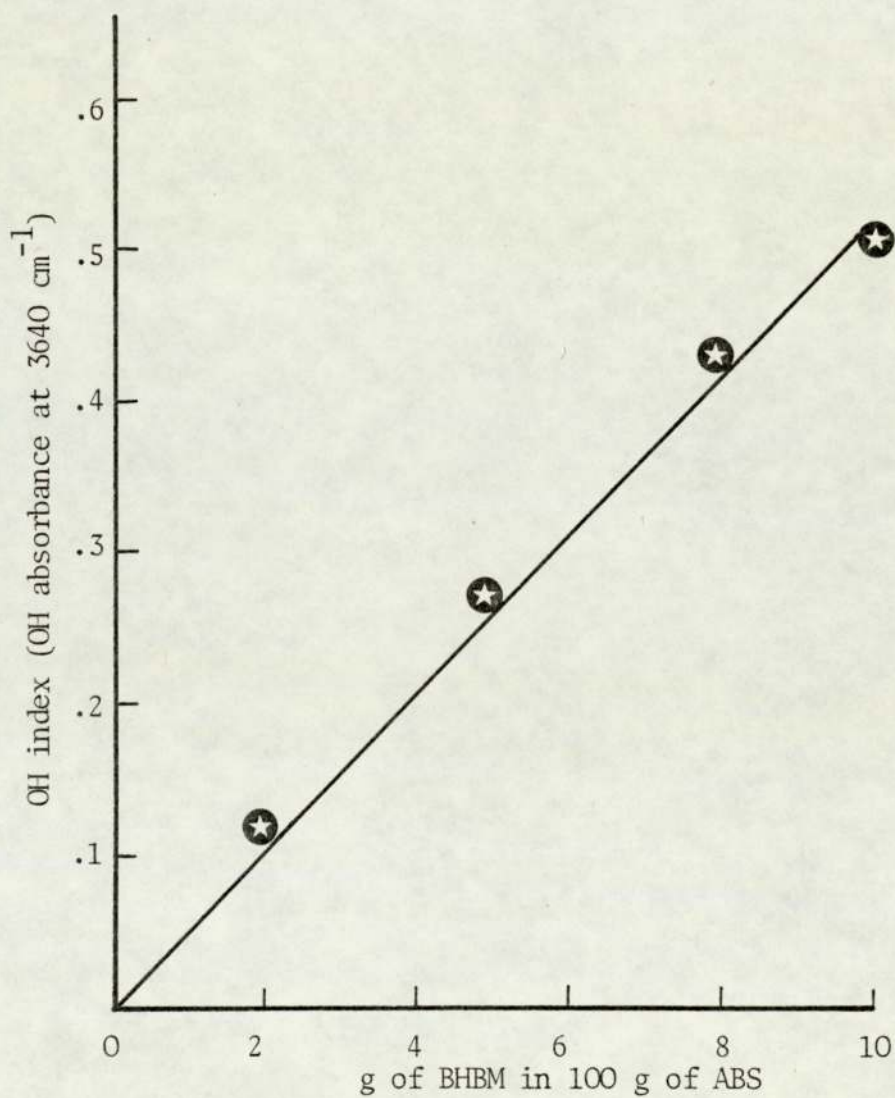
sheets were dried in the vacuum oven at 30°C for 6 hours, (4-5 g) dissolved in dichloromethane and cast on the surface of mercury to give polymer films of thickness 0.125 mm which were used for infra-red spectroscopy for estimation of bound antioxidant by measuring the concentration of OH group at 3640 cm^{-1} using calibration curve (Fig 5.2). The calibration curve for BHBM was made by casting films of ABS powder with different concentrations of BHBM and measuring OH group absorbance using infra-red spectrometry. A second calibration curve for BHBM was made by measuring OH group in a solvent such as chlorobenzene (Fig 5.3). The bound antioxidant was estimated in the extract by rotary evaporating and dissolving the residue in chlorobenzene for OH group measurement. Estimation of bound antioxidant using this technique cannot be as accurate due to the oxidation of OH group of phenolic antioxidant during processing in torque rheometer and extraction. Therefore, the cast film method is more reliable because it measures the OH group remaining after extraction directly in the polymer film.

In the case of polymer film containing EBHPT, the concentration of EBHPT was too high after extraction to measure the benzophenone absorption at 330 nm. The adduct was diluted with unstabilised ABS to a lower concentration, eg 1%, (in the torque rheometer) to bring the benzophenone absorption to the correct level for accurate measurement.

Fig 5.3 Calibration curve for BHBM made by measuring absorbance of OH group of BHBM in chlorobenzene
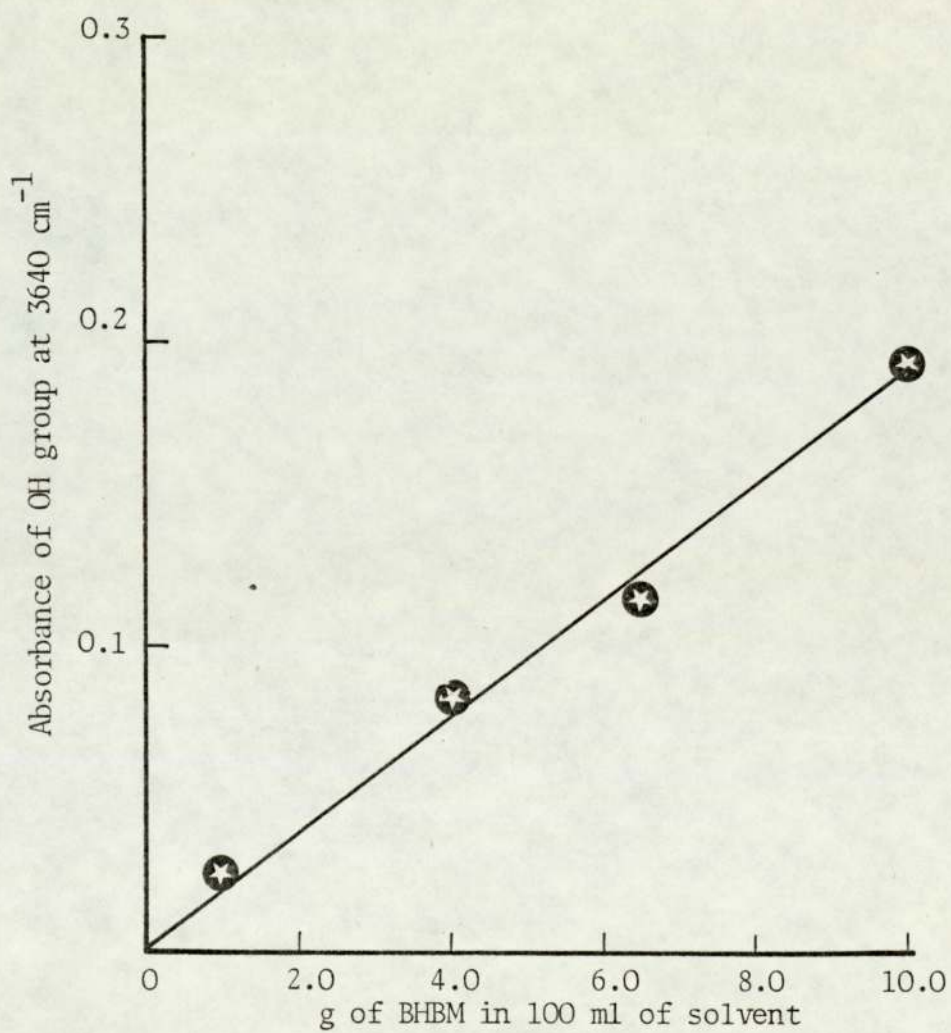
5.2.c Results

Five percent of EBHPT and 5% BHBM were processed separately with unstabilised ABS powder in the torque rheometer for 3 mins at various temperatures. The embrittlement time of the extracted samples were determined and are plotted against processing temperatures for both stabilisers in Fig 5.4.

Embrittlement testing was by flexing pieces of the sample through $180^{o}C$, the sample being considered brittle if a fracture occurred. Normally, five samples with identical thickness for each temperature of processing were used and the repeat tests gave values for embrittlement time lying within $\pm$ 10% of the mean value.

The extracted polymer films containing bound EBHPT were exposed to uv irradiation and the changes in the functional group (C=O, 1,4 C=C) were monitored by infra-red spectrometry. These are shown as a function of uv exposure in Figs 5.5 and 5.6. In the case of polymer films containing bound BHBM, the extracted polymer films were used for thermal ageing at $100^{o}C$ and the changes in the functional groups were again measured. The changes in the carbonyl index of samples processed at various temperatures are shown in Fig 5.7 against time of heating at $100^{o}C$ in air.

Fig 5.4 Embrittlement time (hr) of ABS pressed films containing bound stabilisers
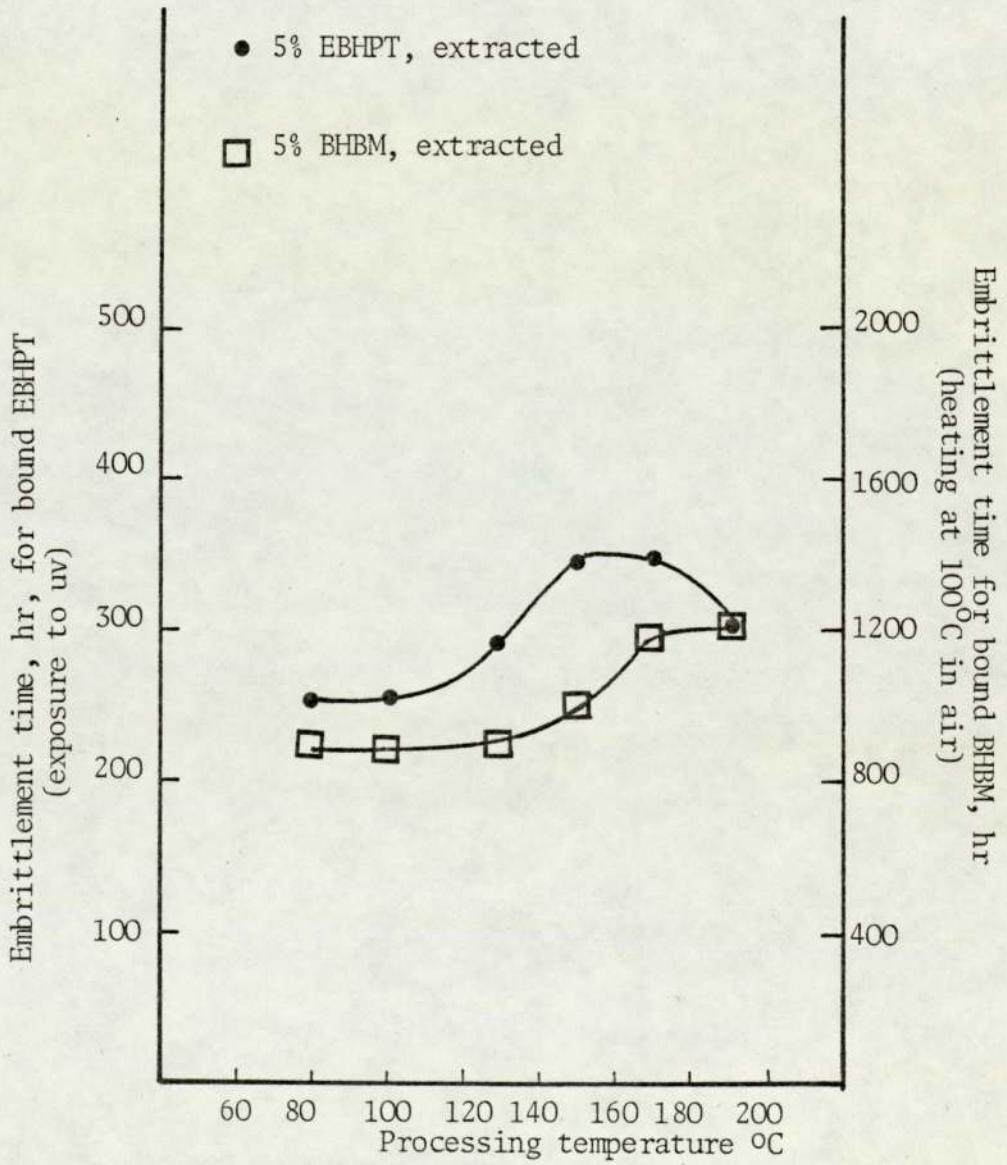
203

Fig 5.5   Development of carbonyl functional group on uv exposure
           of ABS which was processed with 5% EBHPT in torque
           rheometer, extracted

Processing temperature ^{o}C

■ 170

● 130

□ 150

● 80

□ 100

▲ 190

C=0 index

Uv exposure, hr

Fig 5.6   Decay of trans-1,4-PBD unsaturation on uv exposure of ABS
which was processed with 5% EBHPT in torque rheometer,
extracted

Processing temperature ^{o}C

■   170

▲   150

□   130

●   100

■   190

Trans 1,4 C=C index
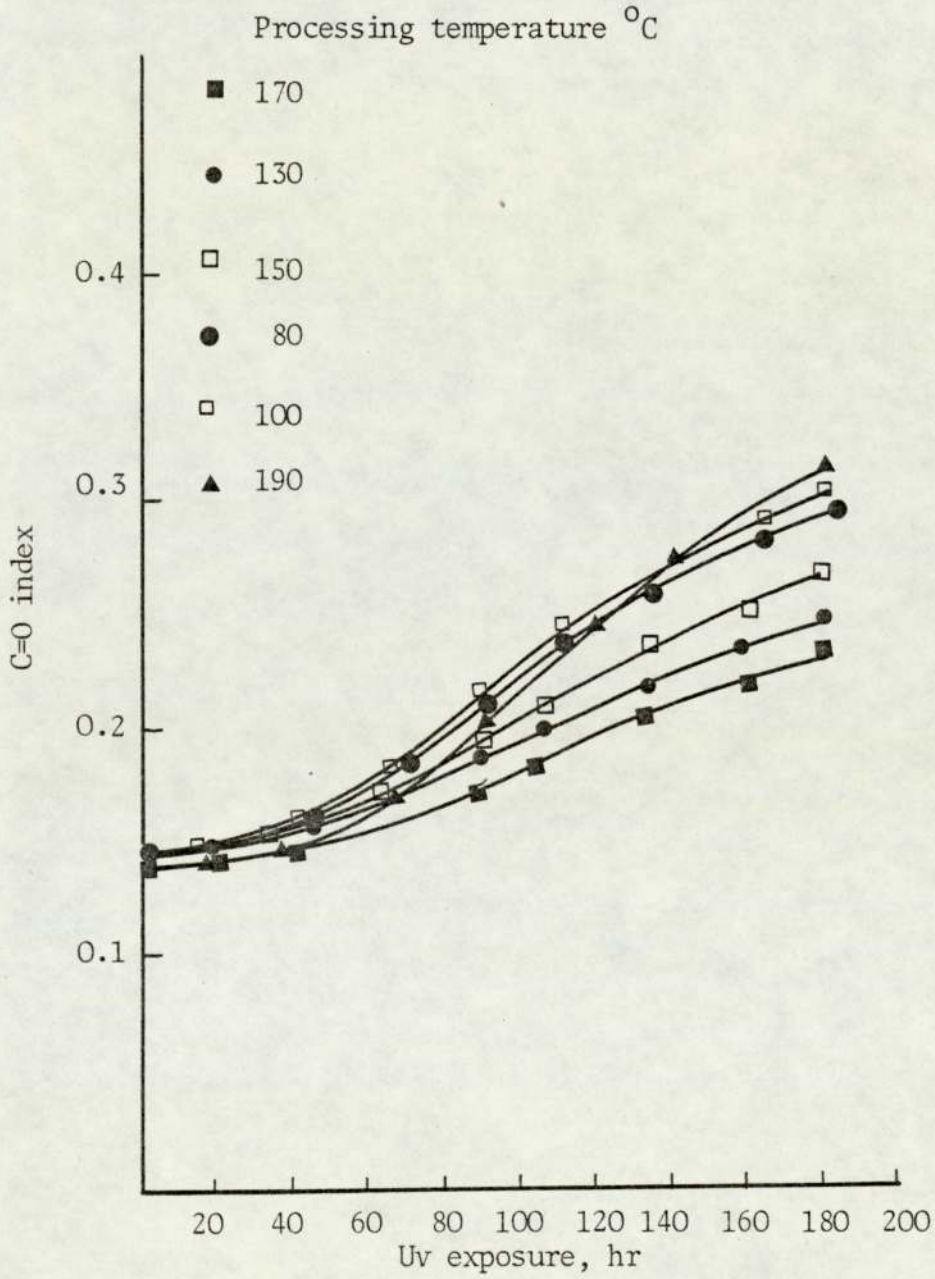
Uv exposure, hr
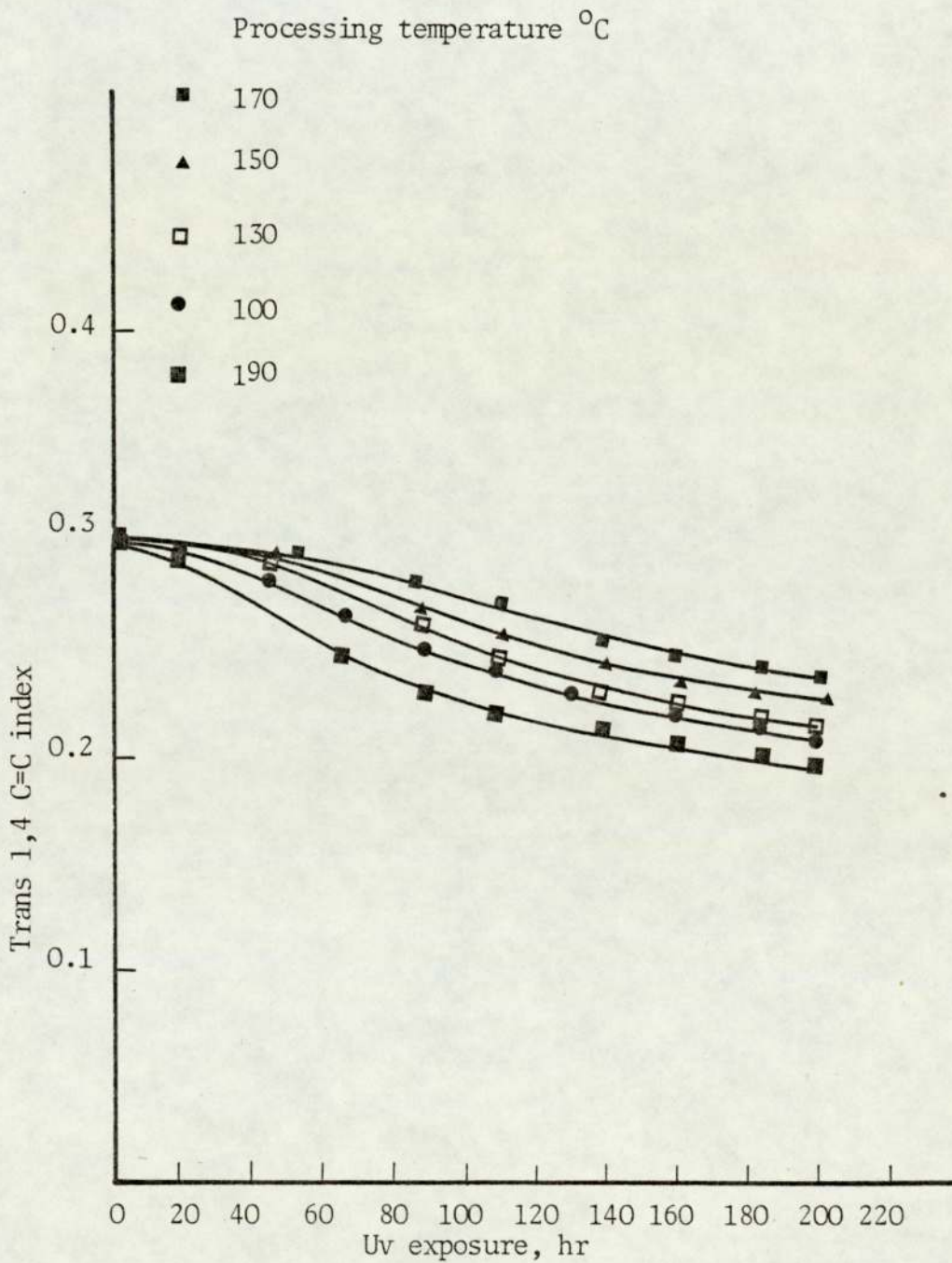
Fig 5.7 Development of carbonyl on heating of ABS which was processed with 5% BHBM in torque rheometer, extracted
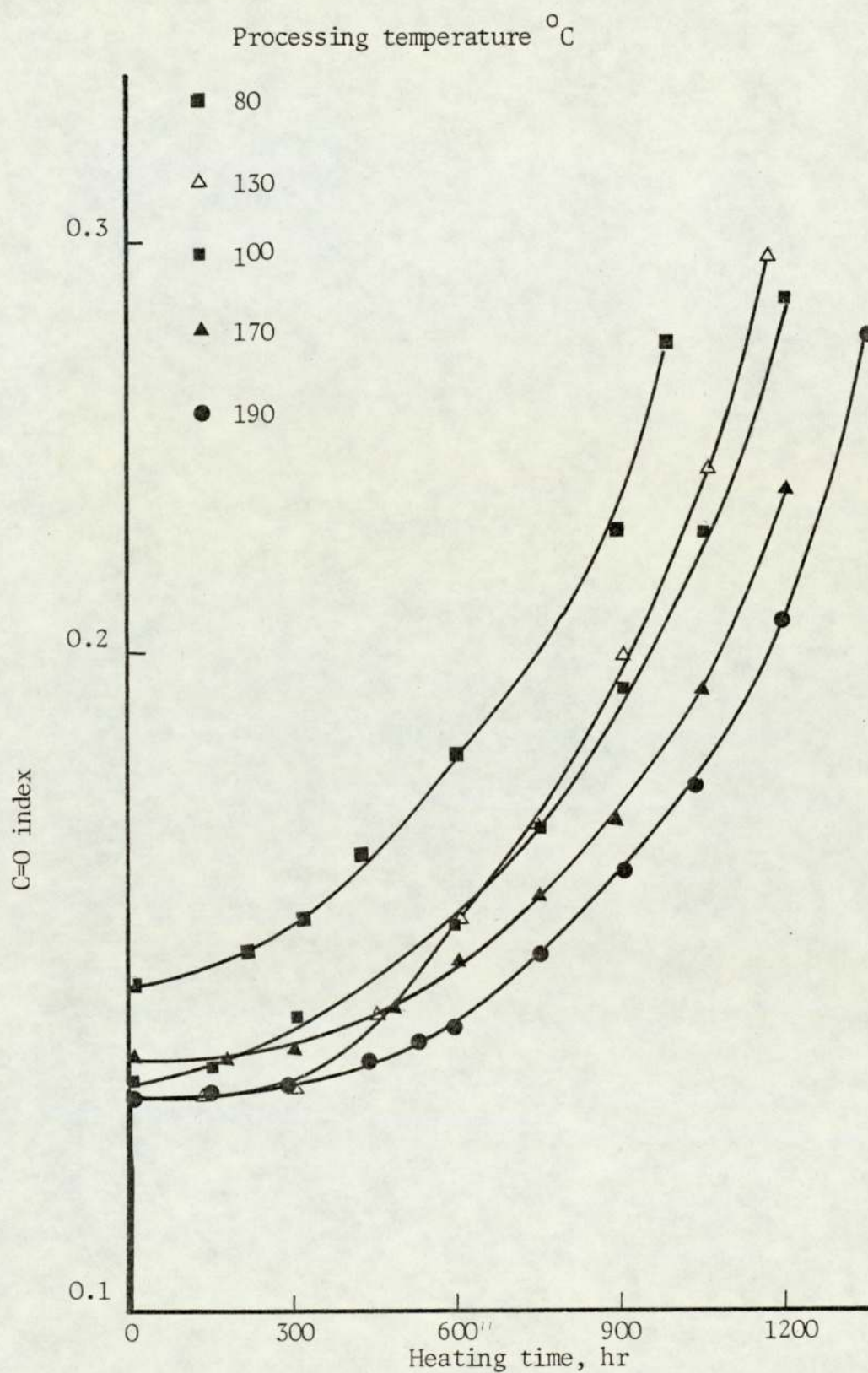
5.3 Masterbatch Formation

The above results (Section 5.2.c) showed that the optimum temperature for obtaining maximum binding with EBHPT was $170^{o}C$ and with BHBM was $170-190^{o}C$. Processing time was 3 mins, in all cases. Similar conditions were used for masterbatch formation (10, 20 and 30%) with EBHPT, BHBM, I, and BTGA.

5.3.1 Results

The extent of binding of EBHPT (measured on the film directly) as a function of EBHPT concentration is shown in Fig 5.8. The amount of binding increased up to 84% for 30 g of EBHPT. The percentage of binding of other stabilisers are shown in Table 5.1. Estimation of bond for compound BTGA was made using the calibration curve given in Fig 5.9. This calibration curve was made using the same procedure as that used for BHBM (see Sections 2.5, 2.20 and Fig 5.2). ABS containing BTGA and compound I were extracted with a more effective solvent, hot methanol, for 50 hours. Estimation of bound stabiliser of compound I was similar to EBHPT (see Section 5.2.b) using the calibration curve which was made for EBHPT (Fig 4.1).

5.3.2 Discussion

5.3.2.a Discussion on the Previous Reported Results

The shear applied during the cold mastication of rubbers ruptures

Fig 5.8 The extent of binding of EBHPT as a function of EBHPT
concentration in ABS by processing in torque rheometer

Percentage of bound stabiliser

g of EBHPT in 100 g of ABS
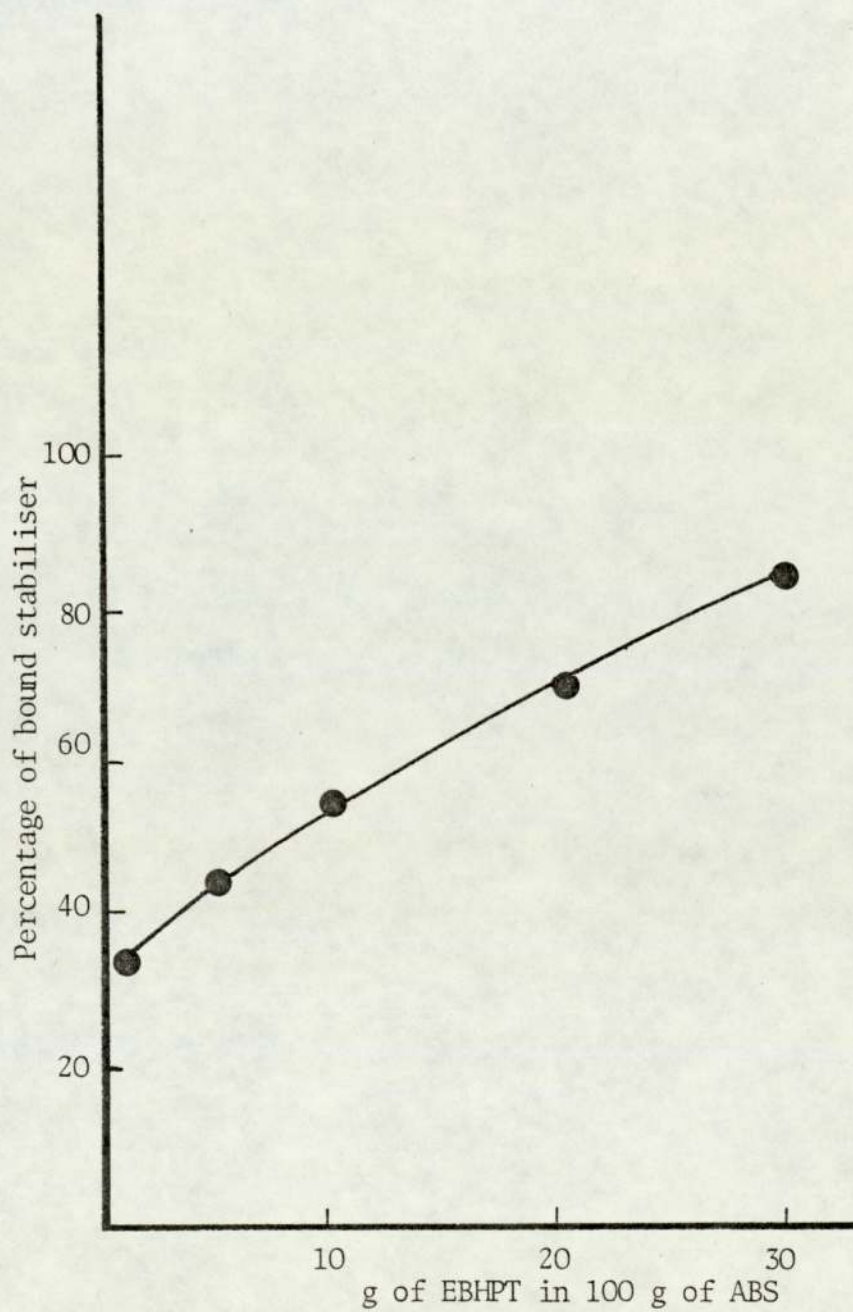
Fig 5.9 Calibration curve for BTGA made by measuring absorbance of OH group at 3640 cm^{-1} on ABS cast film
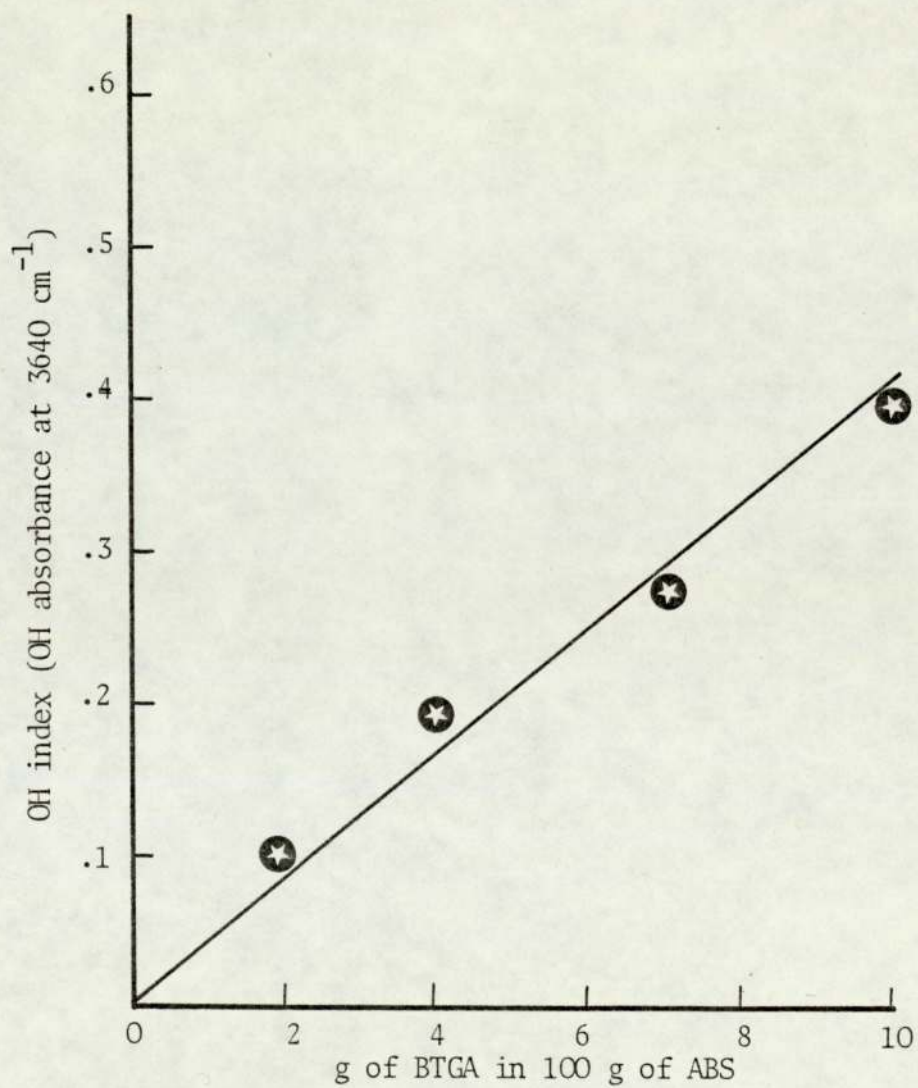
Table 5.1: Estimation percentage of bounding of stabilisers

(measured on the film directly)

Concentration of stabiliser (pph)	Estimated percentage of binding			
	EBHPT	I	BHBM	BTGA
1	34	-	Unknown	Unknown
5	44	-	42	47
10	57	60	6 0	45
20	72	58	12	-
30	84	-	7	-

some of the rubber molecules to form terminal free radicals[122]:

$$R-R \longrightarrow 2R\cdot \qquad (1)$$

The 'softening' of rubber on conventional mastication in air is a consequence of this scission reaction followed by deactivation of these radicals by oxygen to give alkylperoxy radicals. The terminal polymeric radicals in the case of rubbers have been shown to initiate polymerisation of monomer present in the rubber to form predominantly a block copolymer with the rubber[126]. It was reported that polymerisation initiated by mechanical degradation occurs with a wide range of polymer-monomer systems and constitutes a general method of preparing block polymers[127,128]. There appeared to be a limit in the rate of conversion of monomer to polymer which is largely dependent on the viscosity of the molten polymer. The rate of shear may also be altered by softening the mixture by rise in temperature. Degradation of natural rubber during mastication has been shown to proceed[128] via two alternative mechanisms, oxidative scission at high temperatures and mechanical scission at low temperatures. The low temperature, cold mastication, has received the greater attention as a basis of chemical reaction. The mechanism of mastication involves the primary step of mechanical scission of a polymer chain into polymeric free radicals at carbon-to-carbon or other covalent bonds. The reaction of the polymer radicals can be summarised as follows[129].

Recombination: $2R\cdot \longrightarrow R\text{-}R$ (2)

Peroxy radical: $R\cdot + O_2 \longrightarrow RO_2\cdot$ (3)

Reaction with formation
of a radical acceptor: $R\cdot + HS\text{-}ph \longrightarrow RH + ph\text{-}S\cdot$

   (4)

In the absence of oxygen or other radical acceptors, the free radicals recombine (2). In the presence of oxygen the free radicals react to give alkenylperoxy radicals (3)[130]. The $RO_2\cdot$ radicals so formed are deactivated by hydrogen abstraction from other rubber molecules or from non-rubber constituents present:

$RO_2\cdot + HX \longrightarrow ROOH + X\cdot$ (5)

$X\cdot \longrightarrow$ non-radical products   (6)

$X\cdot + R\cdot \; (-CH=CH-\overset{\cdot}{C}H-) \longrightarrow XR \; (-CH=CH-\underset{\underset{X}{|}}{CH}-)$ (7)

$X\cdot + -CH=CH-CH_2- \longrightarrow -\overset{\bullet}{C}H-\underset{\underset{X}{|}}{CH}-CH_2-$ (8)

Hydroperoxides have been shown to be present after mastication

212

in oxygen[130]. Many polymers which are not rubbery at ordinary temperatures become so within a range of higher temperatures, for instance, polystyrene at 100°C. Deforming forces can then readily be imposed on the polymers, indeed, mastication, milling, extruding, and moulding processes depend on deformation in this state. Degradation under mechanical and thermal treatment during processing in a torque rheometer have been reported by many workers for different polymers. HIPS containing no antioxidant was processed in an open torque rheometer and the amount of hydroperoxide was measured by iodiometrically[39]. The concentration of hydroperoxide started to increase in the early stages of processing. It was also reported[131] that samples of polyethylene processed in a full torque rheometer chamber showed much lower dependence on processing conditions. The slight oxidation that was observed was caused by oxygen absorbed on the polymer powder or entrapped in the mixing chamber.

5.3.2.b Discussion on the Present Results

Unstabilised ABS was processed in a full closed torque rheometer chamber at 190°C for 3 mins showed an OH group index of 0.2 whilst the cast film showed less than 0.02. These observations, illustrate that extensive thermal degradation takes place during processing depending on the polymer, temperature, time and the nature of the gaseous atmosphere. The introduction of thermal oxidation products, however, such as alkoxy radicals (RO·) and alkylperoxy radicals (RO$_2$·) into the polymer might be expected

213

to initiate the binding process as the hydroperoxide is known to behave as an effective initiator at high temperatures or in the presence of light. The alkylperoxy radical ($RO_2 \cdot$) might be expected to abstract α-methylenic hydrogen from the rubber backbone or from the thiol group (ASH) to generate the AS$\cdot$ radical.

The thiyl radicals (AS$^{\cdot}$) may then add to the double bonds of rubber component or alternatively they might react with the

$$CH=CH-CH-CH_2 \quad + \quad AS^{\cdot} \quad \longrightarrow \quad \overset{\displaystyle SA}{\underset{\displaystyle |}{CH-CH-CH-CH_2}}$$

$$\underset{\displaystyle SAN}{|} \qquad\qquad\qquad\qquad \underset{\displaystyle SAN}{|}$$

ASH

$$ASSA \quad \longleftarrow \quad AS\cdot \; + \quad \overset{\displaystyle SA}{\underset{\displaystyle |}{CH_2-CH-CH-CH_2}}$$

$$\underset{\displaystyle SAN}{|}$$
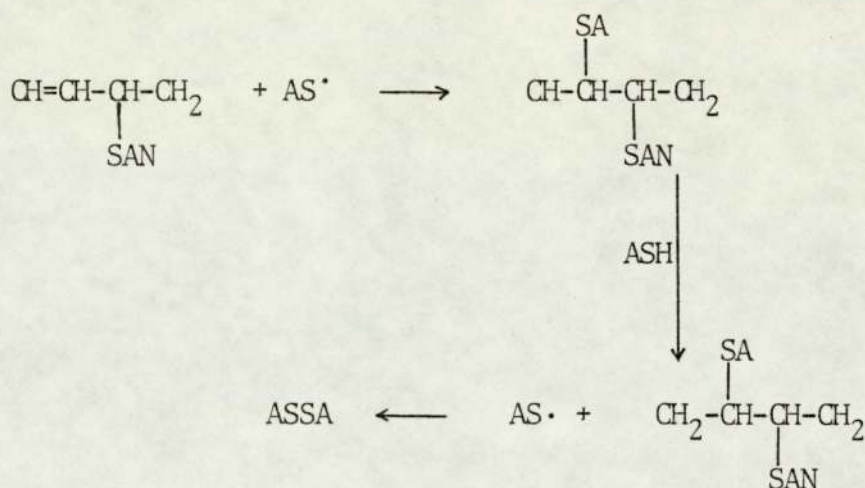
α-methylenic radical in the rubber backbone.

$$CH=CH-\overset{\displaystyle \cdot}{C}-CH_2 \quad + \quad AS^{\cdot} \quad \longrightarrow \quad \overset{\displaystyle SA}{\underset{\displaystyle |}{CH=CH-\overset{|}{C}-CH_2}}$$

$$\underset{\displaystyle SAN}{|} \qquad\qquad\qquad\qquad\qquad \underset{\displaystyle SAN}{|}$$
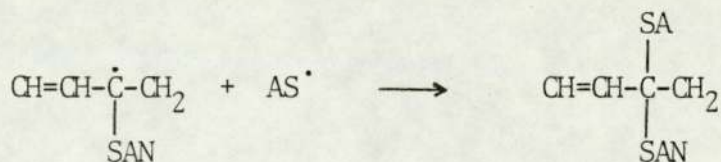
It was however reported that hydroperoxide so formed in the polymer was involved in the initiation process[132] and this was consistent with the fact that the absence of air during

214

grafting (grafting under uv irradiation) leads to a less effective antioxidant graft[132]. The stability of ABS films after an exhaustive extraction can be seen from Fig 5.4 to increase for both stabilisers (BHBM and EBHPT) with increase in temperature of processing. Similar results were observed when the changes in the concentration of functional groups were measured by infra-red during thermal and photodegradation (Figs 5.5-5.7); the most effective stabilisation being produced for polymers processed at 170°C. This behaviour is best explained by the fact that plastics can be transformed into a rubber-like state by raising the temperature or adding plasticisers and they can be masticated in this form with a considerable molecular degradation. Therefore, for 5% stabiliser (BHBM or EBHPT) which is equal to 1.75 g of stabiliser for 35 g of unstabilised ABS, it seems that normal ABS processing temperatures (ranging from 170-190°C) is suitable for the achievment of maximum binding.

There are several important factors which could effect the binding reaction during mechanochemical masterbatch formation. These factors are: temperature, plasticity, rate of shear, initial molecular weight and the compatibility of the stabiliser. Also in the presence of oxygen, the phenolic antioxidants might oxidise at high temperatures. Polymers must be brought into a deformable state during processing either by raising the temperature or by addition of plasticiser; thus the bulk viscosity of the polymer decreases with rise in temperature or addition of plasticiser. At high temperature with increasing amount of

antioxidant, the rate of shear applied to the polymer decreases and causes less breakdown of the polymer. This plasticising effect could be one explanation for the lower bonding above 10 g/100 g polymer in the case of BHBM. The rate of loss of antioxidant from the polymer by volatilisation is another important factor. It has been shown[133] that as the molecular weight of antioxidants increases, the volatility decreases. A study has been carried out[134] of the loss of mononuclear phenolic antioxidants from polypropylene under conditions which simulate the commercial incorporation of the antioxidant into the polymer at $190^{o}C$. It was shown that the loss of the antioxidant 2,6-di-tert-butyl-4-methylphenol at $190^{o}C$ was rather high. Substitution at position -4 by ethyl or i-propyl caused some decrease in volatilisation and n-butyl caused very low loss of the initial concentration. Factors such as volatility, diffusibility and compatibility contribute together with basic chemical activity to the total technological efficiency of an antioxidant[135-137]. It has been shown that the efficiency of the antioxidants depended on polar and steric factors but also on factors leading to low volatility at high temperatures such as suitable molecular weight and compatibility with the polymer. Increases in molecular weight reduces these losses and good compatibility may be ensured by suitable choice of relative molecular weight and aliphatic chain length. Therefore, all these factors, such as increase in viscosity and subsequent decrease in shear force, volatility and compatibility of the stabilisers with the polymer which depend on molecular weight and

216

Fig 5.10 Decay of trans 1,4-PBD unsaturation of ABS films on uv
exposure, masterbatches were made by mechanochemical
processing in torque rheometer

■   1% EBHPT from 20% masterbatch, unextracted

●   1% EBHPT from 30% masterbatch, extracted

□   1% EBHPT from 20% masterbatch, extracted

△   1% EBHPT from 10% masterbatch, extracted

▲   1% EBHPT from 5% masterbatch, extracted

▲   1% EBHPT extracted

●   Control (Borg-Warner latex)

Trans 1,4 C=C index

Uv exposure, hr

217
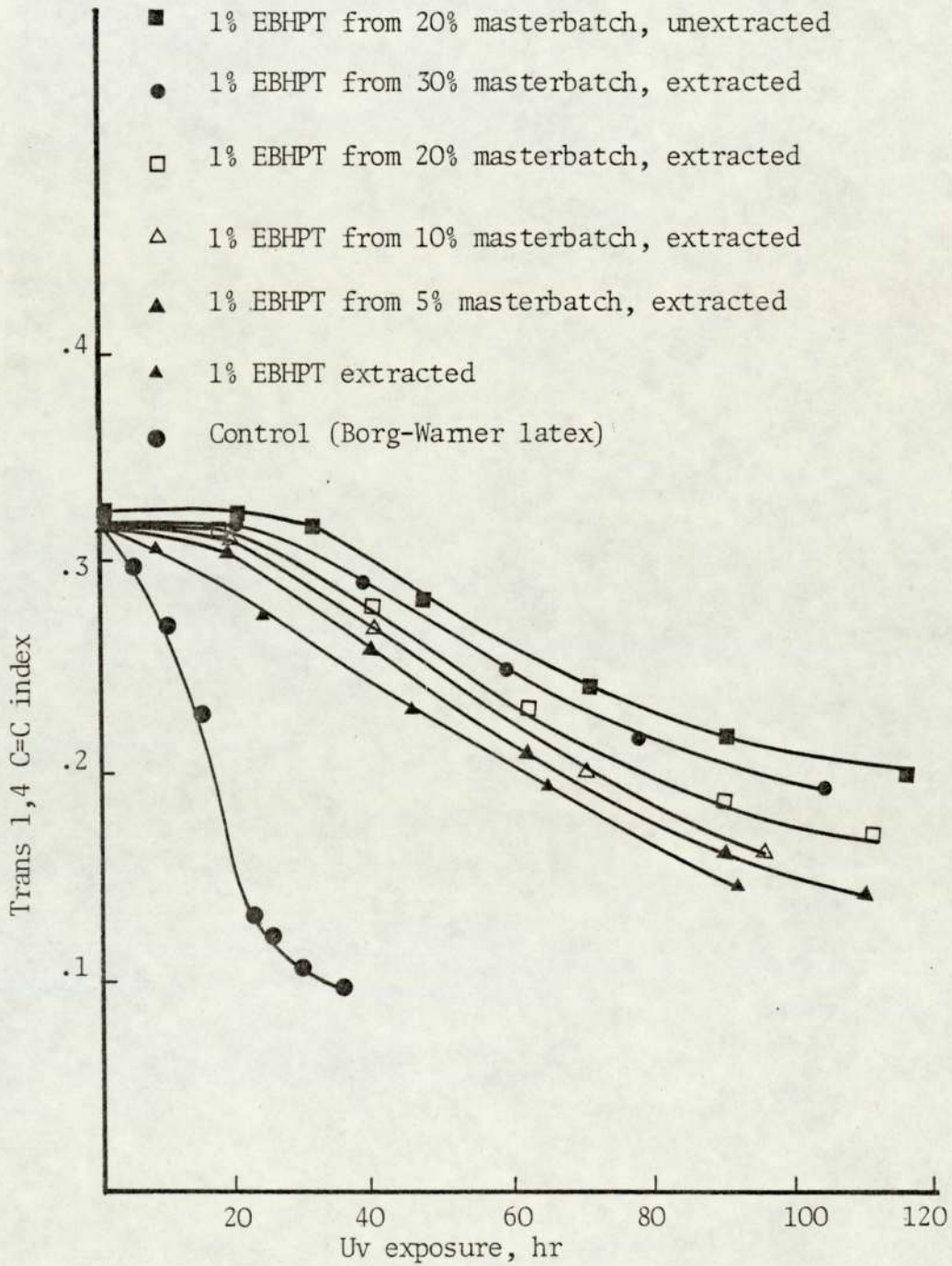
Fig 5.11   Development of carbonyl on uv exposure of ABS films,
masterbatches were made by mechanochemical processing
in torque rheometer

■ 1% EBHPT from 30% masterbatch, extracted

● 1% EBHPT from 20% masterbatch, extracted

■ 1% EBHPT from 10% masterbatch, extracted

□ 1% EBHPT from 5% masterbatch, extracted

▲ 1% EBHPT extracted

● Control

218
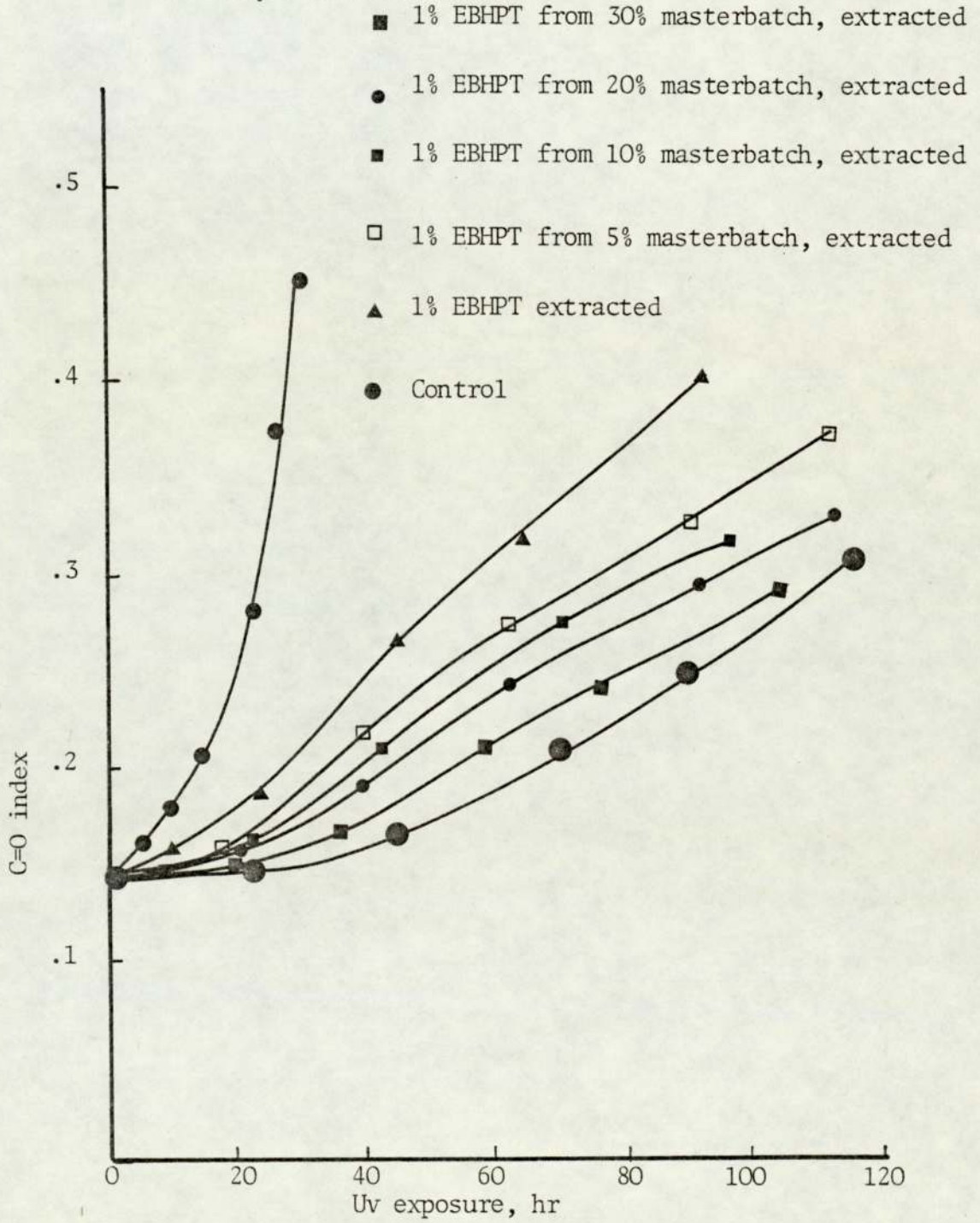
polarity, are probably involved in the formation of masterbatch with EBHPT and BHBM during processing. EBHPT has higher molecular weight and lower volatility and this together with the presence of polar groups should lead to good compatibility with a polar polymer such as ABS. In this connection, it is significant that it gave very similar results by the latex and mechanochemical procedures.

Further work is required and some proposals are made in Section 6.2.

5.3.3 Photo-oxidation of Stabilised ABS (Borg-Warner)

Masterbatches of EBHPT, 10, 20 and 30% were diluted to one percent in the torque rheometer. Photo-oxidation of these samples were followed before and after extraction by measuring the changes in the concentration of functional groups (C=O, 1,4 C=C) and of impact strength. Figs 5.10 and 5.11 show a decrease in 1,4 unsaturation and an increase in carbonyl concentrations respectively. Samples with identical thickness (0.0045 ins) were used for each measurement. The extracted samples containing 0.84 pph of EBHPT from 30% masterbatch showed almost 32 hours induction period. The changes in the impact strength are shown in Fig 5.12 against time of exposure to uv light. The impact strength drops sharply after induction period but the subsequent rate of decrease is rather slower than what was observed in Chapter 4 (masterbatch formation in the latex) which

219

Fig 5.12 Decay of impact strength of ABS films on uv exposure
masterbatches were made by mechanochemical processing in
torque rheometer

● 1% EBHPT from 20% masterbatch, unextracted

■ 1% EBHPT from 30% masterbatch, extracted

■ 1% EBHPT from 20% masterbatch, extracted

▲ 1% EBHPT from 10% masterbatch, extracted

△ 1% EBHPT from 5% masterbatch, extracted

□ 1% EBHPT extracted

● Control

Energy, erg/mm x 10^{-6}

Uv exposure hr

220
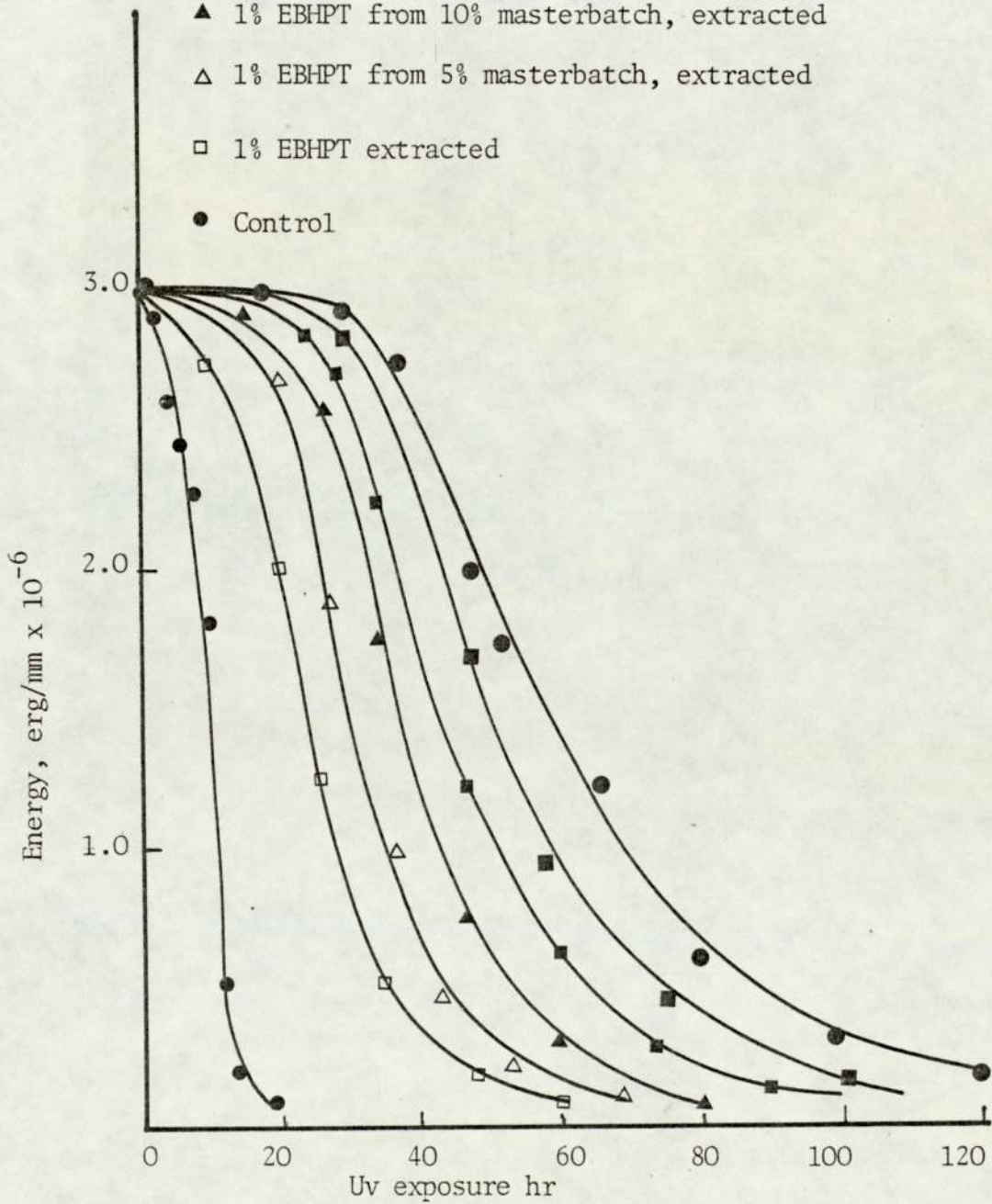
Fig 5.13 Changes in the maximum height of $\tan\delta$ peak at -80°C of ABS films on uv exposure, masterbatches were made by mechanochemical processing in torque rheometer

■ 1% EBHPT from 20% masterbatch, unextracted

○ 1% EBHPT from 30% masterbatch, extracted

▽ 1% EBHPT from 20% masterbatch, extracted

● 1% EBHPT from 10% masterbatch, extracted

▼ 1% EBHPT from 5% masterbatch, extracted

■ 1% EBHPT, extracted

● Control
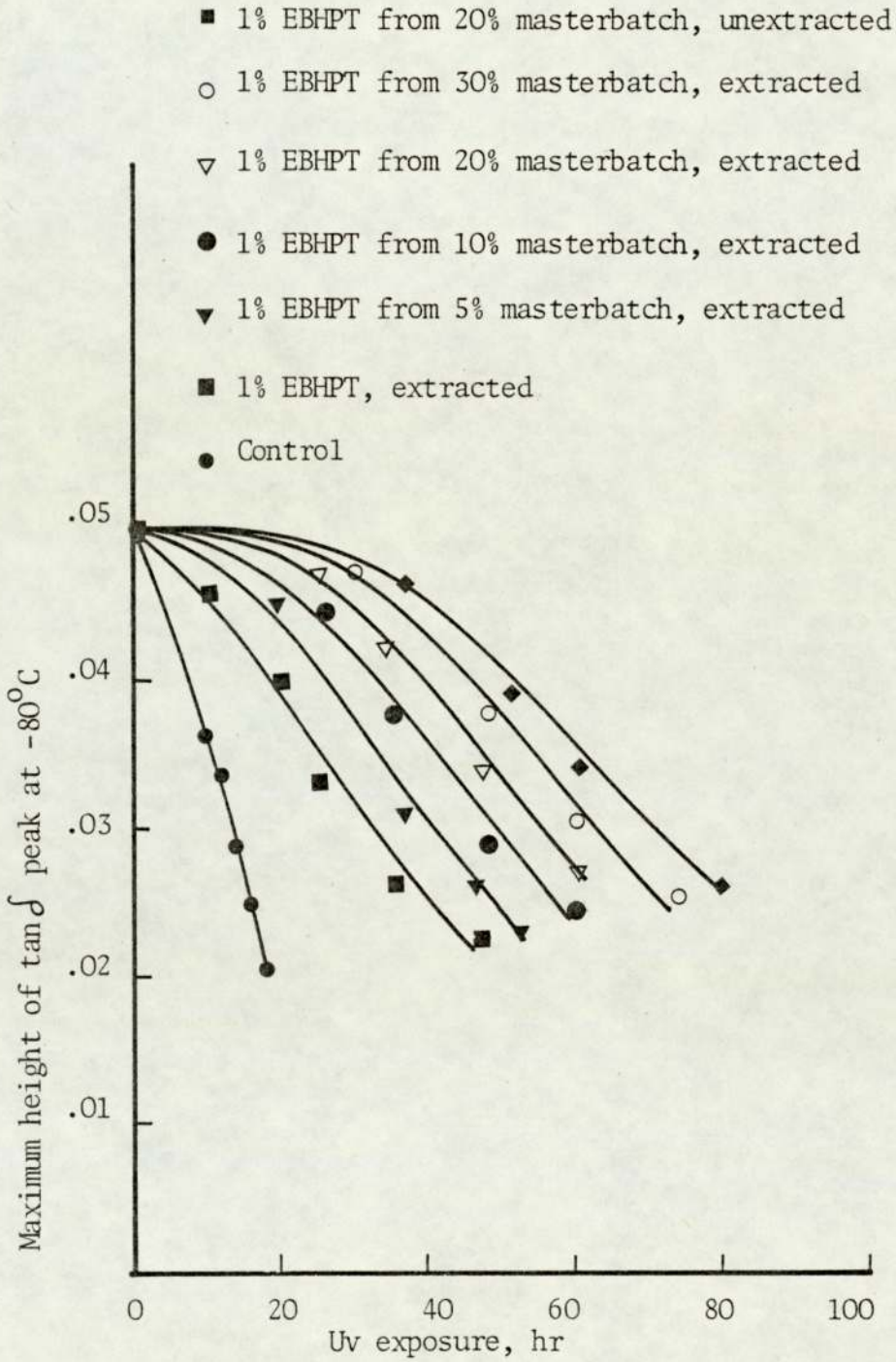
Table 5.2: Concentration of EBHPT before and after extraction of diluted samples and induction periods for formation of carbonyl. *1% unextracted sample was made from 30% masterbatch of EBHPT

Masterbatch concentration pph	Conc of EBHPT before extraction	Conc of EBHPT after extraction	Induction period h
1	1	0.34	10
5	1	0.44	18
10	1	0.57	20
20	1	0.72	25
30	1	0.84	32
*unextracted	1	1	40
Control	-	-	2

is due to the thicker polymer films used (0.1125 mm) (Figs 5.10-5.12). (The increase in thickness of the films resulted from an obligatory change in the compression moulding machine.) Table 5.2 shows the induction periods and embrittlement times of samples, thickness 0.1125 mm, containing different amounts of bound uv stabiliser.

The loss of tan δ peak at -80°C for the samples in Table 5.2 shown in Fig 5.13 against time of irradiation. These curves were made by using the measured impact strengths in Fig 5.12 and the correlation curve between impact strength and loss of tan δ peak at -80°C in Fig 3.22. Although ABS adduct containing 30% EBHPT prepared in torque rheometer was completely rigid with no impact resistance, nevertheless it produced ABS with normal properties when it was diluted to low (1%) concentration with unstabilised ABS.

5.4 Photostabilisation of Monsanto (Lustran) ABS

Monsanto ABS was processed in the torque rheometer with EBHPT up to 2% at 190°C for 3 minutes. Polymer films were prepared using the procedure given in Section 2.5.a and were extracted with hot hexane in a Soxhlett for 4 days. The opaque polymer films were pressed using procedure given in Section 5.2.b to obtain clear films for measurement of functional groups, impact strength and dynamic mechanical property during photodegradation. Samples with standard thickness (0.003 in) were used for all the

223

Fig 5.14 Photo-oxidation of stabilised Monsanto ABS

2% EBHPT, extracted   1% EBHPT, extracted   0.5% EBHPT, extracted   Control (Monsanto ABS)

Trans 1,4 C=C index

Uv exposure, hr

224

Fig 5.15 Photo-oxidation of stabilised Monsanto ABS

O 2% EBHPT, extracted

▼ 1% EBHPT, extracted

O 0.5% EBHPT, extracted

● Control (Monsanto ABS)

C=O index

Uv exposure, hr
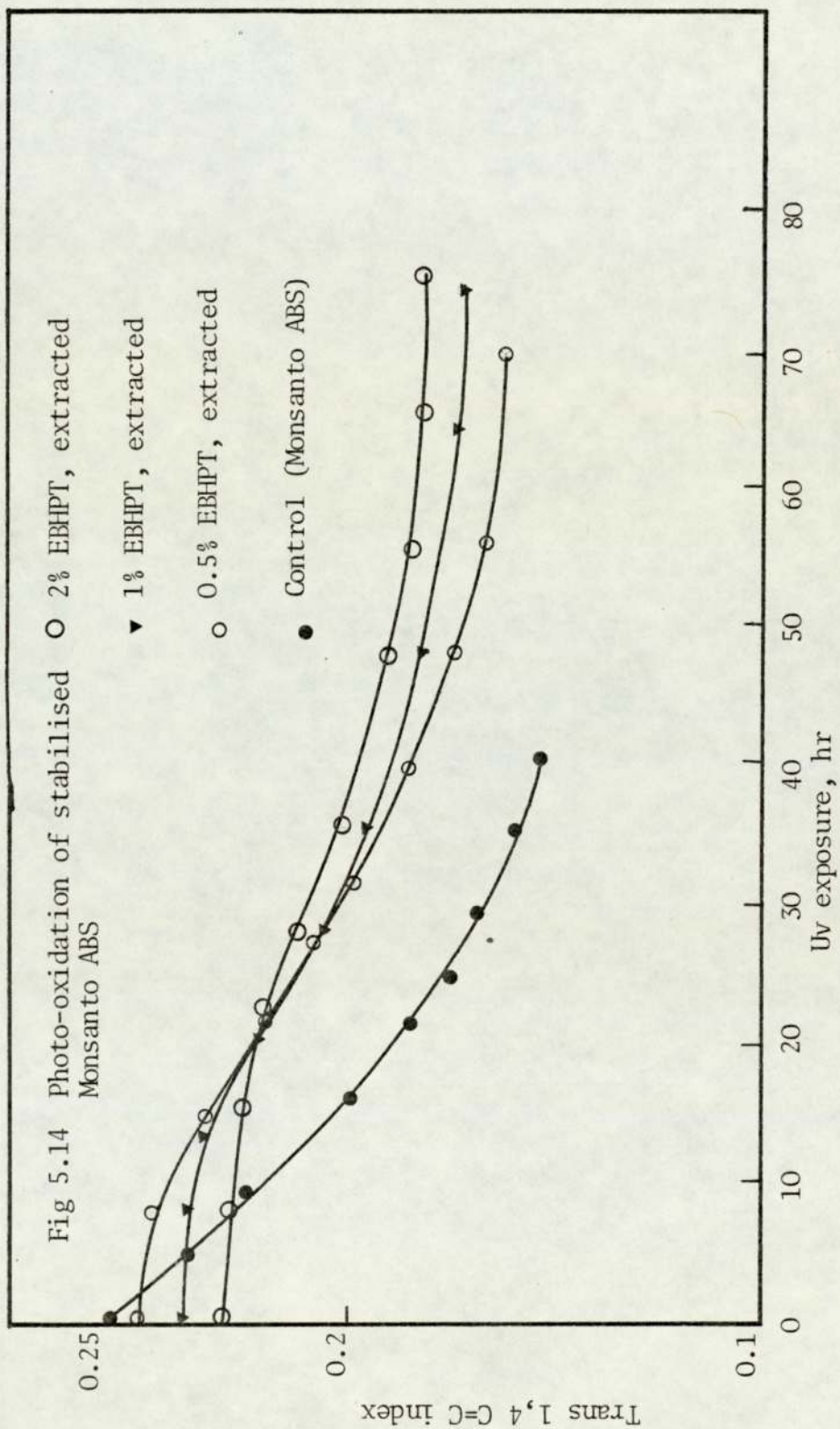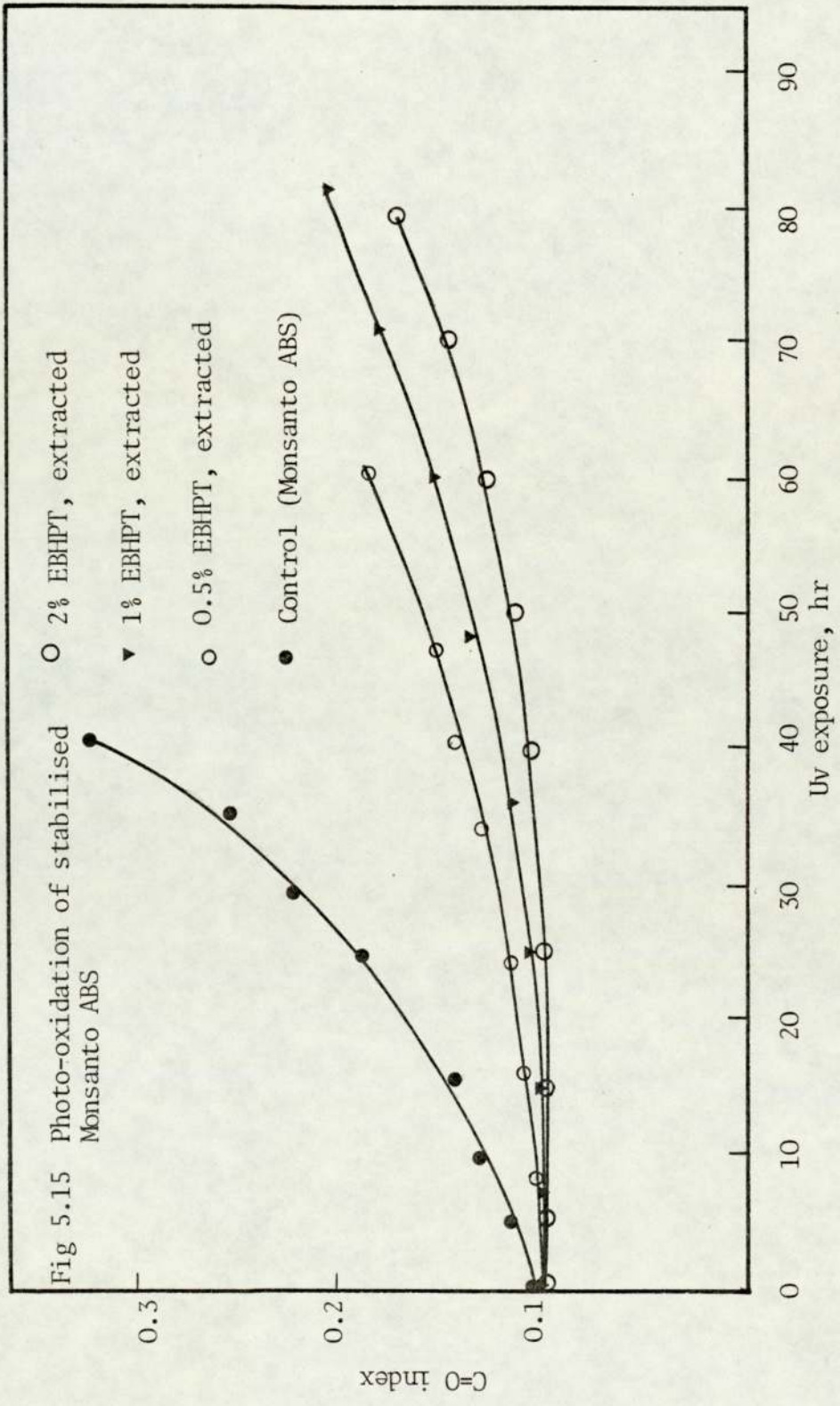
measurements. The changes in the concentrations of functional groups for extracted samples are shown in Figs 5.14 and 5.15 for trans-1,4-unsaturation and carbonyl group respectively. The concentrations of EBHPT used were 0.5, 1 and 2% and led to a great improvement in the photostability of this polymer. The changes in the impact strengths against time of irradiation are shown in Fig 5.16. The induction period and embrittlement time for each concentration of EBHPT after extraction are given in Table 5.3α.

The changes in the heights of tan δ peaks at -80°C were measured by means of Rheovibron viscoelastometer in the temperature range from -120 to 0°C. Figs 5.17, 5.18 and 5.19 show the changes in damping behaviour at low temperature (Tg of rubber) during photo-oxidation for samples containing 0.5, 1 and 2% EBHPT respectively. The maximum heights of tan δ at -80°C were plotted against time of exposure to uv light (Fig 5.20). All these tests show improvement in the stability of Monsanto (Lustran) ABS after extraction with hot hexane, establishing that the thiol containing stabiliser (EBHPT) was bound chemically to ABS during mechano-chemical processing in torque rheometer. As the concentration of EBHPT increased up to 2% the initial concentration of 1,4-unsaturation decreased to some extent (Fig 5.13). The subsequent effect of decrease in unsaturation corresponding to initial decrease in the impact strength and of the height of the tan δ peak at -80°C are shown in Figs 5.17 and 5.20. Since the impact strength and the height of damping peak at low temperature

Fig 5.16 Decrease in the impact strength on uv exposure of Monsanto ABS processed with EBHPT in torque rheometer

★ Control (Monsanto ABS)
○ 0.5% EBHPT, extracted
□ 1% EBHPT, extracted
● 2% EBHPT, extracted
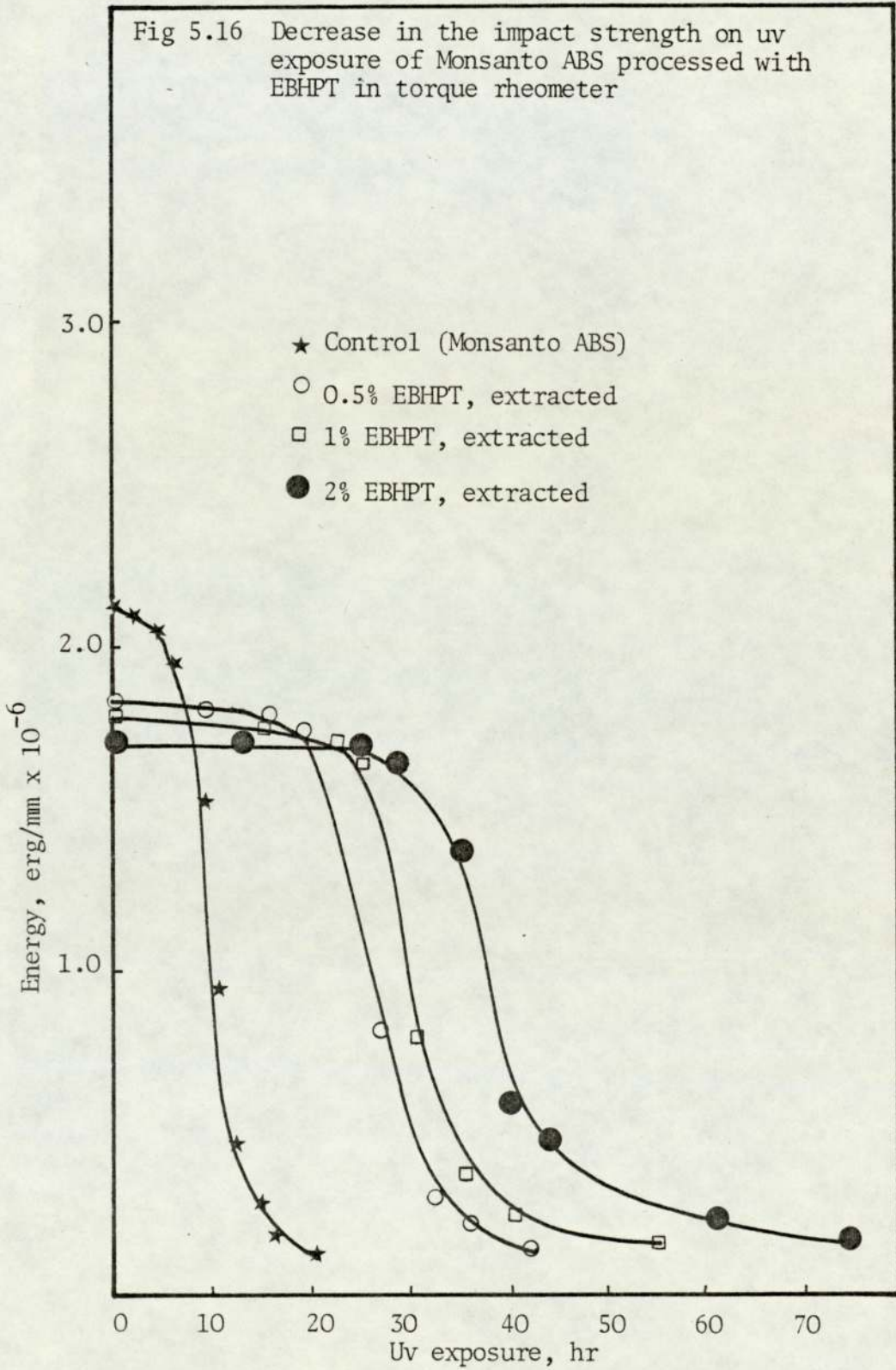
Table 5.3a Induction period and embrittlement time of
extracted samples

Concentration of EBHPT pph	Induction period h	Embrittlement time h
0.5	12	45
1.0	20	55
2.0	30	78

Table 5.3b Loss of unsaturation and impact strength of Monsanto ABS
during processing with EBHPT in torque rheometer

	Initial C=C index	Impact strength erg/mm
Borg-Warner ABS Latex (conc of PBD 30%)	0.425	3.0×10^6
Monsanto ABS (Lustran) (calc conc of PBD 20%)	0.270	2.10×10^6

C=C index of Monsanto ABS (measured by ir)	g EBHPT/ 100 g ABS	Loss of PBD unsaturation %	Impact strength erg/mm theoretically	Impact strength erg/mm practically
0.250	0.5	1.42	1.95×10^6	1.85×10^6
0.240	1.0	2.12	1.88×10^6	1.80×10^6
0.230	2.0	3.0	1.80×10^6	1.70×10^6

Fig 5.17 Effect of uv exposure on low temperature damping (-80°C) of Monsanto ABS containing 0.5% bound EBHPT

229
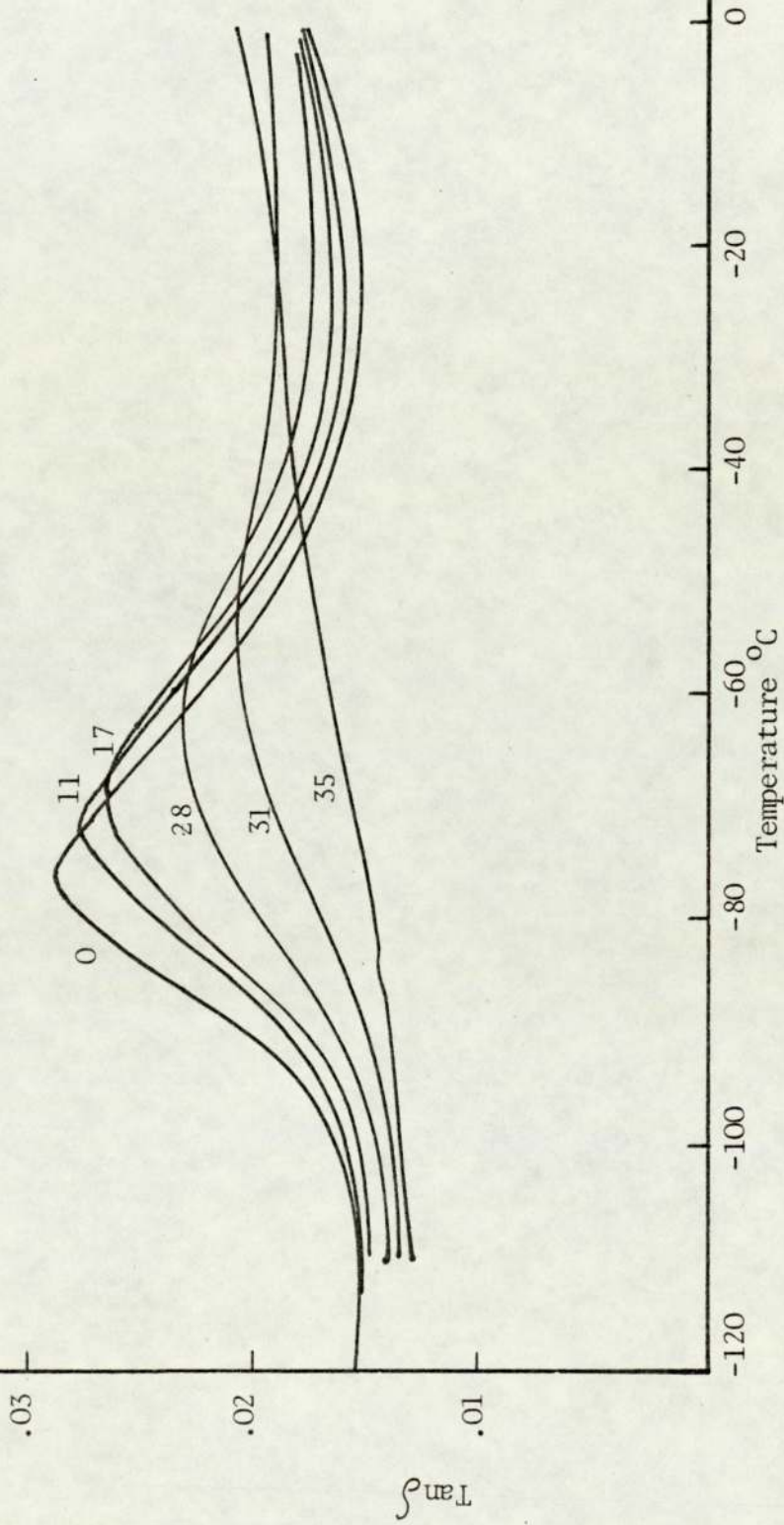
Fig 5.18 Effect of uv exposure on low temperature damping of Monsanto ABS containing 1% bound EBHPT, extracted (numbers on spectra represent h of uv irradiation)

230

Fig 5.19 Effect of uv exposure on low temperature damping of Monsanto ABS containing 2% bound EBHPT, extracted (numbers on spectra represent hrs of uv exposure)

231
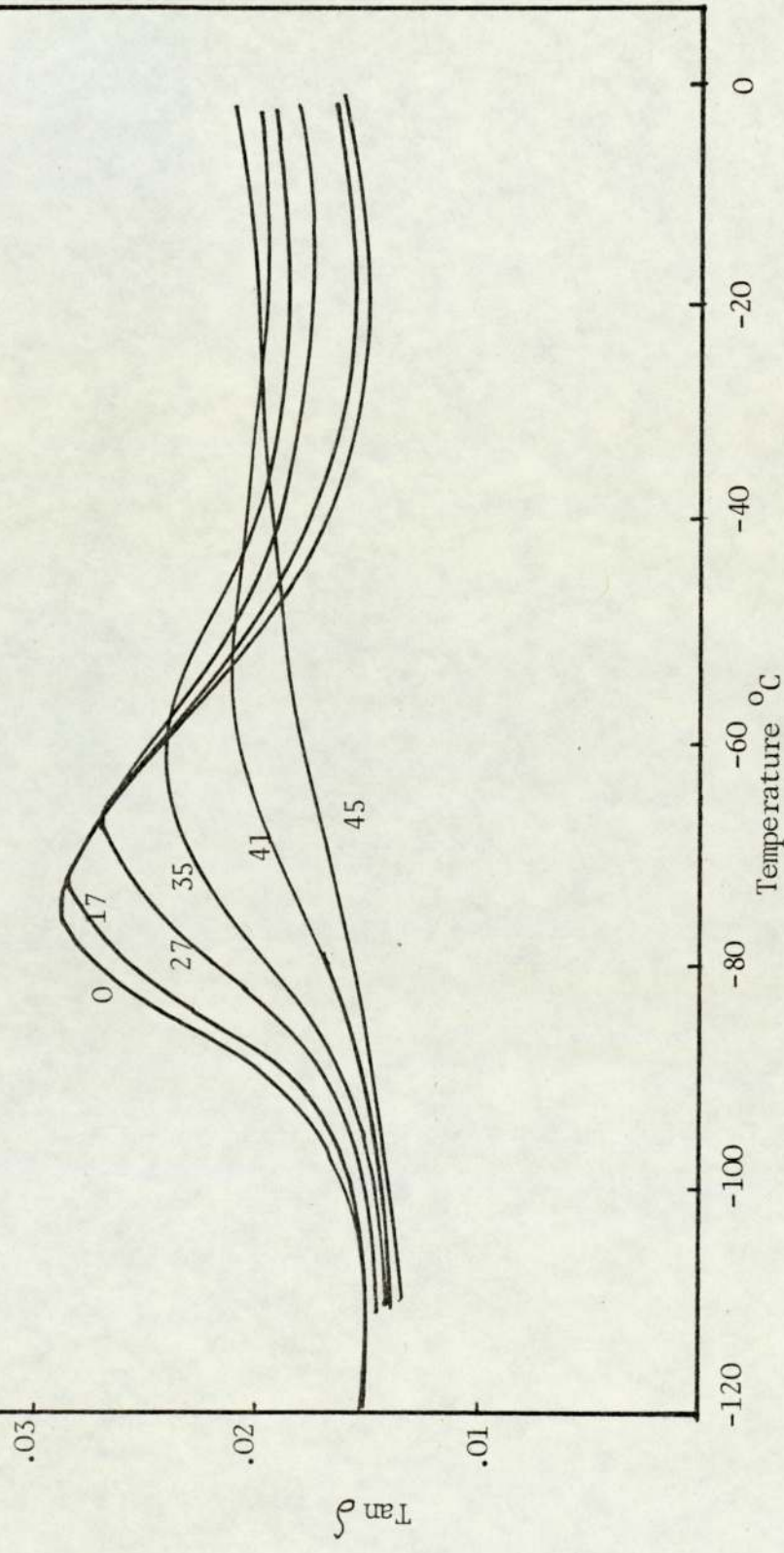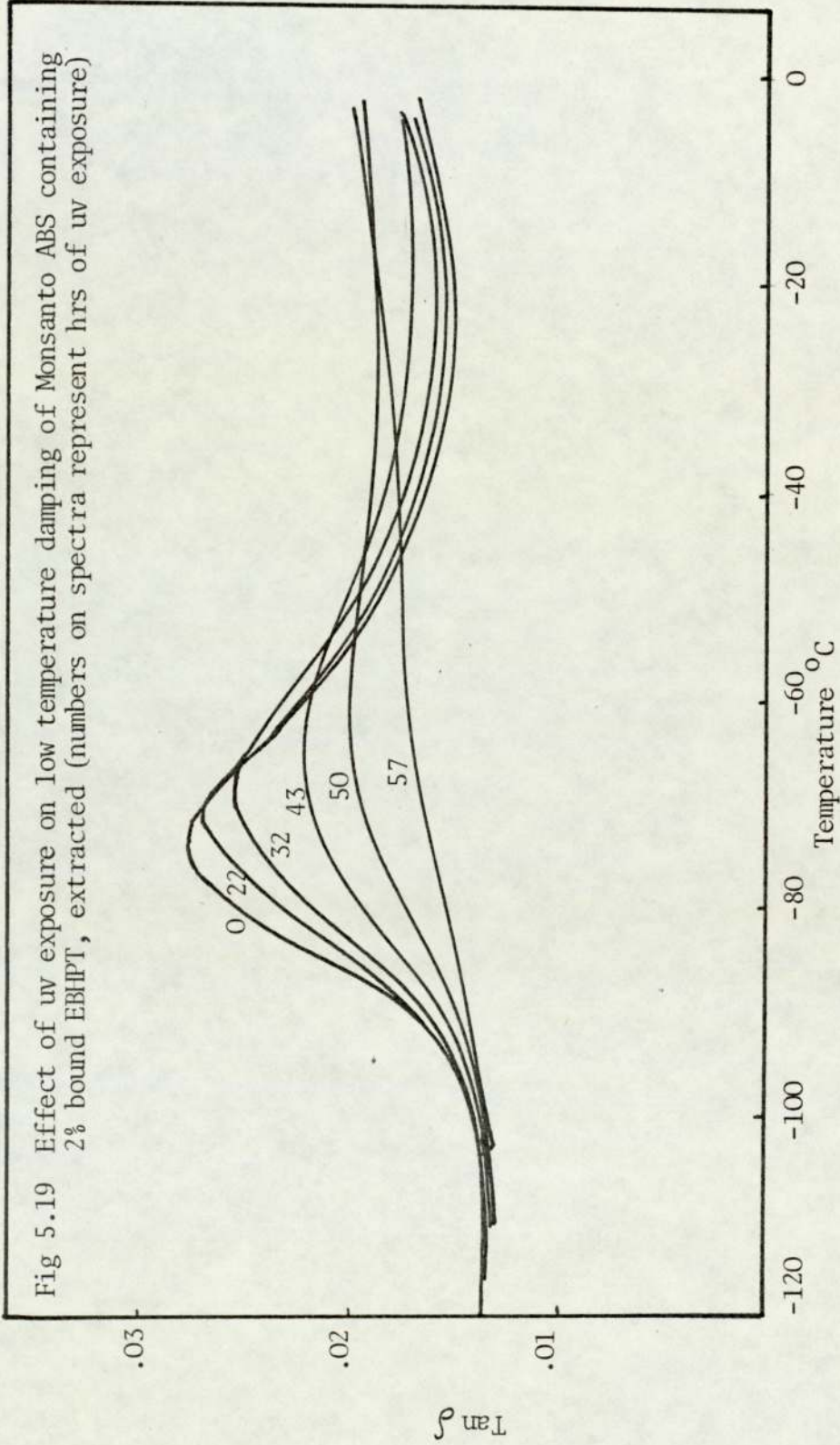
both depend on the concentration of unsaturation in rubber modified polymers[22] this result is inevitable. These results also show that some of the double bonds in the rubber backbone are removed by the thiol compound as well as reaction of these radicals with the allylic radicals. The allylic radicals are generated due to the abstraction of allylic hydrogen by alkyl peroxy or alkoxy radicals.

$$
\overset{\displaystyle H}{\underset{\displaystyle SAN}{-CH=CH-\overset{|}{\underset{|}{C}}-CH_2-}} \quad \xrightarrow{RO_2\cdot} \quad RO_2H + \underset{\displaystyle SAN}{-CH=CH-\overset{\cdot}{\underset{|}{C}}-CH_2-} \quad (1)
$$

$$
\underset{\displaystyle SAN}{-CH=CH-\overset{\cdot}{\underset{|}{C}}-CH_2-} \quad \xrightarrow{AS\cdot} \quad \overset{\displaystyle SA}{\underset{\displaystyle SAN}{-CH=CH-\overset{|}{\underset{|}{C}}-CH_2-}} \quad (2)
$$

$$
\underset{\displaystyle SAN}{-CH=CH-\overset{\cdot}{\underset{|}{C}H}-CH_2-} + AS\cdot \quad \longrightarrow \quad \overset{\displaystyle SA}{\underset{\displaystyle SAN}{-\overset{\cdot}{C}H-CH-CH-CH_2-}} \quad (3)
$$

$$
\overset{\displaystyle SA}{\underset{\displaystyle SAN}{-CH_2-CH-CH-CH_2-}} \quad \xleftarrow[ASH]{RH}
$$
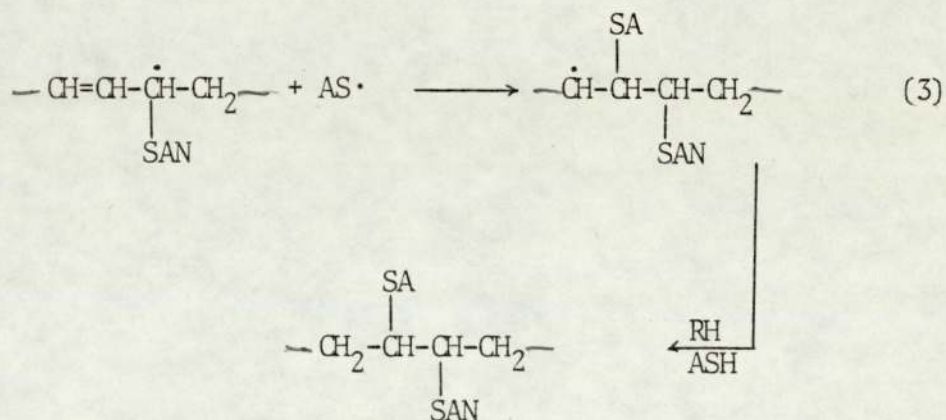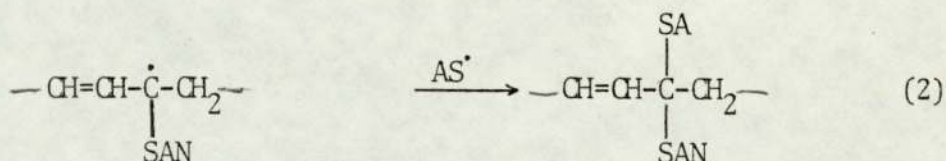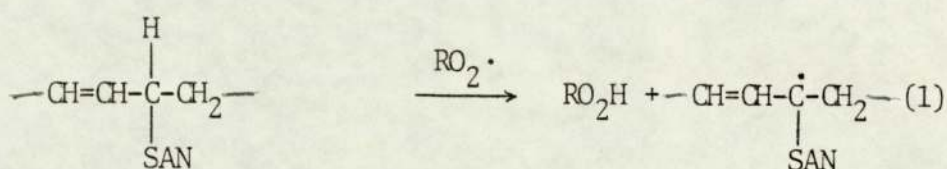
Reaction (2) will also depend on the concentration of oxygen since oxygen at processing temperature could react with the allylic radical to produce peroxy radical.

232

Fig 5.20 Decrease in the height of tan δ peak at -80°C are shown against time of uv exposure for Monsanto ABS processed with EBHPT in torque rheometer

✳ Control (Monsanto ABS)
☐ 0.5% EBHPT, extracted
○ 1% EBHPT, extracted
● 2% EBHPT extracted

Maximum height of tan δ peak at -80°C

Uv exposure, hr

$$-CH=CH-\overset{\bullet}{C}-CH_2- \;+\; O_2 \quad\longrightarrow\quad -CH=CH-\overset{\overset{\displaystyle O-O^{\bullet}}{|}}{C}-CH_2-$$

$$\underset{\text{SAN}}{|} \qquad\qquad\qquad\qquad\qquad \underset{\text{SAN}}{|}$$
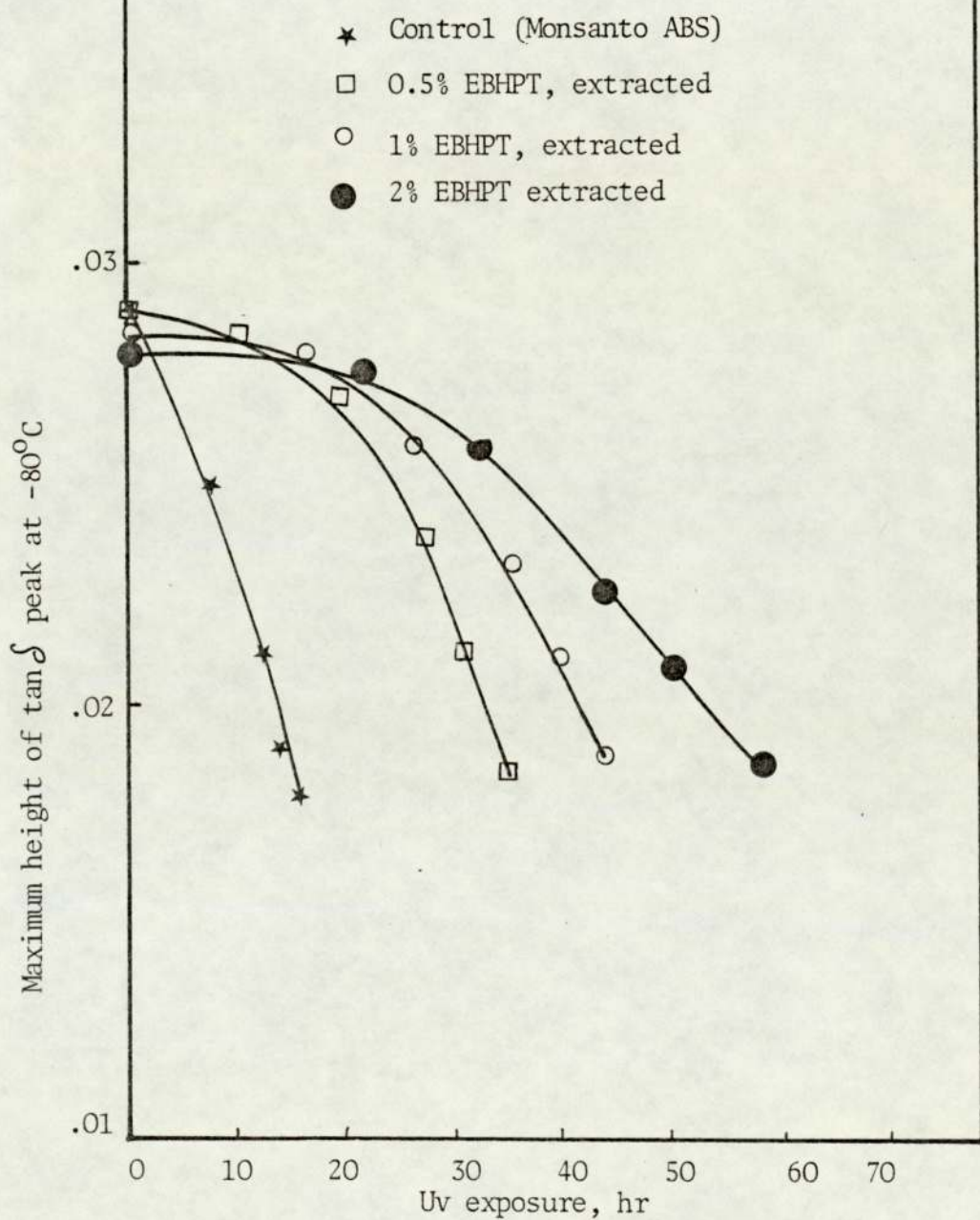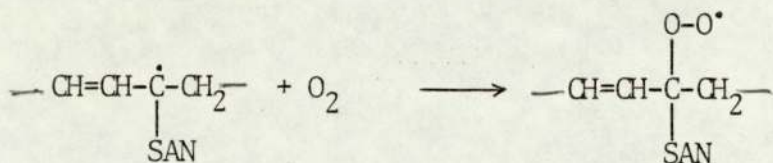
However, both of these reactions could possibly be involved in the binding reaction during mechanochemical process.

5.5 Thermal Oxidation of Stabilised ABS

5.5.a Measurements of Functional Groups, Impact Strength and Loss Factor

Unstabilised ABS (Borg-Warner) was processed with BHBM up to 30% and the amounts bound are given in Table 5.4. The masterbatches were all diluted to a lower concentration (1%). The estimation of bound antioxidant and the extraction procedure were discussed in Section 5.2.a and Section 5.2.b. Thermal oxidation was followed by measuring the changes in the concentration of functional groups (C=O, trans-1,4 C=C), impact strength and the changes in the height of tan at $-80^{\circ}C$ (Tg of PBD component). Samples with thickness 0.1 mm were used for all measurements. (Carbonyl absorbance at 1720 cm^{-1} and trans-1,4 C=C absorbance at 965 cm^{-1} started to increase gradually just after induction period.) The changes in the concentration of functional groups as a function of time against heating (at $100^{\circ}C$ in air) are shown in Figs 5.21 and 5.22. The induction period for increase in carbonyl concentration and decrease in trans-1,4 C=C increased from 1%

234

Fig 5.21 Development of carbonyl on heating at 100°C in air of ABS containing bound
BHBM (key to curves, page 236)

235
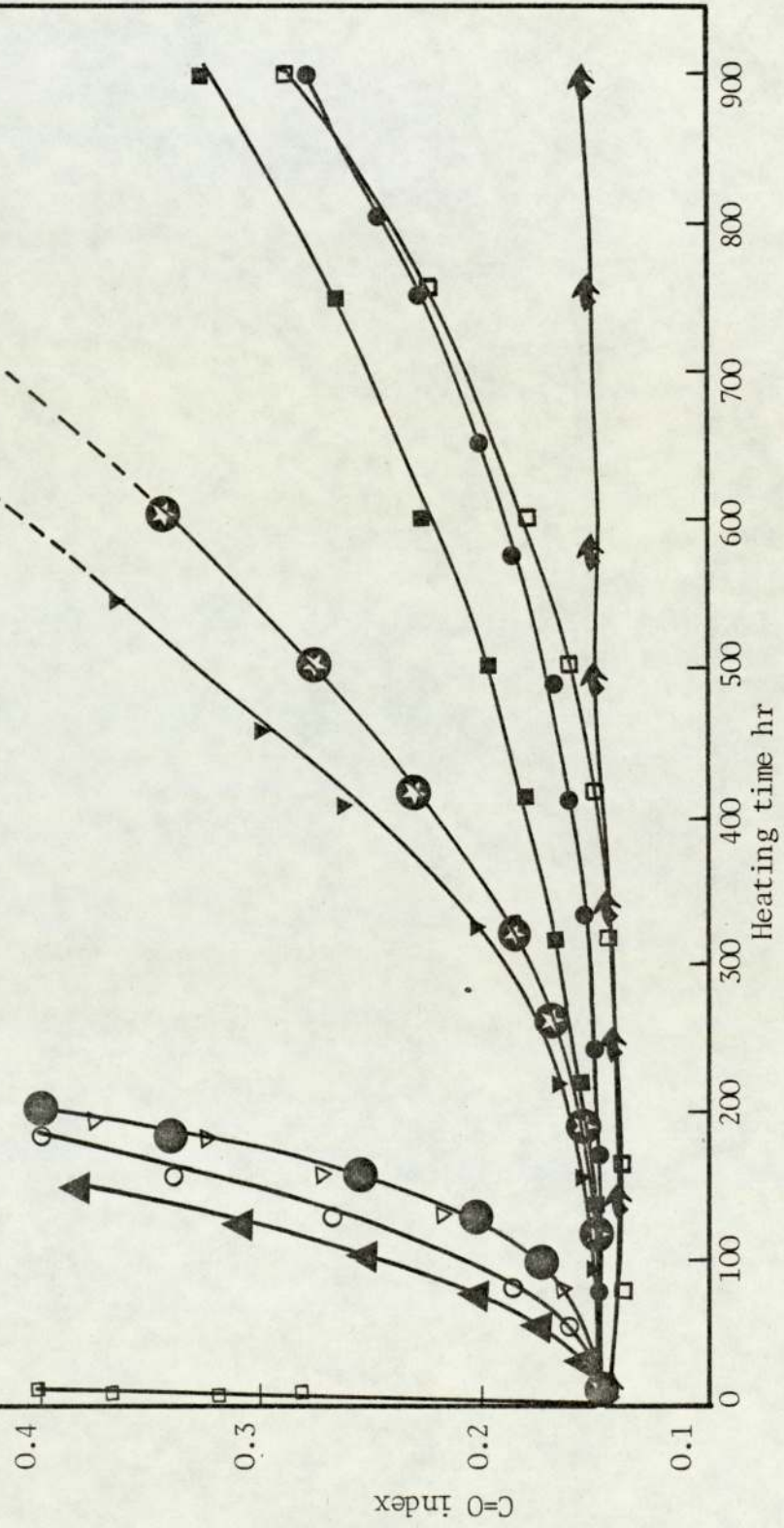
Key to curves for Figs 5.21 and 5.22

➤ 1% BHBM from 10% masterbatch, unextracted

● 1% BHBM from 10% masterbatch, extracted

☐ 1% BTGA from 10% masterbatch, extracted

◼ 2% BTGA from 5% masterbatch, extracted

✪ 1% BTGA from 5% masterbatch, extracted

▼ 1% BHBM from 5% masterbatch, extracted

⬤ (1% BHBM, extracted (1,4 C=C index)
  (1% BTGA, extracted (C=O index)

▪ 1% BTGA, extracted (1,4 C=C index)

△ 1% BHBM from 20% masterbatch, extracted

▲ 1% BHBM from 30% masterbatch, extracted

○ 1% BHBM, extracted (C=O index)

☐ Control (Borg-Warner latex)

236

Fig 5.22 Decay of trans 1,4 PBD unsaturation of ABS containing bound BHBM

Trans 1,4 C=C index

Heating time, hr

237
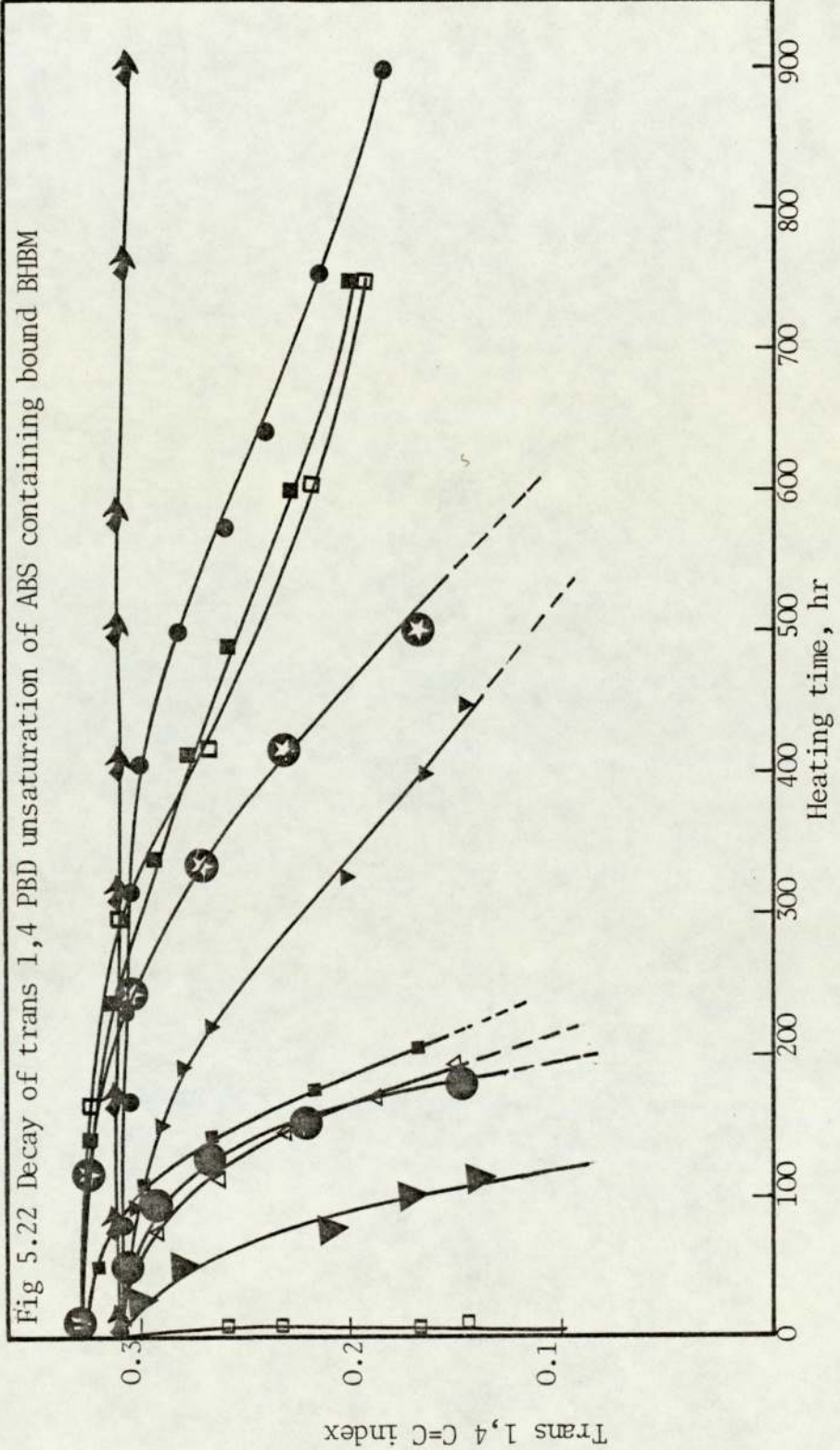
Table 5.4: Induction periods and embrittlement times of ABS containing bound antioxidant (BHBM

No	Masterbatch pph	Diluted pph	Conc of BHBM after extraction	Ind before extraction,h	Emb before extraction,h	Ind after extraction,h	Emb after extraction,h
1	1	1	Unknown	-	-	50	120
2	5	1	0.42	-	-	200	380
3	10	1	0.60	900	1500	400	750
4	20	1	0.12	-	-	70	150
5	30	1	0.07	-	-	25	72

of BHBM up to 10% corresponding to the increase in the amount of bound antioxidant (see Table 5.4) and decreased sharply for 20 and 30% of BHBM. Polymer films containing 1% of BTGA made from 6 and 10% masterbatch showed similar stability (Figs 5.21 and 5.22). There is some difference in the stability of the ABS containing these two antioxidants (BHBM, BTGA) which will be discussed in Section 5.5.b.

The impact strengths of ABS containing bound antioxidant were measured by falling weight tester during thermal oxidation (see Fig 5.23).

The low temperature damping behaviours were measured during thermal oxidation by means of Rheovibron viscoelastometer. Only one sample was used throughout the measurements and oven ageing was interupted frequently for measurements of $\tan \delta$ from -120 to $0^{o}C$. Four ABS films containing different concentrations of bound antioxidant were used and dynamic spectral were similar to those obtained for unstabilised ABS (Fig 3.24). The changes in the height of $\tan \delta$ at $-80^{o}C$ for samples containing different concentrations of bound antioxidants are shown in Figs 5.24, 5.25, 5.26 and 5.27. The maximum height of $\tan \delta$ at $-80^{o}C$ was also plotted against time of heating, see Fig 5.28.

The embrittlement times and induction periods of ABS films containing bound BHBM were plotted against percentage of bound (Fig 5.29). The percentage of bound obtained from 5 g of BHBM

239

Fig 5.23 Decay of impact resistance on heating at 100°C in air of ABS pressed films, masterbatches were made during mechanochemical processing in torque rheometer

● 1% BHBM from 10% masterbatch unextracted

● 1% BHBM from 10% masterbatch extracted

▦ 1% BHBM from 5% masterbatch, extracted

■ 1% BHBM, extracted

▼ Control (Borg-Warner latex)

Heating time, hr

Energy, erg/mm x 10⁻⁶

240

Fig 5.24 Effect of heating (100°C in air) on low temperature damping of ABS processed with 1% BHBM in torque rheometer, extracted (numbers on spectra represent hours of heating)
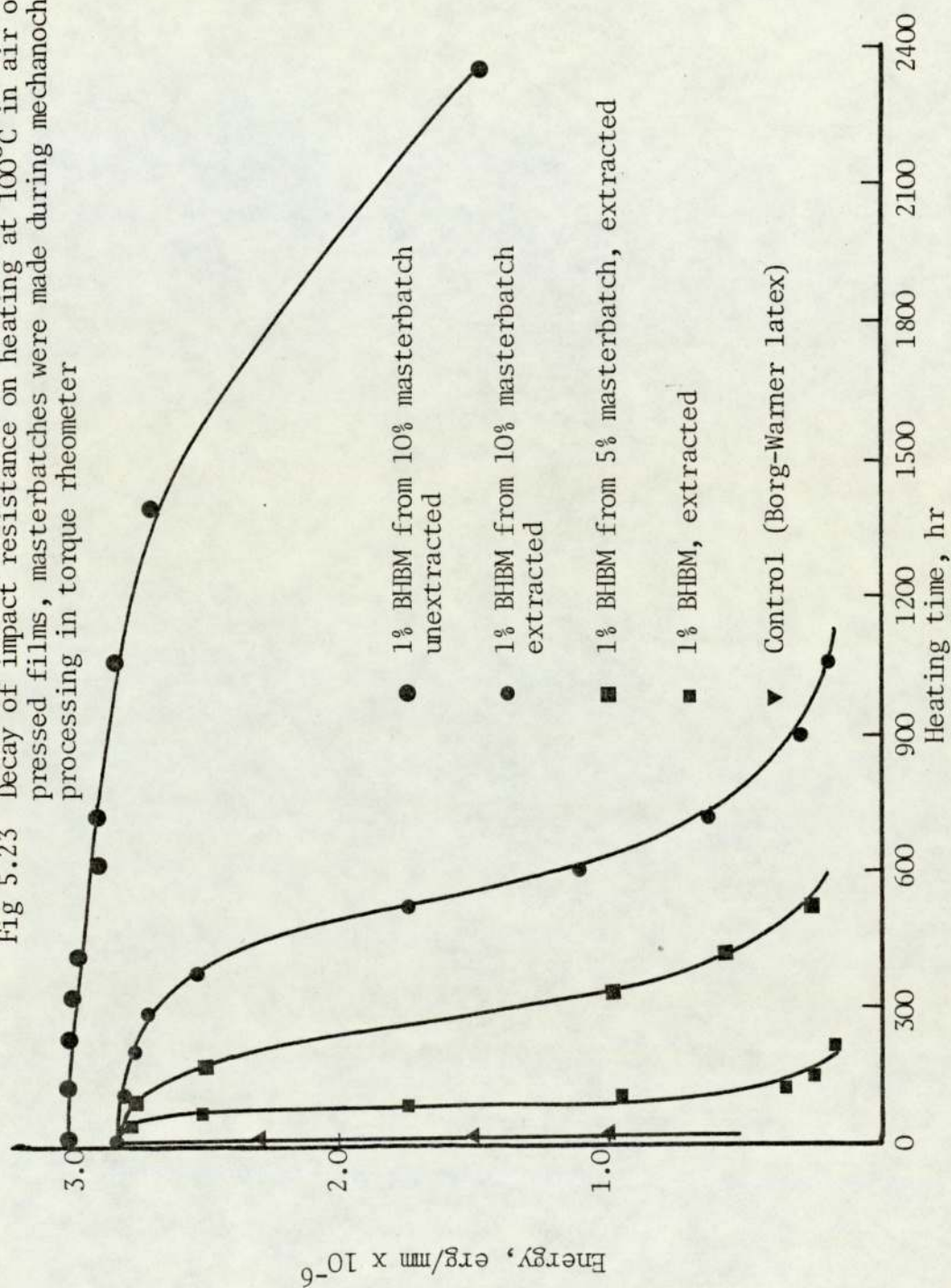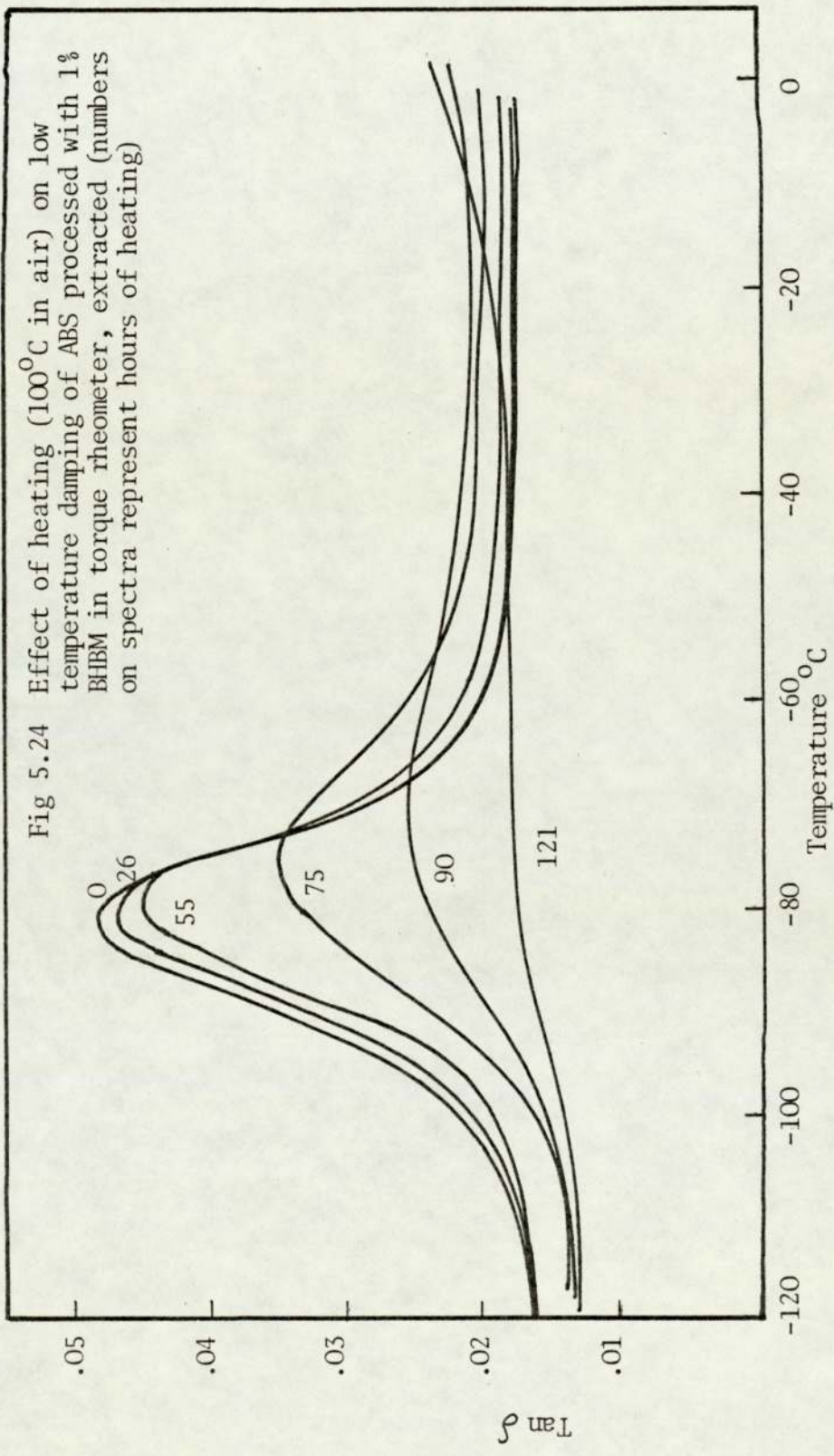
in 100 g of ABS at different processing temperatures, from 80 to 190°C were calculated using the correlation curves between stability and percentage of bound in Fig 5.29 and embrittlement times and processing temperatures in Fig 5.4. The estimated percentages of bound for 5 g of BHBM are given in Table 5.5 with processing temperatures.

5.5.b Discussion

Oven ageing behaviour of extracted ABS films containing bound BHBM at 100°C show a remarkable improvement in stability over the conventional phenolic antioxidants. A conventional phenolic antioxidant was used by Fernando et al[75] and the results are compared with BHBM in the same molar concentration (Table 5.6).

The formation of an adduct saturates a double bond. Such a system can undergo reactions involving β-hydrogen atoms, during the decomposition of hydroperoxides by sulphur compounds as shown by Scott[64,63], scheme 1. According to these references it is possible to arrive at the following mechanism for the decomposition of hydroperoxides.

Fig 5.25 Effect of heating (100°C in air) on low temperature
damping of ABS containing 1% BHBM from 5% masterbatch
extracted

243
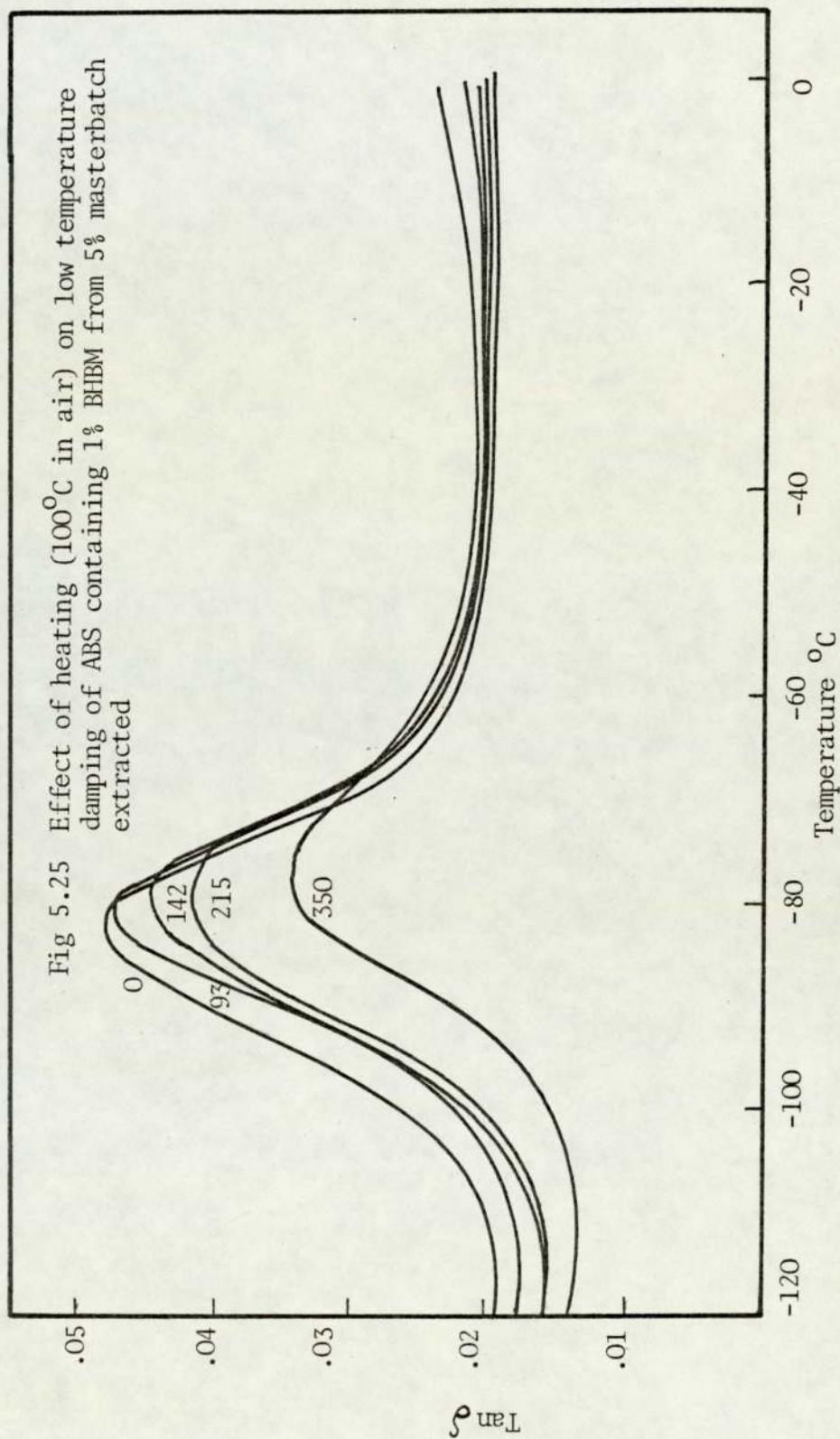
Table 5.5: The estimated percentages of bound of 5 g of BHBM/100 g
of ABS at different processing temperatures

Processing temperatures °C	Estimated percentage of bound	Embrittlement time, h
80	68	900
100	68	900
130	68	900
150	77	1000
170	85	1200
190	85	1200

Table 5.6: Induction periods (carbonyl) on oven ageing of ABS
films at 100°C containing BHBM adduct after
extraction, BHT as additive

Antioxidant	Conc mol/100 g ABS	Induction period,h
BHT	1.86×10^{-3}	100
BHBM	1.86×10^{-3}	200
BHT	2.38×10^{-3}	160
BHBM	2.38×10^{-3}	400
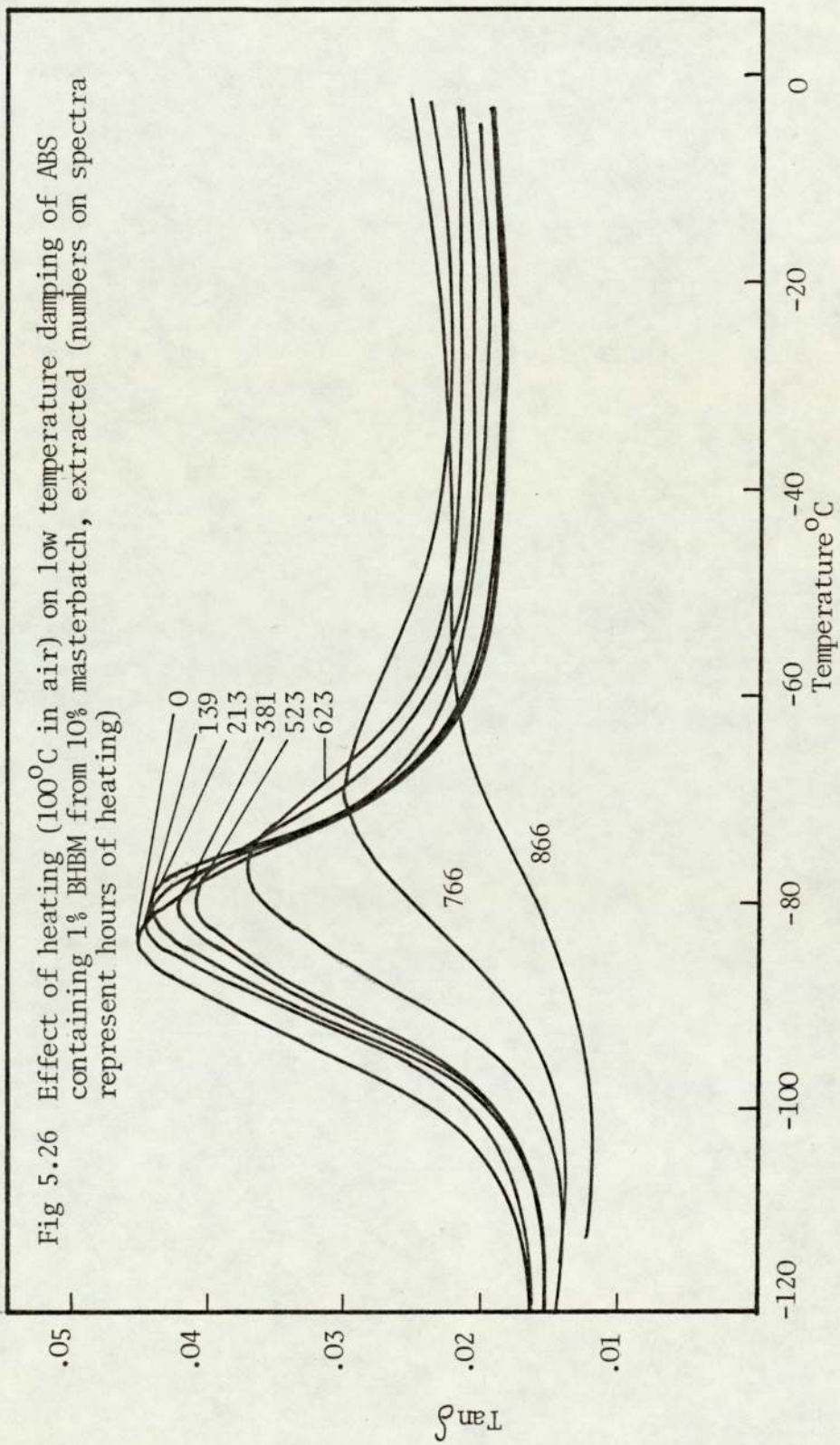
Fig 5.26   Effect of heating (100°C in air) on low temperature damping of ABS containing 1% BHBM from 10% masterbatch, extracted (numbers on spectra represent hours of heating)

245

Scheme 1

The following mechanism has been suggested for the oxidation of the sulphenic acid derivative of the phenolic antioxidant formed[75,76].

Scheme 2

246

Fig 5.27 Effect of heating (100°C in air) on low temperature damping of ABS containing 1% BHBM from 10% masterbatch, unextracted (numbers on spectra represent hours of heating)

247
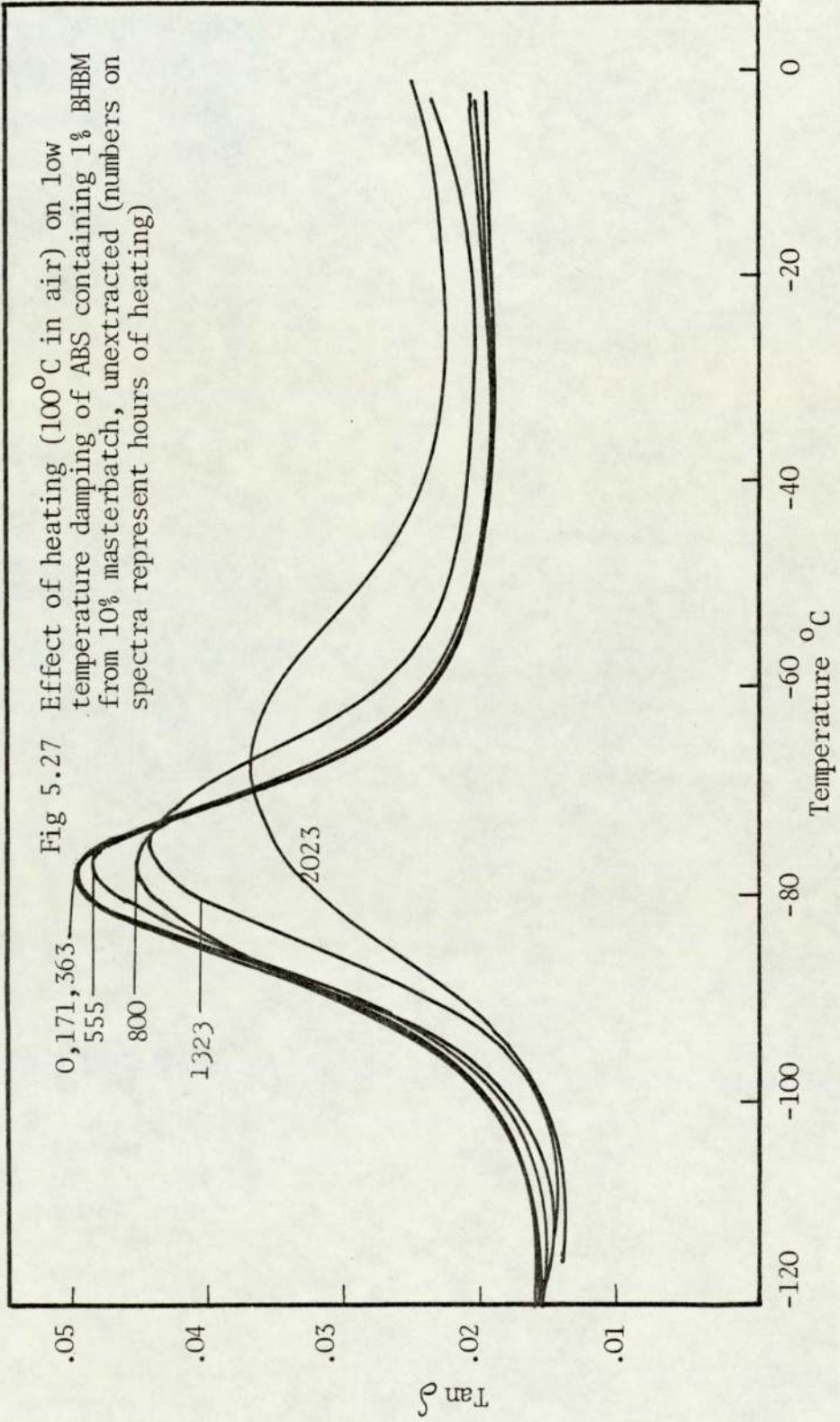
It has been shown[132] that the intermediate sulphinic acids (RSO$_2$H) undergo redox reactions with hydroperoxides in parallel with their acidic decomposition of hydroperoxide. This reaction(s) leads to the formation of free radicals with consequent pro-oxidant effects particularly during the initial stages of peroxide initiated thermal oxidative reactions (5).

$$RSO_2H + R'OOH \xrightarrow{(5)} R\dot{S}O_2 + H_2O + R'O^{\cdot} \qquad (5)$$
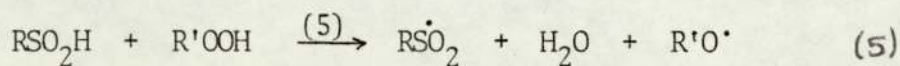
This effect was not seen in antioxidants having hindered phenolic groups and the latter seem to play an important role during the early stages of thermal oxidation in scavenging free radicals produced in reactions (4) and (5).

The results from the present study (Figs 5.21 - 5.28 and Table 5.5) confirm the view that the powerful antioxidant activity of BHBM adducts is primarily due to their ability to destroy hydroperoxides. Hindered phenolic groups in BHBM play the role of chain-breaking antioxidants in scavenging free radicals produced in thermal oxidation of polymer (RO$^{\cdot}$, RO$_2^{\cdot}$) and hydroperoxide decomposition reactions (ArSO$H \xrightarrow[ROOH]{} $ArSO$^{\cdot}$). Chain-breaking antioxidants (InH) act according to the following general reaction:

$$RO_2^{\cdot} + InH \longrightarrow ROOH + I\dot{n} \qquad (6)$$
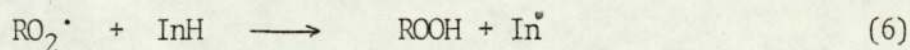
where in the case of BHBM the In$\cdot$ is a phenoxyl radical. The

248

Fig 5.28 Decrease in height of low temperature damping peak (-80°C) are shown against heating (100°C in air) time, masterbatches were prepared during mechanochemical processing in torque rheometer

●   1% BHBM from 10% masterbatch, unextracted

●   1% BHBM from 10% masterbatch, extracted

■   1% BHBM from 5% masterbatch, extracted

■   1% BHBM, extracted

▼   Control (Borg-Warner latex)

Heating time, hr

Maximum height of tan δ peak at -80°C

249
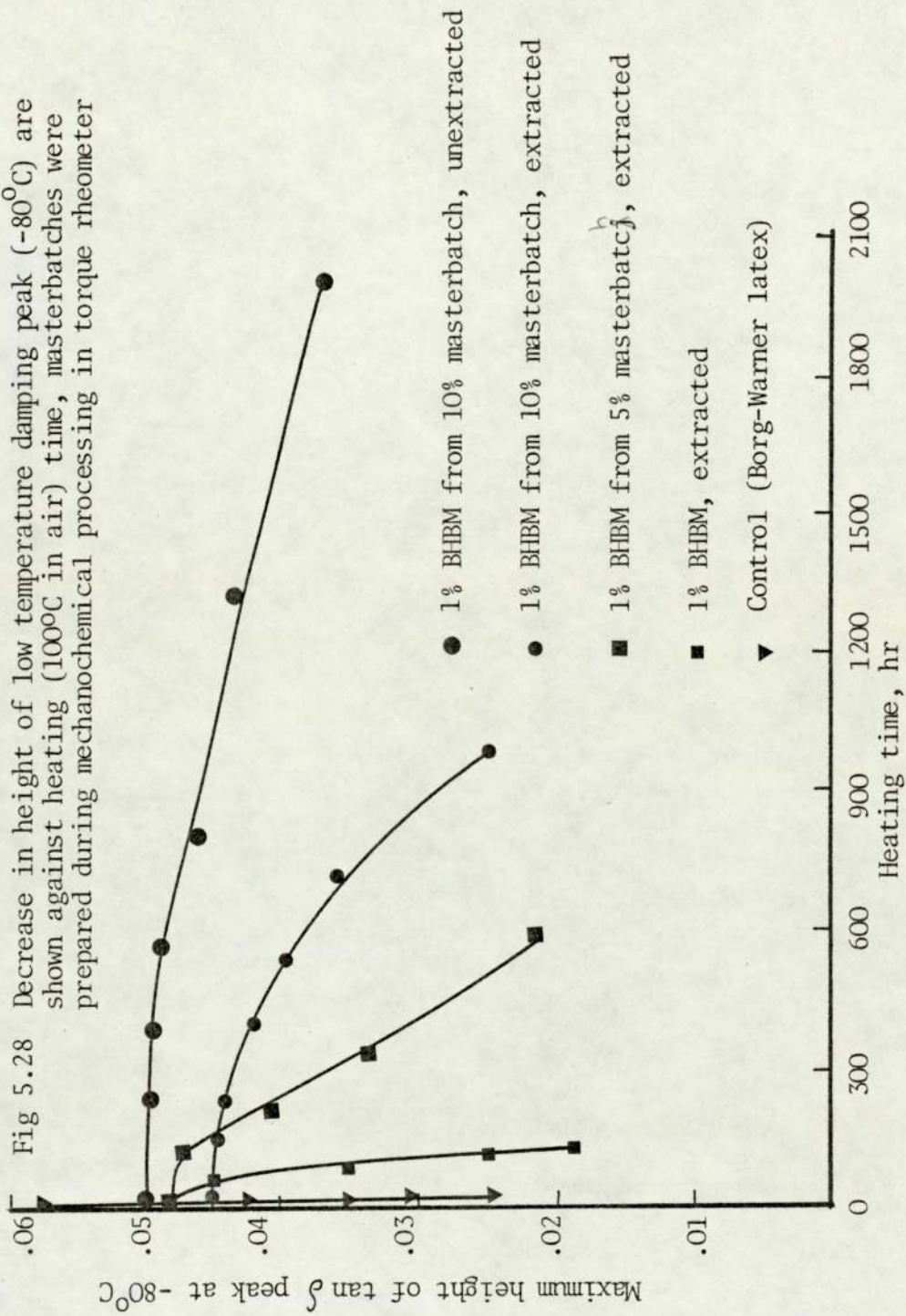
Fig 5.29   Induction period and embrittlement time on oven ageing
of ABS films at 100°C containing BHBM adduct after
extraction

chemistry of phenoxyl radicals has been previously reviewed[139,140]
and the reactions involved are summarised in Scheme 3 for a
typical phenolic antioxidant (BHT).

Scheme 3

The release of the antioxidant as the sulphenic acid derivative
on oxidation of the bound BHBM reintroduces the lost double bond
to the system (Scheme 1). This process probably takes place
during the induction period, observed in the scavenging process.

Oven ageing of extracted ABS containing bound BHBM and BTGA

at 100°C shows some differences in stability. In spite of lower

percentage of bound BTGA, the adduct of BTGA shows better stability

over the BHBM adduct. The structure of BTGA has been shown to be

3,4-di-tert-butyl-4-hydroxybenzyl carboxymethyl sulphide[141].

$$\text{HO}-\overset{\displaystyle tBu}{\underset{\displaystyle tBu}{\bigcirc}}-CH_2SCH_2COOH \qquad \text{(BTGA)}$$
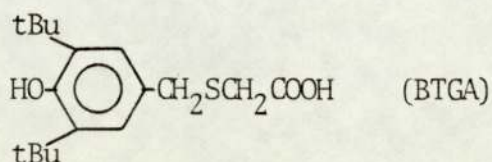
The mechanism of the binding reaction in this case is not yet

clearly known but it has been suggested that the sulphonyl

radical due to the further reaction of sulphenic during

processing might attack double bond in the rubber backbone to

give adduct with the following structure.

$$\text{HO}-\overset{\displaystyle tBu}{\underset{\displaystyle tBu}{\bigcirc}}-CH_2SCH_2COOH \xrightarrow{ROOH} \text{HO}-\overset{\displaystyle tBu}{\underset{\displaystyle tBu}{\bigcirc}}-CH_2\overset{\displaystyle O}{\overset{\|}{S}}CH_2COOH \rightarrow \text{HO}-\overset{\displaystyle tBu}{\underset{\displaystyle tBu}{\bigcirc}}-CH_2SOH$$

$$\xrightarrow{ROOH} \text{HO}-\overset{\displaystyle tBu}{\underset{\displaystyle tBu}{\bigcirc}}-CH_2SO \xrightarrow{-CH=CH-CH-} -\overset{\displaystyle SAN}{CH}-CH-\overset{\displaystyle SAN}{CH}-$$

$$O=S-CH_2$$

$$tBu-\underset{\displaystyle OH}{\bigcirc}-tBu$$

252
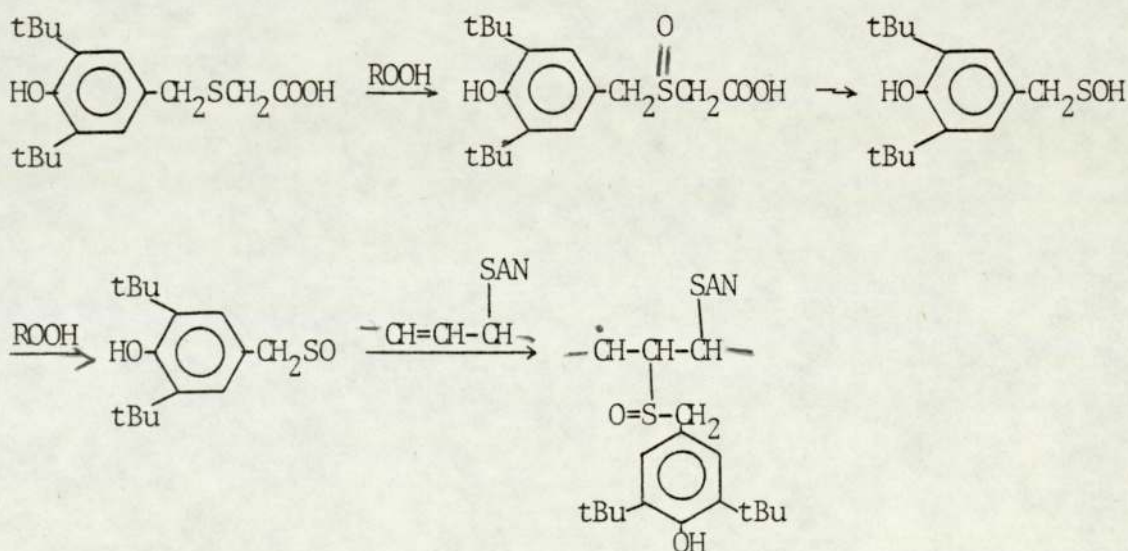
These results reported in Figs 5.20 and 5.21 confirm this suggestion since it was reported[50] that the oxidation products of sulphides function as more active inhibitors of autoxidation than sulphides themselves, and it was found that sulphoxides derived from monosulphides are the precursors of the active inhibitors. The activity of sulphoxides as inhibitor appears to be due to their instability leading to products which convert hydroperoxides to inactive products without formation of free radicals. Oven ageing of unextracted ABS films containing bound BHBM at 100°C in air (Fig 5.21) showed almost 1.5 times more stability over the result reported by Fernando[75] on unextracted sample with the same concentration (1% BHBM). The remarkable improvement in stability of 1% unextracted adduct can be seen in all figures 5.21-5.28. The thiol-containing by-products improve the stability of unextracted samples over extracted samples. However, it seems that during preparation of the BHBM adduct in torque rheometer, sulphoxides which are more active inhibotors of autoxidation are formed.

5.6 Synergistic Combination

5.6.a Efficiency of Adduct Stabilisers BHBM and EBHPT in Combination

It was reported[75] that the individual performance of TBMP and EBHPT as additives in ABS towards thermal oxidative degradation and photo-oxidation respectively was marginally higher than other stabilisers tested, at approximately the same molar concentrations.

253

HO–⬡(X, X)–CH$_2$SCH$_2$–⬡(X, X)–OH   (TBMP)
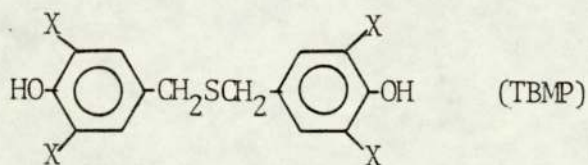
The combined effect of these two on the photo-oxidation of ABS was found[75] to be much higher than that expected on an additive basis. In view of the success of the adduct formation reactions with EBHPT up to 30% in latex and during processing and with BHBM up to 10% during processing, the possibility of solid blending in the torque rheometer was explored to obtain a synergistic combination of the two.

5.6.a.1 Procedure

Maximum bonding of stabilisers was obtained with 30 g of EBHPT and 10 g of BHBM with 100 g of dry ABS during processing in the torque rheometer. The 30% masterbatch of EBHPT and 5% masterbatch of BHBM were used for making synergism combinations of the two. Nine combinations were made from these two extracted masterbatches. The weight ratios of EBHPT to BHBM and the concentration of each component are given in Table 5.7. The synergism combinations were prepared by processing unstabilised ABS with required amount of solid extracted masterbatches of EBHPT and BHBM for 3 mins (in torque rheometer) at 190°C. Polymer films were made by compression moulding machine.

Table 5.7: Synergistic combinations of EBHPT and BHBM made from extracted masterbatches

No	Calculations were made on the basis of unextracted masterbatches				Conc after ext
	Ratio of EBHPT/BHBM by w/w%	g wt of solid masterbatch of 30% EBHPT used	g wt of solid masterbatch of 5% BHBM used	g wt of unstabilised solid ABS	Conc ratio of (w/w) EBHPT/BHBM in 100 g of dry ABS
	a	b	c	d	e
1	0/2	0	14	21	0/0.94
2	0.2/1.8	0.231	12.60	22.17	0.168/0.846
3	0.5/1.5	0.581	10.50	23.92	0.42/0.70
4	0.7/1.3	0.815	9.10	25.08	0.58/0.61
5	1/1	1.16	7	26.82	0.84/0.47
6	1.2/0.8	1.40	5.60	28.0	1.00/0.37
7	1.5/0.5	1.75	3.50	29.75	1.26/0.235
8	1.9/0.1	2.20	2.10	30.70	1.59/0.047
9	2/0	2.33	0	32.67	1.68/0

These films with thickness of 0.1 mm were used for the experimental tests. A total concentration (EBHPT/BHBM) of 2% by weight of unextracted masterbatch was used as the basis for calculating synergistic combinations.

To understand Table 5.7 better it needs to be more explained. Calculations given in columns a, b, c and d were made by imagining that the masterbatches were unextracted, for example 30% masterbatch of EBHPT meant 30 g of EBHPT in 100 g of ABS, knowing that the extracted sample of this masterbatch contains 25.2 g of EBHPT in 100 g of ABS. Therefore column e shows the actual amounts of bound EBHPT and BHBM as grammes/100 g dry ABS.

5.6.a.2 Results

The synergistic combinations made by the procedure given in Section 5.6.a.1 were examined by infra-red. The changes in the concentration of functional groups (C=O, trans-1,4 C=C) were followed during photodegradation. Fig 5.30 shows changes in the concentration of carbonyl groups of synergistic combinations against time of irradiation. The combination 1/1 (EBHPT/BHBM) was selected due to its good stability for measurements of impact strengths and low temperature damping behaviour (Tg of rubber component). For this purpose, samples with identical thicknesses (0.1 mm) were used for impact strength measurements, only one unextracted sample and one extracted sample were used throughout the measurements of $\tan \delta$ at -80°C. The changes

256

Fig 5.30 Development of carbonyl group on uv exposure of ABS film containing synergistic combinations extracted (*refer Table 5.7)

257
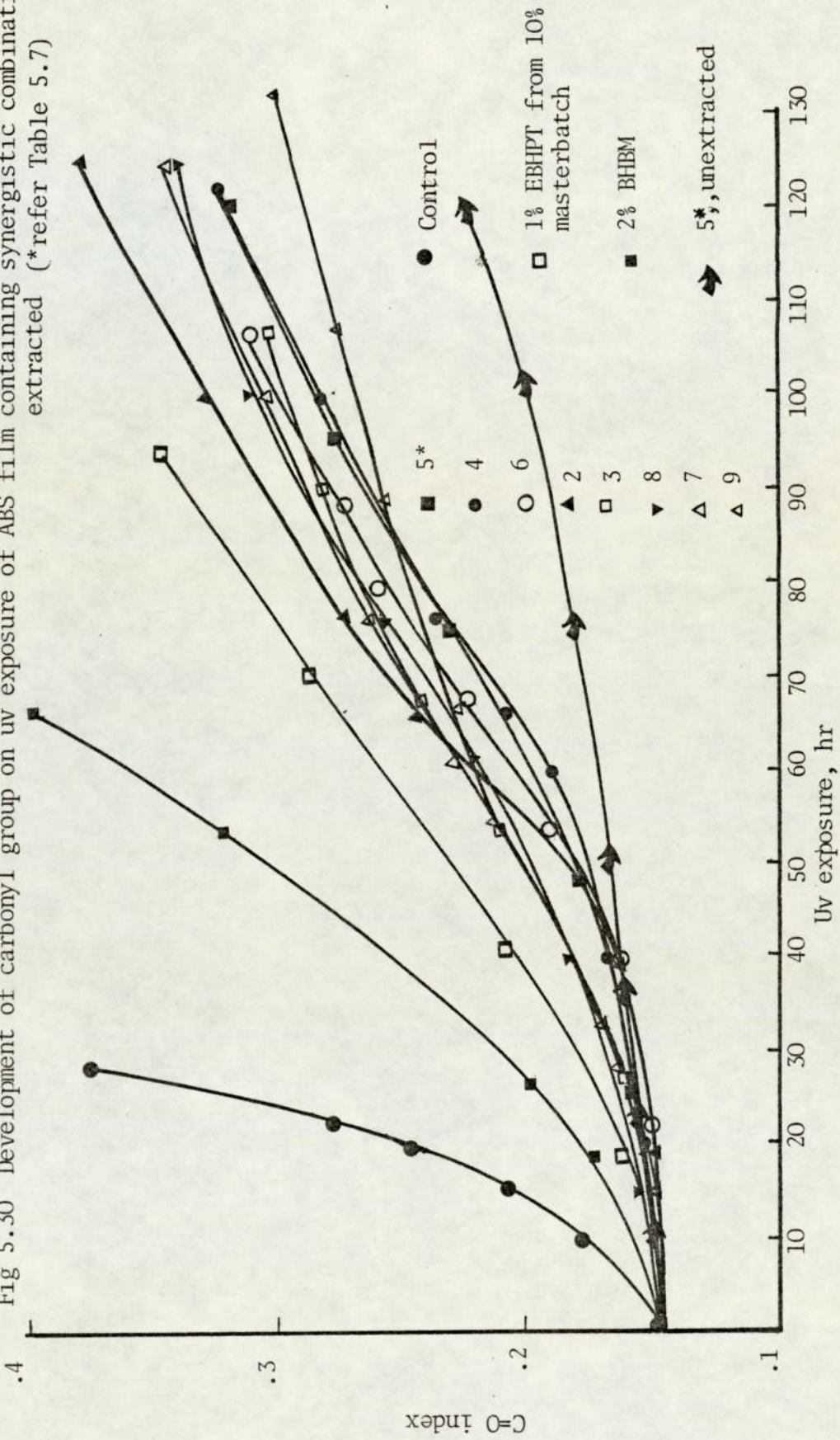
in the height of tan δ at -80°C are shown in Figs 5.31 and 5.32.
The maximum heights of tan δ at -80°C and changes in the impact
strengths were plotted against time of exposure to uv light
(Fig 5.33). The induction periods and embrittlement times are
given in Table 5.8.

5.6.b Discussion

The above results were obtained from ABS of solid blends mixed in
torque rheometer at 190°C for 3 minutes. Application of this
procedure to ABS using a combination of thermal antioxidant
(BHBM) and a light stabiliser (EBHPT) results in modification of
the rubber segment of ABS to give uv lifetime many times longer
than commercially stabilised grades of ABS (Table 5.7). It has
been shown[66] and discussed in Section 5.5.b that BHBM is an
exceptionally powerful catalyst for decomposition of
hydroperoxides to non-radical products.

$$\{CH_2CH=CHCH_2\}_n CH_2 CH_2 CHCH_2 \{CH_2CH=CHCH_2\}_m CH_2 CH$$

$$\underset{SA}{|} \qquad \underset{SB}{|}$$

$$A \equiv$$
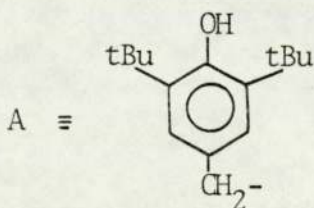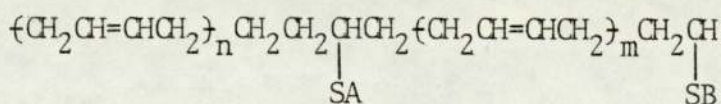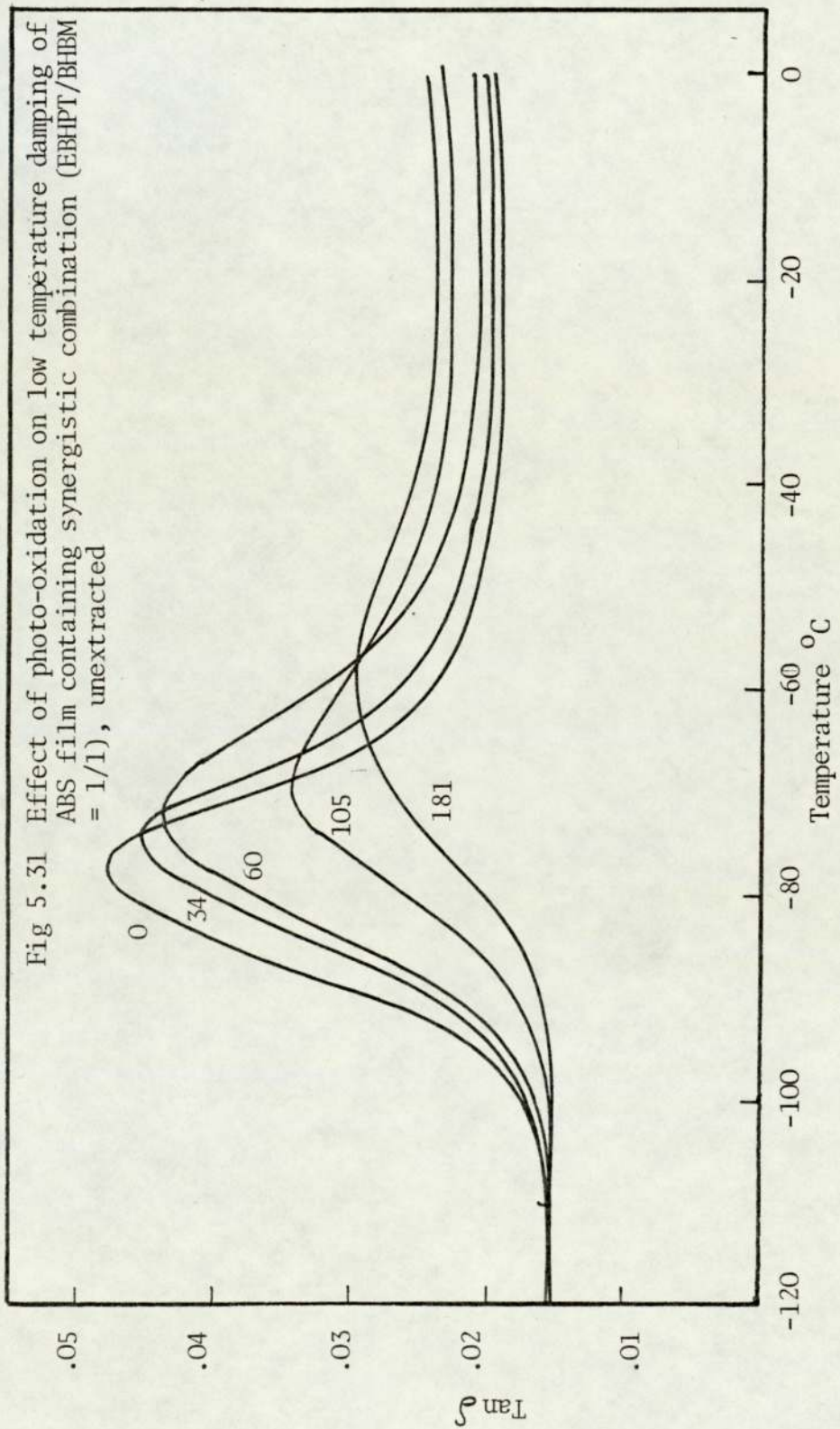
Fig 5.31 Effect of photo-oxidation on low temperature damping of ABS film containing synergistic combination (EBHPT/BHBM = 1/1), unextracted

Fig 3.32 Effect of photo-oxidation on low temperature damping of ABS film containing synergistic combination (EBHPT/BHBM = 1/1) extracted
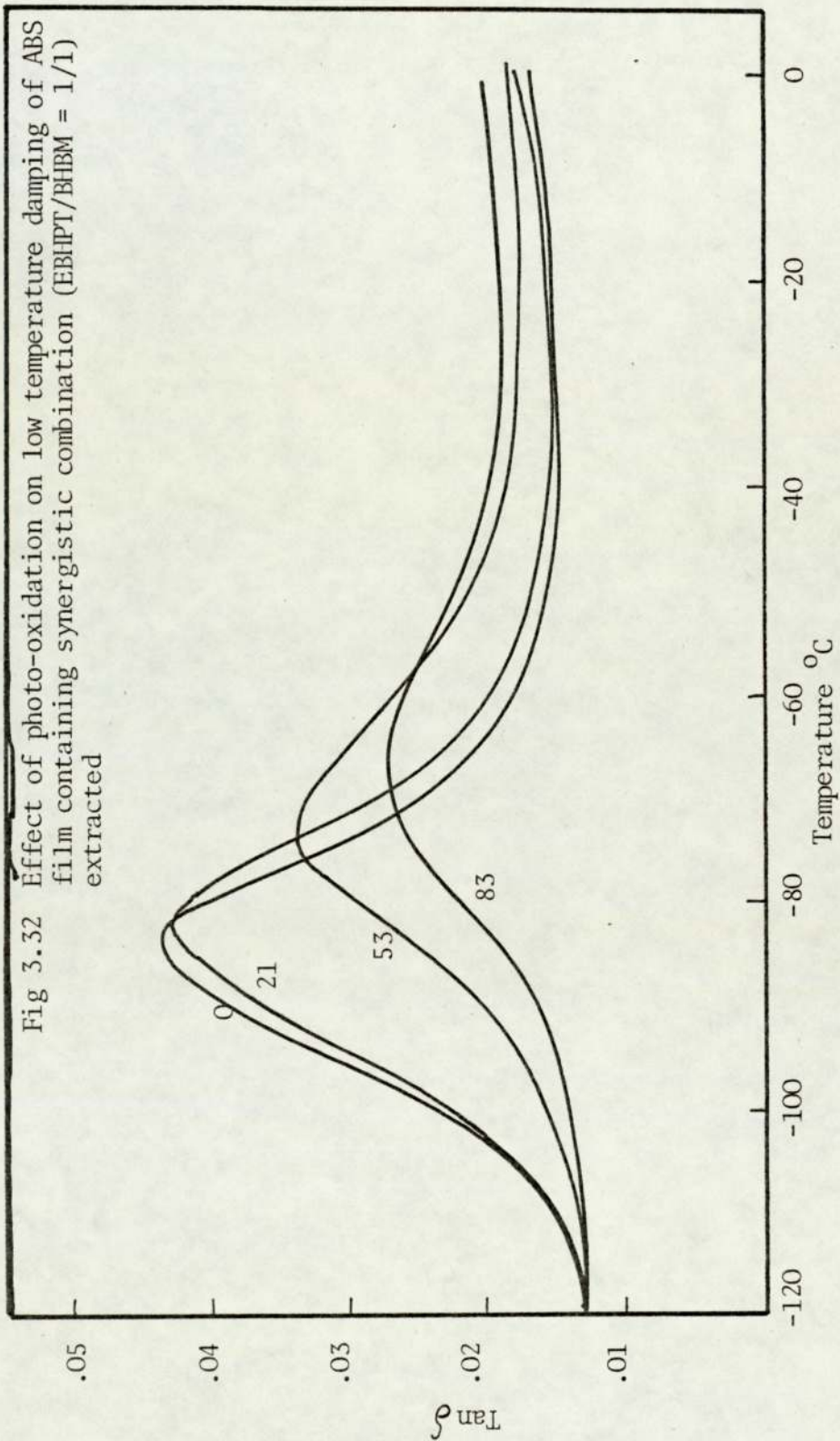
Table 5.8: Induction periods and embrittlement times of
synergistic combinations

No*	Induction period,h	Embrittlement time,h
1	10	45
2	15	100
3	22	136
4	45	170
5	50	220
6	50	180
7	30	170
8	30	170
9	30	155
EBH''T/BHBM = 1/1 unextracted	80	380
0.72 g EBHPT in 100 g of ABS	20	70
Control	2	25
Phosphite stabilised[75]	6	32

* No is from Table 5.7

261

Fig 5.33 * Refer Table 5.7

▲ 1,4 C=C, No* 5, unextracted
☆ Max height of tan δ ,No* 5, unextracted
○ 1,4 C=C, No* 5, extracted
● Impact strength, No* 5, unextracted
▼ Max height of tan δ ,No* 5, extracted
■ Max height of tan δ , 1% EBHPT from 30% masterbatch, extracted
■ Impact strength, No* 5, extracted
□ Impact strength, 1% EBHPT from 30% masterbatch, extracted
☆ Max height of tan δ , control
● Impact strength, control

Uv exposure, hr

Trans 1,4 C=C

Max height of tan δ peak at -80°C

Energy, erg/mm x 10⁻⁶

262

$$B = \langle O \rangle - CO - \langle O \rangle - OCH_2CH_2OCOCH_2-$$

with HO above the second ring.

Whilst SA, the adduct of BHBM with ABS, is an effective thermal antioxidant, SB, the adduct of EBHPT, is not. The antioxidant activity of the sulphur compounds is very specific to the structure of the rest of the molecule since the phenolic function is very important as discussed in Section 5.5.b.

$$-CH_2-\underset{SB}{\overset{H}{C}}-CH_2- \xrightarrow{ROOH} -CH_2-\underset{O=SB}{C}-CH_2- \longrightarrow -CH=C-CH_2- + BSOH$$

$$BSOH + ROOH \longrightarrow RO^{\cdot} + H_2O + B\overset{\cdot}{S}O$$

Initiation   Inhibition
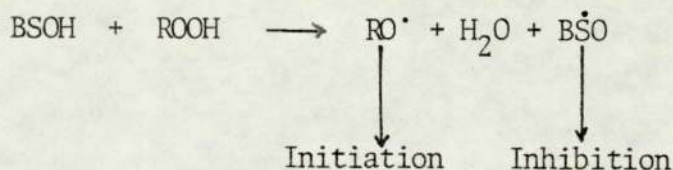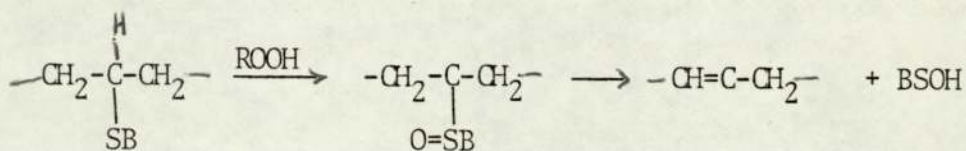
According to the above mechanism for every two molecules of ROOH decomposed, an alkoxy radical capable of chain initiation is formed[63]. The chances of neutralisation of an alkoxy radical formed increases in the presence of increased concentration of a chain-breaking antioxidant. It was pointed out earlier that the parameter most sensitive to uv degradation in ABS is impact resistance, which is related to the residual rubber unsaturation in the polyblend. Fig 5.33 compares the loss of falling weight impact resistance with the loss of unsaturation and loss of maximum height of tan δ at -80°C for solvent extracted ABS

263

containing 1 g of synergistic bound stabiliser. Comparison of Fig 5.33 with the behaviour of unstabilised ABS in the same figure shows that under the same conditions, the time to 50% loss of energy to break has been increased from almost 8 hours to 65 hours for extracted sample to 90 hours for unextracted sample. Comparison of changes in the maximum height of $\tan \delta$ at $-80^{o}C$ in Fig 5.33 shows that the time to 40% loss of the $\tan \delta$ peak has been increased from 15 hours to 90 hours for extracted synergistic sample and to 140 hours for the unextracted. The reason for faster loss of impact resistance is that impact changes reflect chemical and hence physical changes in the surface of the polymer where degradation is most severe, whereas damping measures changes through the bulk of the polymer.

CHAPTER SIX

CONCLUSIONS AND SUGGESTIONS FOR FURTHER WORK

6.1 Conclusions

Photo and thermal oxidation of ABS leads to cross-linking of the rubber phase in the early stages of oxidation. This was confirmed in the present study by the integral rise in complex modulus at $20^{o}C$ and loss of impact strength. The impact resistance is destroyed both by destruction of the elastomeric properties of the interphase and by the destruction of the chemical bond between the SAN copolymer and the interphase. In practice, the loss of impact resistance is much faster than the loss of $\tan\delta$ peak at $-80^{o}C$ and loss of 1,4-PBD unsaturation. The reason for this is that impact changes reflect chemical and hence physical changes occurring in the surface of the polymer where degradation is most severe, whereas transmission infra-red spectroscopy and damping under low strain deformation measure changes through the bulk of the polymer. In view of the differences in the techniques used, fairly good correlations were obtained between trans-1,4-PBD unsaturation, impact strength and maximum height of $\tan\delta$ at $-80^{o}C$ during photo and thermal oxidative degradation. The change in the properties of ABS as measured by destructive (impact) and non-destructive (unsaturation and $\tan\delta$ peak) tests provide linear relationships between impact strenth, trans-1,4-PBD unsaturation and the maximum height of $\tan\delta$ at $-80^{o}C$. Since

265

impact strength measurements need a great number of samples for each period of oxidative degradation, by measuring trans-1,4-PBD unsaturation or tan δ at -80°C (by ir or Rheovibron respectively) the impact strength can be obtained from the correlation curves, thus saving both on polymer samples and in time for the preparation of polymer films and measurement of impact resistance.

Effective stabilisation of ABS depends on the protection by the polybutadiene component of the polymer against oxidative degradation. It was found that a latex bound uv stabiliser (EBHPT) could be produced in concentrated form and that this, when diluted at both latex and solid stages to normal concentration (1%) with unstabilised ABS markedly improved the stability of ABS and did not show any unusual effect on the mechanical properties of the ABS. It was observed that by increasing the amount of EBHPT up to 30 g in 330 ml of latex (100 g of dry ABS) and keeping the amount of initiator (CHP) constant, 0.8 g, the bound uv stabiliser increased up to 82%. These masterbatches can be used as additive for unstabilised ABS and can also be blended with other polymers which in addition to the improving the mechanical properties of the polyblend due to the ABS impact modifier should also improve the environmental stability of the polyblend. The mercapto phenol, ie BHBM, inhibited the adduct formation in latex and the previously reported results were not reproducible. The possible reasons for this have been discussed in Chapter 4.

However, all the mercapto derivatives (EBHPT, BHBM, BTGA) have also been bound to ABS in the melt state through the thiol group by free radical addition to the double bond during processing in the torque rheometer. The amount of bound uv stabiliser (EBHPT) increased up to 84% for the 30 g EBHPT during processing in torque rheometer at 170°C for 3 minutes, the results were quite similar to those obtained in latex. This indicates that in the case of EBHPT the formation of thiyl radicals (RS·) increase with increase in the amount of EBHPT up to 30 g in 100 g ABS. The percentage of bound BHBM increased to 60% for 10 g of BHBM during processing in torque rheometer at 190°C for 3 minutes but decreased sharply to much lower values for 20 and 30 g of BHBM per 100 g of ABS at the same conditions. The possible reasons for the decrease of bound BHBM above 10 g have been discussed in Section 5.2.D.2. The masterbatches made by the mechanochemical process were diluted to normal concentration after exhaustive solvent extractions, the adducts led to remarkable improvement in the stability of useful properties of ABS towards photo and thermal degradation.

A range of combinations were made from the two masterbatches of EBHPT and BHBM. The observed stability is due to the synergistic combination of a chain breaking antioxidant (phenol), peroxide decomposer (sulphide) and uv absorber (benzophenone). The synergistic combinations not only lengthen the induction period but also slow down the auto-accelerating process of the oxidative degradation. It was observed under the same conditions that the

267

time to 50% loss of energy to break was increased from about 8 hours to 65 hours and the time to 40% loss of tan δ peak at -80°C was increased from 15 hours to 90 hours for the extracted bound synergistic combination (EBHPT/BHBM = 1/1).

6.2 Suggestions for Further Work

The adduct preparation with BHBM in ABS latex was not successful. To understand the reason for this several factors need to be considered:

(1)   The effect of possible stabilisers present in some commercial latices will need to be examined.

(2)   Swelling of BHBM emulsion in ABS latex before addition of initiator (CHP).

The easiest way of preparation of masterbatches with thiol containing compounds is processing in torque rheometer in proper conditions. The optimum condition for obtaining maximum bound uv stabiliser (EBHPT) was given in this Thesis. The optimum condition for BHBM up to 10 g was shown to be as given in earlier work but it failed above 10 g, ie 20 and 30 g of BHBM. Several factors could be involved for this:

(1)   Purity of BHBM.

(2)   Shear force. The shear force depends on two factors: temperature and plasticiser. Shear force decreases with increase in temperature and in the amount of plasticiser. The antioxidant (BHBM) reduces the bulk viscosity of the polymer. Therefore the shear force must be increased either by decreasing the processing temperature (processing time may have to be increased) or addition of antioxidant

269

into the processing chamber in several times. For example
20% BHBM can be added to the polymer melt (normal
processing temperature, 190°C) 4 or 5 times and the
processing time must also be adjusted.

REFERENCES

1   R Buchdahl, L E Nielsen, J Poly Sci, vol XV, 1, 1955

2   K Kato, Polymer, 8, 33, 1966

3   R H Boundy, R F Bayer, Styrene, its polymers, copolymers and derivatives, Reinhold, New York, 1952

4   D J Angier, E M Fetters, Rubb Chem and Tech, 38, 1164, 1965

5   J Bevilacqua, J Poly Sci, 24, 292, 1957

6   H Willersin, Die Makromol Chemie, 101, 297, 1967

7   W C Calvert, US Patent, Mar 1, 1966, 3,238,275

8   C H Basdekis, ABS Plastic, Reinhold, New York, 1964

9   W Mayo, Smith, Manufacturing of Plastics, vol 1, New York, Reinhold, 1964

10   J A Brydson, Plastics Materials, Butterworth, 1966

11   R Buchdahl, L E Nielsen, J App Phys, 21, 482, 1950

12   E H Merz et al, Studies on heterogeneous polymeric system, J Poly Sci, 22, 325, 1956

13   C B Bucknall, R R Smith, Polymer, 1, 437, 1965

14   M Matsuo, C Nozaki, Y Jyo, Poly Eng Sci, 9, 197, 1969

15   G Michlev, K Grunber, G Pohl, K Kaestner, Plasteukant, 20, 756, 1973

16   R Boyer, H Keskkula, Styrene, Polymers, Ency Poly Sci and Tech, 13, 375, 1970, Wiley Interscience

17   L E Nielsen, Mechanical Problems of Polymers, New York, Reinhold, 1962

18   M Matsuo et al, Poly Eng Sci, 10, 253, 1970

19   L W Sperling (ed), Polymer Blends, Grafts and Blocks, p 63

20   C B Bucknall, Brit Plastics, Dec 1967, 84

21   C B Bucknall, D G Street, SCI Monograph, No 26, 272, 1967

      (C B Bucknall, Toughened Plastics, 296)

22   C B Bucknall, Toughened Plastics, App Sci Pub, London, 1977

23   L E Nielsen, Mechanical Properties of Polymers and

      Composites, vol 1, Dekker, New York, 1974

24   L E Nielsen, Mechanical Properties of Polymers and

      Composities, vol 2, New Uork, 1974

25   S L Rosen, SPE Tech Paper, vol XII, p1, Two-phase

      polymer systems

26   L E Nielsen, J Am Chem Soc, 75, 1435, 1953

27   R Buchdahl, L E Nielsen, J Poly Sci, XV, 1, 1955

28   R Buchdahl, L E Nielsen, J App Phys, 21, 482, 1950

29   D J Angier, E M Peters, Rubb Chem Tech, 38, 1164, 1965

30   E R Wagner, L M Robeson, Rubb Chem Tech, 43, 1129, 1970

31   M Takayanagi, H Harima, Y Iwata, Mem Fac Eng Kyushu Univ,

      23, 1, 1963

32   S G Turley, J Poly Sci, C1, 101, 1963

33   C B Bucknall, J Mat (ASTM), 4, 214, 1969

34   K Sears, J R Derby, SPEJ, 18, 671, 1962

35   R Shelton, Rubb Chem Tech, 45, 359, 1972

36   L Bateman, H Hughes, J Chem Soc, 4592, 1952

37   G Scott, Atmospheric Oxidation and Antioxidants, Elsevier,

      New York, London, 1965

38   C H Bamford, D F H Tipper (eds), Comprehensive Chemical

      Kinetics, 14, Elsevier, 425, 1975

39   A Scott, PhD Thesis, University of Aston, 1976

40   J Shimada, K Kabuki, J App Poly Sci, 12, 671, 1968

41   J Shimada, K Kabuki, J App Poly Sci, 12, 655, 1968

42   B D Gesner, J App Poly Sci, 9, 3701, 1965

43   G H Hartley, J E Guillet, Macromolecules, 1, 165, 1968

44   R P R Ranaweera, G Scott, J Poly Sci, Poly Lett Ed, 13,
      71, 1975

45   D J Carlsson, D M Wiles, Macromol, 2, 597, 1969

46   J S Hargreaves, D Phillips, J Poly Sci, Poly Chem Ed, 17,
      1711, 1979

47   A Ghaffar, A Scott, G Scott, Europ Poly J, 12, 615, 1975

48   A Scott, G Scott, Europ Polym J, 12, 615, 1976

49   J R Shelton, J App Poly Sci, 2, 345, 1959

50   W L Hawkins, Polymer Stabilisation, Wiley Interscience, 1972

51   B Ranby, J F Rabek, Photodegradation, photo-oxidation and
      photostabilisation of polymers, Wiley Interscience, New
      York, 1975

52   J H Chandot, G C Newland, H W Patten, J W Tamblyn, SPE
      Trans, 1, 26, 1961

53   E J O'Connel, J Am Chem Soc, 90, 6550, 1968

54   H J Heller, Europ Poly J, Supp, 105, 1969

55   J R Shelton, Rubb Chem Tech, 45, 359, 1972

56   G Scott, Atmospheric Oxidation and Antioxidants, Elsevier,
      Amsterdam, 1965

57   G Scott, Chem and Ind, Feb 1963

58   W L Hawkins, H Sautter, Chem Ind (Lond), 1825,1962

59   B A Marshall, Hydroperoxide decomposition by some sulphur
      compounds, in R F Gould (ed) Stabilisation of Polymers and

273

stabiliser processes, Adv Chem Ser, 85, Am Chem Soc, Washington DC, <u>82</u>, 1810, 1960

60   R P R Ranaweera, G Scott, Europ Poly J, <u>12</u>, 825, 1976

61   J D Holdsworth, G Scott, D Williams, J Chem Soc, 4692, 1964

62   K B Chakraborty, G Scott, Europ Poly J, <u>13</u>, 1007, 1977

63   G Scott, Mechanisms of Reactions of Sulphur Compounds (ed N Kharasch), <u>4</u>, 99, 1969

64   C Armstrong, F A A Ingham, J G Pimblott, G Scott, J E Stuckey, Int Rubb Conf, Brighton, F2.1, 1972

65   M J Husbands, G Scott, Europ Poly J, <u>15</u>, 879, 1979

66   V M Farzaliev, W S E Fernando, G Scott, Europ Poly J, <u>14</u>, 785, 1978

67   K W S Kularatne, G Scott, Europ Poly J, 827, 1979

68   J R Shelton, Rubb Rev Rubb Chem Tech, <u>30</u>, 1270, 1957

69   G Scott, Europ Poly J Supp, 189, 1969

70   Instruction manual for Rheovibron DDVII, Toyo Measuring Instruments Co Ltd, Tokyo, 1969

71   Ewing, Instrumental Methods of Chemical Analysis, McGraw Hill, 82, 1960

72   D J Massa, J App Phys, <u>44</u>, No 6, June 1963

73   M Yoshino, M Takayanagi, Jap Soc Testing Materials, <u>8</u>, 330, 1959

74   J R Danby, R Sears, SPEJ, <u>18</u>, 671, 1962

75   W S E Fernando, PhD Thesis, University of Aston, 1977

76   K Metcalf, R F Tomlinson, Plastics, <u>25</u>, 319, 1960

77   M Szwarc, J Poly Sci, <u>19</u>, 589, 1956

78   G Scott, Development in Polymer Stabilisation -1, App Sci
        Pub, 1979

79   L J Bellamy, The infra-red spectra of complex molecules,
        Wiley, New York, 1959

80   G E Boyce, Brit Plast, $\underline{43}$, 122, 1970

81   A Davis, D Gordon, J App Poly Sci, $\underline{13}$, 1159, 1974

82   B D Gesner, SPE Tech Papers, $\underline{XLV}$, 178

83   G Scott, M Tahan, Europ Poly J, $\underline{13}$, 981, 1977

84   A Ghaffar, A Scott, G Scott, Europ Poly J, $\underline{11}$, 271, 1975

85   A Ghaffar, A Scott, G Scott, Europ Poly J, $\underline{13}$, 89, 1977

86   A Ghaffar, A Scott, G Scott, Europ Poly J, $\underline{13}$, 83, 1976

87   M Gordon, Physics of Plastics, (ed P D Ritchie), Iliffe
        Book, London, 1965, 224

88   H Keskkula, S G Turley, R F Boyer, J App Poly Sci, $\underline{15}$,
        351, 1971

89   T Ricco, A Pavan, F Danusso, Polymer, $\underline{16}$, 685, 1975

90   H Keskkular, App Poly Symp, No 15, 51, 1970

91   W P Coh, R A Isaksen, E H Merz, J Poly Sci, $\underline{XLIV}$, 149, 1960

92   B D Gesner, SPEJ, $\underline{25}$, 73, 1969

93   P G Kelleher, D J Boyle, B D Gesner, J App Poly Sci, $\underline{11}$,
        1731, 1967

94   P G Kelleher, D J Boyle, R J Miner, Mod Plast, Sep 1969, 188

95   J Shimada, K Kabuki, M Ando, Rev Elect Comm Lab, $\underline{20}$, No 5-6,
        553, 1972

96   A D McIntyre, J App Poly Sci, $\underline{5}$, 195, 1961

97   P J Donnelly, R H Ralston, App Poly Symp, $\underline{1}$, 71, 1965

98   R M Evans, H R Nara, E G Babalek, SPEJ, $\underline{40}$, 76, 1960

99   S G Turley, J Poly Sci, C1, 101, 1963

100   J Posner, Chem Ber, 38, 646, 1965

101   W A Pryer, Mechanism of Sulphur Reactions, McGraw Hill, 1962

102   Morrison and Boyd, Organic Chemistry, Allyn and Bacon, 1966

103   R Back, G Trick, C McDonald, C Siverts, Canad J Chem, 32, 1078, 1954

104   R Griesbaum, Angew Chem Int Ed, 9, 273, 1970

105   D C Blackley, Emulsion Polymerisation, App Sci Pub, London, Chap 8, 328, 1975

106   C F Fryling, Chem ABs, 45, 4960, 1951

107   G Scott, Pure App Chem, 30, 267, 1972

108   K M Oo, M Tahan, Europ Poly J, 13, 915, 1977

109   J W Horvath, J R Burdon, G E Meyer, E J Naples, J App Poly Symp, 25, 393, 1974

110   M R N Fernando, G Scott, J E Stuckey, Lecture given at Centenary Rubb Conf, Sri Lanka, Dec 1976, J Rubb Res Inst Sri Lanka

111   W S E Fernando, MSc Thesis, University of Aston, 1974

112   G Scott, P A Shearn, J App Poly Sci, 13, 1329, 1969

113   C Armstrong, G Scott, J Chem Soc, 3, 1747, 1971

114   W V Smith, JACS, 68, 2059, 1946; 68, 2069, 1946

115   E G Kolawole, Int Report, Aston University, 1978

116   G Scott, Plast and Rubb: Processing, 1977, p41

117   K W S Kularatne, G Scott, Europ Poly J, 15, 827, 1979

118   W Kauzman, H Eyring, J Am Chem Soc, 62, 3113, 1940

119   M Pike, W F Watson, J Poly Sci, 9, 229, 1952

120   D J Angier, W F Watson, Trans IRI, 33, 22, 1957

121   G Ayrey, C G Moore, W F Watson, J Poly Sci, $\underline{19}$, 1, 1956

122   D J Angier, E D Farlie, W F Watson, Trans IRI, $\underline{34}$, 8, 1958

123   P Yu Butagin, V F Drozdovskii, D R Razgon, J V Kolbanev,

        Sov Phys, Solid State, $\underline{7}$, 757, 1965

124   Ye V Reztsova, G V Chubarova, Poly Sci, USSR, No 7, 1481, 1965

125   W D Potter, G Scott, Europ Poly J, $\underline{7}$, 489, 1970

126   D J Angier, R J Ceresa, W F Watson, J Poly Sci, $\underline{XXXIV}$,

        699, 1959

127   R J Ceresa, W F Watson, Trans IRI, $\underline{35}$, 19, 1959

128   R J Ceresa, Polymer, $\underline{1}$, 72, 1960

129   R J Ceresa, Trans IRI, $\underline{36}$, No 2, 45, 1960

130   R J Ceresa, Plastics Institute Transaction, $\underline{28}$, 178, 1960

131   G V Hutson, G Scott, Europ Poly J, $\underline{10}$, 45, 1974

132   M U Amin, B W Evans, G Scott, Chem Ind, 206, 1974

133   B W Evans, G Scott, Europ Poly J, $\underline{10}$, 453, 1974

134   J Holcik, M Karvas, D Kassovicova, J Durmis, Europ Poly

        J, $\underline{12}$, 173, 1976

135   M A Plant, G Scott, Europ Poly J, $\underline{7}$, 1173, 1971

136   J Durmis, M Karvas, P Cancik, J Holcik, Europ Poly J, $\underline{11}$,

        219, 1975

137   M U Amin, G Scott, L M K Tillekeratne, Europ Poly J, $\underline{11}$,

        85, 1975

138   C Armstrong, M J Husbands, G Scott, to be published

139   A R Forrester, J M Hay, R H Thompson, Organic Chemistry of

        Stable Free Radicals, 1968, Acad Press, London

140   Developments in Polymer Stabilisation (ed G Scott) 1979

141   R Dyke, Diamond Shamrock Europe, unpublished work